Exploring the role of CXCL4 in modulating immune responses triggered by monocyte-derived dendritic cells:

beyond what the eyes can see

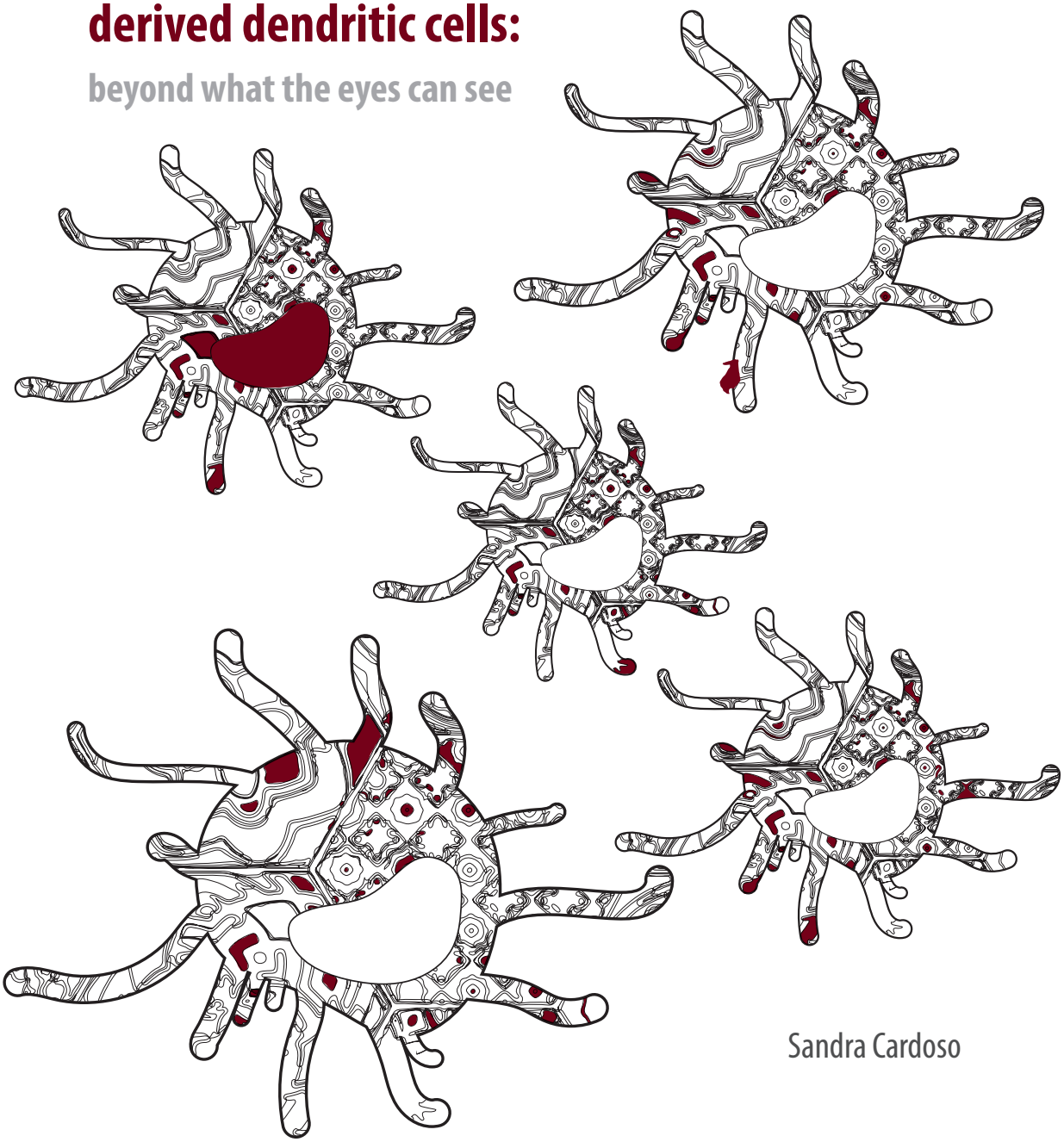

Sandra Cardoso

Exploring the role of CXCL4 in modulating immune responses triggered by monocyte-derived dendritic cells: beyond what the eyes can see

Sandra Cristina Silva Cardoso

ISBN: 978-94-93184-15-2

Layout and print: proefschrift-aio.nl

Printing of this thesis was financially supported by:
Peprotech
PhD program Infection and Immunity Utrecht
Department of Rheumatology & Clinical Immunology
ChipSoft
Stichting NVLE Fonds

Exploring the role of CXCL4 in modulating immune responses triggered by monocyte-derived dendritic cells: beyond what the eyes can see

Zoektocht naar de rol van CXCL4 in het bijsturen van immuunresponsen die door uit monocyt gedifferentieerde dendritische cellen geïnitieerd worden: voorbij aan wat de ogen kunnen zien

(met een samenvatting in het Nederlands)

Proefschrift

ter verkrijging van de graad van doctor aan de
Universiteit Utrecht
op gezag van de
rector magnificus, prof.dr. H.R.B.M. Kummeling,
ingevolge het besluit van het college voor promoties
in het openbaar te verdedigen op

maandag 9 december 2019 des middags te 2.30 uur

door

Sandra Cristina Silva Cardoso

geboren op 6 september 1988
te Viseu, Portugal

Promotor:
Prof. dr. T.R.D.J. Radstake

Copromotoren:
Dr. A. Pandit
Dr. M.L. Boes

Part of the work presented in this thesis was financially supported by a PhD fellowship from: Fundação para a Ciência e a Tecnologia (FCT, Portugal): SFRH/BD/89643/2012

Às minhas estrelinhas que olharam por mim durante esta aventura,
Especialmente à *Luzinha, Mariana, Isabel*
Às guerreiras da minha vida, *Mamã e Lúcia*

To my shining stars that have watched over me during this adventure,
Especially to *Luzinha, Mariana, Isabel*
To the warriors of my life: *Mom and Lúcia*

Manuscriptcommissie: Prof. dr. Theo Geijtenbeek
Prof. dr. Linde Meyaard
Prof. dr. Rene Toes
Prof. dr. Gerard Pasterkamp
Prof. dr. Roel Goldschmeding

Paranymphs: Ana Costa
Chiara Angiolilli

Thesis contents

Chapter 1.	General introduction Aim and Scope of the Thesis	9
Chapter 2.	CXCL4 exposure potentiates TLR-driven polarization of human monocyte-derived dendritic cells and increases stimulation of T-cells	31
Chapter 3.	CXCL4 is a novel inducer of human Th17 cells and correlates with IL-17 and IL-22 in psoriatic arthritis.	55
Chapter 4.	CXCL4 links inflammation and fibrosis through transcriptional and epigenetic reprogramming of inflammatory monocyte-derived cells	83
Chapter 5.	CXCL4 suppresses tolerogenic immune signature of monocyte-derived dendritic cells	135
Chapter 6.	CXCL4 is a driver of cytokine mRNA stability in monocyte-derived dendritic cells	153
Chapter 7.	General discussion	187
Appendix	English summary	204
	Nederlandse samenvatting	208
	Acknowledgments	212
	Curriculum vitae	220
	List of publications	222

Chapter 1

General introduction

CXCL4 as a driver of physiological processes and immune cell modulation

CXC chemokine ligand 4 (CXCL4), previously known as Platelet factor 4 (PF4), is one of the most abundant proteins released at sites of inflammation. CXCL4 is stored in α-granules of platelets and abundantly released upon platelet activation[1,2]. Besides, CXCL4 is also produced by immune cells, such as mast cells[3], dendritic cells (DCs)[4–6], monocytes[7] and activated T-cells [8]. Normal levels of CXCL4 present in plasma are approximately 2-10ng/ml, whereas in serum (enriched by thrombin-mediated platelet aggregation and coagulation) CXCL4 levels are about 5-10μg/ml. Strikingly, human platelets store about 20μg of CXCL4/10^9 platelets[9]. Local levels of CXCL4 are likely to be high in wounds or inflamed tissues, as these are sites of platelet activation. Indeed, increased platelet frequency and activation are implicated in the presence of an injured endothelium, extensive activation of the immune system and amplified inflammation in several autoimmune diseases[10–12].

Most of the chemokines play a critical role in the recruitment of cells to inflammatory sites. However, rather than chemotactic activity, CXCL4 plays a key role in biological processes and pathological conditions[13] like inhibition of hematopoiesis and angiogenesis[14–18], platelet coagulation, wound healing[19–22], atherosclerosis development[23–26] and immune cell activation and differentiation.

CXCL4 plays a critical role in modulating the function of endothelial cells, monocytes, macrophages, DCs and T-cells[27–37]. For instance, CXCL4 prevents monocytes from undergoing apoptosis, promotes their differentiation into a specialized subset of macrophages (M4), augments the production of inflammatory cytokines, and oxygen radical species (ROS) by using distinct signaling pathways[29,30,34,38–40]. Additionally, it has been described that exposure of monocyte-derived dendritic cells (moDCs) to CXCL4 during differentiation alters the phenotype and function of the cells[27,28,33].

Furthermore, studies on T-cells indicated that CXCL4 inhibits proliferation and IL-2 production on activated T-cells[31], induces regulatory CD4+CD25+ T-cell proliferation while impairing CD4+CD25+ T-cell proliferation[41] and drives T-cell polarization by inducing pro-fibrotic Th2 cytokines (IL-13) and by reducing Th1 cytokines (IFNγ) production by naïve CD4+ T-cells through the regulation of transcription factors such as T-bet and GATA-3[36].

CXCL4 is a 70-amino acid protein, located on the chromosome 4q13.3 in humans[42]. Other than many CXC-chemokines, CXCL4 does not comprise an N-terminal Glutamic acid-Leucine-Arginine (ELR) motif within its N-terminal portion of the protein. CXCL4 binds strongly to heparin and negatively charged cell surface glycosaminoglycans (GAGs) such as chondroitin, dermatan and heparin sulfates[43–46]. Furthermore, CXCL4

modulation of endothelial and T-cell function is driven by the CXCL4-high affinity binding to CXCR3B[36,37,47], though modulation of monocyte responses was shown independent of CXCL4-signaling through this receptor[35]. Recently, it has been proposed that CXCL4-induced migration on monocytes is mediated by CCR1[40].

CXCL4 role in autoimmunity

Due to its abundance at sites of platelet activation and pleotropic functions, CXCL4 is implicated in diverse pathological conditions including thrombosis[22]; cancer[48], several autoimmune diseases such as atherosclerosis[23–26], inflammatory bowel disease (IBD)[49,50], heparin-induced thrombocytopenia[51], rheumatoid arthritis (RA)[52], antiphospholipid antibody syndrome (APS)[53], sjögren's syndrome (SS)[54], and infectious diseases like human immunodeficiency virus (HIV)[55] and malaria[56]. Our group was the first to identify CXCL4 as an early serum biomarker for systemic sclerosis (SSc)[5]. Later reports corroborated the contribution of CXCL4 to the pathogenesis of SSc[6,57,58]. Interestingly, increased platelet number and their activation are implicated also in this disease[11,59,60].

SSc is a complex autoimmune disease of unknown etiology. The three hallmarks that characterizes SSc are: vasculopathy, dysfunction of immune cells that leads to exacerbated inflammation and production of autoantibodies, and dysfunction of non-immune cells such as fibroblasts that contribute to the excessive deposition of extracellular matrix (ECM) components. Indeed, due to the increased levels of inflammatory cytokines and growth factors in SSc, they have been proposed as diagnostic and prognostic markers, and therapeutic targets in SSc[61,62]. Supporting *in vitro and in vivo* studies have described that immune and non-immune cells from SSc patients contribute to aberrant production of inflammatory (e.g. IL-6, type-I interferon, IL-12 family members, IL-13, IL-17) and fibrotic (TGFβ, collagen, fibronectin) mediators[63–69].

The heterogeneous clinical manifestations contribute to the complexity of SSc, where extensive fibrosis results in the thickening of the skin and involvement of internal organs may result in mortality. A considerable improvement in diagnosis and patient care in the last years has made possible better clinical outcomes, although no cure has been discovered to date[70–72]. Thus, understanding how disease-biomarkers such as CXCL4 contribute at the molecular level to the development of SSc and targeting either these biomarker or CXCL4-downstream pathways may contribute to the development of new therapeutic strategies.

The research performed in this thesis aimed to assess whether CXCL4 potentiates pro-inflammatory and pro-fibrotic responses that contribute to the development of SSc, and identify CXCL4-downstream signalling.

Dendritic cells: the bridge between innate and adaptive immune responses

Human DCs comprise of several subsets with distinct origin, phenotype, transcriptome and transcription factor profiling, capability of Ag processing, response to stimuli and ability to specifically dictate T-cell activation[73–76]. DCs are divided in two main subsets: conventional or myeloid DCs (mDCs) and plasmacytoid DCs (pDCs)[75,76].

The ability of pDCs to produce high levels of type I interferon (IFN) upon immune recognition of viral antigens (specially by TLR7 and TLR9) attribute to these cells a critical role on antiviral responses[77]. pDCs are identified by high expression of CD303 (BDCA2) and CD304 (BDCA4)[78]. Steady state pDCs are not efficient on Ag presentation, however cells develop this function after stimulation[77,79].

The mDCs are specialised APCs very effective on Ag presentation and stimulation of T-cell responses. mDCs are subdivided in two groups, CD1c+ mDCs (BDCA1 expressing DCs) and CD141+ mDCs (BDCA3 expressing DCs), defined by the distinct expression of surface molecules, TLRs and CLRs expression and production of different cytokines. Compared to other DC subsets, mDCs are a) superior in Ag uptake, processing and presentation, b) characterized by high capability to migrate to the lymph nodes for Ag presentation and c) potent inducers of T-cell responses[73,80,81]. On one hand, CD1c+ mDCs represent a heterogeneous and complex subset that express high levels of CD1c and CD11c, migrate to lymph nodes in response to triggering of several TLRs (except TLR9) to activate CD4+ T-cell responses and produce distinct inflammatory cytokines[73,80,82]. On the other hand, CD141+ mDCs possess superior ability of Ag cross-presentation to CD8+ T-cells to generate cytotoxic T-lymphocyte (CTL) responses and express high levels of TLR3, CLEC9A and unique high expression of XCR1[80,81,83–87].

Notably, early in the 90s, Sallusto and Lanzavecchia[88] and Romani et al.[89] proposed that combination of GM-CSF and IL-4 induce *in vitro* differentiation of monocytes into immature DC-like cells - monocyte-derived DCs (moDCs). Besides their high plasticity, moDCs are also very versatile depending on the micro milieu and the presence of growth factors, cytokines or dangers signals during differentiation and stimulation[90]. As observed for mDCs, the triggering with danger signals induces the maturation of moDCs both at a phenotypic and functional level, and the ability to induce Th1, Th2 or Th17 responses[91–96]. Multiple studies in human and mouse have proposed that cells functionally similar to *in vitro* moDCs are found in tissues under inflammatory conditions, thus named inflammatory DCs[76,83,92,97–99].

Throughout our research, we studied the role of CXCL4 on immune responses by *in vitro* generated moDCs due to the need of high number of cells for our functional experiments and transcriptomic and DNA methylation high through put profiling.

DCs are professional antigen presenting cells (APCs) that play a crucial role in bridging innate and adaptive immune responses. For instance, DCs initiate immune responses by recognizing either danger-associated molecular patterns (DAMPs) from damaged tissues or pathogen-associated molecular patterns (PAMPs) from microorganisms by pattern-recognition receptors (PRRs)[100,101]. Toll-like receptors (TLRs) are one subtype of PPRs, expressed on cell surface, endosomes or lysosomes, that sense components of bacteria, viruses and parasites[101]. Other subtypes of PPRs are the cytosolic NOD-like receptors (NLRs) that sense bacterial products, RIG-I-like receptors (RLRs) that bind to nucleic acids and C-type lectin receptors (CLRs) that recognize β-glucans[100,102]. The triggering of PRR signalling in DCs leads to the activation of several downstream pathways that culminate in a mature phenotype, inflammatory cytokine production and activation of T-cell responses. Thus, signalling through PRRs in DCs instructs adaptive immune responses.

Furthermore, the recognition of microbial components by phagocytosis, macropinocytosis or receptor-mediated endocytosis is pursued by antigen (Ag) processing. Processed peptides are then loaded onto the major histocompatibility complex (MHC) molecules and presented on DC surface to T-cells. Indeed, DCs are potent inducers of T-cell proliferation and polarization into Ag specific effector T-cells (Th1, Th2, Th17, Th22) in the presence of three signals: 1) co-stimulatory molecules, 2) cytokines (e.g. IL-12, TNF, IL-23); 3) TCR engagement (T-cell recognition of peptide bound to MHC molecules of the surface of DCs)[102–104].

Multiple studies reported that CXCL4 modulates the phenotype and function of immune cells, including DCs and T-cells.

In fact, disturbed DC frequencies in circulation and in inflammatory tissues, impaired immune function and aberrant TLR-mediated responses have been associated with several inflammatory autoimmune conditions[105–107], including SSc[108–112]. Strikingly, *in vitro* triggering of mDCs and moDCs from SSc patients with TLR2, TLR3 and TLR4 agonists results in aberrant production of IL6, TNF and IL12. Also, stimulation of pDCs with TLR9 agonist induced increased production of type-I interferon (IFN-I)[5,6,57,111,113–118]. Endogenous ligands of TLR2 (serum amyloid A (SAA)) and TLR4 (S100A8/9) were shown to be increased in patients with SSc[119–121]. The expression of TLR4-pathway associated molecules were found increased in SSc skin and lungs, and were associated with several SSc hallmarks[122,123]. In line with these findings, studies in murine models of chronic inflammation and fibrosis confirmed the implication of immune activation driven by TLR signalling, especially TLR3-mediated responses[124–127].

Moreover, deregulated T-cell responses, namely by Th1, Th2 and Th17 subsets, contribute to tissue fibrosis and inflammation and represent also hallmarks of SSc pathogenesis[64,128–133].

Thus, both innate and adaptive immune responses are compromised in SSc patients, however the contribution of CXCL4 to this aberrant phenotype remains poorly described. Therefore, we investigated how CXCL4 modulates DC innate and adaptive immune responses that culminate in chronic inflammatory responses in SSc and other autoimmune diseases.

Tolerogenicity and Immunogenicity: a balance required for immune homeostasis

DCs are sentinel cells crucial for the initiation of immune responses and the maintenance of immune tolerance[134–137]. The plasticity in phenotype and function confers to DCs two distinct roles: i) in response to inflammatory triggers, immunogenic DCs act as potent activators of T-cells thereby promoting inflammatory responses; ii) conversely, tolerogenic DCs (tol-DCs) in response to self-antigens may deplete self-reactive T-cells promoting the generation of regulatory T-cells, and drive T-cell anergy to maintain the balance of peripheral tolerance[102,138,139].

In steady state, DCs express on cell-surface Ag presenting molecules (MHC class I and II), co-stimulatory molecules and chemokine receptors such as CCR7 in order to promote homing to the lymph nodes. Furthermore, they express low levels of chemokine receptors for local inflammatory mediators (e.g. CCR5 and CCR6) and phagocytic competence. However, when DCs encounter either foreign- or self-danger signals, they initiate, modulate and sustain either immunogenic or tolerogenic responses, according to the presence or absence of inflammatory signals[103,139].

Exposure of immunogenic DCs to inflammatory mediators leads to dramatic upregulation of MHC and co-stimulatory molecules (e.g. CD86, CD80, CD40), cell adhesion molecules such as ICAM1 and pro-inflammatory cytokines. Ag presentation to T-cells, co-stimulation and secretion of cytokines and chemokines that attract T-cells culminates with the expansion and differentiation into effector T-cells with a particular cytokine profile (e.g. Th1, Th2, Th17)[103,140]. However, in the absence of inflammatory mediators tol-DCs are poorly immunogenic, they express low levels of co-stimulatory molecules and do not produce pro-inflammatory cytokines. Presentation of self- or harmless- Ag by tol-DCs to T-cells generates regulatory T-cells (Tregs), which suppress effector functions of CD4+ and CD8+T-cells[103,104,135,141,142]. Moreover, the production of mediators such as IL-10, TGF-β, indolamine 2,3-dioxygenase (IDO) and retinoic acid (RA) by DCs promotes adaptive immune responses by regulatory T-cells (Tregs) rather than effector T-cells[143–147].

Tolerogenic or immunogenic responses are critical for the maintenance of immune homeostasis. Though, when these responses are prolonged and amplified may contribute towards the development of immunodeficiency or autoimmune diseases.

Multiple protocols were established for the *in vitro* generation of DCs with immunogenic and tolerogenic properties[104,148–151]. Recent transcriptomic and proteomic studies provided new understanding of their molecular profiles, and identified several candidate molecules associated with immunogenic and immune-regulatory functions despite the diversity of mediators used to generate these cells[152–158]. Remarkably, the generation of tolDCs represent an attractive target for immunotherapy, especially for the treatment of autoimmune diseases[159–162]. Alternatively, current investigation on discovering candidate biomarkers implicated on immunogenic responses may provide potential targets for therapeutically intervention in multiple immune and non-immune diseases.

In our research, we observed that CXCL4 exposure during moDC differentiation instructs moDCs to distinct phenotype and T-cell activation. Thereby, we explored the role of CXCL4 in the modulation of immunogenic and tolerogenic signatures in order to identify therapeutically targetable markers, which would rescue cells, back to a homeostatic equilibrium.

Transcriptional and post-transcriptional regulation of gene expression by CXCL4

In our functional experiments performed in the first part of this thesis, we observed dramatic changes on the morphology and phenotype of moDCs, and enhanced immunogenic response as result of exposure to CXCL4. Therefore, in the second part, we further investigated the underlying signalling pathways and master regulators implicated in cell reprogramming to elucidate how CXCL4 potentiates pro-inflammatory cytokine production and the association with fibrotic responses implicated in the pathogenesis of SSc.

Exposure to danger signals results in loss of cellular and tissue homeostasis and culminates in complex transcriptional reprogramming which initiates, maintains and lately confines inflammatory responses. For instance, genes associated with cell migration, Ag presentation, tissue remodelling and metabolic reprogramming are some examples of the thousands of genes that are induced or repressed in response to self- and foreign- danger signals[163,164]. The transcriptional regulation of multiple signalling pathways may differ between species, cell type, location of the cells, and function in a gene-specific manner. Transcription factors and transcriptional

co-regulators are crucial players in the regulation of these signalling pathways or transcriptional modules[165,166]. Interestingly, genes belonging to a specific transcriptional module are functionally associated, and regulated in a coordinated manner by master regulators of this module[165,166].

Alongside to the tight control at the transcriptional level, inflammatory cytokines are also regulated at post-transcriptional levels which includes regulation of mRNA stability[167,168]. Adenosine uridine (AU)-rich elements (AREs) present on the 3 prime untranslated region (3'UTR) of many cytokines mediate the regulation of mRNA decay. The binding of trans-acting ARE-binding proteins (ARE-BPs) to AREs in the 3'UTR of inflammatory cytokines ultimately defines the stability or instability of mRNA[167–169]. Deregulation of mRNA regulatory mechanisms have been associated with autoimmune conditions and cancer[170–174].

Furthermore, epigenetic mechanisms such as DNA methylation and histone modifications also regulate gene repression[175] and epigenetic imprinting[176], for instance by modulating the access of transcription factors to DNA regulatory elements[177,178]. DNA methylation is mediated by the addition of a methyl group to the fifth carbon of cytosine (C), forming 5-methylcytosine (5mC) catalysed by DNA methyltransferases (DNMTs)[179,180]. DNMTs comprise of 5 enzymes: DNMT1, DNMT2, DNMT3a, DNMT3b and DNMT3L, that play distinct roles[181,182]. In vertebrates, DNA methylation predominantly occurs in CpG dinucleotides sites (CpGs), however in pluripotent stem cells it has been found also non-CpG sites[180,183,184].

One of the mechanisms that result in transcriptional suppression is accomplished when methyl groups interfere with the binding of transcription factors to CpG sequences. Methylation of gene promoter regions is associated with down-regulation of gene expression by altering the chromatin structure and blocking transcription initiation[185]. Recent studies have shown that environmental perturbations drive rapid changes on DNA methylation and gene regulation, and modulate immune responses[178,186–188]. Indeed, aberrant hyper- or hypo-methylation levels have been associated with autoimmunity[189] and cancer[190,191].

The potential reversibility of epigenetic marks makes them an attractive therapeutic target in several diseases[192–194], including autoimmune conditions[189,195], although much remains to be elucidated. Thus, exploring the transcriptional, post-transcriptional and epigenetic mechanisms implicated in CXCL4 immune-modulatory effects may open new possibilities for therapeutic applications.

Aim and Scope of the Thesis

In this thesis, I aimed to investigate the role of CXCL4 on remodelling the immune landscape of human monocyte-derived dendritic cells (moDCs) and the underlying transcriptional, post-transcriptional and epigenetic mechanisms.

Firstly, in **Chapter 2** we differentiated moDCs in the presence of CXCL4 and explored the effects of CXCL4 exposure on the morphology and phenotype of moDCs. By exposing moDCs and CXCL4-moDCs to a large panel of TLR agonists and by evaluating both the phenotype and pro-inflammatory cytokine production, we further investigated how CXCL4 affects TLR-mediated responses. Moreover, we studied how CXCL4 primes moDCs to activate autologous and Ag specific T-cells.

In **Chapter 3**, we studied the contribution of CXCL4 on the activation of Th17 responses, either directly on CD3/CD28-activated CD4+ T-cells or indirectly via antigen presenting cells (APCs), such as plasmacytoid dendritic cells (pDCs), myeloid dendritic cells (mDCs), monocytes and B cells. Furthermore, we assessed the implication of our findings in a Th17-mediated disease context by studying the relationship of CXCL4 with Th17 cytokine levels in synovial fluid of PsA patients.

To further elucidate how CXCL4 reprograms moDC's innate and adaptive immune responses, in **Chapter 4** we performed high-throughput transcriptome sequencing and DNA methylation profiling on 65 paired longitudinal samples from moDCs and CXCL4-moDCs during differentiation (day 0, 2, 4 and 6) and TLR3-mediated stimulation (0, 4 and 24 hours stimulation). Besides extensively studying the downstream pathways affected by CXCL4 on the transcriptional and DNA methylation levels, we validated multiple candidate molecules modulated by CXCL4 on the protein level. We found an upregulation of pro-inflammatory and pro-fibrotic mediators implicated in diseases where CXCL4 has been implicated, such as Systemic Sclerosis. Notably by applying our new developed methodology (RegEnrich), we created gene regulatory networks based on co-expression and co-methylation patterns of clustered genes in distinct modules. We identified key transcriptional regulators that modulate CXCL4-signature genes.

Chapter 5 reveals how the exposure of moDCs to CXCL4 affects the immunogenic and tolerogenic gene signature on the transcriptional and DNA methylation level in moDCs.

In **Chapter 6,** we investigated the transcriptional and post-transcriptional mechanisms underlying the augmented pro-inflammatory cytokine production in TLR3-stimulated CXCL4-moDCs. We analyzed the expression of primary and mature transcripts of inflammatory cytokines and performed mRNA decay experiments to investigate whether CXCL4 regulates these cytokines on the mRNA stability level. Additionally, we studied the implication of AU-rich element binding proteins (ARE-

BPs) on mRNA stability regulation by CXCL4. Finally, we explored the upstream regulation of the ARE-BP TTP by MAPK-p38 signaling and the consequences of TTP knockdown on inflammatory cytokine production in moDCs.

Finally, the findings of all the research performed in this thesis are summarized and discussed in **Chapter 7**.

Overall, the work performed throughout this thesis provides new insights on the impact of CXCL4 in priming immunogenic innate and adaptive immune responses in moDCs, but also in promoting pro-inflammatory and pro-fibrotic responses that culminate in autoimmune conditions.

References

1. Levine, S. P. & Wohl, H. Human platelet factor 4: Purification and Characterization by affinity chromatography. Purification of human platelet factor 4. *J. Biol. Chem.* **251,** 324–328 (1976).
2. Zucker, M. B. & Katz, I. R. Platelet factor 4: prodution, structure, and physiologic and immunologic action. *Proc. Soc. Exp. Biol. Med.* **198,** 693–702 (1991).
3. McLaren, K. M., Holloway, L. & Pepper, D. S. Human platelet factor 4 and tissue mast cells. *Thromb. Res.* **19,** 293–297 (1980).
4. Maier, M. *et al.* Platelet factor 4 is highly upregulated in dendritic cells after severe trauma. *Mol. Med.* **15,** 384–91 (2009).
5. van Bon, L. *et al.* Proteome-wide analysis and CXCL4 as a biomarker in systemic sclerosis. *N. Engl. J. Med.* **370,** 433–43 (2014).
6. Kioon, M. D. A. *et al.* Plasmacytoid dendritic cells promote systemic sclerosis with a key role for TLR8. *Sci. Transl. Med.* **10,** (2018).
7. Schaffner, A., Rhyn, P., Schoedon, G. & Schaer, D. J. Regulated expression of platelet factor 4 in human monocytes--role of PARs as a quantitatively important monocyte activation pathway. *J. Leukoc. Biol.* **78,** 202–9 (2005).
8. Lasagni, L. *et al.* PF-4/CXCL4 and CXCL4L1 exhibit distinct subcellular localization and a differentially regulated mechanism of secretion. *Blood* **109,** 4127–34 (2007).
9. Files, J. C., Malpass, T. W., Yee, E. K., Ritchie, J. L. & Harker, L. A. Studies of human plate alpha-granule release in vivo. *Blood* **58,** 607–618 (1981).
10. Lood, C. *et al.* Platelet transcriptional profile and protein expression in patients with systemic lupus erythematosus: Up-regulation of the type I interferon system is strongly associated with vascular disease. *Blood* **116,** 1951–1957 (2010).
11. Agache, I., Radoi, M. & Duca, L. Platelet activation in patients with systemic scleroderma--pattern and significance. *Rom. J. Intern. Med.* **45,** 183–191 (2007).
12. Boilard, E. *et al.* Platelets amplify inflammation in arthritis via collagen-dependent microparticle production. *Science (80-.).* **327,** 580–583 (2010).
13. Vandercappellen, J. *et al.* Stimulation of angiostatic platelet factor-4 variant (CXCL4L1/PF-4var) versus inhibition of angiogenic granulocyte chemotactic protein-2 (CXCL6/GCP-2) in normal and tumoral mesenchymal cells. *J. Leukoc. Biol.* **82,** 1519–30 (2007).
14. Han, Z. C., Bellucci, S., Walz, A., Baggiolini, M. & Caen, J. P. Negative regulation of human megakaryocytopoiesis by human platelet factor 4 (PF4) and connective tissue-activating peptide (CTAP-III). *Int. J. Cell Cloning* **8,** 253–259 (1990).
15. Han, Z. C., Sensébe, L., Abgrall, J. F. & Brière, J. Platelet Factor 4 Inhibits Human Megakaryocytopoiesis In Vitro. *Blood* **75,** 1234–1239 (1990).
16. Zhang, C. *et al.* Localization of distal regulatory domains in the megakaryocyte-specific platelet basic protein/platelet factor 4 gene locus. *Blood* **98,** 610–617 (2001).
17. Maione, T. E. *et al.* Inhibition of angiogenesis by recombinant human platelet factor-4 and related peptides. *Science (80-.).* **247,** 77–79 (1990).
18. Sharpe, R. J., Byers, H. R., Scott, C. F., Bauer, S. I. & Maione, T. E. Growth inhibition of murine melanoma and human colon carcinoma by recombinant human platelet factor 4. *J. Natl. Cancer Inst.* **82,** 848–853 (1990).
19. Kowalska, M. A., Rauova, L. & Poncz, M. Role of the platelet chemokine platelet factor 4 (PF4) in hemostasis and thrombosis. *Thromb. Res.* **125,** 292–6 (2010).
20. Dehmer, G. J., Fisher, M., Tate, D. A., Teo, S. & Bonnem, E. M. Reversal of Heparin Anticoagulation by Recombinant Platelet Factor 4 in Humans. *Circulation* **91,** 2188–2194 (1995).
21. Slungaards, A. & Key, N. S. Platelet Factor 4 Stimulates Thrombomodulin Protein C-activating Cofactor Activity. *J. Biol. Chem.* **269,** 25549–25556 (1994).

22. Eslin, D. E. *et al.* Transgenic mice studies demonstrate a role for platelet factor 4 in thrombosis: dissociation between anticoagulant and antithrombotic effect of heparin. *Blood* **104,** 3173–3180 (2004).
23. Erbel, C. *et al.* Prevalence of M4 macrophages within human coronary atherosclerotic plaques is associated with features of plaque instability. *Int. J. Cardiol.* **186,** 219–225 (2015).
24. Pitsilos, S. *et al.* Platelet factor 4 localization in carotid atherosclerotic plaques: correlation with clinical parameters. *Thromb. Haemost.* **90,** 1112–1120 (2003).
25. Sachais, B. S. *et al.* Elimination of platelet factor 4 (PF4) from platelets reduces atherosclerosis in C57Bl/6 and apoE-/- mice. *Thromb. Haemost.* **98,** 1108–1113 (2007).
26. Huo, Y. *et al.* Circulating activated platelets exacerbate atherosclerosis in mice deficient in apolipoprotein E. *Nat. Med.* **9,** 61–67 (2003).
27. Xia, C.-Q. & Kao, K.-J. Effect of CXC chemokine platelet factor 4 on differentiation and function of monocyte-derived dendritic cells. *Int. Immunol.* **15,** 1007–1015 (2003).
28. Fricke, I. *et al.* Platelet factor 4 in conjunction with IL-4 directs differentiation of human monocytes into specialized antigen-presenting cells. *FASEB J.* **18,** 1588–90 (2004).
29. Scheuerer, B. *et al.* The CXC-chemokine platelet factor 4 promotes monocyte survival and induces monocyte differentiation into macrophages. *Blood* **95,** 1158–1166 (2000).
30. Gleissner, C. A., Shaked, I., Little, K. M. & Ley, K. CXC Chemokine Ligand 4 Induces a Unique Transcriptome in Monocyte-Derived Macrophages. *J. Immunol.* **184,** 4810–4818 (2010).
31. Fleischer, J. *et al.* Platelet Factor 4 Inhibits Proliferation and Cytokine Release of Activated Human T Cells. *J. Immunol.* **169,** 770–777 (2002).
32. Schwartzkopff, F., Petersen, F., Grimm, T. A. & Brandt, E. CXC chemokine ligand 4 (CXCL4) down-regulates CC chemokine receptor expression on human monocytes. *Innate Immun.* **18,** 124–39 (2012).
33. Gouwy, M. *et al.* CXCL4 and CXCL4L1 differentially affect monocyte survival and dendritic cell differentiation and phagocytosis. *PLoS One* **11,** (2016).
34. Woller, G., Brandt, E., Mittelstädt, J., Rybakowski, C. & Petersen, F. Platelet factor 4/CXCL4-stimulated human monocytes induce apoptosis in endothelial cells by the release of oxygen radicals. *J. Leukoc. Biol.* **83,** 936–45 (2008).
35. Gleissner, C. A., Shaked, I., Erbel, C., Böckler, D. & Katus, H. A. CXCL4 downregulates the Atheroprotective Hemoglobin Receptor CD163 in Human Macrophages. **106,** 203–211 (2011).
36. Romagnani, P. *et al.* CXCR3-mediated opposite effects of CXCL10 and CXCL4 on TH1 or TH2 cytokine production. *J. Allergy Clin. Immunol.* **116,** 1372–1379 (2005).
37. Mueller, A. *et al.* CXCL4-induced migration of activated T lymphocytes is mediated by the chemokine receptor CXCR3. *J. Leukoc. Biol.* **83,** 875–882 (2008).
38. Pervushina, O. *et al.* Platelet Factor 4/CXCL4 Induces Phagocytosis and the Generation of Reactive Oxygen Metabolites in Mononuclear Phagocytes Independently of Gi Protein Activation or Intracellular Calcium Transients. *J. Immunol.* **173,** 2060–2067 (2004).
39. Kasper, B., Brandt, E., Brandau, S. & Petersen, F. Platelet factor 4 (CXC chemokine ligand 4) differentially regulates respiratory burst, survival, and cytokine expression of human monocytes by using distinct signaling pathways. *J. Immunol.* **179,** 2584–91 (2007).
40. Fox, J. M. *et al.* CXCL4/Platelet Factor 4 is an agonist of CCR1 and drives human monocyte migration. *Sci. Rep.* **8,** (2018).
41. Liu, C. Y. *et al.* Platelet factor 4 differentially modulates CD4+CD25+ (regulatory) versus CD4+CD25- (nonregulatory) T cells. *J. Immunol.* **174,** 2680–2686 (2005).

42. Zlotnik, A., Yoshie, O. & Nomiyama, H. The chemokine and chemokine receptor superfamilies and their molecular evolution. *Genome Biology* **7,** (2006).
43. Petersen, F., Brandt, E., Lindahl, U. & Spillmann, D. Characterization of a neutrophil cell surface glycosaminoglycan that mediates binding of platelet factor 4. *J. Biol. Chem.* **274,** 12376–12382 (1999).
44. Loscalzo, J., Melnick, B. & Handin, R. I. The interaction of platelet factor four and glycosaminoglycans. *Arch. Biochem. Biophys.* **240,** 446–455 (1985).
45. Sachais, B. S., Higazi, A. A. R., Cines, D. B., Poncz, M. & Kowalska, M. A. Interactions of platelet factor 4 with the vessel wall. *Seminars in Thrombosis and Hemostasis* **30,** 351–358 (2004).
46. Handin, R. I. & Cohen, H. J. Purification and binding properties of human platelet factor 4. *J. Biol. Chem.* **251,** 4273–4282 (1976).
47. Lasagni, L. *et al.* An alternatively spliced variant of CXCR3 mediates the inhibition of endothelial cell growth induced by IP-10, Mig, and I-TAC, and acts as functional receptor for platelet factor 4. *J. Exp. Med.* **197,** 1537–49 (2003).
48. Cervi, D. *et al.* Platelet-associated PF-4 as a biomarker of early tumor growth. *Blood* **111,** 1201–1207 (2007).
49. Vrij, A. A., Rijken, J. & Van Wersch, J W Stockbrügger, R. W. Platelet factor and beta-thromboglobulin in inflammatory bowel disease and giant cell arteritis. *Eur. J. Clin. Invest.* **30,** 188–194 (2000).
50. Meuwis, M. A. *et al.* Biomarker discovery for inflammatory bowel disease, using proteomic serum profiling. *Biochem. Pharmacol.* **73,** 1422–1433 (2007).
51. Visentin, G. P., Ford, S. E., Scott, J. P. & Aster, R. H. Antibodies from patients with heparin-induced thrombocytopenia/thrombosis are specific for platelet factor 4 complexed with heparin or bound to endothelial cells. *J. Clin. Invest.* **93,** 81–88 (1994).
52. Yeo, L. *et al.* Expression of chemokines CXCL4 and CXCL7 by synovial macrophages defines an early stage of rheumatoid arthritis. *Ann. Rheum. Dis.* **75,** 763–71 (2016).
53. Patsouras, M. D. *et al.* Elevated expression of platelet-derived chemokines in patients with antiphospholipid syndrome. *J. Autoimmun.* **65,** 30–7 (2015).
54. Vettori, S. *et al.* Serum CXCL4 increase in primary Sjögren ' s syndrome characterizes patients with microvascular involvement and reduced salivary gland infiltration and lymph node involvement. *Clin. Rheumatol.* **35,** 2591–2596 (2016).
55. Schwartzkopff, F. *et al.* Platelet factor 4 (CXCL4) facilitates human macrophage infection with HIV-1 and potentiates virus replication. *Innate Immun.* **15,** 368–379 (2009).
56. Srivastava, K. *et al.* Platelet factor 4 mediates inflammation in experimental cerebral malaria. *Cell Host Microbe* **4,** 179–187 (2008).
57. Lande, R. *et al.* CXCL4 assembles DNA into liquid crystalline complexes to amplify TLR9-mediated interferon-α production in systemic sclerosis. *Nat. Commun.* **10,** (2019).
58. Volkmann, E. R. *et al.* Changes in plasma CXCL4 levels are associated with improvements in lung function in patients receiving immunosuppressive therapy for systemic sclerosis-related interstitial lung disease. *Arthritis Res. Ther.* **18,** (2016).
59. Ramirez, G. a *et al.* The role of platelets in the pathogenesis of systemic sclerosis. *Front. Immunol.* **3,** 160 (2012).
60. Postlethwaite, A. E. & Chiang, T. M. Platelet contributions to the pathogenesis of systemic sclerosis. *Current Opinion in Rheumatology* **19,** 574–579 (2007).
61. Baraut, J., Michel, L., Verrecchia, F. & Farge, D. Relationship between cytokine profiles and clinical outcomes in patients with systemic sclerosis. *Autoimmunity Reviews* **10,** 65–73 (2010).
62. Varga, J. & Pasche, B. Transforming growth factor β as a therapeutic target in systemic sclerosis. *Nat. Rev. Rheumatol.* **5,** 200–206 (2009).
63. Komura, K. *et al.* Increased serum interleukin 23 in patients with systemic sclerosis. *J. Rheumatol.* **35,** 120–125 (2008).

64. Kurasawa, K. *et al.* Increased interleukin-17 production in patients with systemic sclerosis. *Arthritis Rheum.* **43,** 2455–2463 (2000).
65. Sato, S. *et al.* Levels of interleukin 12, a cytokine of type 1 helper T cells, are elevated in sera from patients with systemic sclerosis. *J. Rheumatol.* **27,** 2838–2842 (2000).
66. Yoshizaki, A. *et al.* Elevated serum interleukin-27 levels in patients with systemic sclerosis: Association with T cell, B cell and fibroblast activation. *Ann. Rheum. Dis.* **70,** 194–200 (2011).
67. Nakayama, W. *et al.* Dysregulated interleukin-23 signalling contributes to the increased collagen production in scleroderma fibroblasts via balancing microRNA expression. *Rheumatology (Oxford).* **56,** 145–155 (2017).
68. Yousif, M., Habib, R., Esaely, H., Yasin, R. & Sonbol, A. Interleukin-6 in systemic sclerosis and potential correlation with pulmonary involvement. *Egypt. J. Chest Dis. Tuberc.* **64,** 237–241 (2014).
69. Varga, J., Rosenbloom, J. & Jimenez, S. A. Transforming growth factor β (TGF β) causes a persistent increase in steady-state amounts of type I and type III collagen and fibronectin mRNAs in normal human dermal fibroblasts . *Biochem. J.* **247,** 597–604 (2015).
70. Gabrielli, A., Avvedimento, E. V. & Krieg, T. Scleroderma. *N. Engl. J. Med.* **360,** 1989–2003 (2009).
71. Varga, J. & Abraham, D. Systemic sclerosis: A prototypic multisystem fibrotic disorder. *Journal of Clinical Investigation* **117,** 557–567 (2007).
72. Pattanaik, D., Brown, M., Postlethwaite, B. C. & Postlethwaite, A. E. Pathogenesis of Systemic Sclerosis. *Front. Immunol.* **6,** 755–759 (2015).
73. MacDonald, K. P. A. *et al.* Characterization of human blood dendritic cell subsets. *Blood* **100,** 4512–20 (2002).
74. Banchereau, J. & Steinman, R. M. Dendritic cells and the control of immunity. *Nature* **392,** 245–252 (1998).
75. Steinman, R. M. Decisions about dendritic cells: past, present, and future. *Annu. Rev. Immunol.* **30,** 1–22 (2012).
76. Shortman, K. & Naik, S. H. Steady-state and inflammatory dendritic-cell development. *Nature Reviews Immunology* **7,** 19–30 (2007).
77. Liu, Y.-J. IPC: Professional Type 1 Interferon-Producing Cells and Plasmacytoid Dendritic Cell Precursors. *Annu. Rev. Immunol.* **23,** 275–306 (2005).
78. Colonna, M., Trinchieri, G. & Liu, Y.-J. Plasmacytoid dendritic cells in immunity. *Nat. Immunol.* **5,** 1219–26 (2004).
79. Villadangos, J. A. & Young, L. Antigen-Presentation Properties of Plasmacytoid Dendritic Cells. *Immunity* **29,** 352–361 (2008).
80. Hémont, C., Neel, A., Heslan, M., Braudeau, C. & Josien, R. Human blood mDC subsets exhibit distinct TLR repertoire and responsiveness. *J. Leukoc. Biol.* **93,** 599–609 (2013).
81. Jongbloed, S. L. *et al.* Human CD141+ (BDCA-3)+ dendritic cells (DCs) represent a unique myeloid DC subset that cross-presents necrotic cell antigens. *J. Exp. Med.* **207,** 1247–60 (2010).
82. Mittag, D. *et al.* Human Dendritic Cell Subsets from Spleen and Blood Are Similar in Phenotype and Function but Modified by Donor Health Status. *J. Immunol.* **186,** 6207–6217 (2011).
83. Haniffa, M. *et al.* Human Tissues Contain CD141 hi Cross-Presenting Dendritic Cells with Functional Homology to Mouse CD103 + Nonlymphoid Dendritic Cells. *Immunity* **37,** 60–73 (2012).
84. Huysamen, C., Willment, J. A., Dennehy, K. M. & Brown, G. D. CLEC9A is a novel activation C-type lectin-like receptor expressed on BDCA3+ dendritic cells and a subset of monocytes. *J. Biol. Chem.* **283,** 16693–16701 (2008).

85. Bachem, A. *et al.* Superior antigen cross-presentation and XCR1 expression define human CD11c+CD141+ cells as homologues of mouse CD8+ dendritic cells. *J. Exp. Med* **207,** 1273–1281 (2010).
86. Schreibelt, G. *et al.* The C-type lectin receptor CLEC9A mediates antigen uptake and (cross-)presentation by human blood BDCA3+ myeloid dendritic cells. *Blood* **119,** 2284–2292 (2012).
87. Poulin, L. F. *et al.* Characterization of human DNGR-1 + BDCA3 + leukocytes as putative equivalents of mouse CD8α + dendritic cells . *J. Exp. Med.* **207,** 1261–1271 (2010).
88. Sallusto, F. & Lanzavecchia, A. Efficient presentation of soluble antigen by cultured human dendritic cells is maintained by granulocyte/macrophage colony-stimulating factor plus interleukin 4 and downregulated by tumor necrosis factor alpha. *J. Exp. Med.* **179,** 1109–18 (1994).
89. Romani, N. Proliferating dendritic cell progenitors in human blood. *J. Exp. Med.* **180,** 83–93 (1994).
90. Watchmaker, P. B. *et al.* Comparative transcriptional and functional profiling defines conserved programs of intestinal DC differentiation in humans and mice. *Nat. Immunol.* **15,** 98–108 (2014).
91. de Jong, E. C. *et al.* Microbial compounds selectively induce Th1 cell-promoting or Th2 cell-promoting dendritic cells in vitro with diverse th cell-polarizing signals. *J. Immunol.* **168,** 1704–9 (2002).
92. Segura, E. *et al.* Human Inflammatory Dendritic Cells Induce Th17 Cell Differentiation. *Immunity* **38,** 336–348 (2013).
93. Inaba, K. Dendritic cell progenitors phagocytose particulates, including bacillus Calmette-Guerin organisms, and sensitize mice to mycobacterial antigens in vivo. *J. Exp. Med.* **178,** 479–488 (2004).
94. Inaba, K., Metlay, J. P., Crowley, M. T. & Steinman, R. M. Dendritic cells pulsed with protein antigens in vitro can prime antigen-specific, MHC-restricted T cells in situ. *J. Exp. Med.* **172,** 631–40 (1990).
95. Dhodapkar, M. V. *et al.* Rapid generation of broad T-cell immunity in humans after a single injection of mature dendritic cells. *J. Clin. Invest.* **104,** 173–180 (1999).
96. Dhodapkar, M. V., Krasovsky, J., Steinman, R. M. & Bhardwaj, N. Mature dendritic cells boost functionally superior CD8+ T-cell in humans without foreign helper epitopes. *J. Clin. Invest.* **105,** (2000).
97. Guttman-Yassky, E. *et al.* Major differences in inflammatory dendritic cells and their products distinguish atopic dermatitis from psoriasis. *J. Allergy Clin. Immunol.* **119,** 1210–1217 (2007).
98. Domínguez, P. M. & Ardavín, C. Differentiation and function of mouse monocyte-derived dendritic cells in steady state and inflammation. *Immunological Reviews* **234,** 90–104 (2010).
99. Fei, M. *et al.* TNF- from inflammatory dendritic cells (DCs) regulates lung IL-17A/IL-5 levels and neutrophilia versus eosinophilia during persistent fungal infection. *Proc. Natl. Acad. Sci.* **108,** 5360–5365 (2011).
100. Kawai, T. & Akira, S. The role of pattern-recognition receptors in innate immunity: Update on toll-like receptors. *Nature Immunology* **11,** 373–384 (2010).
101. Kawai, T. & Akira, S. Toll-like Receptors and Their Crosstalk with Other Innate Receptors in Infection and Immunity. *Immunity* **34,** 637–650 (2011).
102. Joffre, O., Nolte, M. A., Spörri, R. & Sousa, C. R. E. Inflammatory signals in dendritic cell activation and the induction of adaptive immunity. *Immunological Reviews* **227,** 234–247 (2009).
103. Hubo, M. *et al.* Costimulatory molecules on immunogenic versus tolerogenic human dendritic cells. *Front. Immunol.* **4,** (2013).
104. Gordon, J. R., Ma, Y., Churchman, L., Gordon, S. A. & Dawicki, W. Regulatory dendritic cells for immunotherapy in immunologic diseases. *Frontiers in Immunology* **5,** (2014).
105. Ganguly, D., Haak, S., Sisirak, V. & Reizis, B. The role of dendritic cells in autoimmunity. *Nature Reviews Immunology* **13,** 566–577 (2013).

106. Drexler, S. K. & Foxwell, B. M. The role of toll-like receptors in chronic inflammation. *Int. J. Biochem. Cell Biol.* **42,** 506–18 (2010).
107. Jongbloed, S. L. *et al.* Enumeration and phenotypical analysis of distinct dendritic cell subsets in psoriatic arthritis and rheumatoid arthritis. *Arthritis Res. Ther.* **8,** (2005).
108. Affandi, A. J., Carvalheiro, T., Radstake, T. R. D. J. & Marut, W. Dendritic cells in systemic sclerosis: Advances from human and mice studies. *Immunology Letters* **195,** 18–29 (2018).
109. O'Reilly, S. Pound the alarm: danger signals in rheumatic diseases. *Clin. Sci.* **128,** 297–305 (2014).
110. Ciechomska, M., Cant, R., Finnigan, J., van Laar, J. M. & O'Reilly, S. Role of toll-like receptors in systemic sclerosis. *Expert Rev. Mol. Med.* **15,** e9 (2013).
111. O'Reilly, S. Toll Like Receptors in systemic sclerosis: An emerging target. *Immunology Letters* **195,** 2–8 (2018).
112. Rossato, M. *et al.* Association of MicroRNA-618 Expression With Altered Frequency and Activation of Plasmacytoid Dendritic Cells in Patients With Systemic Sclerosis. *Arthritis Rheumatol.* **69,** 1891–1902 (2017).
113. Broen, J. C. a *et al.* A rare polymorphism in the gene for Toll-like receptor 2 is associated with systemic sclerosis phenotype and increases the production of inflammatory mediators. *Arthritis Rheum.* **64,** 264–71 (2012).
114. van Bon, L. *et al.* Distinct evolution of TLR-mediated dendritic cell cytokine secretion in patients with limited and diffuse cutaneous systemic sclerosis. *Ann. Rheum. Dis.* **69,** 1539–47 (2010).
115. Farina, G. A. *et al.* Poly(I:C) drives type i IFN- and TGFB-mediated inflammation and dermal fibrosis simulating altered gene expression in systemic sclerosis. *J. Invest. Dermatol.* **130,** 2583–2593 (2010).
116. van Lieshout, A. W. *et al.* Enhanced interleukin-10 production by dendritic cells upon stimulation with Toll-like receptor 4 agonists in systemic sclerosis that is possibly implicated in CCL18 secretion. *Scand. J. Rheumatol.* **38,** 282–290 (2009).
117. Ciechomska, M. *et al.* Toll-like receptor-mediated, enhanced production of profibrotic TIMP-1 in monocytes from patients with systemic sclerosis: role of serum factors. *Ann Rheum Dis* **72,** 1382–1389 (2013).
118. van Bon, L. *et al.* Low heme oxygenase-1 levels in patients with systemic sclerosis are associated with an altered Toll-like receptor response: Another role for CXCL4? *Rheumatol. (United Kingdom)* **55,** 2066–2073 (2016).
119. Van Bon, L. *et al.* Proteomic analysis of plasma identifies the Toll-like receptor agonists S100A8/A9 as a novel possible marker for systemic sclerosis phenotype. *Ann. Rheum. Dis.* **73,** 1585–1589 (2014).
120. Bhattacharyya, S. & Varga, J. Endogenous ligands of TLR4 promote unresolving tissue fibrosis: Implications for systemic sclerosis and its targeted therapy. *Immunology Letters* **195,** 9–17 (2018).
121. O'Reilly, S. *et al.* Serum amyloid A induces interleukin-6 in dermal fibroblasts via Toll-like receptor 2, interleukin-1 receptor-associated kinase 4 and nuclear factor-κB. *Immunology* **143,** 331–340 (2014).
122. Stifano, G. *et al.* Chronic Toll-like receptor 4 stimulation in skin induces inflammation, macrophage activation, transforming growth factor beta signature gene expression, and fibrosis. *Arthritis Res. Ther.* **16,** (2014).
123. Bhattacharyya, S. *et al.* Toll-like receptor 4 signaling augments transforming growth factor-β responses: A novel mechanism for maintaining and amplifying fibrosis in scleroderma. *Am. J. Pathol.* **182,** 192–205 (2013).
124. Farina, G., York, M., Collins, C. & Lafyatis, R. dsRNA activation of endothelin-1 and markers of vascular activation in endothelial cells and fibroblasts. *Ann. Rheum. Dis.* **70,** 544–550 (2011).
125. Agarwal, S. K. *et al.* Toll-like receptor 3 upregulation by type I interferon in healthy and scleroderma dermal fibroblasts. *Arthritis Res. Ther.* **13,** R3 (2011).

126. Farina, G. a *et al.* Poly(I:C) drives type I IFN- and TGFβ-mediated inflammation and dermal fibrosis simulating altered gene expression in systemic sclerosis. *J. Invest. Dermatol.* **130,** 2583–93 (2010).
127. Ciechomska, M. *et al.* Histone Demethylation and Toll-like Receptor 8-Dependent Cross-Talk in Monocytes Promotes Transdifferentiation of Fibroblasts in Systemic Sclerosis Via Fra-2. *Arthritis Rheumatol.* **68,** 1493–1504 (2016).
128. O'Reilly, S., Hügle, T. & Van Laar, J. M. T cells in systemic sclerosis: A reappraisal. *Rheumatology (United Kingdom)* **51,** 1540–1549 (2012).
129. Parel, Y. *et al.* Presence of CD4+CD8+ double-positive T cells with very high interleukin-4 production potential in lesional skin of patients with systemic sclerosis. *Arthritis Rheum.* **56,** 3459–3467 (2007).
130. Li, G. *et al.* Skin-Resident Effector Memory CD8+CD28– T Cells Exhibit a Profibrotic Phenotype in Patients with Systemic Sclerosis. *J. Invest. Dermatol.* **137,** 1042–1050 (2017).
131. Fuschiotti, P., Larregina, A. T., Ho, J., Feghali-Bostwick, C. & Medsger, T. A. Interleukin-13-producing CD8+ T cells mediate dermal fibrosis in patients with systemic sclerosis. *Arthritis Rheum.* **65,** 236–246 (2013).
132. Mavalia, C. *et al.* Type 2 helper T-cell predominance and high CD30 expression in systemic sclerosis. *Am. J. Pathol.* **151,** 1751–8 (1997).
133. Yang, X., Yang, J., Xing, X., Wan, L. & Li, M. Increased frequency of Th17 cells in systemic sclerosis is related to disease activity and collagen overproduction. *Arthritis Res. Ther.* **16,** (2014).
134. Meredith, M. M. *et al.* Expression of the zinc finger transcription factor zDC (Zbtb46, Btbd4) defines the classical dendritic cell lineage. *J. Exp. Med.* **209,** 1153–1165 (2012).
135. Groux, H., Fournier, N. & Cottrez, F. Role of dendritic cells in the generation of regulatory T cells. *Semin. Immunol.* **16,** 99–106 (2004).
136. Birnberg, T. *et al.* Lack of Conventional Dendritic Cells Is Compatible with Normal Development and T Cell Homeostasis, but Causes Myeloid Proliferative Syndrome. *Immunity* **29,** 986–997 (2008).
137. Chen, M., Huang, L. & Wang, J. Deficiency of Bim in dendritic cells contributes to overactivation of lymphocytes and autoimmunity. *Blood* **109,** 4360–4367 (2007).
138. Steinman, R. M., Hawiger, D. & Nussenzweig, M. C. T <scp>OLEROGENIC</scp> D <scp>ENDRITIC</scp> C <scp>ELLS</scp>. *Annu. Rev. Immunol.* **21,** 685–711 (2003).
139. Lewis, K. L. & Reizis, B. Dendritic cells: Arbiters of immunity and immunological tolerance. *Cold Spring Harb. Perspect. Biol.* **4,** (2012).
140. Kaliński, P., Hilkens, C. M. U., Wierenga, E. A. & Kapsenberg, M. L. T-cell priming by type-1 and type-2 polarized dendritic cells: The concept of a third signal. *Immunology Today* **20,** 561–567 (1999).
141. Caux, C. *et al.* Dendritic cell biology and regulation of dendritic cell trafficking by chemokines. *Springer Seminars in Immunopathology* **22,** 345–369 (2000).
142. Saeki, H., Moore, A. M., Brown, M. J. & Hwang, S. T. Cutting edge: secondary lymphoid-tissue chemokine (SLC) and CC chemokine receptor 7 (CCR7) participate in the emigration pathway of mature dendritic cells from the skin to regional lymph nodes. *J. Immunol.* **162,** 2472–5 (1999).
143. Ghiringhelli, F. *et al.* Tumor cells convert immature myeloid dendritic cells into TGF-β–secreting cells inducing CD4 + CD25 + regulatory T cell proliferation . *J. Exp. Med.* **202,** 919–929 (2005).
144. Fujita, S. *et al.* Regulatory dendritic cells protect against cutaneous chronic graft-versus-host disease mediated through CD4+CD25 +Foxp3+ regulatory T cells. *Blood* **110,** 3793–3803 (2007).
145. Puccetti, P. & Grohmann, U. IDO and regulatory T cells: A role for reverse signalling and non-canonical NF-κB activation. *Nature Reviews Immunology* **7,** 817–823 (2007).

146. Belladonna, M. L. *et al.* Cutting edge: Autocrine TGF-beta sustains default tolerogenesis by IDO-competent dendritic cells. *J. Immunol.* **181,** 5194–8 (2008).
147. Matteoli, G. *et al.* Gut CD103+ dendritic cells express indoleamine 2,3-dioxygenase which influences T regulatory/T effector cell balance and oral tolerance induction. *Gut* **59,** 595–604 (2010).
148. Torres-Aguilar, H., Sánchez-Torres, C., Jara, L. J., Blank, M. & Shoenfeld, Y. IL-10/TGF-β-treated dendritic cells, pulsed with insulin, specifically reduce the response to insulin of CD4+ effector/memory T cells from type 1 diabetic individuals. *J. Clin. Immunol.* **30,** 659–668 (2010).
149. Boks, M. A. *et al.* IL-10-generated tolerogenic dendritic cells are optimal for functional regulatory T cell induction - A comparative study of human clinical-applicable DC. *Clin. Immunol.* **142,** 332–342 (2012).
150. Bosma, B. M. *et al.* Dexamethasone transforms lipopolysaccharide-stimulated human blood myeloid dendritic cells into myeloid dendritic cells that prime interleukin-10 production in T cells. *Immunology* **125,** 91–100 (2008).
151. Schinnerling, K., García-González, P. & Aguillón, J. C. Gene expression profiling of human monocyte-derived dendritic cells - Searching for molecular regulators of tolerogenicity. *Frontiers in Immunology* **6,** (2015).
152. Torres-Aguilar, H. *et al.* Tolerogenic Dendritic Cells Generated with Different Immunosuppressive Cytokines Induce Antigen-Specific Anergy and Regulatory Properties in Memory CD4 + T Cells. *J. Immunol.* **184,** 1765–1775 (2010).
153. Perrier, P. *et al.* Distinct transcriptional programs activated by interleukin-10 with or without lipopolysaccharide in dendritic cells: induction of the B cell-activating chemokine, CXC chemokine ligand 13. *J. Immunol.* **172,** 7031–42 (2004).
154. Zimmer, A. *et al.* A regulatory dendritic cell signature correlates with the clinical efficacy of allergen-specific sublingual immunotherapy. *J. Allergy Clin. Immunol.* **129,** 1020–1030 (2012).
155. Ferreira, G. B. *et al.* Proteome analysis demonstrates profound alterations in human dendritic cell nature by TX527, an analogue of vitamin D. *Proteomics* **9,** 3752–3764 (2009).
156. Ferreira, G. B. *et al.* Vitamin D3 induces tolerance in human dendritic cells by activation of intracellular metabolic pathways. *Cell Rep.* **10,** 711–725 (2015).
157. Malinarich, F. *et al.* High Mitochondrial Respiration and Glycolytic Capacity Represent a Metabolic Phenotype of Human Tolerogenic Dendritic Cells. *J. Immunol.* **194,** 5174–5186 (2015).
158. Ferreira, G. B. *et al.* Differential protein pathways in 1,25-dihydroxyvitamin D 3 and dexamethasone modulated tolerogenic human dendritic cells. *J. Proteome Res.* **11,** 941–971 (2012).
159. Banchereau, J. & Palucka, A. K. Dendritic cells as therapeutic vaccines against cancer. *Nature Reviews Immunology* **5,** 296–306 (2005).
160. Kalinski, P., Wieckowski, E., Muthuswamy, R. & de Jong, E. in 117–133 (2009). doi:10.1007/978-1-60761-421-0_7
161. Hilkens, C. M. U. & Isaacs, J. D. Tolerogenic dendritic cell therapy for rheumatoid arthritis: Where are we now? *Clin. Exp. Immunol.* **172,** 148–157 (2013).
162. Thomas, R. Dendritic cells as targets or therapeutics in rheumatic autoimmune disease. *Current Opinion in Rheumatology* **26,** 211–218 (2014).
163. Ramsey, S. A. *et al.* Uncovering a macrophage transcriptional program by integrating evidence from motif scanning and expression dynamics. *PLoS Comput. Biol.* **4,** (2008).
164. Ravasi, T., Wells, C. A. & Hume, D. A. Systems biology of transcription control in macrophages. *BioEssays* **29,** 1215–1226 (2007).
165. Medzhitov, R. TLRs & innate immunity. *Nat. Rev. Immunol.* (2001).

166. Smale, S. T. Selective Transcription in Response to an Inflammatory Stimulus. *Cell* **140,** 833–844 (2010).
167. Barreau, C., Paillard, L. & Osborne, H. B. AU-rich elements and associated factors: Are there unifying principles? *Nucleic Acids Research* **33,** 7138–7150 (2005).
168. Stoecklin, G. & Anderson, P. In a tight spot: ARE-mRNAs at processing bodies. *Genes and Development* **21,** 627–631 (2007).
169. Carpenter, S., Ricci, E. P., Mercier, B. C., Moore, M. J. & Fitzgerald, K. A. Post-transcriptional regulation of gene expression in innate immunity. *Nature Reviews Immunology* **14,** 361–376 (2014).
170. Brooks, S. A., Connolly, J. E., Diegel, R. J., Fava, R. A. & Rigby, W. F. C. Analysis of the function, expression, and subcellular distribution of human tristetraprolin. *Arthritis Rheum.* **46,** 1362–1370 (2002).
171. Huang, L. *et al.* Interaction with Pyruvate Kinase M2 Destabilizes Tristetraprolin by Proteasome Degradation and Regulates Cell Proliferation in Breast Cancer. *Sci. Rep.* **6,** (2016).
172. Khabar, K. S. A. Post-transcriptional control during chronic inflammation and cancer: A focus on AU-rich elements. *Cellular and Molecular Life Sciences* **67,** 2937–2955 (2010).
173. Seko, Y., Cole, S., Kasprzak, W., Shapiro, B. A. & Ragheb, J. A. The role of cytokine mRNA stability in the pathogenesis of autoimmune disease. *Autoimmunity Reviews* **5,** 299–305 (2006).
174. Zhang, H. *et al.* MRNA-binding protein ZFP36 is expressed in atherosclerotic lesions and reduces inflammation in aortic endothelial cells. *Arterioscler. Thromb. Vasc. Biol.* **33,** 1212–1220 (2013).
175. Newell-Price, J., Clark, A. J. L. & King, P. DNA methylation and silencing of gene expression. *Trends in Endocrinology and Metabolism* **11,** 142–148 (2000).
176. Li, E., Beard, C. & Jaenisch, R. Role for DNA methylation in genomic imprinting. *Trends Genet.* **10,** 78 (2003).
177. Bierne, H., Hamon, M. & Cossart, P. Epigenetics and bacterial infections. *Cold Spring Harb. Perspect. Med.* **2,** (2012).
178. Pacis, A. *et al.* Bacterial infection remodels the DNA methylation landscape of human dendritic cells. *Genome Res.* **25,** 1801–1811 (2015).
179. Yong, W. S., Hsu, F. M. & Chen, P. Y. Profiling genome-wide DNA methylation. *Epigenetics and Chromatin* **9,** (2016).
180. Smith, Z. D. & Meissner, A. DNA methylation: roles in mammalian development. *Nat. Rev. Genet.* **14,** 204–20 (2013).
181. Berkyurek, A. C. *et al.* The DNA methyltransferase Dnmt1 directly interacts with the SET and RING finger-associated (SRA) domain of the multifunctional protein Uhrf1 to facilitate accession of the catalytic center to hemi-methylated DNA. *J. Biol. Chem.* **289,** 379–386 (2014).
182. Okano, M., Bell, D. W., Haber, D. A. & Li, E. DNA methyltransferases Dnmt3a and Dnmt3b are essential for de novo methylation and mammalian development. *Cell* **99,** 247–257 (1999).
183. Ramsahoye, B. H. *et al.* Non-CpG methylation is prevalent in embryonic stem cells and may be mediated by DNA methyltransferase 3a. *Proc. Natl. Acad. Sci. U. S. A.* **97,** 5237–42 (2000).
184. Ziller, M. J. *et al.* Genomic distribution and Inter-Sample variation of Non-CpG methylation across human cell types. *PLoS Genet.* **7,** (2011).
185. Jones, P. A. Functions of DNA methylation: Islands, start sites, gene bodies and beyond. *Nature Reviews Genetics* **13,** 484–492 (2012).
186. Klug, M. *et al.* Active DNA demethylation in human postmitotic cells correlates with activating histone modifications, but not transcription levels. *Genome Biol.* **11,** (2010).
187. Dowen, R. H. *et al.* Widespread dynamic DNA methylation in response to biotic stress. *Proc. Natl. Acad. Sci. U. S. A.* **109,** E2183-91 (2012).
188. Marr, A. K. *et al.* Leishmania donovani Infection Causes Distinct Epigenetic DNA Methylation Changes in Host Macrophages. *PLoS Pathog.* **10,** (2014).

189. Wang, X. *et al.* A DNA-Methylated Sight on Autoimmune Inflammation Network across RA, pSS, and SLE. *J. Immunol. Res.* **2018,** 1–13 (2018).
190. Kulis, M. & Esteller, M. in *Epigenetics and Cancer, Part A* **70,** 27–56 (2010).
191. Moarii, M., Boeva, V., Vert, J. P. & Reyal, F. Changes in correlation between promoter methylation and gene expression in cancer. *BMC Genomics* **16,** (2015).
192. Tsai, H. C. *et al.* Transient Low Doses of DNA-Demethylating Agents Exert Durable Antitumor Effects on Hematological and Epithelial Tumor Cells. *Cancer Cell* **21,** 430–446 (2012).
193. Sobolewski, C., Sanduja, S., Blanco, F. F., Hu, L. & Dixon, D. A. Histone deacetylase inhibitors activate tristetraprolin expression through induction of early growth response protein 1 (EGR1) in colorectal cancer cells. *Biomolecules* **5,** 2035–2055 (2015).
194. Griffiths, E. A. & Gore, S. D. Epigenetic therapies in MDS and AML. *Adv. Exp. Med. Biol.* **754,** 253–283 (2013).
195. Joosten, L. A. B., Leoni, F., Meghji, S. & Mascagni, P. Inhibition of HDAC Activity by ITF2357 Ameliorates Joint Inflammation and Prevents Cartilage and Bone Destruction in Experimental Arthritis. *Mol. Med.* **17,** 391–396 (2011).

1

Chapter 2

CXCL4 exposure potentiates TLR-driven polarization of human monocyte-derived dendritic cells and increases stimulation of T cells

Sandra C. Silva-Cardoso[*†], Alsya J. Affandi[*†], Lotte Spel[*‡], Marta Cossu[*†], Joel A.G. van Roon[*†], Marianne Boes[*‡1], Timothy R.D.J. Radstake[*†1]

[*] Laboratory of Translational Immunology, University Medical Center Utrecht, the Netherlands

[†] Department of Rheumatology & Clinical Immunology, University Medical Center Utrecht, the Netherlands

[‡] Department of Pediatrics, University Medical Center Utrecht, the Netherlands

[1] M.B. and T.R.D.J.R. contributed equally to this work

J Immunol 2017;199:253–262 doi: 10.4049/jimmunol.1602020

Abstract

Chemokines have been shown to play immune-modulatory functions unrelated to steering cell migration. CXCL4 is a chemokine abundantly produced by activated platelets and immune cells. Increased levels of circulating CXCL4 are associated with immune-mediated conditions, including systemic sclerosis. Considering the central role of dendritic cells (DCs) in immune activation, in this article we addressed the effect of CXCL4 on the phenotype and function of monocyte-derived DCs (moDCs). To this end, we compared innate and adaptive immune responses of moDCs with those that were differentiated in the presence of CXCL4. Already prior to TLR- or Ag-specific stimulation, CXCL4-moDCs displayed a more matured phenotype. We found that CXCL4 exposure can sensitize moDCs for TLR-ligand responsiveness, as illustrated by a dramatic upregulation of CD83, CD86, and MHC class I in response to TLR3 and TLR7/8-agonists. Also, we observed a markedly increased secretion of IL-12 and TNF-α by CXCL4-moDCs exclusively upon stimulation with polyinosinic-polycytidylic acid, R848, and CL075 ligands. Next, we analyzed the effect of CXCL4 in modulating DC-mediated T cell activation. CXCL4-moDCs strongly potentiated proliferation of autologous $CD4^+$ T cells and $CD8^+$ T cells and production of IFN-γ and IL-4, in an Ag-independent manner. Although the internalization of Ag was comparable to that of moDCs, Ag processing by CXCL4-moDCs was impaired. Yet, these cells were more potent at stimulating Ag-specific $CD8^+$ T cell responses. Together our data support that increased levels of circulating CXCL4 may contribute to immune dysregulation through the modulation of DC differentiation.

Abbreviations used in this article: CL075, thiazoloquinoline; CTV, CellTrace Violet; DC, dendritic cell; HV, healthy volunteer; MFI, median fluorescence intensity; MHC-I, MHC class I; moDC, monocyte-derived DC; O/N, overnight; PAMP, pathogen-associated molecular pattern; poly(I:C), polyinosinic-polycytidylic acid; R848, resiquimod; SSc, systemic sclerosis.

Introduction

Stored in α-granules of platelets and released upon platelet activation, CXCL4 is a 7.8 kDa chemokine[1,2]. CXCL4 is also produced and released by various immune cells including mast cells[3], dendritic cells (DCs)[4,5], monocytes[6] and activated T-cells[7]. It has been described that CXCL4 plays a role in several physiological processes[8–10]. However, increased levels of CXCL4 have been implicated in pathological conditions such as cancer[11] and infectious[12,13] and inflammatory diseases[14–19]. Indeed, a strong correlation was found between elevated CXCL4 levels in the circulation and the clinical features of patients with systemic sclerosis (SSc)[5]. Monocytes and professional APCs are essential players in both innate defense and in the initiation of adaptive immune responses, thereby contributing to both immune activation and the maintenance of immune peripheral tolerance[20,21]. Accordingly, upon detection of pathogen (PAMPs) or danger-associated molecular patterns, DCs undergo further maturation into potent APCs now able to prime and induce the clonal expansion of antigen (Ag)-specific T-cells[22].

The imbalance of homeostasis because of the presence of inflammatory mediators such as CXCL4 lead to the modulation of phenotype and function of immune cells[23–32]. In monocytes, for instance, CXCL4 not only functions as a chemoattractant mediator but also promotes survival the production of TNF-α, release of reactive oxygen species (ROS) and differentiation into macrophage-like phenotype cells[26,31,33]. Gleissner et al.[34] found that the exposure of monocytes-derived macrophages to CXCL4 induces unique transcriptomic changes, in comparison with M1 and M2 macrophages, and named these M4 macrophages. Genes involved in inflammatory responses, Ag presentation and lipid metabolism were overexpressed in M4 macrophages. In addition, monocytes exposed to CXCL4 and IL-4 alone or in the presence of GM-CSF for 6 d were shown to result in a functionally distinct APC[24,25,31].

To date, it is not clear how CXCL4 might affect DC function, and thus influence innate and adaptive immune responses. In this study, we hypothesized that CXCL4 may modulate the phenotype and potentiate the innate function of DCs, as triggered by recognition of danger-associated molecular patterns and PAMPs. Such recognition occurs via germline-encoded immune receptors including TLRs, which represent the frontline of innate defense. Indeed, dysfunction of TLR-mediated responses has been associated with immune and nonimmune cell reprograming[35,36] and several autoimmune diseases such as atherosclerosis[37], rheumatoid arthritis (RA)[38], psoriasis[39] and SSc[40–45]. Notably, CXCL4 has been described as being involved in the same set of diseases[5,14,17,19].

We found that CXCL4 reprograms monocytes as they differentiate into DCs, imprinting a more mature phenotype and an augmented responsiveness to TLR ligands: CXCL4-moDCs showed a dramatic increase in IL-12 and TNF-α production

upon stimulation with TLR3, TLR7/8 and TLR8 ligands. Moreover, CXCL4-moDCs were more potent at inducing the proliferation of polyclonal $CD4^+$ T and $CD8^+$ T cells and cytokine production. Finally, Ag processing was impaired in CXCL4-moDCs, as they exhibited a superior ability to cross-present endocytosed Ags to HCMV-specific $CD8^+$ T-cells. Altogether, here we reveal novel functions of CXCL4 both in innate as well as adaptive immune responses.

Materials and Methods

Monocyte isolation

Blood from healthy volunteers (HV) was obtained following institutional ethical approval. PBMCs were isolated from heparinized venous blood by density-gradient centrifugation over Ficoll Paque Plus (GE Healthcare). Fresh monocytes were isolated by Ab-based positive separation according to the manufacturer's protocol, using anti-CD14 magnetic beads and auto-MACS assisted cell sorting (Miltenyi Biotec). Purity of isolated monocytes was > 95% for all the independent samples. Negative fractions following monocyte isolation consisting of PBLs were cryopreserved in FCS containing 20% (v/v) DMSO and thawed after 6 d to be used for $CD3^+$ T-cell isolation and autologous co-culture experiments.

MoDC differentiation

Monocytes were cultured at a density of 1 x 10^6 cells/ml using complete medium: RPMI 1640 with GlutaMAX (Life Technologies), supplemented with 10% (v/v) heat-inactivated FCS (Biowest) and 1% (v/v) antibiotics (penicillin and streptomycin) (both from Life Technologies). To generate moDCs, recombinant human IL-4 (500 U/ml; R&D Systems**)** and GM-CSF (800 U/ml; R&D Systems) were added to the medium, in the presence or absence of recombinant human CXCL4 (10 µg/ml; PeproTech). The MoDCs were differentiated for 6 d at 37°C in the presence of 5% CO_2. At day 3, medium supplemented with the same concentration of IL-4, GM-CSF and CXCL4 was added.

Confocal microscopy

Nunc Lab-Tek II chamber slides (Thermo Scientific) were pre-coated with 1% (w/v) Alcian blue 8GX (Klinipath) in PBS for 30 min at 37°C, washed with PBS and air-dried inside culture hood prior to moDC differentiation culture (as described in the *MoDC differentiation* section). On day 6, the chamber slide was spun for 2 min at 500 x g. Next, 75% of the culture medium was removed, and cells were incubated with 500 µl of the Fixation/Permeabilization solution (eBioscience) for 30 min at room temperature (RT). Fixed cells were washed twice with Permeabilization buffer

(eBioscience) and incubated with phalloidin-labeled FITC (0.5 mg/ml; ENZO) and Hoechst 33342 (1 µM; Invitrogen) in Permeabilization buffer for 30 min in dark (RT). Afterwards, cells were washed once with Permeabilization buffer and the last wash with 1% (w/v) BSA and 0.1% (v/v) sodium azide (NaN_3; Sigma-Aldrich) in cold PBS (designated here as FACS buffer). At last, chambers were removed and dried slides were mounted in Mowiol (Sigma-Aldrich) and coverslipped. Slides were left at 4°C (O/N) until the measurement. Acquisition of imaging data was performed on a Zen2009 LSM 710 (Zeiss) confocal microscope. To determine the cell area and perimeter, confocal images were obtained with the x63 1.40 oil objective and analyzed using ImageJ software.

TLR stimulation

A total of 50 x 10^3 immature moDCs (day 6 of differentiation) were plated in a 96-well flat-bottom plate (Thermo Scientific) in medium (0.5 x 10^6 moDCs/ml) and rested O/N. Next, cells were left unstimulated or stimulated for 24 h at 37°C with the following TLR ligands: Pam3CSK4 (5 µg/ml), polyinosinic-polycytidylic acid [poly(I:C); 25 µg/ml], LPS (100 µg/ml), flagellin (2 µg/ml), resiquimod (R848; 1 µg/ml), loxoribine (500 µM), imiquimod (R837; 3 µg/ml), thiazoloquinoline (CL075; 0.3 µg/ml), and CpG-B (ODN684; 5 µM), all purchased from InvivoGen. Surface expression of maturation markers and MHC molecules on moDCs after TLR stimulation was measured by flow cytometry. Cell-free supernatants were stored at -20°C for measurement of cytokine levels by Luminex technology, as described before [46] at the MultiPlex Core Facility of the Laboratory of Translational Immunology, University Medical Center of Utrecht.

Stimulation of polyclonal T-cells

One day prior to moDC coculture with polyclonal T cells, 50 µl of anti-CD3 Ab (0.01 µg/ml) in PBS (clone OKT3; eBioscience) was immobilized to the surface of 96-well round-bottom plate (Thermo Scientific) at 37°C O/N. Unbound Ab was removed by washing the wells three times with PBS. Autologous $CD3^+$ T-cells were purified by positive selection according to the manufacturer's protocol using anti-CD3 magnetic beads and autoMACS-assisted cell sorting (Miltenyi Biotech). Purity of $CD3^+$ T-cells was >95% for all the samples. $CD3^+$ T-cells were labeled with CellTrace Violet (CTV) fluorescent dye (1.5 µM; Invitrogen) and cocultured with moDCs or CXCL4-moDCs (1:5 ratio) in a final volume of 150 µl. After 5 d of coculture, $CD4^+$ T and $CD8^+$ T cell proliferation and cytokine production was assessed by flow cytometry. The division index was calculated as a measure of proliferation, following FlowJo guidelines and previous publications[47,48].

BSA uptake and processing

The moDC and CXCL4-moDCs were pulsed with BSA-labeled Alexa Fluor 647 (0.1 µg/ml, Invitrogen) or DQ-Green BSA (0.1 µg/ml), a self-quenched dye conjugate of BSA (Life Technologies) for 10 min at 37°C to measure specific uptake or processing, respectively; or at 4°C to assess non-specific cell surface binding. Cells were subsequently washed with cold medium and chased at 37°C for 10, 20, 40 or 100 min or left at 4°C. Next, cells were washed twice with FACS buffer and analyzed by flow cytometry. Ag uptake and processing were determined by analysis of median fluorescence intensity (MFI) for Alexa Fluor 647- or FITC-expressing cells. MFI measured at starting point $t = 0$ (0 min chase) was established as 100%. To calculate the percentage of BSA uptake or processing, the MFI for the time points: 10, 20, 40 and 100 min of chasing were normalized to the respective $t = 0$.

Direct Ag presentation and cross-presentation

MoDCs from HLA-A2$^+$ HV were differentiated as described above with or without CXCL4. Direct presentation of recombinant NLVPMVATV (NLV)-pp65 peptide (ProImmune) or cross-presentation of soluble recombinant HCMV-pp65 protein (Miltenyi Biotec) to HCMV-specific CD8$^+$ T cell clones that we have generated, was performed as previously described[49]. Briefly, 50 x 10^3 moDCs or CXCL4-moDCs were loaded either with the peptide NLV-pp65 (10^0 - 10^{-3} µM) or with 30 µg/ml of the full protein HCMV-pp65 in 96-well round-bottom plates (on a final volume of 100 µl) O/N at 37°C. Where indicated, cells were pre-treated with MG132 (2 µM; Calbiochem), hydroxychloroquine (50 µM; Sigma), brefeldin A (2.5 µg/ml; Sigma), or DMSO (Sigma) as control vehicle, for 30 min before Ag loading. The next day, cells were washed vigorously with complete medium and cocultured with 50x10^3 HCMV-specific CD8$^+$ T cells in the presence of GolgiStop (1/1500; BD). After 5 h of coculture, activation of CD8$^+$T cells was assessed by flow cytometry analyses.

Flow cytometry

Prior to Ab staining, moDCs were incubated with fixable viability dye eFluor780 or T cells with eFluor506 (eBioscience) in PBS, to allow exclusion of dead cells. After washing with FACS buffer, cells were treated with 10% (v/v) mouse serum (Fitzgerald) in FACS buffer to prevent non-specific Ag binding. MoDC sets were stained for 20 min at 4°C with the following anti-human fluorochrome-conjugated mAbs: CD1a (clone HI149), CD11b (clone ICRF44), CD205 (clone DEC-205), CD206 (clone 19.2), CD80 (clone L307.4), HLA-DR (clone G46-6), HLA-ABC (clone G46-2.6) obtained from BD; CD14 (clone M5E2), CD1c (BDCA1; clone L161), CD83 (clone HB15e), CD86 (clone IT2.2) obtained from Biolegend; CD11c (clone 3.9) and CD40 (clone 5C3) obtained eBioscience and CD141 (BDCA3; clone AD5-14H12) obtained from Miltenyi or the isotype control-matched Ab.

To measure intracellular cytokine expression by polyclonal T cells after 5-d coculture with moDCs, cells were restimulated for 5 h with PMA (50 ng/ml; Sigma) and ionomycin (1 µg/ml; Sigma) in the presence of GolgiStop (1/1500, BD). After incubation with fixable viability dye and mouse serum, cells were stained for 20 min with the anti-human mAbs: CD3 (UCHT1, eBioscience), CD4 (clone RPA-T4, eBioscience) and CD8 (clone RPA-T8, Biolegend) in FACS buffer. To analyze intracellular cytokine production, cells were fixed and permeabilized for 30 min using Fixation/ Permeabilization solution (eBioscience), according to the manufacturer's instructions, and washed twice with Permeabilization buffer (eBioscience). Intracellular staining for IL-10 (clone JES3-19F1) and IL-4 (clone MP4-25D2) obtained from BD; IL-22 (clone IL22JOP) and IFN-γ (clone 4S.B3) obtained from eBioscience; and IL-13 (clone JES10-5A2) obtained from BioLegend, was performed for 30 min in Permeabilization buffer. Finally, cells were washed twice with Permeabilization buffer, and the last wash with FACS buffer. Autologous $CD4^+$ T and $CD8^+$ T cell proliferation and cytokine production was measured by flow cytometry. To analyze the cytokine expression by HCMV-specific $CD8^+$ T cells after coculture with pp65-loaded moDCs, we used a staining protocol to similar to the above. The following anti-human mAbs were used for extracellular staining: CD3 (clone UCHT1; Biolegend), CD8 (clone RPA-T8; BD) and CD107a (LAMP1; clone H4A3, BD), followed by intracellular staining of IFN-γ (clone 4S.B4, BD) and TNF-α (clone MAB11; Sony Biotechnology). The cell acquisition of flow cytometry data was performed using LSR Fortessa (BD), and FlowJo software (Version 7.6.5; Tree Star. Inc.) was used for data analyses. In all flow cytometry analyses, cell debris were first excluded, then $CD3^+CD4^+$ T and $CD3^+CD8^+$ T cells were gated, and analyzed for the expression of activation markers, or dilution of CTV in proliferation experiments. Data was represented as MFI or the percentage of positive cells for a specific cell marker, as mentioned in the figures.

Statistical analysis

Graphs and statistical analyses were performed with GraphPad Prism software (version 6.0). Paired *t* test were used to compare two groups, and one-way ANOVA when more than two groups were compared. In all cases, the significance was defined as P-value ≤ 0.05.

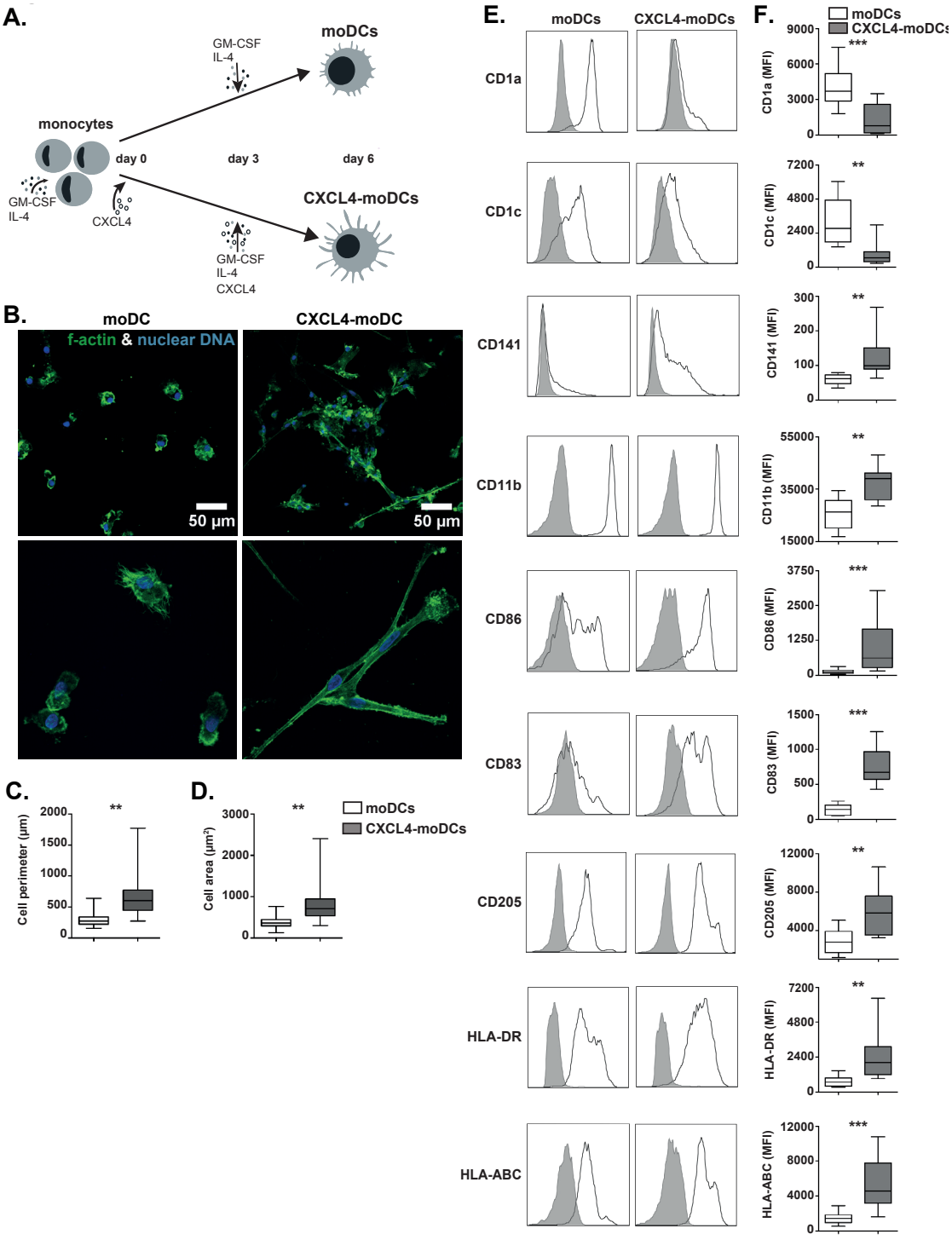
A.
GM-CSF
IL-4
moDCs
monocytes
day 0
day 3
day 6
GM-CSF
IL-4
CXCL4
CXCL4-moDCs
GM-CSF
IL-4
CXCL4
B.
moDC
CXCL4-moDC
f-actin & nuclear DNA
50 µm
50 µm
C.
Cell perimeter (µm)
2000
1500
1000
500
0
**
D.
Cell area (µm²)
3000
2000
1000
0
**
moDCs
CXCL4-moDCs
E.
moDCs
CXCL4-moDCs
CD1a
CD1c
CD141
CD11b
CD86
CD83
CD205
HLA-DR
HLA-ABC
F.
moDCs
CXCL4-moDCs
CD1a (MFI)
9000
6000
3000
0
***
CD1c (MFI)
7200
4800
2400
0
**
CD141 (MFI)
300
200
100
0
**
CD11b (MFI)
55000
35000
15000
**
CD86 (MFI)
3750
2500
1250
0
***
CD83 (MFI)
1500
1000
500
0
***
CD205 (MFI)
12000
8000
4000
**
HLA-DR (MFI)
7200
4800
2400
0
**
HLA-ABC (MFI)
12000
8000
4000
0
***

Figure 1. CXCL4 exposure alters moDC morphology and phenotype. (**A**) MoDCs from HVs were differentiated for 6 d with IL-4 and GM-CSF (moDCs) or in the additional presence of CXCL4 (CXCL4-moDCs). (**B**) Fluorescence-confocal microscopy analyses of representative images from the morphology of moDCs and CXCL4-moDCs. Top panels show images acquired with original magnification ×40; lower panels, original magnification ×63 1.40 oil objective. Cells were stained with phalloidin, which binds to f-actin (green), and Hoechst 33,342 to show the nuclear DNA (blue). (**C**) Quantification of cell perimeter and (**D**) area on day 6 of differentiation by confocal microscopy was determined for three HV, using 75 cells per condition for each HV. Data are shown as mean and SD. (**E**) Representative flow cytometry histograms for one experiment, in which black lines show the expression of several APC and maturation markers, as well as HLA-ABC and HLA-DR by moDCs (left panel) and CXCL4-moDCs (right panel). Gray-shaded histograms show the respective isotype controls. (**F**) Flow cytometry analyses showing the MFI expression for several markers by moDCs and CXCL4-moDCs (10 HVs). Boxes show upper and lower quartiles (interquartile range), with the horizontal line within the boxes indicating the median. Whiskers represent the highest and lowest values. Paired t test. **P<0.01, ***P<0.001.

Results

CXCL4 exposure alters differentiation of moDCs

To examine the contribution of CXCL4 to moDC differentiation, we generated moDCs for 6 d, with our without CXCL4 (**Fig. 1A**). We observed that CXCL4-treated moDC formed plate-adherent cell aggregates, with very heterogeneous morphology and extended dendrites, in contrast to moDCs (**Fig. 1B**). As a quantitative measurement to determine the cell size and formation of branched protrusions we analyzed the area and perimeter of the cells based on the expression f-actin. We observed that moDCs exposed to CXCL4 display a bigger perimeter (**Fig. 1C**) and area (**Fig. 1D**).

In addition, CXCL4-moDCs showed downregulation of the lipid-presenting molecules CD1a and CD1c, whereas the integrin CD11b involved in cell adhesion and migration, myeloid marker CD141, endocytic receptor CD205, maturation markers CD86 and CD83, MHC class I (MHC-I) and class II (MHC-II) molecules were expressed at higher levels (**Fig. 1C,D**). No differences were observed for the lineage marker CD11c, the mannose receptor CD206, the costimulatory molecules CD80 and CD40, and macrophage markers CD14, CD64, and CD163 (data not shown). These results demonstrate that CXCL4 exposure alters the differentiation and maturation of moDCs, suggesting that CXCL4-moDCs might perform differently on innate and adaptive immune responses in comparison with moDCs.

CXCL4 enhances TLR-mediated responses of moDCs

As DCs from SSc patients have been shown to display augmented response to TLR agonists, we next explored whether this could be attributed to the increased levels of CXCL4 observed in these patients[41]. With this purpose, moDCs and CXCL4-moDCs were challenged for 24 h with TLR agonists or left unstimulated (**Fig. 2A**). Stimulation

with poly(I:C) (TLR3), LPS (TLR4) and R848 (TLR7/8) resulted in upregulation of co-stimulatory and MHC molecules on both moDCs as well as CXCL4-moDCs (**Fig. 2B**). However, these TLR ligands induced upregulation of CD86, CD83 and MHC-I expression to a greater extent on CXCL4-moDCs compared to moDCs (**Fig. 2B).** We compared the ability of CXCL4-moDCs to produce proinflammatory cytokines in response to a panel of nine different TLR ligands. Stimulation with poly(I:C), R848, and CL075 resulted in a markedly higher production of IL-12 (an average 64-fold, 5-fold and 6-fold increase, respectively) and TNF-α (an average 15-fold, 7-fold and 6-fold increase, respectively) by CXCL4-moDCs as compared with moDCs. Stimulation with Pam3CSK4 (TLR2), LPS, flagellin (TLR5), loxoribine or imiquimod (both TLR7) did not result in significant differences on IL-12 and TNF-α production (**Fig. 2C,D**). Altogether, these results point towards CXCL4 as a modulator of TLR3 and TLR8-mediated innate responses in moDCs.

CXCL4-moDCs are strong inducers of $CD4^+$ T and $CD8^+$ T cell responses

DCs are crucial for the initiation of T cell responses; thus they function as a bridge between the innate and adaptive immune system. To evaluate if CXCL4-moDCs were more potent in activation of T cell responses, immature moDCs and CXCL4-moDCs were cocultured with autologous $CD3^+$ T cells. CXCL4 strongly potentiated the proliferation of $CD4^+$ T cells and $CD8^+$ T cells (**Fig. 3A,B**), in this study determined as division index (**Fig. 3C**). In addition, the frequencies of $CD4^+IFN\text{-}\gamma^+$ (**Fig. 3D,E**) as well as $CD8^+IFN\text{-}\gamma^+$ and $CD8^+IL\text{-}4^+$ (**Fig. 3F,G**) expressing T-cells were significantly higher after coculture with CXCL4-moDC, in comparison to conventional moDCs. No differences were observed for $CD8^+IL\text{-}10^+$, $CD8^+IL\text{-}22^+$ and $CD8^+IL\text{-}13^+$ T cells (data not shown). Based on these results, we propose CXCL4-moDCs as potent inducers of both $CD4^+$ T cell and $CD8^+$ T cell responses in an Ag-independent manner.

CXCL4-moDCs display impaired Ag processing

To study whether CXCL4 could affect Ag presentation, we analyzed the ability of moDCs to uptake and process Ag, using BSA as a model. Uptake of Alexa Fluor 647 BSA by both moDC and CXCL4-moDCs was comparable over the 100 min duration of the pulse-chase experiment, with the greatest increase on uptake seen at 40 min of Ag exposure (**Fig. 4A**). Moreover, CXCL4-moDCs displayed impaired processing of Ag (DQ-BSA) compared to moDCs at 10, 20 and 40 minutes of chase. The highest Ag processing level was observed at the time point 20 min (**Fig. 4B**). Taken together, whereas uptake of Ag by moDCs is not affected by the exposure to CXCL4, exogenous Ag, when taken up by early stages of maturated DCs might be retained intracellularly longer, thus kept preserved for slower degradation, implying that CXCL4 might modulate Ag cross-presentation capacities of moDCs.

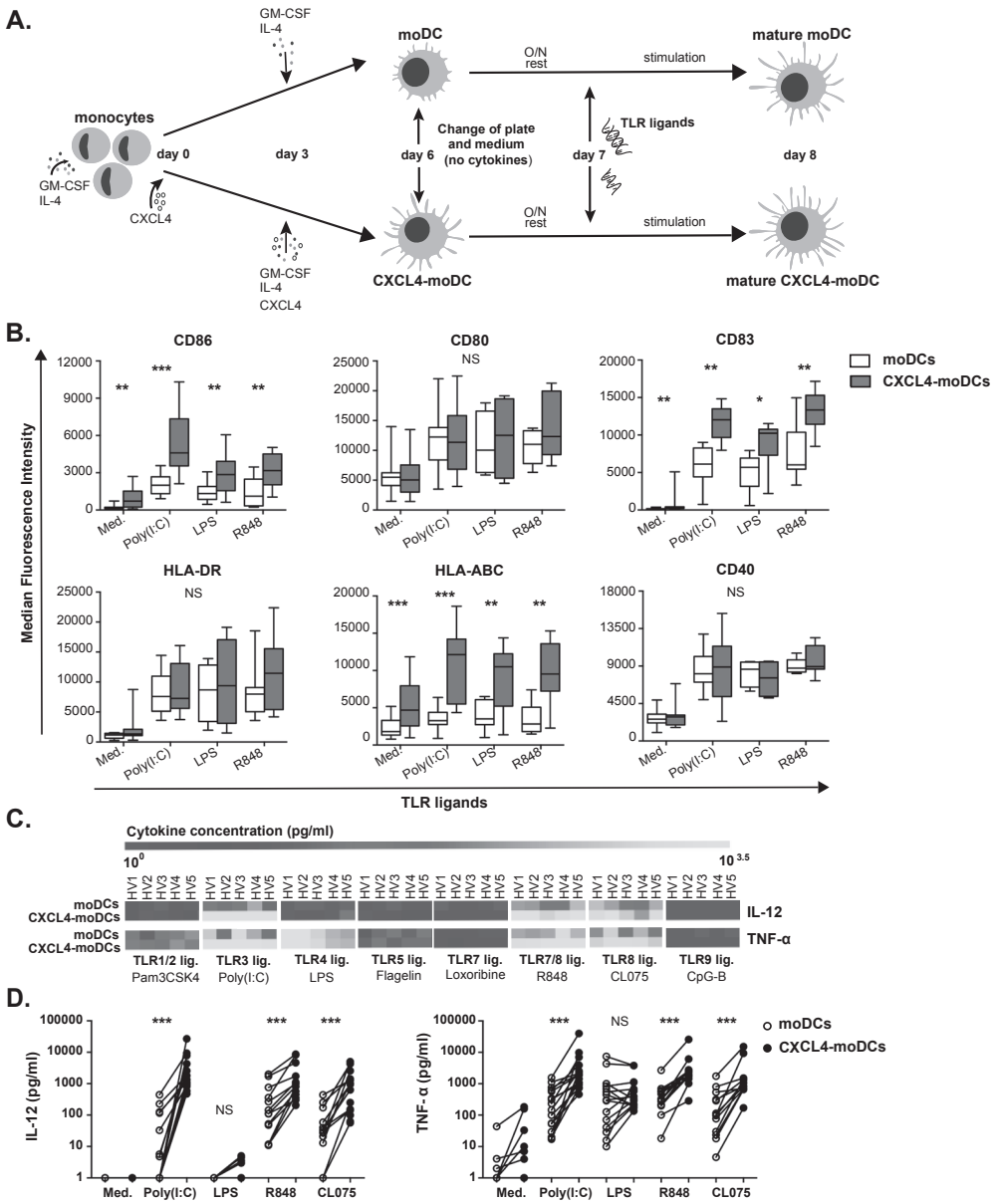

Figure 2. CXCL4-moDCs are more sensitized to TLR reactivity. (**A**) After O/N resting with new complete medium without cytokines, both day 7 moDCs and CXCL4-moDCs were either left unstimulated or stimulated with TLR ligands for 24 h. Phenotype was analyzed by flow cytometry, and supernatants were used to measure cytokine levels by a Luminex-based assay. (**B**) Flow cytometry analyses on day 8 show the MFI of DC maturation markers as well as HLA-ABC and HLA-DR expressed by both moDCs and CXCL4-moDCs upon stimulation with poly(I:C), LPS, and R848 (data are shown for eight HVs). Boxes show upper and lower quartiles (interquartile range). Horizontal line within the boxes indicate median. Whiskers represent the highest and lowest values. (**C**) Gray scale profile shows for five representative HVs the concentration levels of IL-12 and TNF-α produced by moDCs and CXCL4-moDCs upon stimulation with a panel of TLR ligands. Concentration of cytokines is shown in $\log_{10}$ scale. (**D**) Production of IL-12 and TNF-α by moDCs and CXCL4-moDCs upon stimulation with poly(I:C), LPS, R848, and CL075 is shown for each paired individual sample. Each symbol represents an individual donor; lines connect the same donor. Results were obtained from a total of 12 HVs. Paired t test. * P<0.05, **P<0.01, *** P<0.001. lig., ligand; Med., medium.

CXCL4 potentiates pp65 presentation and cross-presentation

CXCL4-moDCs display increased expression of MHC-I, and our data proposes that these cells process Ag more efficiently, suggested by the longer Ag preservation on processing compartments. To investigate whether CXCL4-moDCs may be superior on direct Ag presentation or cross-presentation, we analyzed the response of HCMV-specific $CD8^+$ T cell clones to their cognate peptide (NLV-pp65 or HCMV-pp65 protein after processed into peptides), either pulsed or endogenously processed by the moDCs. The moDCs and CXCL4-moDCs were first loaded with NLV-pp65 peptide or HCMV-pp65 protein and then co-cultured with HCMV-specific $CD8^+$ T cells (**Fig. 5A**). $CD8^+$ T cells in the absence of NLV-pp65 or HCMV-pp65 protein did not produce IFN-γ and TNFα (**Fig. 5B-D**). To control for differences on MHC-I expression, we assessed direct presentation of NLV-pp65 peptide. We observed a trend for it to be increased, but not significantly so, upon $CD8^+$ T cell activation, which showed as frequency of $CD8^+IFN\text{-}\gamma^+$ T cells and $CD8^+$ $TNF\alpha^+$ T cells after presentation of NLV-pp65 (10^0 – 10^{-3} μM) by CXCL4-moDCs (**Fig. 5B,C**). Strikingly, CXCL4-moDCs induced potent activation of HCMV-specific $CD8^+$ T cell responses after cross-presentation of HCMV-pp65 protein, measured as the production of IFN-γ and TNF-α (**Fig. 5D-F**). Next, to better understand the effects of CXCL4 on Ag processing pathways, moDCs were treated with proteasome or endosomal inhibitors prior to Ag loading. The moDCs and CXCL4-moDCs conserved their ability to direct present NLV-pp65 peptide and stimulate $CD8^+$ T-cells after treatment with the inhibitors (data not shown). Treated moDCs and CXCL4-moDCs with proteasome (MG132) or endosomal (hydroxychloroquine) inhibitors displayed a reduced ability to stimulate HCMV-specific $CD8^+$ T cells (**Fig. 5G**). Nevertheless, CXCL4-moDCs were still superior in activating $CD8^+$ T cells, despite the inhibition of processing in both compartments. Blocking the transport of newly synthesized molecules from the endoplasmic reticulum (ER) to the golgi with brefeldin A completely abrogated Ag cross-presentation by moDCs and CXCL4-moDCs (**Fig. 5E**). Overall, these results indicate that CXCL4-moDCs potentiate the activation of Ag-specific $CD8^+$ T cells.

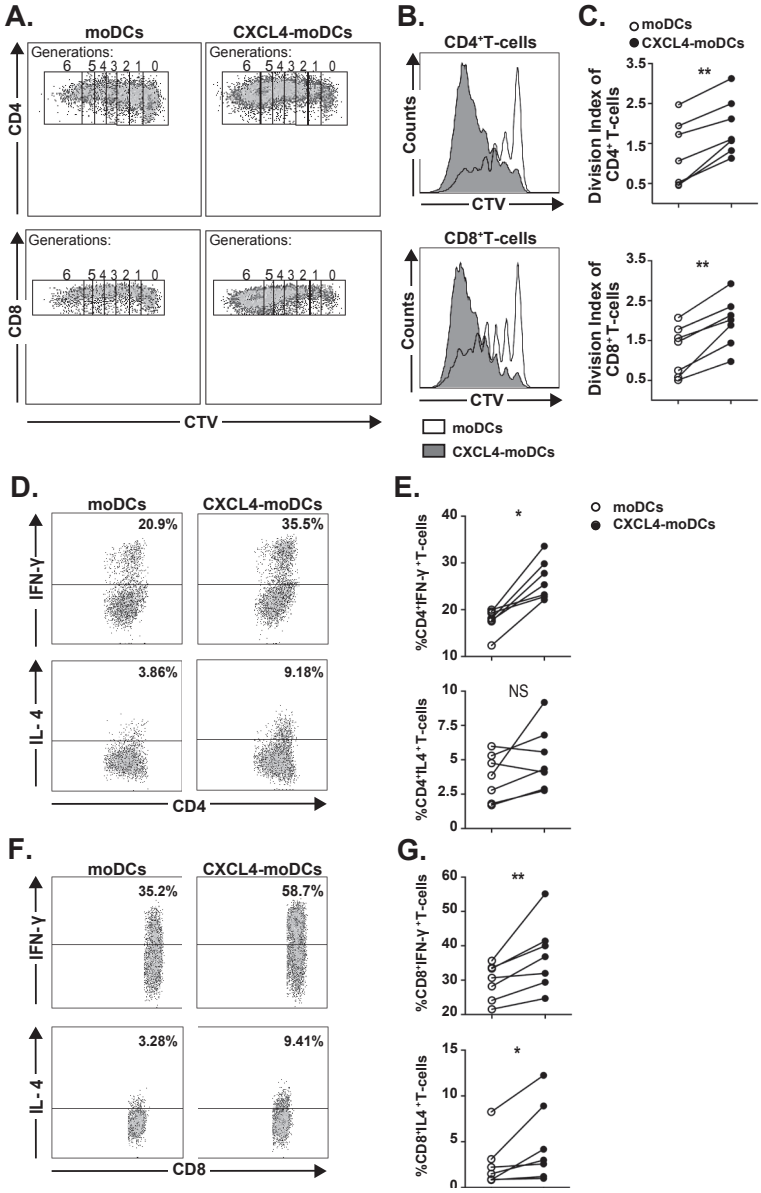

Figure 3. CXCL4-moDCs are more potent activators of polyclonal CD4⁺ and CD8⁺ T cells. (**A**) Flow cytometry dot plots show the expression of diluted CTV by live $CD3^+CD4^+$ T cells (upper panel) and $CD3^+CD8^+$ T cells (lower panel), and represent cell proliferation after 5-d coculture with autologous moDCs or CXCL4-moDCs. Outlined areas indicate the percentage of T cells gated accordingly to increasing dilution of CTV, representing subsequent generations of divided cells. (**B**) Representative histograms of one experiment show CTV expression by $CD4^+$ T cells (upper graph) and $CD8^+$ T cells (lower graph), with each pick indicating one subsequent generation of proliferating cells. (**C**) Proliferation was analyzed as division index of $CD4^+$ T cells (upper graph) and $CD8^+$ T cells (lower graph) after coculture for eight HVs. (**D**) Flow cytometry dot plots show the production of IFN-γ and IL-4 by $CD4^+$ T cells and (**F**) $CD8^+$ T cells after coculture with moDCs or CXCL4-moDCs, for one representative experiment. Numbers indicate the percentage of cells expressing IFN-γ^+ (upper panel) or IL-4^+ (lower panel). (**E**) IFN-γ– and IL-4–producing $CD4^+$ T cells and (**G**) $CD8^+$ T cells were measured for eight HVs. Symbols represent each donor, and the same donor is connected with lines. Paired t test. * $P<0.05$, ** $P<0.01$.

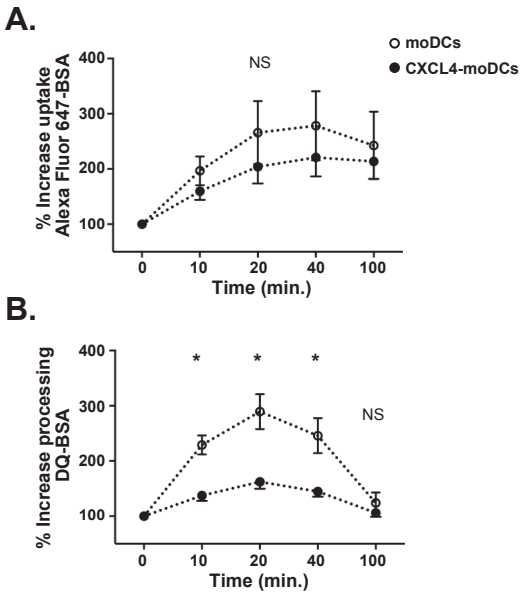

Figure 4. CXCL4-moDCs exhibit comparable rates of Ag uptake but restrained processing capacity. Immature moDCs and CXCL4-moDCs were pulsed with BSA conjugates for 10 min and chased for 10, 20, 40, or 100 min at 37°C. (**A**) Uptake of Alexa Fluor 647–conjugated BSA and (**B**) processing of DQ-BSA were followed over chasing by flow cytometry. Results are shown as percentage of increase normalized to the MFI obtained at the starting point (0 min). Mean and SDs from six HVs are shown. One-way ANOVA. * $P<0.05$.

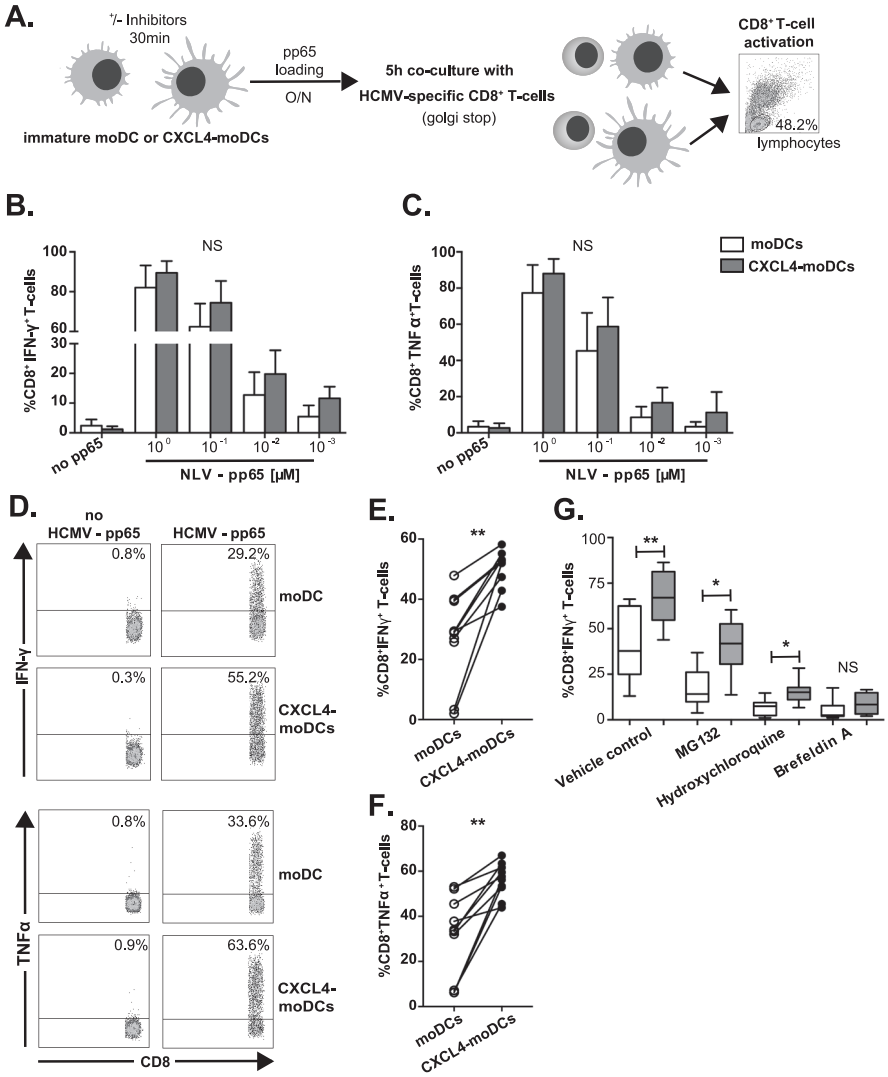

Figure 5. Stimulation of HCMV-specific CD8⁺ T cell responses is potentiated by prior exposure of moDCs to CXCL4. (**A**) Immature HLA-A2⁺ moDCs and CXCL4 moDCs on day 6 of differentiation were loaded O/N with NLV-pp65 peptide or HCMV-pp65 protein and cocultured with HCMV-pp65–specific CD8⁺ T cells for 5 h in the presence of GolgiStop. The moDCs not loaded with pp65 were used as a negative control. Activation of HCMV-specific CD8⁺ T cells was assessed by flow cytometry. (**B**) Shown are the percentages of HCMV-specific CD8⁺IFN-γ⁺ T cells and (**C**) CD8⁺TNF-α⁺ T cells after coculture with moDCs or CXCL4-moDCs loaded with several concentrations of NLV-pp65 peptide. Data are shown as mean and SD. (**D**) Dot plots illustrate for one representative experiment the production of IFN-γ (upper panel) and TNF-α (lower panel) by HCMV-specific CD8⁺ T cells after 5-h coculture with moDCs or CXCL4-moDCs loaded or not with HCMV-pp65 protein. Numbers indicate the percentages of CD8⁺IFN-γ⁺ T cells or CD8⁺TNF-α⁺ T cells, respectively. (**E**) IFN-γ and (**F**) TNF-α production by HCMV-specific CD8⁺ T cells was assessed after cross-presentation for 10 HV. Symbols represent each donor, and the same donor is linked with lines. (**G**) MoDCs and CXCL4-moDCs were pretreated with hydroxychloroquine or MG132 or brefeldin A for 30 min before loading with HCMV-pp65. DMSO was used as vehicle control. Box plots show the percentage of CD8⁺IFN-γ⁺ T cells after cross-presentation of HCMV-pp65. Boxes show upper and lower quartiles (interquartile range), with horizontal lines within the boxes displaying the median. Whiskers represent the highest and lowest values. All experiments were measured for eight HVs. Paired t test. * P<0.05, ** P<0.01.

Discussion

Inflammatory mediators such as cytokines, chemokines or PAMPs are found in circulation and localized at affected tissues from patients suffering from autoimmune diseases or infections, driving inflammation and modulating immune responses. CXCL4, a chemokine involved in several physiological processes has been implicated in many diseases, and was recently proposed as a biomarker in SSc[5,17,50]. Indeed, evidences of its immune-modulatory function on both immune and non-immune cells have emerged in the last decade.

In the current study, we explored the effects of CXCL4 on moDC differentiation and on the initiation of innate and adaptive immune responses.

We showed by confocal microcopy images, that in comparison to conventional differentiated moDCs, most of the CXCL4-moDCs are very heterogeneous, are bigger, and display branched protrusions. These observations suggest that CXCL4 may have an effect on the remodeling of cytoskeleton components, such as f-actin. As a result, CXCL4-moDCs might perform differently in important APC functions—for instance on cell mobility and migration but in cell-cell contact, as well.

Besides the effects on moDC morphology, we also observed that CXCL4 exposure results in downregulation of the lipid-presenting molecules CD1a and CD1c. On the contrary, CD141, CD11b, CD205, maturation markers and MHC molecules were upregulated on CXCL4-moDCs. Partially, these effects were described in previous studies, in which different approaches were used[24,25,31]. To our knowledge, this is the first study to describe that CXCL4 sensitizes moDCs to triggering with several TLR ligands. Expression of maturation and MHC-I molecules were additionally upregulated on CXCL4-moDCs, specifically when triggered with poly(I:C) and R848. Moreover, we also found that CXCL4-moDCs are more potent producers of pro-inflammatory cytokines upon triggering with the poly(I:C), R848 and CL075, compared with moDCs. Proliferation and cytokine production by autologous $CD4^+$ T cells and $CD8^+$ T cells were potentiated by CXCL4-moDCs, in an Ag-independent manner. In a previous study by Xia *et al.*[24], opposite effects were shown on the activation of $CD4^+$ T cell responses, in a very distinct allogeneic culture system. We expanded these findings, showing that CXCL4-moDCs displayed impaired Ag processing in comparison with moDCs, and suggesting that CXCL4 might affect the functional ability of cells to perform Ag cross-presentation. CXCL4-moDCs loaded with HCMV-pp65 were able to potentiate the activation of HCMV-specific $CD8^+$ T cells, in contrast to moDCs. These results suggest that CXCL4-moDCs display improved ability to activate adaptive immune responses.

When molecules resulting from tissue damage and inflammation are sensed by innate recognition receptors such as TLRs, IFN signaling pathway is activated. Accumulating evidences from both human and mouse studies implicate TLR and type I IFN signaling in the pathogenesis of SSc and may be one of the causes leading

to and sustaining autoimmunity and fibrosis[5,36,40,41,43,44,51]. On the basis of this, we hypothesized that CXCL4 could alter TLR-mediated responses and contribute to immune-mediated diseases such as SSc. In this study, we found that CXCL4 exposure enhances TLR3- and TLR8-mediated moDC maturation and pro-inflammatory cytokine production.

Several studies have suggested that activation of TLR responses, like TLR3 (Myd88-independent) and MyD88 signaling on APCs can improve cross-priming and Ag cross-presentation[52–55]. Therefore, our findings showing that CXCL4 exposure modulates TLR signaling may point towards a contribution of these innate effects on the adaptive immune responses.

In addition, the greater stimulating signals provided by the CXCL4-moDCs and T cells during coculture, such as: TCR signaling, CD40-CD40L and other co-stimulating signals, as well as cytokines released by DCs, most likely contribute to the potentiation of T-cell responses by CXCL4-moDCs[56,57]. We also found that CXCL4 exposure upregulated the expression of CD11b. Previous studies showed that $CD11^{high}$ cells, besides expressing a mature phenotype, are potent chemokine-producing cells, both in homeostasis and after stimulation with airway Ag or TLR ligands, and efficiently prime T-cell responses[58,59].

Internalization, processing and presentation of Ag or dangerous molecules resulting from dying cells by DCs as peptide/MHC complexes is critical to the priming of T-cells against tumors, virus infections and inflammation. In our experimental setting, several molecules involved on these adaptive mechanisms were upregulated on CXCL4-moDC. For instance, we found upregulation of CD141 and CD205 expression on CXCL4-moDCs, in comparison to moDCs. DCs expressing these molecules were described to efficiently uptake Ags or molecules derived from dying cells, process, and cross-present via peptide-loaded MHC molecules[60–65]. Of note, CD205 plays a crucial role in these processes as endocytic or non-endocytic receptor on both immature and mature cells[66]. These features also most likely facilitate the efficient activation of Ag-specific $CD8^+$ T-cell responses.

Although it has been described that micropinocytosis is downregulated in mature DCs, the capacity to capture Ag by moDCs and CXCL4-moDCs was not affected, as seen in other studies[67,68]. We propose that due to the mature phenotype of CXCL4-moDCs and the capacity to store Ag for prolonged time, these cells may more efficiently process Ag for continuous supply to MHC-I, as well as promote the stability of these molecules, leading to potentiation of cross-presentation capacities[69–71]. In addition, it was described that increase of immunoproteasome subunit expression during DC maturation[72] and modifications of proteasome and transporter-associated with Ag processing (TAP) activities can promote the presentation of peptide/MHC-I complexes[73,74]. We hypothesize that these pathways may be more activated in CXCL4-moDCs, due to their maturated phenotype, thus contributing also to higher ability for the activation of Ag-specific $CD8^+$ T-cells. Attempts to understand the contribution of endosomal and proteasome compartments for Ag processing by CXCL4-moDCs were confounded with the reduction to the same extent of $CD8^+$ T-cell activation when moDCs and CXCL4-moDCs were treated with MG132 and hydroxychloroquine. Clarification of how CXCL4 impacts Ag processing on early or late endosomes, lysosomes and proteasome compartments requires further investigation since these pathways are crucial for the effective cross-presentation of exogenous Ag to $CD8^+$ T-cells and activation of adaptive immune responses[75]. Further research could make use of more specific inhibitors on cross-presentation assays, perhaps including selective immunoproteasome inhibitors[76,77].

Although the sensitization of DCs by CXCL4 might improve responses against dangerous molecules resulting from dying cells and pathogens, and efficient priming of T-cells contributes to protection against infections and tumors, on the other side, the homeostatic balance of these immune responses have a critical role in the maintenance of self-tolerance [78,79].

Taken together, our findings corroborate and expand upon earlier studies showing that increased circulating levels of CXCL4 modulates inflammatory immune responses [5,24–27,29,32].

Acknowledgments

We thank Lenny van Bon, Maarten van der Linden, Willemijn Janssen, Thijs Flinsenberg, Tessa Kempen, Maud Plantinga and the Flow Core facility for the very helpful work discussions; and the Multiplex Core facility of the Laboratory of Translational Immunology (University Medical Center Utrecht) for performing cytokine measurements.

This work was supported by a PhD grant from the Portuguese Fundação para a Ciência e a Tecnologia (SFRH/BD/89643/2012) to S.C.S.C.; A.J.A. was supported by the grants from the Dutch Arthritis Association (Reumafonds grant NR-10-1-301)

and the Netherlands Organization for Science Research (Mosaic grant 017.008.014) and T.R.D.J.R. was funded by an ERC Starting grant, a grant from the Dutch Arthritis Foundation and Pre-Seed grant Dutch Association of Science (NWO).

Author contributions: S.C.S.C., M.B. and T.R.D.J.R. designed research project; S.C.S.C., A.J.A., L.S., M.C., J.A.G.R and M.B. performed research; S.C.S.C. and A.A. analyzed data; S.C.S.C., M.B. and T.R.D.J.R. wrote the paper.

References

1. Levine, S. P. & Wohl, H. Human Platelet Factor 4: Purification and Characterization by Affinity Chromatography. *J. Biol. Chem.* 251, 324–328 (1976).
2. Zucker, M. B. & Katz, I. R. Platelet factor 4: prodution, structure, and physiologic and immunologic action. *Proc. Soc. Exp. Biol. Med.* 198, 693–702 (1991).
3. McLaren, K. M., Holloway, L. & Pepper, D. S. Human platelet factor 4 and tissue mast cells. *Thromb. Res.* 19, 293–297 (1980).
4. Maier, M. *et al.* Platelet factor 4 is highly upregulated in dendritic cells after severe trauma. *Mol. Med.* 15, 384–91 (2009).
5. van Bon, L. *et al.* Proteome-wide analysis and CXCL4 as a biomarker in systemic sclerosis. *N. Engl. J. Med.* 370, 433–43 (2014).
6. Schaffner, A., Rhyn, P., Schoedon, G. & Schaer, D. J. Regulated expression of platelet factor 4 in human monocytes--role of PARs as a quantitatively important monocyte activation pathway. *J. Leukoc. Biol.* 78, 202–9 (2005).
7. Lasagni, L. *et al.* PF-4/CXCL4 and CXCL4L1 exhibit distinct subcellular localization and a differentially regulated mechanism of secretion. *Blood* 109, 4127–34 (2007).
8. Han, Z. C., Sensébe, L., Abgrall, J. F. & Brière, J. Platelet Factor 4 Inhibits Human Megakaryocytopoiesis In Vitro. *Blood* 75, 1234–1239 (1990).
9. Maione, T. E. *et al.* Inhibition of angiogenesis by recombinant human platelet factor-4 and related peptides. *Science (80-.).* 247, 77–79 (1990).
10. Dehmer, G. J., Fisher, M., Tate, D. A., Teo, S. & Bonnem, E. M. Reversal of Heparin Anticoagulation by Recombinant Platelet Factor 4 in Humans. *Circulation* 91, 2188–2194 (1995).
11. Aivado, M. *et al.* Serum proteome profiling detects myelodysplastic syndromes and identifies CXC chemokine ligands 4 and 7 as markers for advanced disease. *Proc. Natl. Acad. Sci. U. S. A.* 104, 1307–12 (2007).
12. Schwartzkopff, F. *et al.* Platelet factor 4 (CXCL4) facilitates human macrophage infection with HIV-1 and potentiates virus replication. *Innate Immun.* 15, 368–79 (2009).
13. Srivastava, K. *et al.* Platelet factor 4 mediates inflammation in experimental cerebral malaria. *Cell Host Microbe* 4, 179–187 (2008).
14. Pitsilos, S. *et al.* Platelet factor 4 localization in carotid atherosclerotic plaques: correlation with clinical parameters. *Thromb. Haemost.* 4245, 1112–1120 (2003).
15. Visentin, G. P., Ford, S. E., Scott, J. P. & Aster, R. H. Antibodies from patients with heparin-induced thrombocytopenia/thrombosis are specific for platelet factor 4 complexed with heparin or bound to endothelial cells. *J. Clin. Invest.* 93, 81–88 (1994).
16. Vrij, A. A., Rijken, J. & Van Wersch, J W Stockbrügger, R. W. Platelet factor and beta-thromboglobulin in inflammatory bowel disease and giant cell arteritis. *Eur. J. Clin. Invest.* 30, 188–194 (2000).
17. Yeo, L. *et al.* Expression of chemokines CXCL4 and CXCL7 by synovial macrophages defines an early stage of rheumatoid arthritis. *Ann. Rheum. Dis.* 75, 763–71 (2016).
18. Patsouras, M. D. *et al.* Elevated expression of platelet-derived chemokines in patients with antiphospholipid syndrome. *J. Autoimmun.* 65, 30–7 (2015).
19. Tamagawa-Mineoka, R., Katoh, N., Ueda, E., Masuda, K. & Kishimoto, S. Elevated platelet activation in patients with atopic dermatitis and psoriasis: increased plasma levels of beta-thromboglobulin and platelet factor 4. *Allergol. Int.* 57, 391–6 (2008).
20. Banchereau, J. & Steinman, R. M. Dendritic cells and the control of immunity. *Nature* 392, 245–252 (1998).
21. Kapsenberg, M. L. Dendritic-cell control of pathogen-driven T-cell polarization. *Nat. Rev. Immunol.* 3, 984–93 (2003).

22. Mellman, I. & Steinman, R. M. Dendritic cells: Specialized and regulated antigen processing machines. *Cell* 106, 255–258 (2001).
23. Bebawy, S. T., Gorka, J., Hyers, T. M. & Webster, R. O. In vitro effects of platelet factor 4 on normal human neutrophil functions. *J. Leukoc. Biol.* 39, 423–34 (1986).
24. Xia, C.-Q. & Kao, K.-J. Effect of CXC chemokine platelet factor 4 on differentiation and function of monocyte-derived dendritic cells. *Int. Immunol.* 15, 1007–15 (2003).
25. Fricke, I. *et al.* Platelet factor 4 in conjunction with IL-4 directs differentiation of human monocytes into specialized antigen-presenting cells. *FASEB J.* 18, 1588–90 (2004).
26. Scheuerer, B. *et al.* The CXC-chemokine platelet factor 4 promotes monocyte survival and induces monocyte differentiation into macrophages. *Blood* 95, 1158–66 (2000).
27. Fleischer, J. *et al.* Platelet factor 4 inhibits proliferation and cytokine release of activated human T cells. *J. Immunol.* 169, 770–7 (2002).
28. Crisi, G. M., Katz, I. R., Zucker, M. B. & Thorbecke, G. J. Induction of Inhibitory Activity for B Cell Differentiation in Human CD8 T Cells with Pokeweed Mitogen, Dimaprit, and cAMP Upregulating Agents: Countersuppressive Effect of Platelet Factor 4. *Cell. Immunol.* 172, 205–216 (1996).
29. Schwartzkopff, F., Petersen, F., Grimm, T. A. & Brandt, E. CXC chemokine ligand 4 (CXCL4) down-regulates CC chemokine receptor expression on human monocytes. *Innate Immun.* 4, (2010).
30. Martí, F. *et al.* Platelet factor 4 induces human natural killer cells to synthesize and release interleukin-8. *J. Leukoc. Biol.* 72, 590–597 (2002).
31. Gouwy, M. *et al.* CXCL4 and CXCL4L1 Differentially Affect Monocyte Survival and Dendritic Cell Differentiation and Phagocytosis. *PLoS One* 11, e0166006 (2016).
32. Woller, G., Brandt, E., Mittelstädt, J., Rybakowski, C. & Petersen, F. Platelet factor 4/CXCL4-stimulated human monocytes induce apoptosis in endothelial cells by the release of oxygen radicals. *J. Leukoc. Biol.* 83, 936–45 (2008).
33. Pervushina, O. *et al.* Platelet factor 4/CXCL4 induces phagocytosis and the generation of reactive oxygen metabolites in mononuclear phagocytes independently of Gi protein activation or intracellular calcium transients. *J. Immunol.* 173, 2060–7 (2004).
34. Gleissner, C. A., Shaked, I., Little, K. M. & Ley, K. CXCL4 induces a unique transcriptome in monocyte-derived macrophages. *J. Immunol.* 184, 4810–4818 (2010).
35. Sugiura, H. *et al.* Activation of Toll-like receptor 3 augments myofibroblast differentiation. *Am. J. Respir. Cell Mol. Biol.* 40, 654–62 (2009).
36. Ciechomska, M. *et al.* Histone Demethylation and Toll-like Receptor 8-Dependent Cross-Talk in Monocytes Promotes Transdifferentiation of Fibroblasts in Systemic Sclerosis Via Fra-2. *Arthritis Rheumatol.* 68, 1493–1504 (2016).
37. Edfeldt, K., Swedenborg, J., Hansson, G. K. & Yan, Z. Expression of Toll-Like Receptors in Human Atherosclerotic Lesions. *Circulation* 105, 1158 LP-1161 (2002).
38. Ospelt, C. *et al.* Overexpression of toll-like receptors 3 and 4 in synovial tissue from patients with early rheumatoid arthritis: toll-like receptor expression in early and longstanding arthritis. *Arthritis Rheum.* 58, 3684–92 (2008).
39. Édouard Begon *et al.* Expression, subcellular localization and cytokinic modulation of Toll-like receptors (TLRs) in normal human keratinocytes: TLR2 up-regulation in psoriatic skin. *Eur. J. Dermatology* 17, 497–506 (2007).
40. Farina, G. A. *et al.* Poly(I:C) drives type I IFN- and TGFβ-mediated inflammation and dermal fibrosis simulating altered gene expression in systemic sclerosis. *J. Invest. Dermatol.* 130, 2583–93 (2010).

41. van Bon, L. *et al.* Distinct evolution of TLR-mediated dendritic cell cytokine secretion in patients with limited and diffuse cutaneous systemic sclerosis. *Ann. Rheum. Dis.* 69, 1539–47 (2010).
42. Broen, J. C. A. *et al.* A rare polymorphism in the gene for Toll-like receptor 2 is associated with systemic sclerosis phenotype and increases the production of inflammatory mediators. *Arthritis Rheum.* 64, 264–71 (2012).
43. Agarwal, S. K. *et al.* Toll-like receptor 3 upregulation by type I interferon in healthy and scleroderma dermal fibroblasts. *Arthritis Res. Ther.* 13, R3 (2011).
44. Ciechomska, M. *et al.* Toll-like receptor-mediated, enhanced production of profibrotic TIMP-1 in monocytes from patients with systemic sclerosis: role of serum factors. *Ann Rheum Dis* 72, 1382–1389 (2013).
45. York, M. R. *et al.* A macrophage marker, Siglec-1, is increased on circulating monocytes in patients with systemic sclerosis and induced by type I interferons and toll-like receptor agonists. *Arthritis Rheum.* 56, 1010–20 (2007).
46. de Jager, W., Prakken, B. J., Bijlsma, J. W. J., Kuis, W. & Rijkers, G. T. Improved multiplex immunoassay performance in human plasma and synovial fluid following removal of interfering heterophilic antibodies. *J. Immunol. Methods* 300, 124–35 (2005).
47. Roederer, M. Interpretation of cellular proliferation data: Avoid the panglossian. *Cytom. Part A* 79 A, 95–101 (2011).
48. Hawkins, E. D. *et al.* Measuring lymphocyte proliferation, survival and differentiation using CFSE time-series data. *Nat. Protoc.* 2, 2057–2067 (2007).
49. Flinsenberg, T. W. H. *et al.* Fcγ receptor antigen targeting potentiates cross-presentation by human blood and lymphoid tissue BDCA-3+ dendritic cells. *Blood* 120, 5163–5172 (2012).
50. Vettori, S. *et al.* Serum CXCL4 increase in primary Sjögren's syndrome characterizes patients with microvascular involvement and reduced salivary gland infiltration and lymph node involvement. *Clin. Rheumatol.* 35, 2591–6 (2016).
51. Blanco, P., Palucka, A. K., Gill, M., Pascual, V. & Banchereau, J. Induction of Dendritic Cell Differentiation by IFN-α in Systemic Lupus Erythematosus. *Science (80-.).* 294, 1540 LP-1543 (2001).
52. Iwasaki, A. & Medzhitov, R. Toll-like receptor control of the adaptive immune responses. *Nat Immunol* 5, 987–95. (2004).
53. Palliser, D., Ploegh, H. & Boes, M. Myeloid Differentiation Factor 88 Is Required for Cross-Priming In Vivo. *J. Immunol.* 172, 3415–3421 (2004).
54. Schulz, O. *et al.* Toll-like receptor 3 promotes cross-priming to virus-infected cells. *Nature* 433, 887–892 (2005).
55. Burgdorf, S., Schölz, C., Kautz, A., Tampé, R. & Kurts, C. Spatial and mechanistic separation of cross-presentation and endogenous antigen presentation. *Nat. Immunol.* 9, 558–66 (2008).
56. Kaiser, A., Bercovici, N., Abastado, J. P. & Nardin, A. Naive CD8+ T cell recruitment and proliferation are dependent on stage of dendritic cell maturation. *Eur. J. Immunol.* 33, 162–171 (2003).
57. Aerts-Toegaert, C. *et al.* CD83 expression on dendritic cells and T cells: Correlation with effective immune responses. *Eur. J. Immunol.* 37, 686–695 (2007).
58. Beaty, S. R., Edward Rose, C. & Sung, S. J. Inflammation Homeostasis and in Allergic Lung Dendritic Cells in high Lung CD11b Diverse and Potent Chemokine Production by Diverse and Potent Chemokine Production by Lung CD11b high Dendritic Cells in Homeostasis and in Allergic Lung Inflammation. *J Immunol Ref. J. Immunol. Univ. Libr. Utr.* 178, 1882–1895 (2007).
59. Bantsimba-Malanda, C. *et al.* A role for dendritic cells in bleomycin-induced pulmonary fibrosis in mice? *Am. J. Respir. Crit. Care Med.* 182, 385–395 (2010).
60. Mahnke, K. *et al.* The dendritic cell receptor for endocytosis, DEC-205, can recycle and enhance antigen presentation via major histocompatibility complex class II-positive lysosomal compartments. *J. Cell Biol.* 151, 673–683 (2000).

61. Bonifaz, L. *et al.* Efficient Targeting of Protein Antigen to the Dendritic Cell Receptor DEC-205 in the Steady State Leads to Antigen Presentation on Major Histocompatibility Complex Class I Products and Peripheral CD8 2T Cell Tolerance. *J. Exp. Med* 121200, 1627–1638 (2002).
62. Bachem, A. *et al.* Superior antigen cross-presentation and XCR1 expression define human CD11c+CD141+ cells as homologues of mouse CD8+ dendritic cells. *J. Exp. Med* 207, 1273–1281 (2010).
63. Shrimpton, R. E. *et al.* CD205 (DEC-205): A recognition receptor for apoptotic and necrotic self. *Mol. Immunol.* 46, 1229–1239 (2009).
64. Jongbloed, S. L. *et al.* Human CD141+ (BDCA-3)+ dendritic cells (DCs) represent a unique myeloid DC subset that cross-presents necrotic cell antigens. *J. Exp. Med.* 207, 1247–60 (2010).
65. Bozzacco, L. *et al.* DEC-205 receptor on dendritic cells mediates presentation of HIV gag protein to CD8+ T cells in a spectrum of human MHC I haplotypes. *Proc Natl Acad Sci U S A* 104, 1289–1294 (2007).
66. Butler, M. *et al.* Altered expression and endocytic function of CD205 in human dendritic cells, and detection of a CD205-DCL-1 fusion protein upon dendritic cell maturation. *Immunology* 120, 362–371 (2006).
67. West, M. A., Prescott, A. R., Eskelinen, E. L., Ridley, A. J. & Watts, C. Rac is required for constitutive macropinocytosis by dendritic cells but does not control its downregulation. *Curr. Biol.* 10, 839–848 (2000).
68. Garrett, W. S. *et al.* Developmental Control of Endocytosis in Dendritic Cells by Cdc42. *Cell* 102, 325–334 (2000).
69. Van Montfoort, N. *et al.* Antigen storage compartments in mature dendritic cells facilitate prolonged cytotoxic T lymphocyte cross-priming capacity. *PNAS* 106, 6730–6735 (2009).
70. Platt, C. D. *et al.* Mature dendritic cells use endocytic receptors to capture and present antigens. *PNAS* 107, 4287–4292 (2010).
71. Ackerman, A. L. & Cresswell, P. Regulation of MHC class I transport in human dendritic cells and the dendritic-like cell line KG-1. *J. Immunol.* 170, 4178–88 (2003).
72. Macagno, A. *et al.* Dendritic cells up-regulate immunoproteasomes and the proteasome regulator PA28 during maturation. *Eur. J. Immunol.* 29, 4037–4042 (1999).
73. Delamarre, L., Holcombe, H. & Mellman, I. Presentation of Exogenous Antigens on Major Histocompatibility Complex (MHC) Class I and MHC Class II Molecules Is Differentially Regulated during Dendritic Cell Maturation. *J. Exp. Med. J. Exp. Med* 71111200, 111–122 (2003).
74. Gil-Torregrosa, B. C. *et al.* Control of cross-presentation during dendritic cell maturation. *Eur. J. Immunol.* 34, 398–407 (2004).
75. Cohn, L. *et al.* Antigen delivery to early endosomes eliminates the superiority of human blood BDCA3+ dendritic cells at cross presentation. *J. Exp. Med.* 210, 1049–63 (2013).
76. Fehling, H. J. *et al.* MHC class I expression in mice lacking the proteasome subunit LMP-7. *Science (80-.).* 265, 1234–7 (1994).
77. Muchamuel, T. *et al.* A selective inhibitor of the immunoproteasome subunit LMP7 blocks cytokine production and attenuates progression of experimental arthritis. *Nat. Med* 15, 781–788 (2009).
78. Cavassani, K. a *et al.* TLR3 is an endogenous sensor of tissue necrosis during acute inflammatory events. *J. Exp. Med.* 205, 2609–21 (2008).
79. Farina, G., York, M., Collins, C. & Lafyatis, R. dsRNA activation of endothelin-1 and markers of vascular activation in endothelial cells and fibroblasts. *Ann. Rheum. Dis.* 70, 544–50 (2011).

Chapter 3

CXCL4 is a novel inducer of human Th17 cells and correlates with IL-17 and IL-22 in psoriatic arthritis.

Alsya J. Affandi[1,2], Sandra C. Silva-Cardoso[1,2], Samuel Garcia[1,2], Emmerik F.A. Leijten[1,2], Tessa S. van Kempen[1,2], Wioleta Marut[1,2], Joel A.G. van Roon[1,2#], Timothy R.D.J. Radstake[1,2#]

[1] Laboratory of Translational Immunology, University Medical Center Utrecht, Utrecht University, Utrecht, The Netherlands
[2] Department of Rheumatology and Clinical Immunology, University Medical Center Utrecht, Utrecht University, Utrecht, The Netherlands
[#] Shared last co-authors

Eur J Immunol 2017 doi: 10.1002/eji.201747195

Abstract

CXCL4 regulates multiple facets of the immune response and is highly upregulated in various Th17-associated rheumatic diseases. However, whether CXCL4 plays a direct role in the induction of IL-17 production by human $CD4^+$ T cells is currently unclear. Here, we demonstrated that CXCL4 induced human $CD4^+$ T cells to secrete IL-17 that co-expressed IFNγ and IL-22, and differentiated naïve $CD4^+$ T cells to become Th17-cytokine producing cells. In a co-culture system of human $CD4^+$ T cells with monocytes or myeloid dendritic cells, CXCL4 induced IL-17 production upon triggering by superantigen. Moreover, when monocyte-derived dendritic cells were differentiated in the presence of CXCL4, they orchestrated increased levels of IL-17, IFNγ, and proliferation by $CD4^+$ T cells. Furthermore, the CXCL4 levels in synovial fluid from psoriatic arthritis patients strongly correlated with IL-17 and IL-22 levels. A similar response to CXCL4 of enhanced IL-17 production by $CD4^+$ T cells was also observed in patients with psoriatic arthritis. Altogether, we demonstrate that CXCL4 boosts pro-inflammatory cytokine production especially IL-17 by human $CD4^+$ T cells, either by acting directly or indirectly via myeloid antigen presenting cells, implicating a role for CXCL4 in PsA pathology.

Graphical abstract

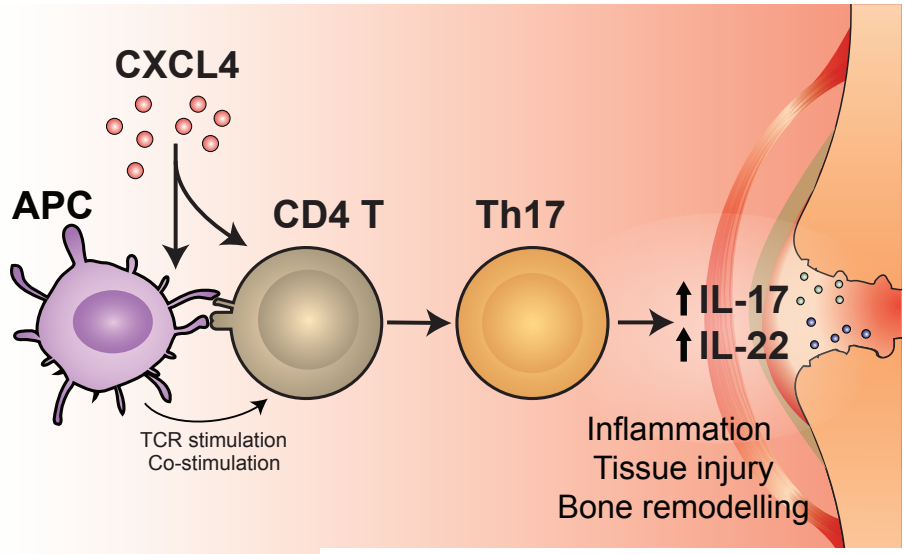

CXCL4 is highly increased in autoimmune and inflammatory disorders. Here we show that CXCL4 directs activated human CD4 T cells toward Th17 cells, by acting directly or indirectly via antigen presenting cells, in healthy and psoriatic arthritis patients. Our findings implicate a novel role for CXCL4 as a Th17 driver.

Introduction

$CD4^+$ T cells orchestrate immune responses in physiological and pathological conditions by secreting a wide array of cytokines. To gain effector functions, $CD4^+$ T cells require the engagement of T cell receptor and costimulatory molecules, in the presence of specific cytokines and chemokines, resulting in distinct subsets of T helper cells (Th). The interferon gamma (IFNγ)-secreting type 1 cells (Th1) and IL-4/IL-5/IL-13-producing type 2 cells (Th2) form the classical subsets of $CD4^+$ T cells, that have been expanded by discoveries of other T helper cells, such as the IL-17-secreting type 17 cells (Th17 cells)[1]. Characterized by expression of IL-17, IL-21, IL-22 and other pro-inflammatory mediators, Th17 cells are potent inducers of immune responses needed for pathogen clearance, but are also pivotal in the development of autoimmunity. Psoriasis (Pso), psoriatic arthritis (PsA), systemic lupus erythematosus, rheumatoid arthritis, and systemic sclerosis, are amongst the diseases where IL-17 involvement in the pathogenesis is evident[2–6]. In PsA, IL-17 producing cells accumulate in skin lesions and synovial fluid and play a destructive role by inducing tissue inflammation and bone erosion[7–9]. Therefore, it is important to understand the key upstream drivers of IL-17 activation in PsA.

CXCL4, previously known as platelet factor 4 (PF4), is an immunomodulatory chemokine produced by multiple immune cells that can target virtually all cells in the vasculature[10]. Besides the crucial role of CXCL4 in maintaining homeostasis, it has been implicated in many inflammatory conditions[11]. We and others reported elevated levels of CXCL4 in various Th17-associated rheumatic diseases[12–16], yet the role of CXCL4 in driving the Th17 pathway is largely unexplored. While it has been indicated previously that blocking CXCL4 in human platelet-$CD4^+$ T cells co-cultures led to a reduction of IL-17 production[17,18], direct effects of CXCL4 on Th17 responses have never been studied. Also, these findings of CXCL4 promoting Th17 activity were not supported by mouse studies[19,20].

Here we sought to investigate whether CXCL4 contributed to Th17 activation in human $CD4^+$ T cells and by which mechanisms it acted, directly on $CD4^+$ T cells or indirectly via antigen presenting cells (APCs). To support these findings, we went on to assess whether CXCL4 was also related to Th17 cytokines in a disease setting-in the inflamed joints of patients with PsA, a prototypical Th17 mediated disease.

Results

CXCL4 increases IL-17 producing cells in CD3/CD28-activated CD4$^+$ T cells

To investigate CXCL4 effect on T helper cell responses, CD4$^+$ T cells isolated from peripheral blood of healthy individuals were stimulated with α-CD3/CD28 in the absence or presence of CXCL4. CXCL4 significantly increased IL-17 production by CD4$^+$ T cells as compared to CD3/CD28 stimulation alone (**Fig. 1A,B**). This was supported by *de novo* synthesis of *IL17A* mRNA in CD4$^+$ T cells upon CXCL4 treatment (**Fig. S1** in Supporting Information). CXCL4 did not significantly alter the levels of other T helper cytokines (**Fig. 1C, Fig. S2A** in Supporting Information) nor did it affect proliferation (**Fig. S3A** in Supporting Information). In contrast, CXCL4 treatment induced co-expression of IFNγ and IL-22 in IL-17 positive cells (**Fig. 1D,E**). Therefore, our data indicates that CXCL4 directly induces human CD4$^+$ T cells to produce IL-17 in co-expression with other pro-inflammatory cytokines such as IFNγ and IL-22.

To further dissect CXCL4 effect on Th17 differentiation, we purified naïve CD4$^+$ T cells from peripheral blood of healthy individuals, and stimulated them with α-CD3/CD28 in the absence or presence of CXCL4. Similar to bulk CD4$^+$ T cells, CXCL4-treated naïve CD4$^+$ T cells showed an increased IL-17 production as compared to CD3/CD28 stimulation alone (**Fig. 2A,B**). CXCL4 did not change the levels of other T helper cytokines (**Fig. 2C**), however CXCL4 elevated the ratio of IL-17$^+$ IL-22$^+$ expressing cells (**Fig. 2D**). Thus, naïve CD4$^+$ T cells preferentially differentiate into Th17 cells when exposed to CXCL4.

CXCL4 induces IL-17 production by CD4$^+$ T cells when co-cultured with myeloid antigen-presenting cells

Next we addressed whether CXCL4-induced IL-17 induction was APCs-dependent. For this purpose, human CD4$^+$ T cells were co-cultured with antigen-presenting cells loaded with superantigen SEB. In an autologous co-culture of monocytes and CD4$^+$ T cells, we found that CXCL4 increased the secretion of IL-17 as compared to superantigen SEB alone (**Fig. 3A**). CXCL4 treatment also seemed to slightly induce IL-5 and IL-22 production. We further assessed the effect of CXCL4 on CD4$^+$ T cell cytokine production using three other APCs: myeloid dendritic cells (mDCs), plasmacytoid dendritic cells (pDCs) and B cells. We observed that CXCL4 significantly enhanced IL-17 production of CD4$^+$ T cells when co-cultured with mDCs (**Fig. 3B**), but not with pDCs or B cells. Previous data from others and our group indicate clear immunomodulatory effects of CXCL4 at higher doses[21,22]. In co-culture with monocytes, increasing amount of CXCL4 up to 5 μg/ml did not additionally enhance the IL-17 induction (**Fig. S4** in Supporting Information). The effect of CXCL4 on CD4$^+$ T

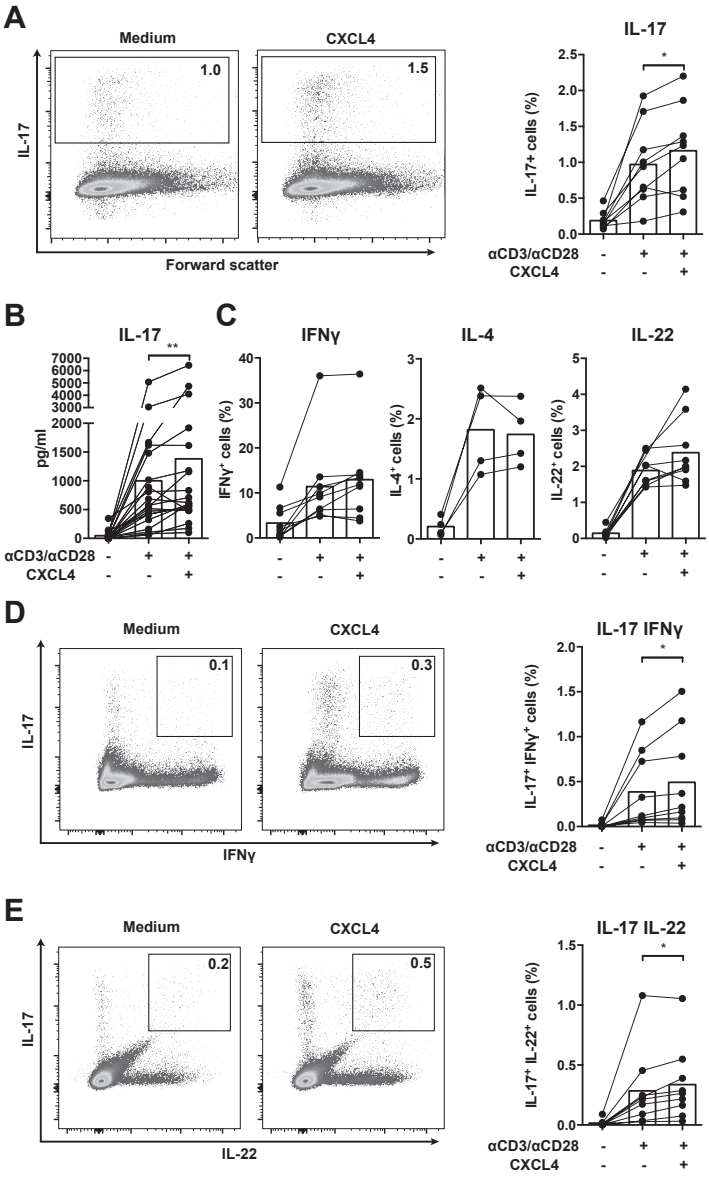

Figure 1. CXCL4 increases the percentage of IL-17 producing cells in CD3/CD28-stimulated human CD4 T cells. CD4 T cells were isolated from healthy donors and cultured with CD3/CD28 coated Dynabeads and CXCL4 for five days. (**A, B**) The effect of CXCL4 on IL-17 production by CD4 T cells was assessed by (**A**) flow cytometric intracellular cytokine staining and (**B**) enzyme-linked immunosorbent assay. (**C**) The percentage of of IFNγ-, IL-4- and IL-22-producing CD4 T cells were measured by flow cytometry. (**D, E**) The amount of IL-17 producing cells co-expressing IFNγ (**D**) or IL-22 (**E**) were measured by flow cytometry. Cells were gated on live, single cells. Means (bars) and values from each donor are shown. Data are pooled from two to four independent experiments, except for panel B from 14 independent experiments, with one to four donor samples per experiment. Each dot on the bar graphs represent a single donor and paired t-test was used for statistical analysis. * P<0.05, ** P<0.01.

cell proliferation upon activation with superantigen SEB-loaded APCs was minimal (**Fig. S3B,C** in Supporting Information). Thus, also in the presence of myeloid APCs, CXCL4 promotes the production of the pro-inflammatory IL-17 production by $CD4^+$ T cells.

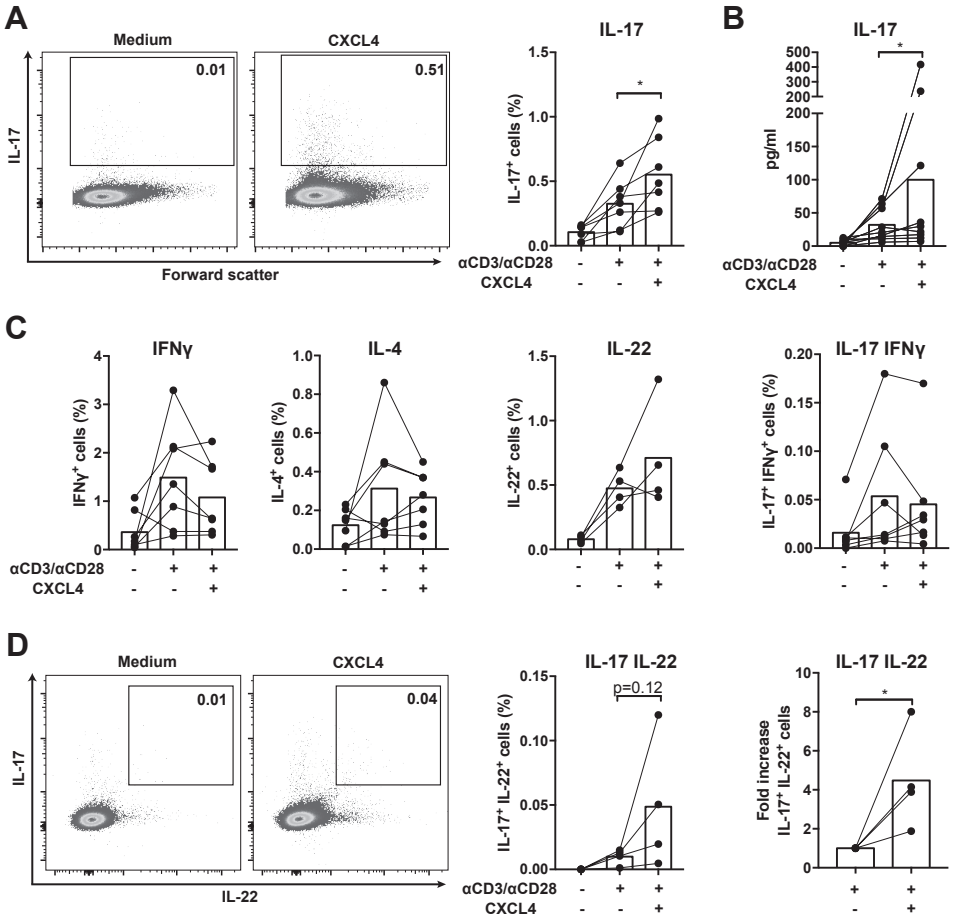

Figure 2. CXCL4 induces IL-17 producing cells differentiated from naïve human CD4 T cells. Naïve CD4 T cells were purified by fluorescence-activated cell sorting and cultured with CD3/CD28 coated Dynabeads and CXCL4 for seven days. (**A, B**) The effect of CXCL4 on IL-17 production by CD4 T cells was assessed by (**A**) flow cytometric intracellular cytokine staining and (**B**) enzyme-linked immunosorbent assay . (**C**) The levels of IFNγ-, IL-4-, IL-22-, and IL-17/IFNγ-producing CD4 T cells were measured by flow cytometry. (**D**) The amount of IL-17 producing cells co-expressing or IL-22 was measured by flow cytometry. Cells were gated on live, single cells. Means (bars) and values from each donor are shown. Data are pooled from four to 10 independent experiments, with one to two donor samples per experiment. Each dot on the bar graphs represent a single donor and paired t-test was used for statistical analysis. * P<0.05, ** P<0.01.

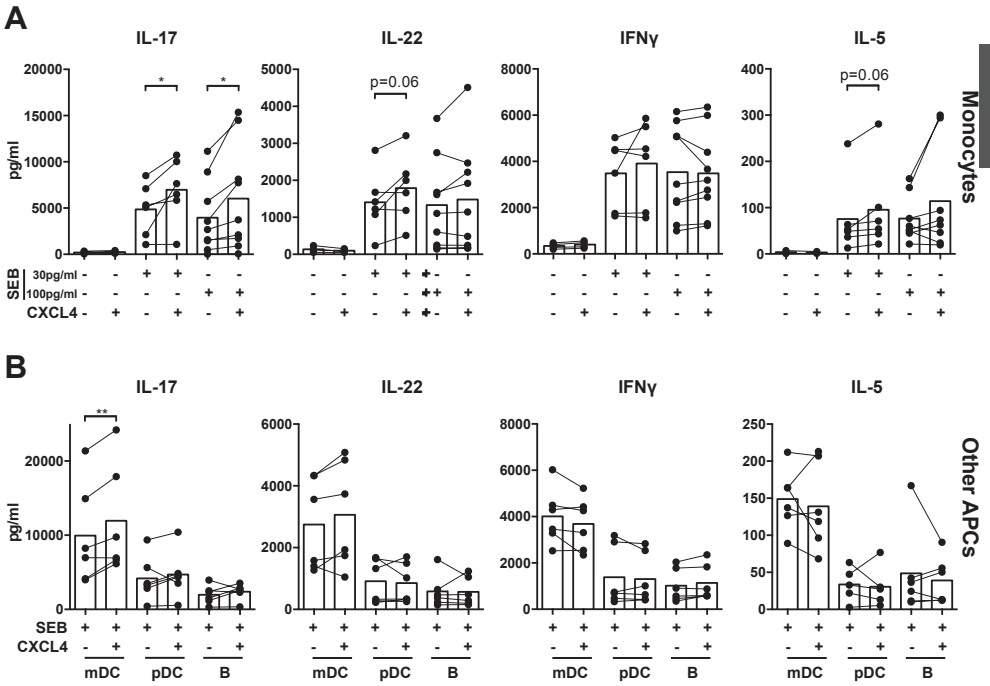

Figure 3. CXCL4 induces IL-17 production in autologous antigen-presenting cells (APCs)-CD4 T cells co-culture. Monocytes, B cells, myeloid dendritic cells (mDCs), plasmacytoid dendritic cells (pDCs), and CD4 T cells were isolated from healthy individuals, co-cultured in the absence or presence of superantigen from Staphylococcal enterotoxin B (SEB) and CXCL4 for three days and restimulated with PMA and ionomycin. (**A**) Supernatant from co-culture of monocytes and CD4 T cells stimulated with superantigen SEB and CXCL4 were measured for IL-17, IL-22, IFNγ, and IL-5. (**B**) The effect of CXCL4 treatment on 100 pg/ml superantigen SEB-activated CD4 T cells co-cultured with myeloid dendritic cells (mDCs), plasmacytoid dendritic cells (pDCs), or B cells, on IL-17, IL-22, IFNγ, and IL-5 production was assessed. Cytokines produced were determined using a Luminex-based assay. Means (bars) and values from each donor are shown. Data are pooled from two to five independent experiments, with one to four donor samples in duplicate per experiment. Each dot on the bar graphs represent a single donor Paired t-test was used for statistical analysis. * $P<0.05$, ** $P<0.01$.

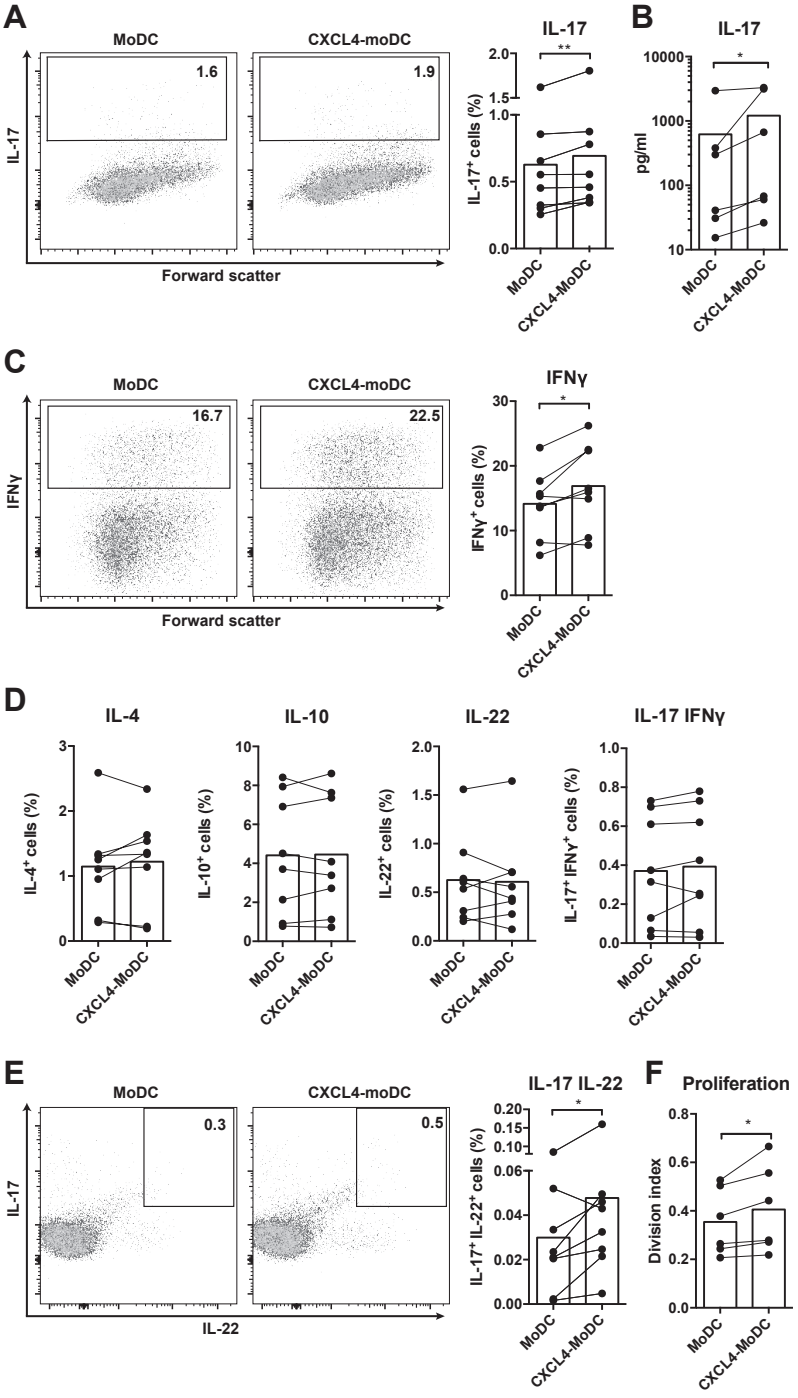
A
MoDC
CXCL4-moDC
1.6
1.9
IL-17
Forward scatter
IL-17
IL-17+ cells (%)
**
MoDC
CXCL4-MoDC
B
IL-17
pg/ml
*
MoDC
CXCL4-MoDC
C
MoDC
CXCL4-moDC
16.7
22.5
IFNγ
Forward scatter
IFNγ
IFNγ+ cells (%)
*
MoDC
CXCL4-MoDC
D
IL-4
IL-4+ cells (%)
MoDC
CXCL4-MoDC
IL-10
IL-10+ cells (%)
MoDC
CXCL4-MoDC
IL-22
IL-22+ cells (%)
MoDC
CXCL4-MoDC
IL-17 IFNγ
IL-17+ IFNγ+ cells (%)
MoDC
CXCL4-MoDC
E
MoDC
CXCL4-moDC
0.3
0.5
IL-17
IL-22
IL-17 IL-22
IL-17+ IL-22+ cells (%)
*
MoDC
CXCL4-MoDC
F
Proliferation
Division index
*
MoDC
CXCL4-MoDC

Figure 4. CXCL4-differentiated monocyte-derived dendritic cells enhance pro-inflammatory cytokine production and proliferation by CD4 T cells . Monocytes from healthy donors were isolated and differentiated into dendritic cells in the absence or presence of CXCL4 (moDCs or CXCL4-moDCs). moDCs were then co-cultured with autologous CD4 T cells in the presence of superantigen from Staphylococcal Enterotoxin B (SEB) for three days and restimulated with PMA and ionomycin. (**A-C**) Comparison of co-culture with moDC or CXCL4-moDC on IL-17 or IFNγ production by CD4 T cells was assessed by (**A, C**) intracellular cytokine staining and (**B**) enzyme-linked immunosorbent assay are shown. (**D**) Intracellular cytokine staining was performed for the measurement of IL-4$^+$, IL-10$^+$, IL-22$^+$, and IL-17$^+$IFNγ$^+$ cells gated on live CD4 T cells. (**E**) The amount of IL-17 producing cells co-expressing IL-22 as measured by flow cytometry. (**F**) CD4 T cells were labeled with CellTrace Violet prior co-culture and proliferation was analyzed as division index. Cells were gated on live, single, CD4 T cells. Means (bars) and values from each donor are shown. Data are pooled from two to three independent experiments, with two to three donor samples per experiment. Each dot on the bar graphs represent a single donor and paired t-test was used for statistical analysis. * P<0.05, ** P<0.01

CXCL4-primed monocyte-derived dendritic cells enhance CD4$^+$ T cell activation

Previous works have shown that during monocyte differentiation into dendritic cell or macrophage, the addition of CXCL4 resulted in an altered expression of cell surface markers and a distinct transcriptomic profile[22–24]. They also differed in their capacity to activate T cells, yet the effect on IL-17 production was not assessed. We added CXCL4 to monocytes differentiating into dendritic cells (moDCs) during culture with GM-CSF and IL-4. After differentiation, moDCs were co-cultured with autologous CD4$^+$ T cells in the presence of SEB. CXCL4-treated moDCs induced a higher IL-17 production by CD4$^+$ T cells as compared to conventional moDCs (**Fig. 4A,B**). CXCL4 treatment also increased the percentage of IFNγ-producing cells (**Fig. 4C**), but not IL-4 or IL-10 producing cells (**Fig. 4D**). Interestingly, CXCL4-treated moDCs increased the percentage of co-expressing IL17$^+$ IL-22$^+$ cells (**Fig. 4E**). CXCL4-treated moDCs also significantly potentiated CD4$^+$ T cell proliferation (**Fig. 4F, Fig. S3D** in Supporting Information). Therefore, our data suggest that CXCL4 modulates moDCs to induce proliferation of CD4$^+$ T cells and production of pro-inflammatory cytokines, especially IL-17.

CXCL4 is increased in Th17 diseases and correlates with Th17 cytokines at the site of inflammation

To assess potential clinical relevance of our findings above, we measured the level of circulating CXCL4 in patients with Pso and PsA, both known to be type 17-driven autoimmune diseases. The level of CXCL4 in the circulation was previously shown to be increased in Pso patients[14]. Here we found that the plasma level of CXCL4 was increased in both Pso and PsA patients as compared to healthy individuals (**Fig. 5A**). We then examined intra-articular level of CXCL4 from patients with PsA

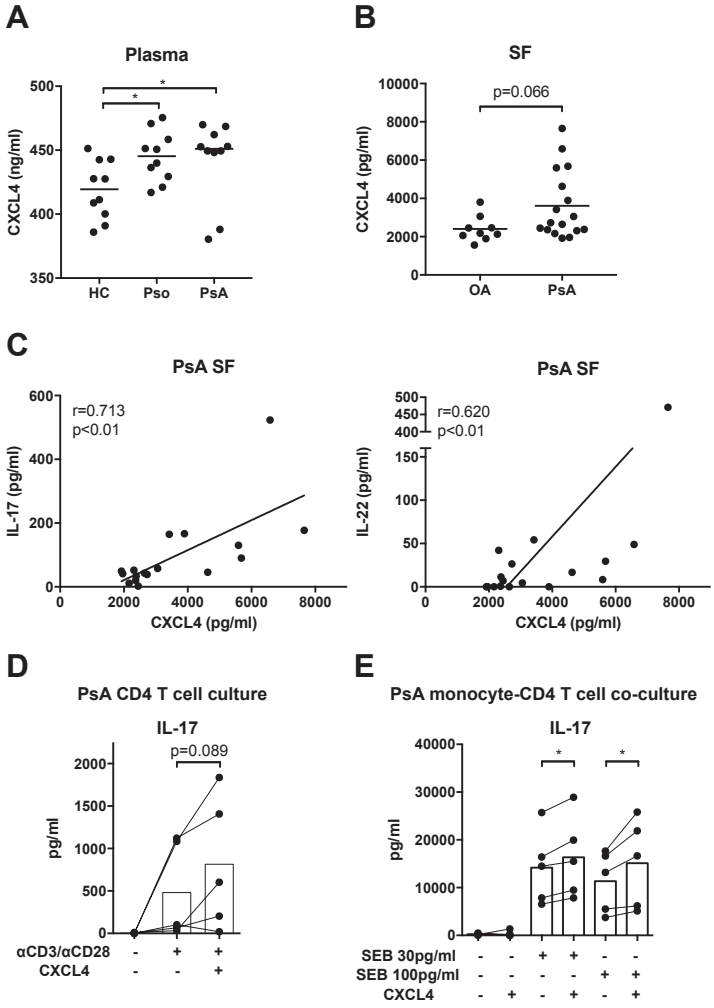

Figure 5. CXCL4 expression is upregulated in Th17-mediated diseases, correlates with Th17 cytokine levels in the synovial fluid of psoriatic arthritis joints, and induces IL-17 production in psoriatic arthritis patients. Plasma was obtained from healthy controls (HC), psoriasis (Pso), or psoriatic arthritis (PsA) patients, and synovial fluid (SF) from PsA and osteoarthritis (OA) patients. Monocytes and CD4 T cells were isolated from PsA patients and CXCL4 effect was assayed in (co-) cultures. (**A**) CXCL4 was measured in the plasma of HC, Pso, or PsA patients by enzyme-linked immunosorbent assay. Kruskal-Wallis test was used for statistical analysis. (**B**) The levels of CXCL4 was measured in SF from OA and PsA patients using a Luminex-based assay. Mann-Whitney test was used for statistical analysis. (**C**) The intraarticular levels of CXCL4, IL-17, and IL-22 in PsA SF were measured using Luminex-based assay. Correlation between cytokine levels was assessed by Spearman's correlation. (**D, E**) The effects of 2 µg/ml CXCL4 on secreted IL-17 by CD4 T cells from PsA patients upon (**D**) CD3/CD28 stimulation or (**E**) co-culture with autologous monocytes in the absence or presence of superantigen from Staphylococcal Enterotoxin B (SEB) as assessed by enzyme-linked immunosorbent assay are shown. Data are pooled from three independent experiments, with one to two patient samples in duplicate per experiment. Means (bars) and values from each patient are shown and paired t-test was used for statistical analysis. * P<0.05.

and patients with osteoarthritis as a non-autoimmune disease control group. In SF, we found a trend toward increased CXCL4 levels in patients with PsA as compared to those with osteoarthritis (**Fig. 5B**, p=0.066). To determine whether CXCL4 mediates Th17 activation *in vivo* at the site of inflammation, we measured CXCL4 and T cell-derived cytokines in the SF of patients with PsA. Remarkably, CXCL4 strongly correlated with both IL-17 (r=0.713, p<0.01) and IL-22 (r=0.620, p<0.01) (**Fig. 5C**), whereas CXCL4 did not correlate with IFNγ, IL-5, IL-10, nor GM-CSF in the SF of PsA patients, clearly mimicking our *in vitro* results. The enhanced IL-17 production by $CD4^+$ T cells upon CXCL4 treatment was also observed in PsA patients (**Fig. 5D,E**). Additionally, we had five donors from which multiple synovial fluid samples was collected multiple times at different time points. CXCL4 level completely mirrored the changes of IL-17 amount in PsA SF over time in four out of five PsA patients (**Fig. S5** in Supporting Information). These data suggest that in PsA, higher CXCL4 levels are associated with increased Th17 cytokines locally at the site of inflammation.

Discussion

IL-17 producing cells have been implicated to play a major role in multiple autoimmune and chronic inflammatory disorders. Here we show that CXCL4 – a chemokine shown to be highly present in many of these disorders – directly and indirectly promotes the production of IL-17 by human $CD4^+$ T cells (**Fig. 6**). In addition to that, CXCL4 enhances the levels IL-17 secreting cells that also produce IFNγ and IL-22. Moreover, in the Th17-mediated disease context of PsA, CXCL4 level in PsA SF is significantly associated with IL-17 and IL-22 levels.

Previous reports on CXCL4 effects on the regulation of T cells have been inconsistent. CXCL4 was described to inhibit the expression of IFNγ (Th1) while favoring IL-13 (Th2) on cultured naïve $CD4^+$ T cells[25]. However, another study suggested that CXCL4 only induced the proliferation and cytokine production of $CD4^+$ $CD25^+$ T cells, but not $CD4^+$ $CD25^-$ T cells[26]. Our data are the first evidence revealing a direct CXCL4 effect on driving IL-17 production by $CD4^+$ T cells. Moreover, multiple studies showed that platelets, that can secrete a large amount of CXCL4, promoted $CD4^+$ T cells IL-17 production in a co-culture, thus supporting our findings[17,18,27]. CXCL4 also increased the amount of $IL\text{-}17^+$ double producers with IFNγ and IL-22. These cells have been found in many human inflammatory conditions[28–32], therefore the induction of $IL\text{-}17^+$ cells and their co-expression with IFNγ and IL-22 by CXCL4 may exacerbate pathological processes.

CXCL4 is known to elicit inflammatory response on myeloid cells. On monocytes, CXCL4 has been shown to promote their survival and pro-inflammatory cytokines

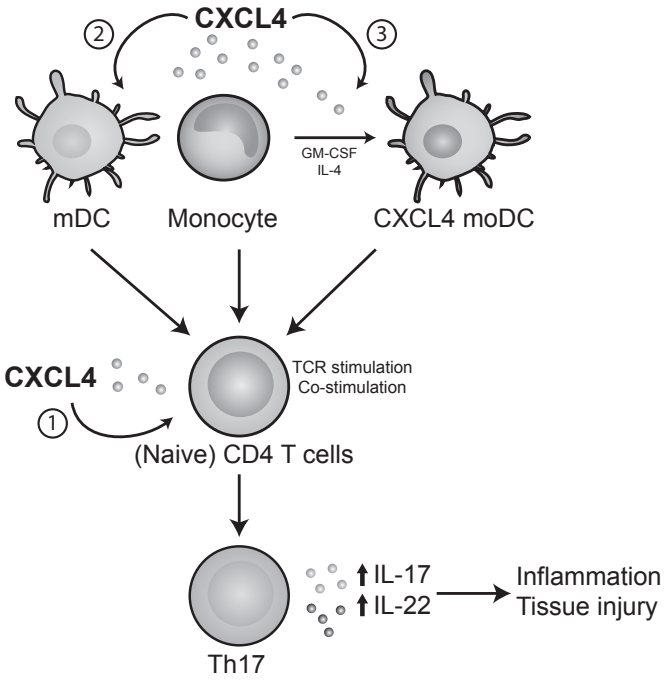

Figure 6. Proposed mechanisms of CXCL4 as a novel Th17 driver. CXCL4 promotes IL-17 production in human CD4 T cells by acting (1) directly on CD3/CD28-activated human (naïve) CD4 T cells, and (2) indirectly in a co-culture of CD4 T cells with monocytes and myeloid dendritic cells (mDCs). (3) CXCL4 also primed monocytes-derived dendritic cells (CXCL4-moDCs) to induce IL-17 production and proliferation in activated CD4 T cells. These IL-17-producing cells also co-produce IL-22, which results in an increased immune response at the site of inflammation, such as a psoriatic arthritis joint.

production, such as IL-6, TNFα, as well as reactive oxygen species[33,34]. While there is little known about the effect of CXCL4 on mDC, we previously showed that CXCL4 could enhance IFNα production by pDCs upon toll-like receptor stimulation[12]. We recently demonstrated that CXCL4 potentiated moDCs cytokine production upon toll-like receptor stimulation[22]. Through regulating APC function, CXCL4 can promote an inflammatory environment that results in an increased IL-17 production by $CD4^+$ T cells.

SF from PsA patients contains many soluble mediators that recruit immune cells and promote tissue inflammation. The source of CXCL4 in PsA SF has yet to be identified. Macrophages have been suggested to contribute to the overexpression of CXCL4 in rheumatoid arthritis synovium[13]. mDCs and pDCs, both capable of producing CXCL4, are increased in PsA and rheumatoid arthritis SF[35–37]. Furthermore, in addition to $CD4^+$ T cells, there are other type 17 cells enriched in the PsA SF,

including the type 3 innate lymphoid cells[38], CD8 T cells[39], and γδ T cells[40]. CXCL4 contribution to the IL-17 regulation in these cells still needs to be evaluated.

Compelling evidence suggests a pro-inflammatory role for CXCL4 in multiple mouse inflammation models[12,41–43], however it is intriguing that some studies showed CXCL4 to suppress IL-17 production[19,20]. The underlying mechanism is unclear, the apparent species-specific prerequisite for Th17 development in human and mice may contribute to this discrepancy[44–46]. Furthermore, human Th17 cells also did not seem to co-produce GM-CSF as seen in mice studies[47], and our data showed that CXCL4 did not influence GM-CSF production by human $CD4^+$ T cells in vitro. In support of this, no correlations were found between CXCL4 and GM-CSF in inflamed PsA joint.

In conclusion, we have identified CXCL4 as a new Th17 driver, that is able to directly and indirectly promote IL-17 production in human $CD4^+$ T cells, and that it correlates with Th17 cytokines levels intra-articularly, at inflammatory site of PsA patients. These data strongly suggest CXCL4 to play a significant role in Th17 regulation in PsA. Further research to dissect the molecular mechanisms involved and to assess the CXCL4 contribution in other Th17-mediated diseases are necessary.

Materials and Methods

Patients population

Peripheral blood and synovial fluid (SF) were obtained in accordance with the local Institutional Review Board's approval and patients gave their written informed consent. For plasma measurement, blood was collected from 10 healthy controls, 10 patients with Pso, and 10 patients with PsA. Venous blood was collected in a 10 ml EDTA vacutainer (#367864, BD Biosciences), centrifuged at 1700xg for 10 min, and plasma was collected. SF samples were isolated from 17 patients with PsA and nine patients with osteoarthritis. All SF samples were collected from effusion of the knee as part of routine clinical care. For SF collection, fluids were centrifuged at 2300 xg for 10 min at 4°C to remove cells and debris. All samples were aliquoted and immediately frozen at –80°C until further use. Patients with PsA fulfilled Classification of Psoriatic Arthritis Study Group criteria and their characteristics are summarized in

Table S1 in Supporting Information.

Cell isolation

Peripheral blood mononuclear cells from healthy donors and PsA patients were isolated by Ficoll gradient (#17-1440-02, GE Healthcare). Cells were processed for further isolation using magnetic beads for plasmacytoid dendritic cells (pDCs, #130-

090-532), myeloid dendritic cells (mDCs) and B cells (#130-094-487), monocytes (#130-050-201), and $CD4^+$ T cells (#130-096-533) on autoMACS Pro Separator according to manufacturer's instructions, all from Miltenyi Biotec. Naïve $CD4^+$ T cells ($CD127^+$ $CD25^-$ $CD27^+$ $CD4^+5RO^-$) were further purified using fluorescence-activated cell sorting on BD FACSAria (BD Biosciences). Purity was routinely above 99% for naïve $CD4^+$ T cells, 95% for bulk $CD4^+$ T cells, and above 90% for other cells as assessed by flow cytometry. Cells were washed and cultured with complete medium of RPMI-GlutaMAX (#61870-010, Thermo Fisher Scientific) supplemented with 10% FBS (Biowest) and Penicillin-Streptomycin (#15070063, Thermo Fisher Scientific).

T cell stimulation

50,000 $CD4^+$ T cells were cultured in a complete medium on a 96-well round bottom plate at 37°C for three to seven days. In $CD4^+$ T cells monoculture, cells were activated with Dynabeads Human T-Activator CD3/CD28 (#111.31D, Thermo Fisher Scientific) at bead-to-cell ratio of 1:5. In autologous co-culture with antigen-presenting cells (APCs), $CD4^+$ T cells were cultured with pDCs, mDCs, B cells, monocytes, or monocytes-derived DCs (moDCs) at APC-to-$CD4^+$ T cell ratio of 1:5, in the presence of superantigen from Staphylococcal Enterotoxin B (SEB) (#S4881, Sigma Aldrich). Recombinant human CXCL4 (#300-16, Peprotech) was added as indicated. For restimulation, cells were stimulated with phorbol 12-myristate 13-acetate (PMA, #P8139) and ionomycin (#I0634, all Sigma Aldrich) overnight. For intracellular cytokine staining, PMA, ionomycin and GolgiStop (#554724, BD Biosciences) was added for the final four hours of culture. For proliferation analysis, $CD4^+$ T cells were labeled with CellTrace Violet (1.5 µM; #C34557 Thermo Fisher Scientific) prior culture.

Monocyte-derived dendritic cells

Monocytes were cultured at a density of 1 million cells/ml in complete medium with 800 IU/ml recombinant human granulocyte-macrophage colony-stimulating factor (GM-CSF, #204-IL, R&D Systems), 500 IU/ml recombinant human IL-4 (#215-GMP, R&D Systems), in the presence or absence of 10 µg/ml recombinant human CXCL4 for six days, with medium and cytokines refreshment on day three. Cells were harvested and remaining cytokines were washed in complete medium and rested for 1-2 h at 37°C prior to co-culture with $CD4^+$ T cells from the same donor.

Flow cytometry

For intracellular cytokine staining, cells were stained with Fixable Viability Dye (#65-0866, eBioscience) for dead cell exclusion, then cells were fixed and permeabilized using Foxp3/Transcription Factor Staining Buffer Set (#00-5523, eBioscience), and stained for IL-17A (#11-7179), IL-22 (#17-7222), IFNγ (#45-7319, #12-7319,

eBioscience), IL-4 (#564112, BD Biosciences), IL-10 (#554706, BD Biosciences), GM-CSF (#502317, Biolegend), CD3 (#48-0038), and $CD4^+$ (#25-0049 eBioscience). Cells were acquired on BD LSRFortessa (BD Biosciences). Cells were gated to exclude debris, doublets, and dead cells and analyzed by FlowJo software (Tree Star). Division index was calculated as a measure of proliferation, following FlowJo guidelines. Alternatively, percentage of proliferated cells (CellTrace $Violet^-$) was shown.

Cytokine measurement

Cytokines in cell-free supernatant, plasma, or synovial fluid, were measured using enzyme-linked immunosorbent assay (IL-17A, #88-7176, eBioscience; CXCL4, #DY795, R&D Systems; GM-CSF, #88-8337, eBioscience) or using a multiplex immunoassay based on xMAP technology (Luminex) at the MultiPlex Core Facility of the Laboratory of Translational Immunology, University Medical Center Utrecht[48]. For the Luminex-based assay, acquisition was performed with a Biorad FlexMap3D system using Xponent 4.2 software and analyzed using Bio-Plex Manager 6.1.1.

Statistical analysis

Paired t-test, Mann-Whitney test, Kruskal-Wallis test, or Spearman's correlation analysis, were calculated using GraphPad Prism 6.0 Software. Differences of $P<0.05$ were considered significantly different.

Acknowledgments

Alsya J. Affandi was supported by the Dutch Arthritis Association (Reumafonds grant NR-10-1-301) and the Netherlands Organization for Scientific Research (Mosaic grant 017.008.014). Sandra C. Silva-Cardoso was supported by a PhD grant from the Portuguese Fundação para a Ciência e a Tecnologia (SFRH/BD/89643/2012). Wioleta Marut obtained funding from Marie Curie Intra-European Fellowship (Proposal number: 624871). Timothy R.D.J. Radstake received funding from ERC Starting Grant (ERC-2011-StG, Circumvent).

All the authors listed have made substantial, direct, and intellectual contribution to the work and approved it for publication. We thank Wilco de Jager (MultiPlex Core Facility, University Medical Center Utrecht) for performing Luminex assays. We thank Sytze de Roock, Gerdien Mijnheer, Tiago Carvalheiro, and Ana P. Lopes for their valuable inputs and technical advices. We acknowledge the contributions of Michel A.M. Olde Nordkamp, Arno N. Concepcion, and Fréderique M. Moret for collection of samples and clinical information.

References

1. Gaffen, S. L., Jain, R., Garg, A. V & Cua, D. J. The IL-23-IL-17 immune axis: from mechanisms to therapeutic testing. *Nat. Rev. Immunol.* **14,** 585–600 (2014).
2. Kim, J. & Krueger, J. G. Highly Effective New Treatments for Psoriasis Target the IL-23/Type 17 T Cell Autoimmune Axis. *Annu. Rev. Med.* **68,** 255–269 (2017).
3. Rother, N. & van der Vlag, J. Disturbed T Cell Signaling and Altered Th17 and Regulatory T Cell Subsets in the Pathogenesis of Systemic Lupus Erythematosus. *Front. Immunol.* **6,** 610 (2015).
4. Pattanaik, D., Brown, M., Postlethwaite, B. C. & Postlethwaite, A. E. Pathogenesis of Systemic Sclerosis. *Front. Immunol.* **6,** 272 (2015).
5. Lubberts, E. The IL-23-IL-17 axis in inflammatory arthritis. *Nat Rev Rheumatol* **11,** 415–429 (2015).
6. Ritchlin, C. T., Colbert, R. A. & Gladman, D. D. Psoriatic Arthritis. *N. Engl. J. Med.* **376,** 957–970 (2017).
7. Adamopoulos, I. E. *et al.* IL-17A gene transfer induces bone loss and epidermal hyperplasia associated with psoriatic arthritis. *Ann. Rheum. Dis.* **74,** 1284–92 (2015).
8. Raychaudhuri, S. P. & Raychaudhuri, S. K. IL-23/IL-17 axis in spondyloarthritis-bench to bedside. *Clin. Rheumatol.* **35,** 1437–41 (2016).
9. Raychaudhuri, S. P., Raychaudhuri, S. K. & Genovese, M. C. IL-17 receptor and its functional significance in psoriatic arthritis. *Mol. Cell. Biochem.* **359,** 419–29 (2012).
10. Kasper, B. & Petersen, F. Molecular pathways of platelet factor 4/CXCL4 signaling. *Eur. J. Cell Biol.* **90,** 521–6 (2011).
11. Karshovska, E., Weber, C. & von Hundelshausen, P. Platelet chemokines in health and disease. *Thromb. Haemost.* **110,** 894–902 (2013).
12. van Bon, L. *et al.* Proteome-wide analysis and CXCL4 as a biomarker in systemic sclerosis. *N. Engl. J. Med.* **370,** 433–43 (2014).
13. Yeo, L. *et al.* Expression of chemokines CXCL4 and CXCL7 by synovial macrophages defines an early stage of rheumatoid arthritis. *Ann. Rheum. Dis.* **75,** 763–71 (2016).
14. Tamagawa-Mineoka, R., Katoh, N., Ueda, E., Masuda, K. & Kishimoto, S. Elevated platelet activation in patients with atopic dermatitis and psoriasis: increased plasma levels of beta-thromboglobulin and platelet factor 4. *Allergol. Int.* **57,** 391–6 (2008).
15. Vettori, S. *et al.* Serum CXCL4 increase in primary Sjögren's syndrome characterizes patients with microvascular involvement and reduced salivary gland infiltration and lymph node involvement. *Clin. Rheumatol.* **35,** 2591–6 (2016).
16. Patsouras, M. D. *et al.* Elevated expression of platelet-derived chemokines in patients with antiphospholipid syndrome. *J. Autoimmun.* **65,** 30–7 (2015).
17. Starossom, S. C. *et al.* Platelets Play Differential Role During the Initiation and Progression of Autoimmune Neuroinflammation. *Circ. Res.* **117,** 779–92 (2015).
18. Gerdes, N. *et al.* Platelets regulate $CD4^+$ T-cell differentiation via multiple chemokines in humans. *Thromb. Haemost.* **106,** 353–62 (2011).
19. Fang, S. *et al.* Platelet factor 4 inhibits IL-17/Stat3 pathway via upregulation of SOCS3 expression in melanoma. *Inflammation* **37,** 1744–50 (2014).
20. Shi, G. *et al.* Platelet factor 4 limits Th17 differentiation and cardiac allograft rejection. *J. Clin. Invest.* **124,** 543–52 (2014).
21. Gouwy, M. *et al.* CXCL4 and CXCL4L1 Differentially Affect Monocyte Survival and Dendritic Cell Differentiation and Phagocytosis. *PLoS One* **11,** e0166006 (2016).
22. Silva-Cardoso, S. C. *et al.* CXCL4 Exposure Potentiates TLR-Driven Polarization of Human Monocyte-Derived Dendritic Cells and Increases Stimulation of T Cells. *J. Immunol.* **199,** 253–262 (2017).
23. Xia, C.-Q. & Kao, K.-J. Effect of CXC chemokine platelet factor 4 on differentiation and function of monocyte-derived dendritic cells. *Int. Immunol.* **15,** 1007–15 (2003).

24. Gleissner, C. a, Shaked, I., Little, K. M. & Ley, K. CXC chemokine ligand 4 induces a unique transcriptome in monocyte-derived macrophages. *J. Immunol.* **184,** 4810–8 (2010).
25. Romagnani, P. *et al.* CXCR3-mediated opposite effects of CXCL10 and CXCL4 on TH1 or TH2 cytokine production. *J. Allergy Clin. Immunol.* **116,** 1372–9 (2005).
26. Liu, C. Y. *et al.* Platelet factor 4 differentially modulates CD4+CD25+ (regulatory) versus CD4+CD25- (nonregulatory) T cells. *J. Immunol.* **174,** 2680–6 (2005).
27. Zhu, L., Huang, Z., Stålesen, R., Hansson, G. K. & Li, N. Platelets provoke distinct dynamics of immune responses by differentially regulating CD4+ T-cell proliferation. *J. Thromb. Haemost.* **12,** 1156–65 (2014).
28. Annunziato, F. *et al.* Phenotypic and functional features of human Th17 cells. *J. Exp. Med.* **204,** 1849–61 (2007).
29. Kryczek, I. *et al.* Induction of IL-17+ T cell trafficking and development by IFN-gamma: mechanism and pathological relevance in psoriasis. *J. Immunol.* **181,** 4733–41 (2008).
30. Nistala, K. *et al.* Th17 plasticity in human autoimmune arthritis is driven by the inflammatory environment. *Proc. Natl. Acad. Sci. U. S. A.* **107,** 14751–6 (2010).
31. Benham, H. *et al.* Th17 and Th22 cells in psoriatic arthritis and psoriasis. *Arthritis Res. Ther.* **15,** R136 (2013).
32. Truchetet, M.-E., Brembilla, N. C., Montanari, E., Allanore, Y. & Chizzolini, C. Increased frequency of circulating Th22 in addition to Th17 and Th2 lymphocytes in systemic sclerosis: association with interstitial lung disease. *Arthritis Res. Ther.* **13,** R166 (2011).
33. Scheuerer, B. *et al.* The CXC-chemokine platelet factor 4 promotes monocyte survival and induces monocyte differentiation into macrophages. *Blood* **95,** 1158–66 (2000).
34. Kasper, B. *et al.* CXCL4-induced monocyte survival, cytokine expression, and oxygen radical formation is regulated by sphingosine kinase 1. *Eur. J. Immunol.* **40,** 1162–73 (2010).
35. Moret, F. M. *et al.* Intra-articular CD1c-expressing myeloid dendritic cells from rheumatoid arthritis patients express a unique set of T cell-attracting chemokines and spontaneously induce Th1, Th17 and Th2 cell activity. *Arthritis Res. Ther.* **15,** R155 (2013).
36. Jongbloed, S. L. *et al.* Enumeration and phenotypical analysis of distinct dendritic cell subsets in psoriatic arthritis and rheumatoid arthritis. *Arthritis Res. Ther.* **8,** R15 (2006).
37. Lande, R. *et al.* Characterization and recruitment of plasmacytoid dendritic cells in synovial fluid and tissue of patients with chronic inflammatory arthritis. *J. Immunol.* **173,** 2815–24 (2004).
38. Leijten, E. F. A. *et al.* Brief report: enrichment of activated group 3 innate lymphoid cells in psoriatic arthritis synovial fluid. *Arthritis Rheumatol. (Hoboken, N.J.)* **67,** 2673–8 (2015).
39. Menon, B. *et al.* Interleukin-17+CD8+ T cells are enriched in the joints of patients with psoriatic arthritis and correlate with disease activity and joint damage progression. *Arthritis Rheumatol. (Hoboken, N.J.)* **66,** 1272–81 (2014).
40. Guggino, G. *et al.* Interleukin (IL)-9/IL-9R axis drives γδ T cells activation in psoriatic arthritis patients. *Clin. Exp. Immunol.* **186,** 277–283 (2016).
41. Koenen, R. R. *et al.* Disrupting functional interactions between platelet chemokines inhibits atherosclerosis in hyperlipidemic mice. *Nat. Med.* **15,** 97–103 (2009).
42. Grommes, J. *et al.* Disruption of platelet-derived chemokine heteromers prevents neutrophil extravasation in acute lung injury. *Am. J. Respir. Crit. Care Med.* **185,** 628–36 (2012).
43. Lapchak, P. H. *et al.* The role of platelet factor 4 in local and remote tissue damage in a mouse model of mesenteric ischemia/reperfusion injury. *PLoS One* **7,** e39934 (2012).

44. Shay, T. *et al.* Conservation and divergence in the transcriptional programs of the human and mouse immune systems. *Proc. Natl. Acad. Sci. U. S. A.* **110,** 2946–51 (2013).
45. Schmitt, N. & Ueno, H. Regulation of human helper T cell subset differentiation by cytokines. *Curr. Opin. Immunol.* **34,** 130–6 (2015).
46. Annunziato, F., Cosmi, L., Liotta, F., Maggi, E. & Romagnani, S. Human Th17 cells: are they different from murine Th17 cells? *Eur. J. Immunol.* **39,** 637–40 (2009).
47. Noster, R. *et al.* IL-17 and GM-CSF expression are antagonistically regulated by human T helper cells. *Sci. Transl. Med.* **6,** 241ra80 (2014).
48. de Jager, W., Prakken, B. J., Bijlsma, J. W. J., Kuis, W. & Rijkers, G. T. Improved multiplex immunoassay performance in human plasma and synovial fluid following removal of interfering heterophilic antibodies. *J. Immunol. Methods* **300,** 124–35 (2005).

Supporting Information

Supplementary Materials and Methods

RNA extraction and gene expression analysis

Total RNA was isolated from cell lysates using the RNeasy Mini Kit (#74106 Qiagen), according to the manufacturer's instructions. Gene expression was analysed by quantitative PCR using a 3 ng RNA-equivalent after retrotranscription with iScript cDNA Synthesis Kit (#1708891 Bio-Rad). Reactions were conducted using the SYBR Select Master Mix with 500 nM specific primer pairs on a StepOnePlus Real-Time PCR System (ThermoFisher Scientific). Fold change was calculated using the comparative cycle threshold (ΔΔCt) method and values were normalized to the expression of B2M. All primers used are listed in **Table S2**.

Naïve $CD4^+$ T cell isolation

Peripheral blood mononuclear cells from healthy donors were isolated by Ficoll gradient (#17-1440- 02, GE Healthcare). Cells were first enriched using magnetic beads for $CD4^+$ T cells (#130-096-533, Miltenyi Biotec) on autoMACS Pro Separator (Miltenyi Biotec) according to manufacturer's instructions. After staining with antibodies for 30 min at 4°C, naïve $CD4^+$ T cells ($CD3^+$ $CD4^+$ $CD127^+$ $CD25^-$ $CD27^+$ $CD4^+5RO^-$) were further purified using fluorescence-activated cell sorting on BD FACSAria (BD Biosciences). Antibodies used are listed in **Table S3**.

Supplementary Figures

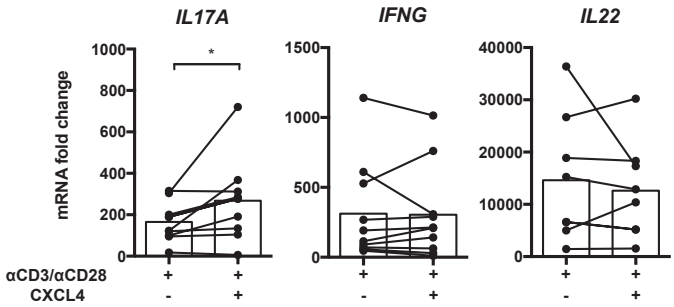

Figure S1. CXCL4 increases IL-17 mRNA in stimulated human CD4 T cells. CD4 T cells were isolated from healthy individuals and cultured with CD3/CD28 Dynabeads and 2 µg/ml CXCL4 for 24 h. RNA was isolated, followed by cDNA synthesis, and gene expressions were assessed. The effect of CXCL4 on *IL17A, IFNG,* and *IL22* mRNA in CD4 T cells was determined by quantitative PCR. Mean and values from each donor are shown and paired t-test was used for statistical analysis. * P<0.05.

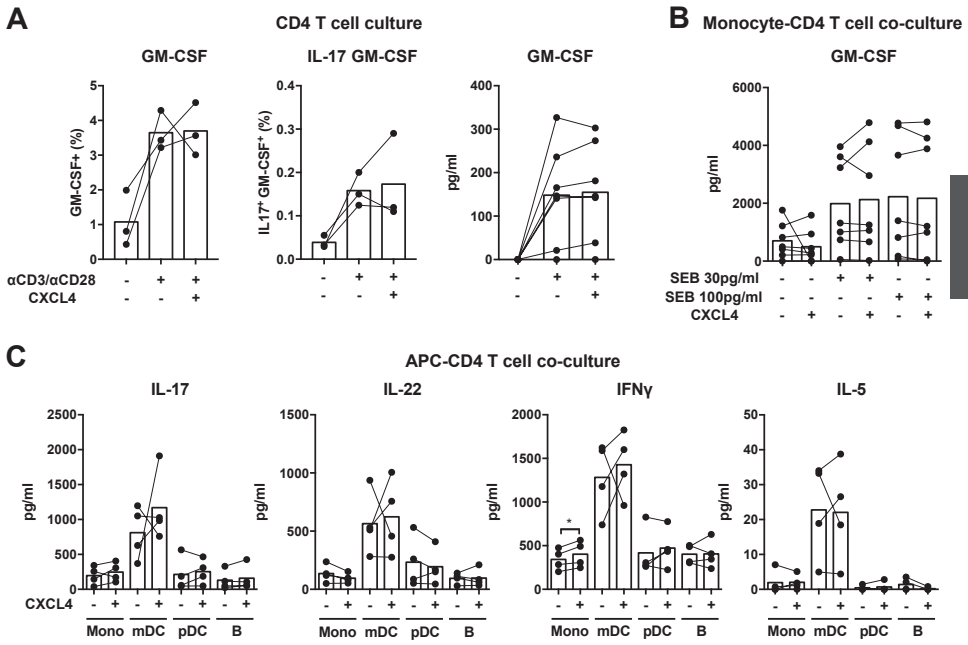

Figure S2. CXCL4 effect on GM-CSF and other cytokines on human CD4 T cells. CD4 T cells and antigen presenting cells (APCs) were isolated from healthy individuals and CXCL4 effect was assessed during (co-) cultures. (**A**) CD4 T cells were cultured with CD3/CD28 Dynabeads and 2 µg/ml CXCL4 for five days. Supernatant was collected for secreted cytokine measurement and cells were fixed and permeabilized for intracellular cytokine staining for GM-CSF+ cells or IL-17+ GM- CSF+ cells. (**B**) Monocytes and CD4 T cells were co-cultured in the absence or presence of superantigen from Staphylococcal enterotoxin B (SEB) and 2 µg/ml of CXCL4 for three days and restimulated with PMA and ionomycin. (**C**) Monocytes (Mono), myeloid dendritic cells (mDC), plasmacytoid dendritic cells (pDC), B cells (B), and CD4 T cells were co-cultured without superantigen SEB in the absence or presence of 2 µg/ml CXCL4 for three days and restimulated with PMA and ionomycin. Cell-free supernatant was collected and secreted cytokines were assessed by enzyme-linked immunosorbent assay or Luminex-based immunoassay. Means (bars) and values from each different donor are shown and paired t-test was used for statistical analysis. * $P<0.05$.

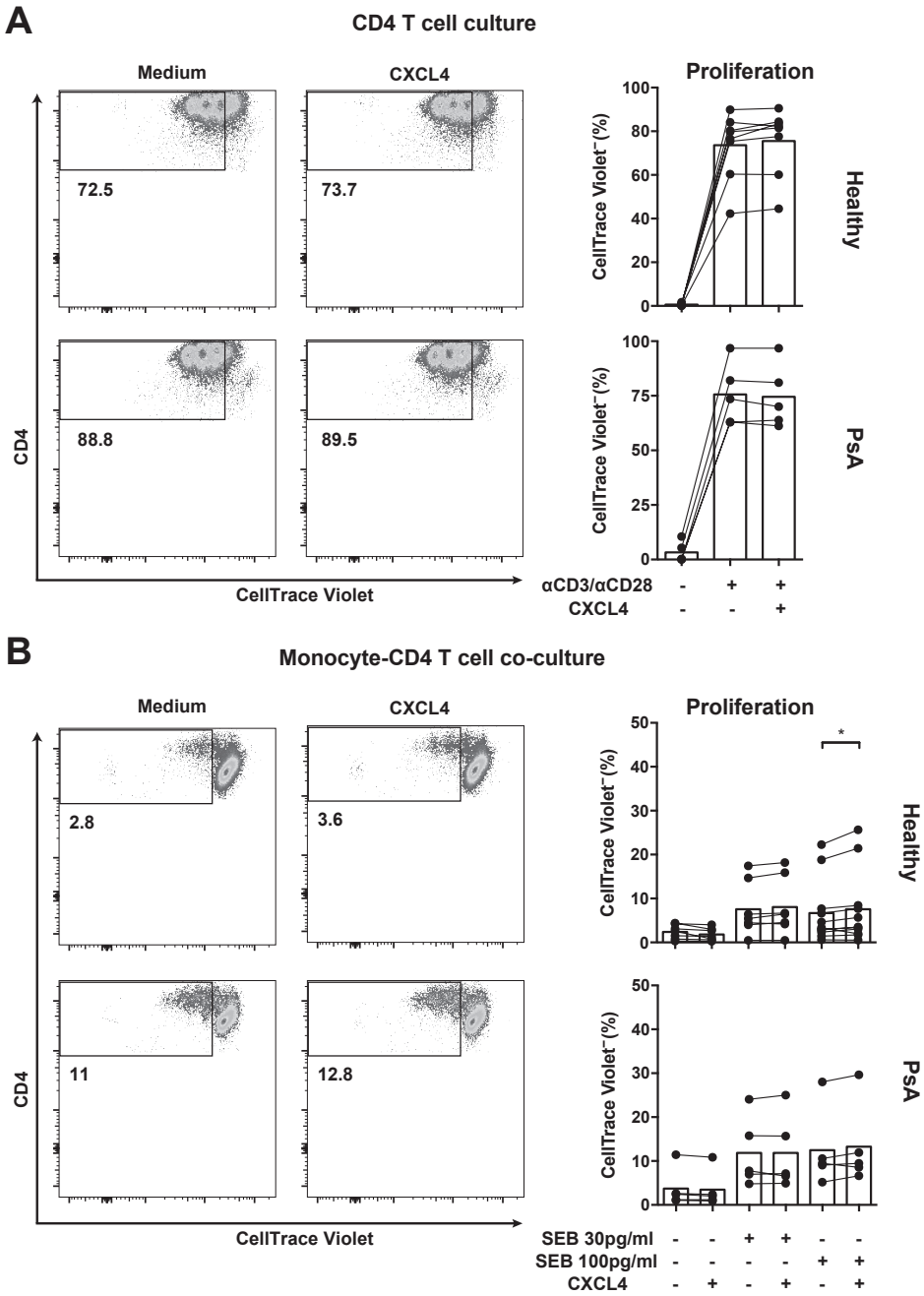
A
CD4 T cell culture
Medium
CXCL4
72.5
73.7
88.8
89.5
CD4
CellTrace Violet
Proliferation
CellTrace Violet⁻ (%)
Healthy
PsA
αCD3/αCD28
CXCL4
B
Monocyte-CD4 T cell co-culture
2.8
3.6
11
12.8
*
SEB 30pg/ml
SEB 100pg/ml

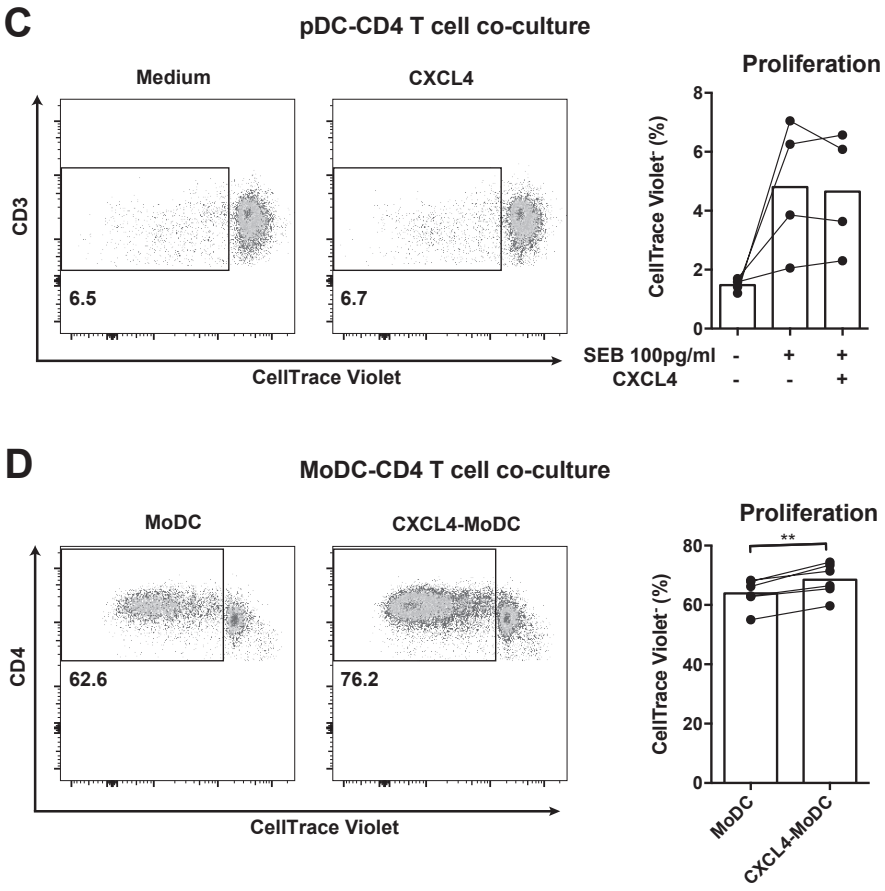

Figure S3. CXCL4 effects on proliferation of stimulated human CD4 T cells. CD4 T cells and monocytes were isolated from healthy individuals or psoriatic arthritis (PsA) patients, then CD4 T cells were stained with CellTrace Violet prior culture. (**A**) CD4 T cells were cultured with CD3/CD28 Dynabeads and 2 µg/ml CXCL4 for three days and cell proliferation was assessed. (**B, C**) CD4 T cells were co-cultured with autologous (**B**) monocytes or (**C**) plasmacytoid dendritic cells in the presence of superantigen from Staphylococcal enterotoxin B (SEB) and 2 µg/ml of CXCL4 for three days and proliferated cells were determined. (**D**) Monocytes were differentiated into dendritic cells (MoDC) in the absence or presence of CXCL4 (CXCL4-MoDC) for six days, then they were co-cultured with autologous CD4 T cells in the presence of superantigen from Staphylococcal enterotoxin B (SEB) for three days, and proliferated cells were assessed. Cells were gated based on CD4 and/or CD3 expression. Means (bars) and values from each different donor are shown and paired t-test was used for statistical analysis. * $P<0.05$, ** $P<0.01$.

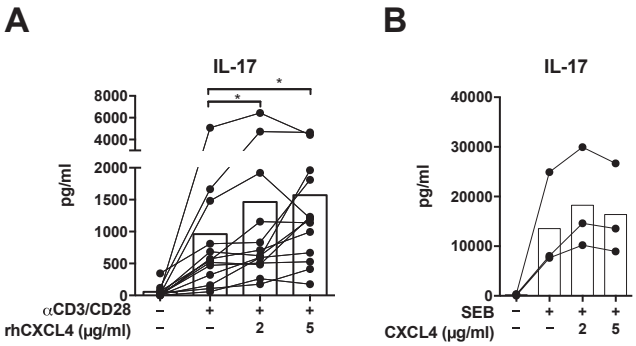

Figure S4. Dose response of CXCL4 on IL-17 production by CD4 T cell cultures. CD4 T cells and monocytes were isolated from healthy individuals and the CXCL4 effect was assessed during culture. (**A**) CD4 T cells were cultured with CD3/CD28 Dynabeads and 2 or 5 μg/ml CXCL4 for five days and supernatant was collected. (**B**) Monocytes and CD4 T cells were co-cultured in the presence of superantigen from Staphylococcal enterotoxin B (SEB) and 2 or 5 μg/ml of CXCL4 for three days and restimulated with PMA and ionomycin. The effect of IL-17 production by CD4 T cells was assessed by enzyme-linked immunosorbent assay. Means (bars) and values from each different donor are shown. Paired t-test was used for statistical analysis. * $P<0.05$.

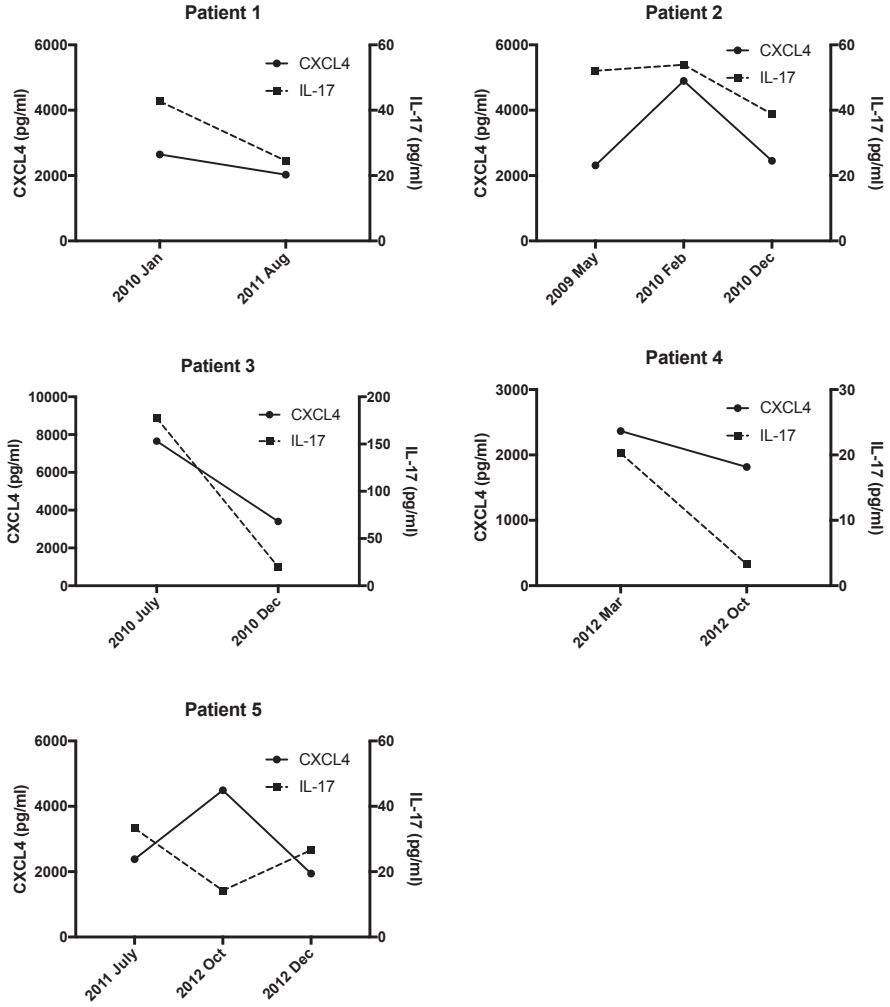

Figure S5. Changes in CXCL4 and IL-17 levels in PsA synovial fluid. Cell-free synovial fluid from five PsA patients were collected from the same knee at different time points. The median time between each collection was 9.2 months (range, 2.8 - 19.1 months). The levels of intra-articular CXCL4 and IL-17 from PsA patients were measured by Luminex-based assay.

Supplementary Tables

Table S1. Clinical and demographic features.

	Plasma and PBMC			SF	
	HC	**Pso**	**PsA**	**OA**	**PsA**
Age (years)	46 ± 11	48 ± 14	47 ± 12	63 ± 8	45 ± 19
Female	40%	40%	27%	67%	18%
DMARD use	-	0%	27%	0%	53%
TNF-inhibitor use	-	0%	0%	0%	12%
CRP	-	2.3 (0.5-15)	7.05 (1.4-41)	10.5 (2-22)	13 (3-87)
ESR	-	5 (2-33)	10 (2-39)	n.d.	12.5 (2-73)
SJC76	-	0 (0-0)	4 (0-22)	n.a.	n.a.
TJC78	-	0 (0-3)	5 (0-13)	n.a.	n.a.

Data are shown as mean ± standard deviation, median (range), or frequency (%). The therapies shown represent therapy at the time of sample collection (note: all the PsA plasma analysis was performed on PsA patients free from DMARDs at the time of sample collection). HC, healthy controls; Pso, psoriasis; PsA, psoriatic arthritis; OA, osteoarthritis; PBMC, peripheral blood mononuclear cell; SF, synovial fluid; DMARD, disease- modifying anti-rheumatic drug; CRP, C-reactive protein; ESR, erythrocyte sedimentation rate; 76SJC 76 swollen-joint count; 78TJC, 78 tender-joint count; n.a., not available; n.d., not detected.

Table S2. Primer sets used in quantitative PCR analysis.

Target	Forward primer	Reverse primer
IL17A	CCGTGGGCTGCACCTGTGTC	GGGAGTGTGGGCTCCCCAGA
IFNG	GCAGAGCCAAATTGTCTCCT	ATGCTCTTCGACCTCGAAAC
IL22	GCTGGCTAAGGAGGCTAGCTT	CATACTGACTCCGTGGAACAGTTT
B2M	GATGAGTATGCCTGCCGTGT	TGCGGCATCTTCAAACCTCC

Table S3. Antibodies used in fluorescence-activated cell sorting.

Antigen	Fluorochrome	Company	Catalog #
CD27	BV510	BD Biosciences	563090
CD25	PE	BD Biosciences	555432
CD45RO	PE-Cy7	BD Biosciences	337168
CD127	Alexa Fluor 647	Sony Biotechnology	2356590
CD3	Alexa Fluor 700	Biolegend	300424
CD4	APC-eFluor 780	eBioscience	47-0049

Chapter 4

CXCL4 links inflammation and fibrosis through transcriptional and epigenetic reprogramming of inflammatory monocyte-derived cells

Authors: Sandra C Silva-Cardoso[1,2,†], Weiyang Tao[1,2,†], Chiara Angiolilli[1,2], Ana P. Lopes[1,2], Cornelis P.J. Bekker[1,2], Abhinandan Devaprasad[1,2], Barbara Giovannone[3], Jaap van Laar[2], Marta Cossu[1,2], Wioleta Marut[1,2], Erik Hack[1], Rob J de Boer[4], Marianne Boes[1,5], Aridaman Pandit[1,2,‡,*], Timothy R.D.J. Radstake1,2,‡,*

Affiliations:

[1] Laboratory of Translational Immunology, Department of Immunology, University Medical Center Utrecht, Utrecht University, The Netherlands

[2] Department of Rheumatology and Clinical Immunology, University Medical Center Utrecht, Utrecht University, The Netherlands

[3] Department of Dermatology and Allergology, University Medical Center Utrecht, Utrecht University, The Netherlands

[4] Theoretical Biology, University Utrecht, The Netherlands

[5] Department of Pediatrics, University Medical Center Utrecht, Utrecht University, The Netherlands

†,‡ authors contributed equally.

Submitted

Abstract

Fibrosis is a condition shared by numerous inflammatory diseases. Our incomplete understanding of the molecular mechanisms underlying fibrosis has severely hampered effective drug development. CXCL4 is associated with the onset and extent of fibrosis development in systemic sclerosis (SSc), a prototypic inflammatory and fibrotic disease. Here, we integrated 65 paired longitudinal whole genome transcriptional and methylation profiles from monocyte-derived cells responding to CXCL4 exposure. Using data-driven gene regulatory network analyses, we demonstrate that CXCL4 dramatically alters the trajectory of monocyte differentiation, inducing a novel pro-inflammatory and pro-fibrotic phenotype mediated via key transcriptional regulators including CIITA. Importantly, pro-inflammatory cells exposed to CXCL4 directly trigger a fibrotic cascade by producing ECM molecules and inducing myofibroblast differentiation. Inhibition of CIITA mimicked CXCL4 in inducing a pro-inflammatory and pro-fibrotic phenotype, validating the relevance of the gene regulatory network. Our study unveils CXCL4 as a key secreted factor driving innate immune training and forming the long-sought link between inflammation and fibrosis.

Introduction

Fibrosis is an uncontrolled accumulation of extracellular matrix (ECM) in multiple organs and accounts for one third of deaths worldwide[1, 2]. Fibrosis is considered to be a result of complex cellular and molecular interplay following tissue inflammation and injury. Across a wide range of diseases, fibroblasts inappropriately synthesize and release increased amounts of ECM components, suggesting a conceptual framework in which myofibroblast transition is the key event leading to fibrosis[1]. Recent studies however, strongly implicate the innate immune system as a critical contributor to fibrosis development[3], in line with clinical observations that an inflammatory phase precedes fibrosis by years. Hence, identification of the molecular pathways linking inflammation to fibrosis will provide unprecedented opportunities for drug development to treat or even reverse tissue fibrogenesis[2, 3].

CXCL4, a chemokine initially identified as a product of activated platelets, is now known to be secreted by a variety of immune cells[4, 5, 6]. CXCL4 drives a broad spectrum of immune-modulatory effects in both hematopoietic stem and progenitor cells, as well as differentiated immune cells, and has been implicated in the pathology of a variety of inflammatory diseases[7, 8, 9]. Systemic sclerosis (SSc) is an archetypical fibrotic disease in which hypoxia, followed by endothelial cell damage and immune activation, typically culminates in fibrosis of the skin and internal organs. Previously, we identified CXCL4 as an early biomarker of this process[5]. Monocytes are indispensable for inflammation and tissue repair. Monocyte-derived dendritic cells (moDCs) can be differentiated *in vitro* by culturing monocytes isolated from human donors and are considered as DC model that mimics *in vivo* inflammatory DCs. Previously, we investigated whether circulating CXCL4 potentiates aberrant TLR-mediated responses and T-cell dysregulated responses observed in autoimmune diseases including SSc (Silva-Cardoso et al. J Immunol 2017, 199:253; Affandi et al. Eur J Immunol. 2018, 48(3):522-531). Considering the presence of CXCL4 during early inflammation and its role in modulating key immune functions, we postulated that CXCL4 might constitute the link between inflammation and fibrosis. Therefore, here, we tested this hypothesis by examining the transcriptional and epigenetic effects of CXCL4 on monocytes during and after differentiation, integrating 65 paired time courses of whole genome transcriptional and methylation profiles, and reconstructed CXCL4-dependent gene regulatory networks.

CXCL4 drastically impacts monocyte differentiation

To study the role of CXCL4 on the possible imprinting of immune cells towards fibrosis, we examined the effects of CXCL4 on the differentiation of monocyte-derived dendritic cells (moDCs)[8]. We cultured monocytes obtained from five healthy donors in the presence of IL-4 and GM-CSF to differentiate them in the absence

(conventional moDCs) and presence of CXCL4 ("CXCL4-moDCs"). To systematically study the effects of CXCL4 on the trajectory of monocyte differentiation into moDCs, we obtained longitudinal transcriptional (RNA-seq) profiles at days 0 (monocytes), 2, 4, and 6. To examine the effects of CXCL4 on moDC maturation, we stimulated the cells on day 7 with the toll-like receptor 3 ligand polyI:C and obtained transcriptional profiles before stimulation (day 7), 4 hours (day 7 + 4 hours) and 24 hours (day 8) after stimulation (**Fig. 1a**).

The differentiation of moDCs from monocytes was accompanied by extensive transcriptional changes, as 13,192 genes underwent significant (likelihood ratio test; FDR corrected p-value ≤ 0.05) alterations in their expression levels (**Fig. 1b**). Nearly half of the differentially expressed genes (6,350) were upregulated. CXCL4-moDCs also underwent widespread transcriptional changes, as 13,110 genes were differentially expressed compared to monocytes, nearly half of those were found to be upregulated (**Fig. 1b** and **S1**). Remarkably, most of this transcriptional shift happens between day 0 and day 2, in both conventional moDCs and CXCL4-moDCs (**Fig. 1d**). Genes characteristic of monocyte differentiation (such as *CD14*, *CD163*, *TLR2*, *TLR4*, and *TLR7*)[10] and cell adhesion molecules (including *LGALS2*, *LGALS9*, and *ICAM2*) were down-regulated in both conventional moDCs and CXCL4-moDCs on day 2 (**Table S3**). After day 2, cells continued to differentiate, as evidenced by their shifting transcriptional profiles (**Fig. 1d**). Genes encoding pattern recognition proteins MRC1, MRC2, growth factors such as CSF1, and the chemokine receptors CCR1, CCR5, and CCR7, were upregulated over time in both conventional moDCs and CXCL4-moDCs (**Table S3**). Together these results indicate that the differentiation of monocytes (with or without CXCL4) leads to massive transcriptional changes as reported by several previous studies[11, 12].

To elicit the transcriptional signature unique to CXCL4 exposure, we compared differentiating CXCL4-moDCs with conventional moDCs from day 2 to day 6 and found differential expression of 5,775 genes (likelihood ratio test, FDR corrected p-value ≤ 0.05; **Fig. 1b**, **S1**, and **Table S1** and **S3**). CXCL4-moDCs follow a distinct molecular differentiation trajectory that progressively diverges from conventional moDCs (**Fig. 1d**, right panel). The CXCL4 signature genes belong to several crucial innate immune system pathways including cytokine signaling, interferon signaling, and antigen processing and presentation (**Fig. S1e**). For instance, CXCL4-moDCs, in the absence of further stimulation, up-regulate expression of several inflammatory molecules such as *CTSL*, *FLT1*, *CD86*, *LAMP1*, *CHI3L1*, and down-regulate signaling receptors such as *CLEC10A, IL1R1, IL1R2* compared to moDCs (**Fig. 1g-i** and **S1a-d**). Strikingly, CXCL4 exposure also leads to dramatic changes in expression of genes regulating metabolism and transcription (**Fig. S1e**), reminiscent of changes previously observed in myeloid cells undergoing immune training[13]. Thus, CXCL4

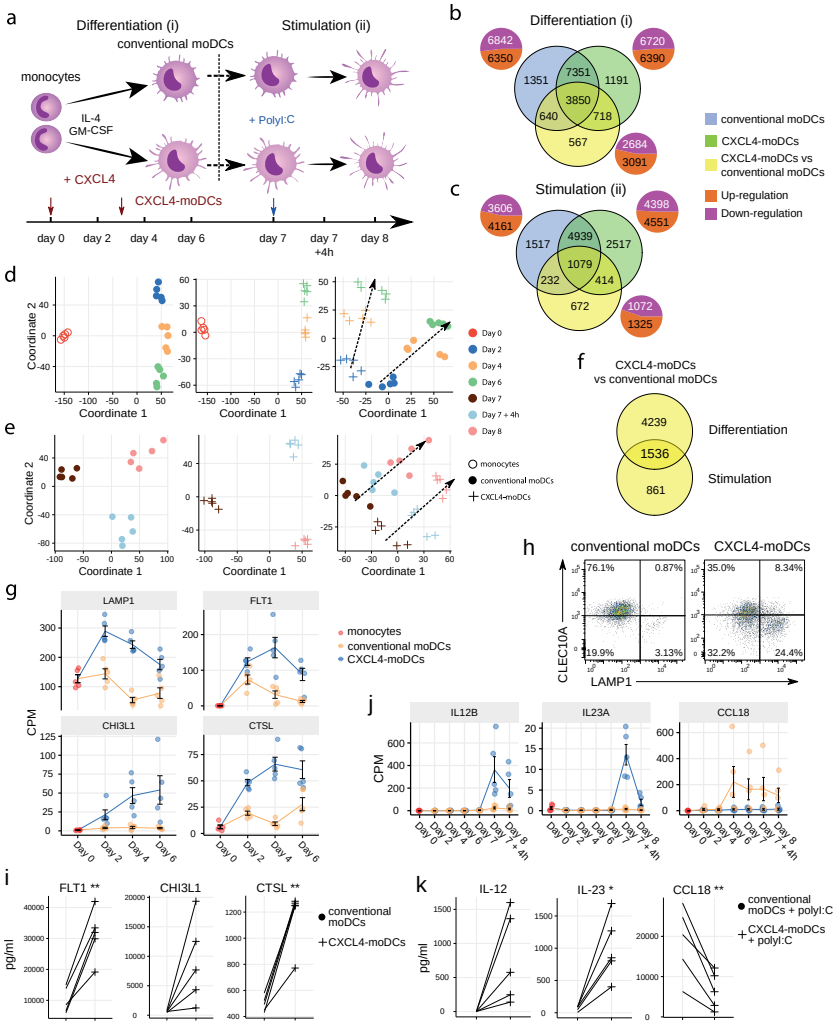

Fig. 1. Transcriptomic programing of CXCL4-moDCs. (a) Schematic overview of the experimental setup: (i) differentiation of monocytes to conventional moDCs or CXCL4-moDCs; (ii) stimulation with polyI:C on day 7, for 4 hours or 24 hours. Overlap of differentially expressed genes (DEGs) during **(b)** differentiation and **(c)** after polyI:C stimulation of: monocytes into conventional moDCs (blue); monocytes into CXCL4-moDCs (green); and between CXCL4-moDCs and moDCs during differentiation (yellow). In **(b)** and **(c)** pie charts showing the number of upregulated (orange) and down-regulated (purple) genes. Multi-dimensional scaling (MDS) plot **(d)** differentiating and **(e)** stimulated conventional moDCs (left panel), CXCL4-moDCs (middle panel), and CXCL4-moDCs vs conventional moDCs (right panel). In **(d)** and **(e)** dotted lines indicate trajectories over time. **(f)** Overlap of DEGs between CXCL4-moDCs and conventional moDCs, during differentiation and upon stimulation. Gene expression of example genes differential during **(g)** differentiation and **(j)** stimulation between CXCL4-moDCs and conventional moDCs. Validation of **(h)** protein expression (flow cytometry) and **(i)** cytokine production (Luminex) on day 6. **(k)** Validation of cytokine production (Luminex) on day 8. Gene expressions are shown as mean±SEM. CPM, count per million. In panels I and K, lines connect individual donors (n=5). *P<0.05; **P< 0.01, paired two-sided Student's t-test.

orchestrates a differentiation process dramatically different than that of the conventional moDCs.

Mature CXCL4-moDCs are functionally distinct from conventional moDCs

To study the effects of CXCL4 on moDC maturation, we stimulated the cells with polyI:C on day 7. This perturbed the expression of 8,949 and 7,767 genes in CXCL4-moDCs and conventional moDCs, respectively, compared to the day 7 transcriptional profiles of their unstimulated counterparts (**Fig. 1c** and **1e**, left and middle panels). 2,397 genes responded differently to polyI:C stimulation in CXCL4-moDCs compared to conventional moDCs (**Fig. 1c** and **S2**). Several pathways involved in inflammatory responses such as TLR signaling, interferon signaling, and cytokine signaling, were significantly upregulated in CXCL4-moDCs compared to conventional moDCs (**Fig. S2e**). Confirming our previous findings[8], these transcriptional changes were followed by increased production of pro-inflammatory mediators such as IL-1β, IL-6, IL-12, IL-23, IL-27, TNF and CCL22, and down-regulation of immune-suppressive mediator CCL18 (validated using Luminex assays; see **Fig. 1j-k** and **S2a-d**). Pathways involved in cellular adhesion, integrin signaling, ECM organization, and collagen formation, among others, were upregulated in CXCL4-moDCs upon polyI:C stimulation compared to stimulated moDCs (**Fig. S2e**), indicating that CXCL4 exposure induces a pro-inflammatory and pro-fibrotic phenotype. Because most of the altered genes were already differentially expressed in immature CXCL4-moDCs (**Fig. 1e**, **f** and **S2b**), the unique molecular program induced by CXCL4 is suggestive of genetic imprinting.

CXCL4 alters epigenetic imprinting during differentiation but not maturation of moDCs

To comprehensively examine whether CXCL4 signaling might alter moDC phenotype via epigenetic modifications[12, 14, 15,] we studied genome wide alterations in DNA methylation. Similar to the transcriptome analysis, we found that a large number of genes, regions and sites were differentially methylated between monocytes and differentiating moDCs and CXCL4-moDCs (**Fig. 2a**, **S3** and **S4**). Interestingly, most of the differentially methylated genes were hypomethylated compared to monocytes (2,617 in conventional moDCs and 2,156 in CXCL4-moDCs) (**Fig. 2a**, **b**, **S3a** and **c**, and **Table S4**).

To discern the epigenetic footprint of CXCL4 during differentiation, we compared the methylome profiles of differentiating CXCL4-moDCs with differentiating conventional moDCs (from day 2 to day 6). CXCL4 exposure led to substantial changes in the DC methylome as 1,065 genes were differentially methylated between CXCL4-moDCs and conventional moDCs (**Fig. 2a** and **S3**). Most of the differentially

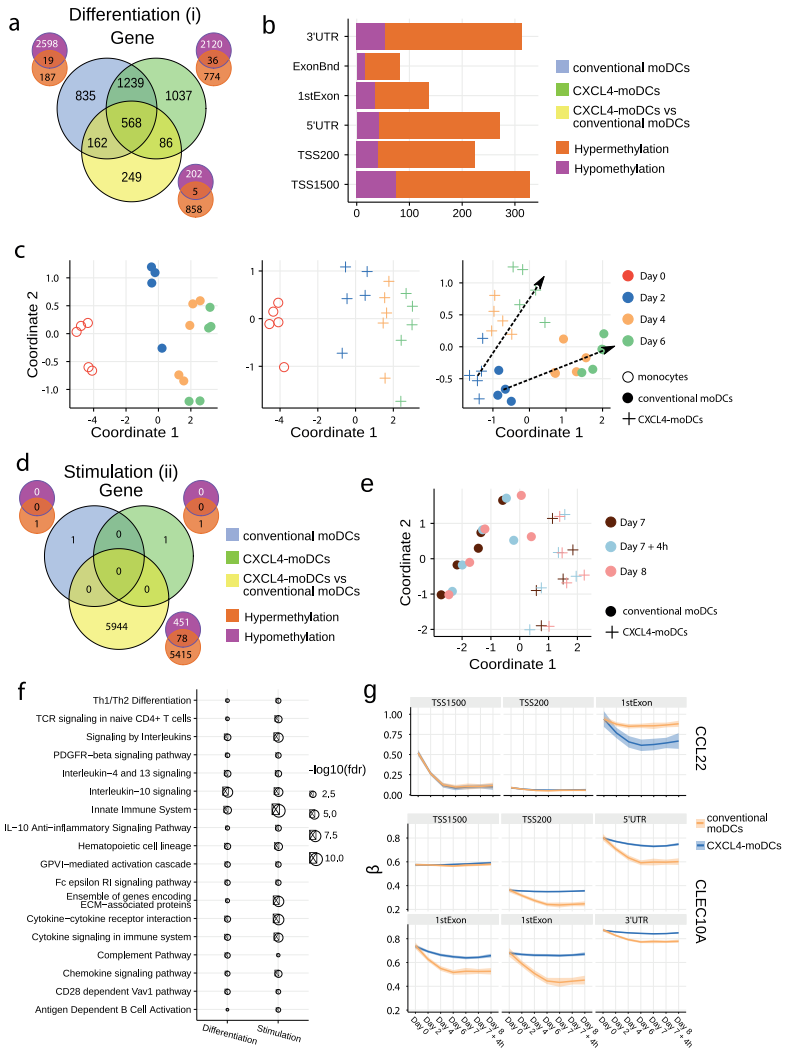

Fig. 2. DNA methylation analysis of CXCL4-moDCs and conventional moDCs. (a) Overlap between differentially methylated genes (DMGs) found during differentiation similar to **Fig. 1b**. A gene is considered differentially methylated if any region on the gene is differentially methylated. Smaller Venn diagram graphs display the overlap of hyper-methylated (orange) and hypo-methylated (purple) genes for each comparison. Note some genes are classified as both hyper-methylated and hypo-methylated based on different regions. **(b)** Distribution of differentially methylated regions (1500 and 200 base pairs upstream of the transcription start site (TSS), 5' untranslated region (UTR), 1st exon, other exons (ExonBnd) and 3'UTR) between CXCL4-moDCs and conventional moDCs during differentiation. **(c)** MDS analysis using DMRs, similar to **Fig. 1d**. **(d)** Overlap between DMGs found during stimulation similar to **Fig. 1c**. **(e)** MDS analysis using all DMRs between CXCL4-moDCs and conventional moDCs during stimulation. **(f)** Top enriched pathways from DMGs between CXCL4-moDCs and conventional moDCs during differentiation and stimulation. **(g)** DNA methylation β values (see Methods) of CCL22 and CLEC10A. Lines represent mean β values and shading represents 95% confidence interval.

methylated genes were hypermethylated in CXCL4-moDCs. The hypermethylation was not restricted to promoter regions, indicating that CXCL4 influences chromatin accessibility at a more global level (**Fig. 2b**). Alterations in DNA methyltransferases and DNA demethylases are known to cause global hypermethylation, which have been implicated in SSc pathogenesis previously[16]. Interestingly, we found transcriptional upregulation of DNA methyltransferases (such as DNMT3A) and downregulation of DNA demethylases (TET2 and TET3) that together can cause global hypermethylation in CXCL4-moDCs (**Fig. S4a**). As in the transcriptional analysis, CXCL4-moDCs progressively diverge from moDCs (**Fig. 2c**, right panel). This progressive and temporal divergence of DNA methylation patterns caused by CXCL4 alters several crucial innate immune system pathways including cytokine signaling, co-stimulatory molecules, and ECM organization (**Fig. 2f**). Thus, we provide direct mechanistic evidence that CXCL4 programs a pro-inflammatory and pro-fibrotic phenotype via epigenetic imprinting that corroborates the transcriptional results (**Fig. S3e** and **3f**).

We also studied the role of epigenetic remodeling in mature moDCs. Surprisingly, stimulation of conventional moDCs and CXCL4-moDCs with polyI:C on day 7 hardly affected the DNA methylation (**Fig. 2d**, **g**, **S3b** and **3d**), an observation confirmed by multivariate analysis as the samples did not exhibit any temporal clustering (**Fig. 2e**). Thus, the altered functional responses exhibited by CXCL4-moDCs were epigenetically imprinted during differentiation rather than maturation (**Fig. S3**).

Gene regulatory network driving the CXCL4-specific transcriptome

Since CXCL4 exposure caused massive alterations in both DNA methylation and transcriptional factors, we next studied the regulatory mechanisms behind the CXCL4 signature. We first assessed the concordance of DNA methylation and mRNA expression and found that the changes in DNA methylation did not correlate with the changes in corresponding gene's expression for majority of the CXCL4 signature genes (**Fig. 3a** and **S4b-e**). Surprised by the lack of correlations for most CXCL4 signature genes, we checked if levels of DNA methylation reflect upon the overall gene expression levels, rather than their differential expression. We indeed found that levels of DNA methylation play a role in overall gene expression levels (**Fig. S4f** and **g**). Given the lack of concordance between individual transcriptional and DNA methylation changes, DNA methylation of individual genes may be a poor guide for further association studies.

Genes rarely work in isolation, and their expression is typically regulated via a complex molecular network[17, 18]. To systematically identify the underlying complexity and inter-connectivity of molecular changes caused by CXCL4, we developed a new methodology (RegEnrich) to integrate the transcriptional and

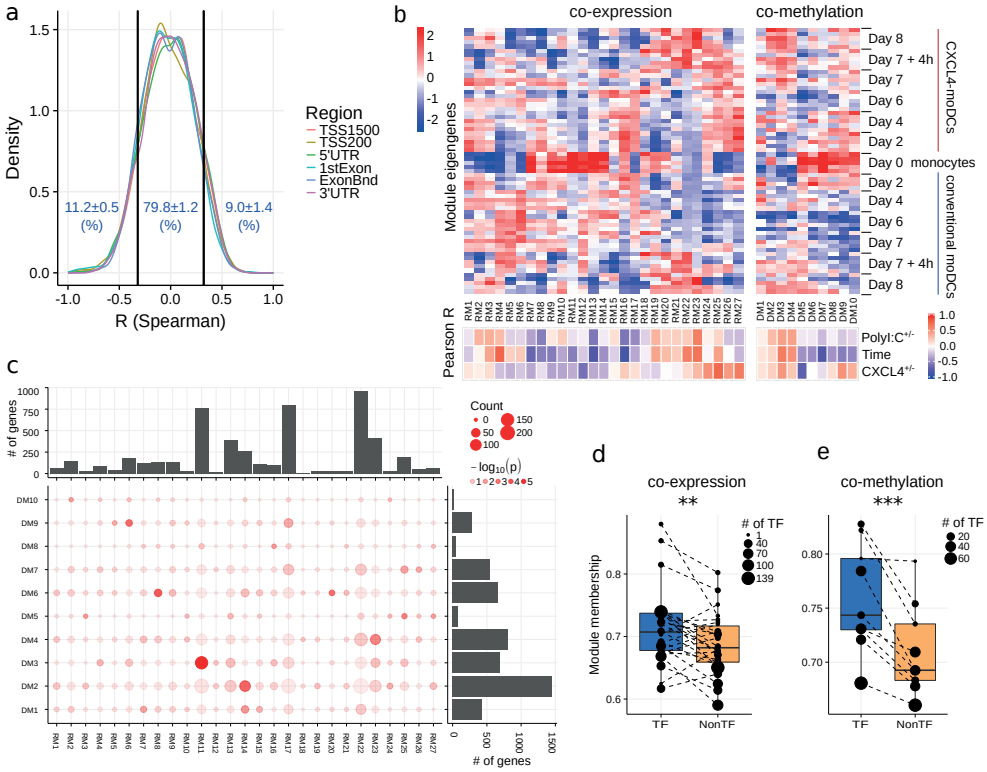

Fig. 3. Co-expression and co-methylation networks. (a) Distribution of spearman correlation coefficients (R) between β values of each region and the corresponding gene expression for all genes that are differentially expressed and methylated. The cutoffs (two vertical lines at R = ±0.32) indicate significant correlation coefficients ($p < 0.01$). **(b)** The top heatmap shows expression/methylation eigengenes of co-expression (left) and co-methylation (right) modules. The bottom heatmap shows the Pearson correlation coefficients between sample traits (i.e. CXCL4+/-, time and polyI:C+/-), and co-expression (left) and co-methylation (right) module eigengenes. **(c)** Concordance of co-expression and co-methylation modules. The bottom left graph shows the number (circle size) and significance (color, p-value calculated by Fisher's exact test) of overlapping genes between co-expression and co-methylation modules. The bar plots show the total number of genes in the co-expression (top) or co-methylation (right) module. Module membership comparisons of transcriptional regulators (TF) and other genes (NonTF) in **(d)** co-expression and **(e)** co-methylation network. Each dot represents a module and the size denotes the number of TFs in the corresponding module. Modules that do not contain TFs were excluded in these analyses. ***P*<0.01, ****P*<0.001, paired two-sided Student's *t*-test.

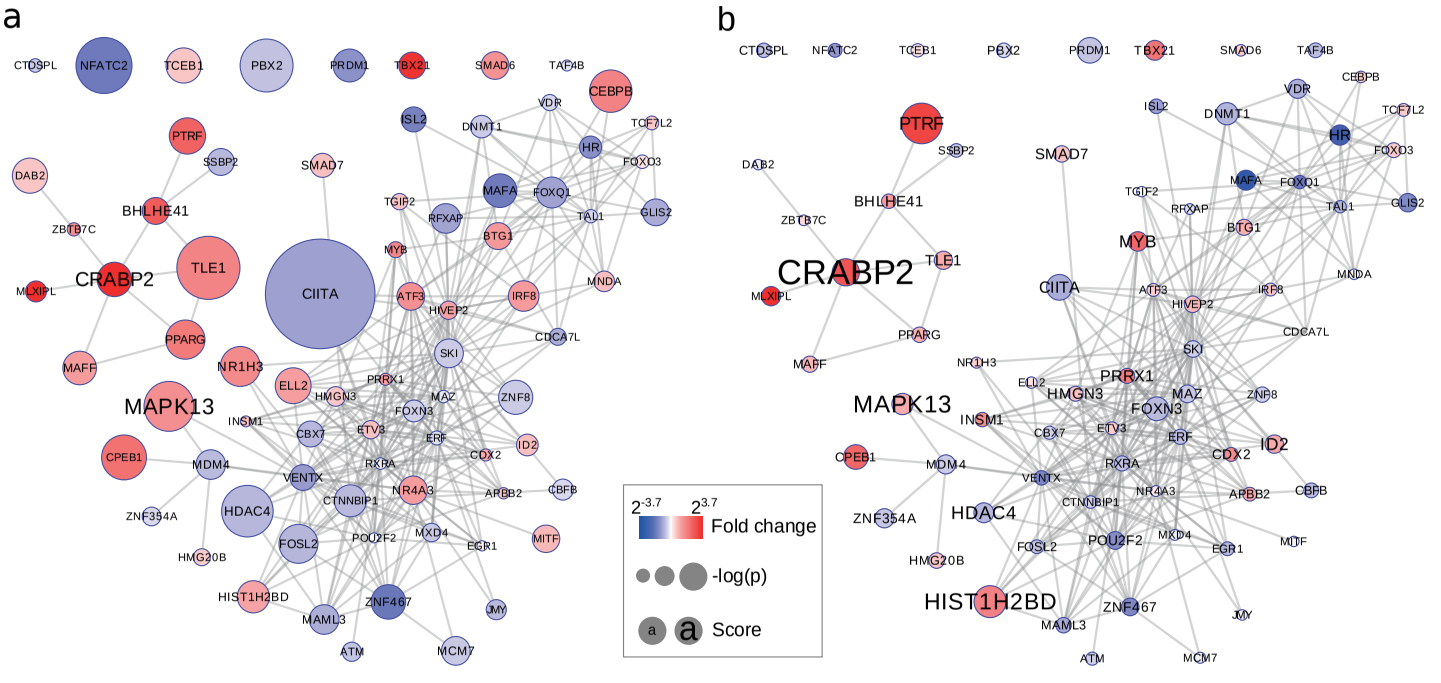
a
b
CTOSPL
NFATC2
TCEB1
PBX2
PRDM1
TBX21
SMAD6
TAF4B
CEBPB
VDR
ISL2
DNMT1
TCF7L2
HR
FOXO3
PTRF
SSBP2
SMAD7
DAB2
MAFA
FOXQ1
TGIF2
BHLHE41
RFXAP
TAL1
GLIS2
ZBTB7C
BTG1
MYB
CRABP2
TLE1
CIITA
MNDA
MLXIPL
ATF3
IRF8
HIVEP2
PPARG
CDCA7L
SKI
MAFF
NR1H3
ELL2
PRRX1
MAPK13
HMGN3
MAZ
ZNF8
FOXN3
INSM1
CBX7
ETV3
ERF
ID2
CPEB1
MDM4
RXRA
COX2
VENTX
NR4A3
ARBB2
CBFB
CTNNBIP1
ZNF354A
HDAC4
FOSL2
POU2F2
MXD4
EGR1
MITF
HMG20B
HIST1H2BD
ZNF467
MAML3
JMY
ATM
MCM7
2-3.7
23.7
Fold change
-log(p)
a
Score

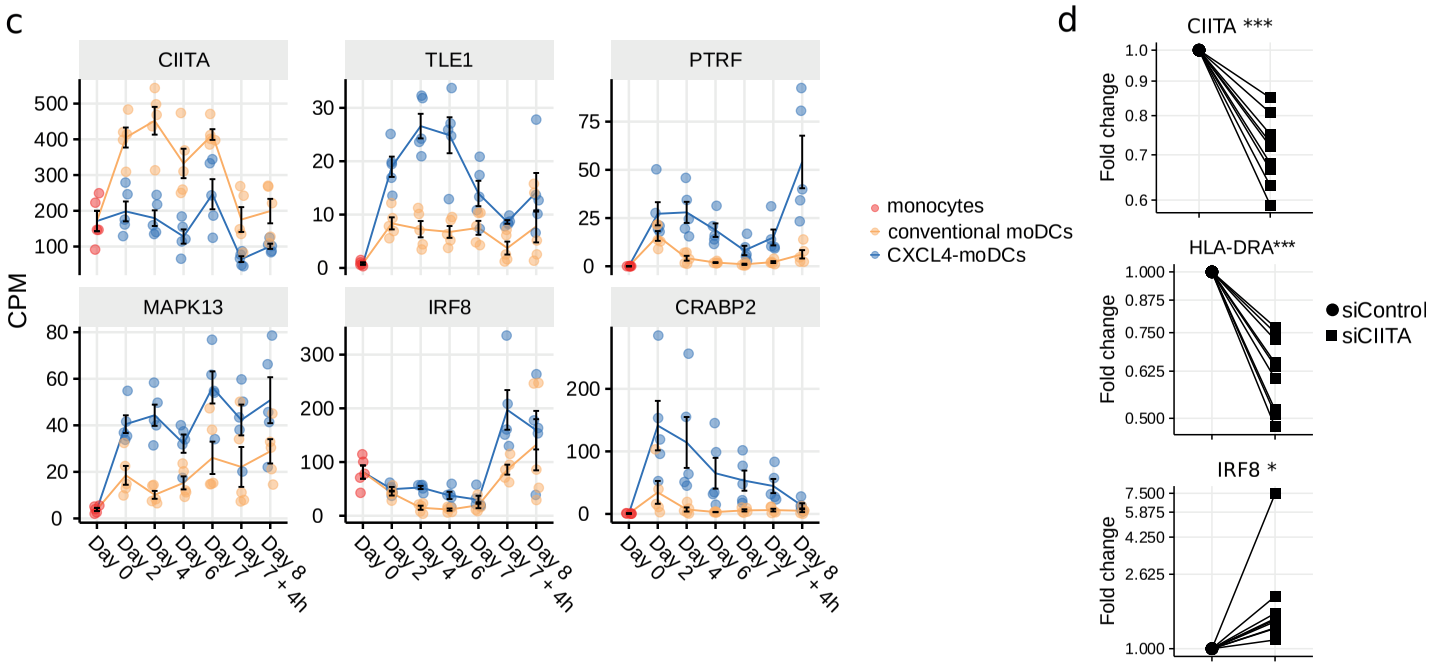

Fig. 4. Transcription regulator enrichment highlights key TF candidates. Co-expression based key TF network during: **(a)** differentiation and **(b)** stimulation. Colors indicate fold change between CXCL4-moDCs and conventional moDCs. Red represents upregulation and blue represents downregulation. Circle size indicates -$\log_{10}$(p) for each comparison, where p is the p-value calculated during differential expression analysis; text size shows the RegEnrich score (see Methods). **(c)** Expression profile (mean±SEM) of key regulators. **(d)** Expression of *CIITA*, *HLADRA*, and *IRF8* on day 6 measured by qPCR in moDCs obtained from monocytes transfected with silencer negative control siRNA (siControl) or silencer CIITA siRNA (siCIITA). qPCR data were normalized using mean expression of *RPL32* and *RPL13A*. Fold change in y-axis (log2 scaled) is relative to the value obtained for siControl for each donor. Lines connect individual donors. **P*<0.05, ****P*<0.001, paired two-sided Student's *t*-test.

epigenetic layers and identify the important transcription factors modulated by CXCL4 (see Methods). Using RegEnrich, we first constructed weighted gene correlation networks, which allowed us to cluster genes into distinct modules (or sets of genes) based upon either their co-expression or co-methylation patterns (**Fig. S5a-b**)[19, 20]. Modular analysis segregated the differentially expressed genes into 27 modules, each exhibiting a distinct co-expression pattern (**Fig. 3b**, **c** and **S5c**). Of these 4 were CXCL4-moDCs-specific modules (RM24-RM27) and contained genes belonging to ECM organization, ion channel transport, IFNα signaling and metabolic pathways, highlighting the impact of CXCL4 upon the DC phenotype (**Fig. 3b** and **S6b**). Similarly, modular analysis segregated all differentially methylated genes into 10 distinct co-methylation modules (**Fig. 3b**). CXCL4-moDC-specific modules (DM5 and DM9) contained genes belonging to transcriptional and translational pathways, antigen presentation pathways, and the innate immune system (**Fig. 3b** and **S6c**; **Table S8**). However, we did not find much overlap between the CXCL4-moDC-specific co-expression and co-methylation modules (**Fig. 3c**). Thus, DNA methylation only partially influences the transcriptional changes of CXCL4 signature genes.

To test whether transcription regulators are the central players (hubs) in our networks[17, 18], we calculated module memberships as a measure to determine the importance of a gene in a given module[19, 20]. Interestingly for both co-expression and co-methylation modules, we found that the transcription regulators typically exhibited higher module membership than the other genes (**Fig. 3d**, **e** and **S5d**). That transcription regulators are typically the hubs in our networks highlights their crucial regulatory function in modulating the expression dynamics of their downstream target genes. Thus, alterations in the expression and activity of a few key transcription regulators can potentially precipitate the large phenotypic differences observed between moDCs and CXCL4-moDCs. Using RegEnrich, we ranked the transcription regulators most prominently dysregulated between CXCL4-moDCs and conventional moDCs during differentiation (**Fig. 4a**), and post stimulation (**Fig. 4b**). Using these gene regulatory networks, we found that key transcription regulators such as *CIITA*, *TLE1*, *PTRF*, *MAPK13*, *CRABP2*, *IRF8*, regulate a large number of the CXCL4 signature genes, including pro-inflammatory and ECM pathway genes (**Fig. 4a** and **b**). We confirmed that these key transcription regulators were significant for CXCL4 signature genes using two independent approaches: i) random forest-based gene regulatory networks (see Methods, and **Fig. S7a-b**), and ii) literature-derived gene regulatory networks (data not shown). Together, the data-driven gene regulatory networks identified a direct mechanistic link between CXCL4, inflammation and ECM modeling in moDCs.

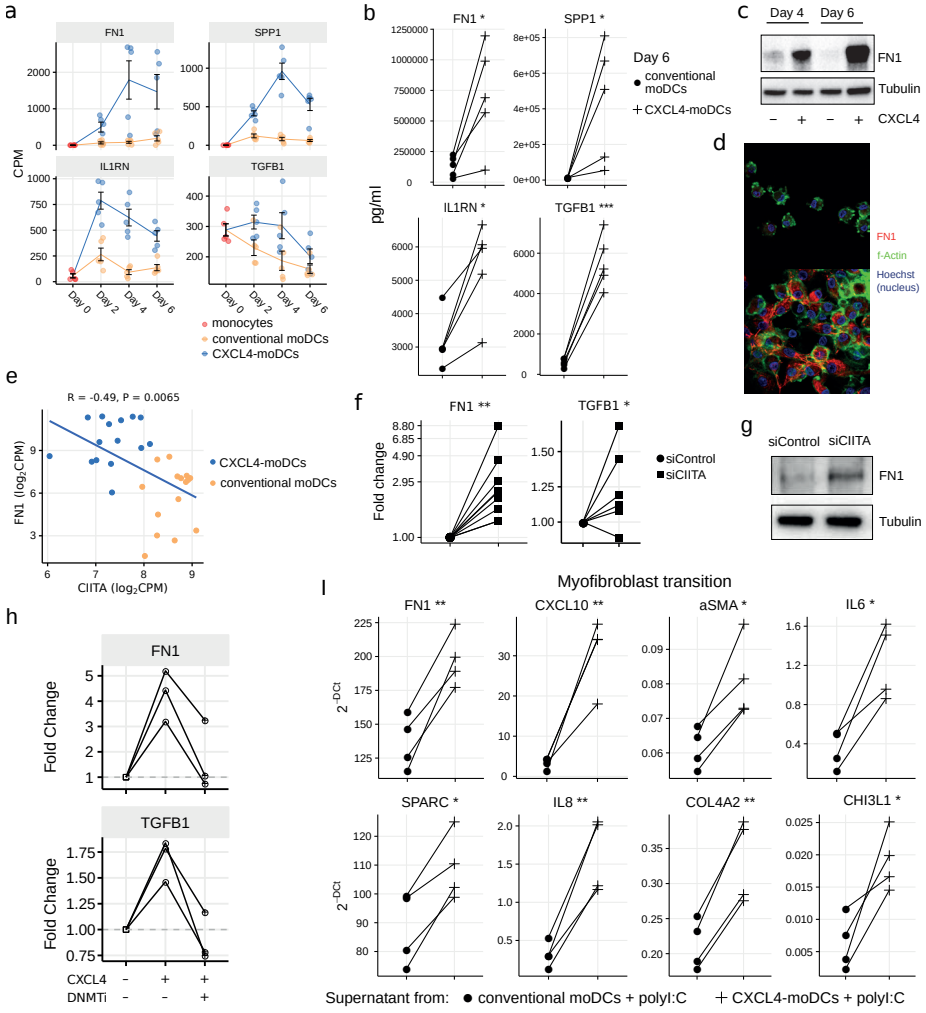

Fig. 5. CXCL4 induces production of ECM components in moDCs and fibroblasts. (a) Expression of genes implicated in ECM remodeling (mean±SEM). **(b)** Validation (luminex) of ECM protein production in CXCL4-moDCs and conventional moDCs on day 6. **(c)** Fibronectin (FN1) expression (tubulin as loading control) determined using Western blot on days 4 and 6 (representative of 5 independent experiments). **(d)** Fibronectin (red) synthesis determined using confocal imaging on day 6 (green: f-actin; and blue: nucleus staining using Hoechst). **(e)** Pearson correlation between gene expression of *CIITA* and *FN1* during differentiation (i.e. on day 2, 4 and 6). **(f)** FN1 and TGFB1 expression measured by qPCR and **(g)** FN1 expression measured by western blot on day 6 moDCs obtained from monocytes transfected with siControl and siCIITA (see **Fig. 4d**). **(h)** FN1 and TGFB1 expression measured by qPCR on day 3 in conventional moDCs, CXCL4-moDCs and CXCL4-moDCs exposed to DNMT inhibitor (100nM 5-Aza-2ƍ-deoxycytidine). **(i)** Expression of ECM genes measured using qPCR in healthy dermal fibroblasts (one representative donor; for others see **Fig. S9**) co-cultured with supernatants from CXCL4-moDCs and moDCs that were stimulated for 24 hours with polyI:C. qPCR data were normalized using mean expression of *RPL32* and *RPL13A*. In panels **b**, **f**, **h** and **i**, lines connect individual donors. **P*<0.05; ***P*<0.01, ****P*<0.001, paired two-sided Student's *t*-test.

CIITA is a key target of CXCL4 signaling

We found that the key transcriptional regulatory proteins exhibit different mRNA expression patterns over time. For example, *TLE1*, *PTRF* and *CRABP2* were expressed at low levels in monocytes but were upregulated during the differentiation of both conventional moDCs and CXCL4-moDCs (**Fig. 4c**). However, these genes exhibited persistently higher expression in CXCL4-moDCs during both differentiation and following polyI:C stimulation (**Fig. 4c**). Another example is the interferon regulatory factor 8 (IRF8), a transcription factor typically associated with pro-inflammatory gene expression in monocytic lineages, which is markedly upregulated in immature CXCL4-moDCs compared to conventional moDCs (**Fig. 4c**). Class II MHC transactivator (CIITA), a transcription co-factor associated with regulation of MHC class II gene expression, was the most significantly down-regulated regulator in CXCL4-moDCs (**Fig. 4c**).

To validate the inter-connectivity of important regulators inferred from the gene regulatory network, we performed siRNA-mediated knockdown to silence CIITA expression. At day 6 following introduction of siRNA, monocyte-derived cells remained viable, and displayed the anticipated phenotype: CIITA-silencing down-regulated expression of both CD74 and HLA-DR (**Fig. 4d** and **S7c-d**)[21]. While IRF8 has not been reported to be regulated by CIITA, our gene regulatory networks predicted direct or indirect regulatory interactions between CIITA and IRF8. Silencing of CIITA led to upregulation of IRF8, mimicking the effects of CXCL4 and validating the prediction of our gene regulatory networks (**Fig. 4d** and **S7c-d**). Hence using our gene regulatory networks, we have elucidated novel gene regulatory interactions in moDCs and found that CXCL4 alters the fate of moDCs by modulating the expression of the key transcription regulator CIITA.

CXCL4 induces fibrotic pathways in moDCs mediated via epigenetic imprinting and CIITA

Our data-driven methodology allowed us to identify several novel regulators and pathways that are differentially regulated due to CXCL4 during moDC differentiation (Fig. 2f, 4a-c and Table S7). As a result, we observed that even unstimulated CXCL4-moDCs exhibit a pro-fibrotic phenotype, as characterized by the increased gene and protein expression of several crucial ECM-related molecules including FN1, SPP1, IL1RN and TGFB1 (for transcriptional changes see Fig. 5a, S8a and b; for protein validations see Fig. 5b-d). Importantly, silencing CIITA mimicked the effects of CXCL4 leading to upregulation of FN1 along with other molecules involved in ECM remodeling validating the relevance of this network in the pro-fibrotic cascade (Fig. 5e-g, S8c and d). Since in CXCL4-moDCs we found that majority of the differential genes were hypermethylated (Fig. 2a and b) and that ECM genes were up-regulated

(including FN1 and TGFB1; see Fig. 5a and b), we next examined whether modulating DNA methylation affects FN1 and TGFB1 expression. In line with our hypothesis, inhibition of DNMTs using 100nM 5-Aza-2'-deoxycytidine restored the expression of FN1 and TGFB1 which were upregulated by CXCL4 in moDCs (Fig. 5h), suggesting that CXCL4 associated epigenetic imprinting also plays a role in promoting expression of pro-fibrotic genes. Although our data provides unprecedented data for the direct implication of CXCL4 in tissue fibrogenesis via CXCL4-moDCs, we next examined the possible implication of these CXCL4-moDCs on fibroblast behavior. By culturing fibroblasts with the supernatant of CXCL4-moDCs stimulated with polyI:C, we demonstrate that these fibroblasts expressed markedly higher levels of inflammatory mediators associated with fibrosis and above all, myofibroblast transition, considered indispensable for fibrosis, compared to conventional moDCs stimulated with the same TLR3 ligand (Fig. 5i and S9). Together, this data unequivocally demonstrates that CXCL4 alters the fate of moDCs differentiation into cells that drive fibrogenesis both directly and, via myofibroblast activation, indirectly.

Discussion

Although the role of inflammation in fibrosis is increasingly recognized, the underlying molecular links between these processes remain elusive and their identification is paramount for the development of medicines to not only halt progression but prevent fibrosis. Using whole genome transcriptional and epigenetic profiling, we find that CXCL4 drives the development of a pro-inflammatory and pro-fibrotic phenotype in moDCs, characterized by the excessive production of ECM components and capacity to promote myofibroblast differentiation. As these are two key mechanisms contributing to tissue fibrogenesis, our study introduces the novel concept that CXCL4-induced inflammatory moDCs constitute the driving force behind both the initiation and progression of fibrosis in diseases where CXCL4 levels are increased such as SSc.

TGF-β is considered a key regulator during fibrosis in physiological and pathological conditions[22]. For instance, TGF-β drives mesenchymal responses during wound healing, where its transiently increased expression promotes myofibroblast transition. However, the initial stage of wound healing is the formation of a platelet plug, followed by monocyte recruitment and monocyte differentiation into M1 macrophages. After this primarily inflammatory phase, a switch to resolution, accompanied by tissue repair and fibrosis, occurs[23]. Platelets, crucial players in the pathogenesis of several diseases including SSc, contain large amounts of CXCL4[4, 5, 24]. Activation of platelets early on in the wound healing process is likely to precede the synthesis and secretion of TGF-β. Notably, CXCL4 was found to play an important role

in lung inflammation and tissue damage[25], and has been identified as a biomarker for early rheumatoid arthritis where it was co-localized with inflammatory cells and platelets in synovial tissue[26]. In contrast to other inflammatory mediators that appear at later stages of disease, CXCL4 levels are also increased in patients at risk for SSc, a disease in which clinical inflammation precedes fibrosis by years[5]. Together, these observations indicate an early role for CXCL4 in inflammatory and subsequent fibrotic processes, placing CXCL4 upstream of TGF-β. This possibility is further substantiated by our finding that CXCL4 clearly induces TGF-β RNA and protein expression (**Fig. 5a** and **b**).

Multiple studies provide compelling evidence for the presence of inappropriately activated and/or trained innate immunity in patients with inflammatory diseases. Recently, several crucial studies have highlighted the molecular basis, relevance and pathological consequences of innate immunity trained by various exogenous ligands and endogenous ligands the latter contributing to atherosclerosis and gout[27, 28, 29, 30]. Following a seminal study which observed enhanced collagen synthesis in SSc patient skin fibroblasts compared to those of healthy control[31], this phenomenon was observed in SSc patient DCs, which had potentiated responses to various TLR agonists[5, 32]. Our study now reveals that differentiating monocytes undergo massive transcriptomic and epigenetic reprogramming upon CXCL4 exposure, and we propose that CXCL4 is a clinically relevant and important endogenous ligand bridging inflammation with fibrosis via trained immunity and provides a rationale for therapeutic targeting of CXCL4 in SSc and other fibrotic diseases.

Methods

Differentiation and stimulation of CXCL4 moDCs

Blood from healthy donors (HDs) was collected in accordance with institutional ethical approval. Peripheral blood mononuclear cell (PBMC) and monocyte isolation, as well as differentiation of monocyte-derived dendritic cells (moDCs) were performed as described previously[8]. Briefly, PBMCs were isolated from heparinized venous blood using Ficoll PaqueTM Plus (GE Healthcare) density gradient. Monocytes were purified with anti-CD14 magnetic beads-based positive isolation using autoMACS Pro Separator-assisted cell sorting (Miltenyi Biotec), according to the manufacturer's protocol. Monocyte purity was above 95% for all of the samples (data not shown). For the differentiation of moDCs, monocytes were cultured at a density of $1x10^6$ cells/ml in culture medium comprised of RPMI 1640 with GlutaMAX (Life Technologies) supplemented with 10% (v/v) heat-inactivated fetal bovine serum (FBS; Biowest) and 1% (v/v) antibiotics (penicillin and streptomycin; Life Technologies). In order to generate moDCs, GM-CSF (800 U/ml; R&D) and IL-4 (500 U/ml; R&D) were added. For

the experiments where we investigated the effects of CXCL4, we added 10 µg/ml of recombinant human CXCL4 (PeproTech) on day 0 and day 3. Medium and cytokines were refreshed on day 3. Differentiated moDCs were obtained after 6 days from monocytes cultured at 37oC in the presence of 5% CO_2. After differentiation, cells were washed, plated at a density of $0.5x10^6$ cells/ml and left overnight (O/N) in new culture medium. Cells were stimulated with 25 µg/ml of polyinosinic-polycytidylic acid (polyI:C; InvivoGen) for 4 hours or 24 hours, or kept unstimulated, as shown in **Fig. 1a**.

DNA and RNA extraction for DNA methylation and RNA sequencing analysis

For DNA methylation and RNA sequencing analysis cells were collected from 5 HDs: on the first day of culture (monocytes, day 0); during differentiation on day 2, day 4 and day 6. After O/N resting, unstimulated cells (day 7), cells stimulated with polyI:C for 4 hours (day 7 + 4h) and 24 hours (day 8) were also lysed in RLTplus buffer (Qiagen) containing 1% (v/v) beta-mercaptoethanol (Sigma). In total, we obtained 65 paired samples for RNA sequencing and DNA methylation profiling. DNA and RNA were extracted using the Allprep Universal Kit (Qiagen) following the manufacturer's instructions. For the experimental validation using transfected moDCs and fibroblasts, due to the limiting number of cells, the total RNA was isolated using an RNeasy Micro Kit (Qiagen) according to the manufacturer's instructions. The concentration of DNA and RNA was assessed using the Qubit RNA HS Assay Kit and Qubit dsDNA HS Assay Kit (Life Technologies), respectively, and measured in the Qubit 2.0 fluorimeter (Invitrogen).

RNA sequencing

RNA Sequencing (RNA-seq) was performed at the Genomic Facility from the University Medical Center of Utrecht. RNA integrity was first evaluated using a Bioanalyzer (Agilent). RNA-seq library was prepared using 100ng total RNA using the TruSeq kit (Illumina). Oligo(dT) magnetic beads were used to enrich for messenger RNAs which were then fragmented (about 200 bp). Random hexamer-primers were used to reverse transcribe mRNA into double stranded cDNA, which was then end-repaired followed by addition of 3'-end single nucleotide adenine. Sequencing adaptors were ligated to the resulting cDNA that was subsequently amplified using PCR. Agilent 2100 Bioanaylzer and the ABI StepOnePlus Real-Time PCR System were used to assess the quality and quantity of RNA-seq libraries. The library products were sequenced on an Illumina NextSeq 500 sequencer using 75bp single-end reads, generating on average 26.2 million clean reads per sample.

Transcriptional data analysis

For each of the 65 transcriptional profiles, reads were aligned using STAR aligner using the default parameters to the 65,217 annotated genes obtained from the GrCh38 (v79) built from the human genome (http://www.ensembl.org). On average 22.5 million uniquely mapped reads were obtained per sample. The read counts per gene were quantified by the Python package HTSeq[33] using annotations from the GrCh38 (v79) built from the human genome (http://www.ensembl.org). Differentially expressed genes (DEGs) were identified by using the DESeq2 (1.8.2) Bioconductor/R package[34] using likelihood ratio test (LRT), and genes with FDR adjusted p-value < 0.05 were considered differentially expressed. Raw count data were transformed to count per million (CPM) for gene expression visualization. Variance stabilizing transformation (VST) was applied to obtain the VSD data for further analysis[34].

DNA methylation profiling

DNA methylation profiling was performed at the GenomeScan (GenomeScan B.V., Leiden, The Netherlands). Genomic DNA was bisulfite-converted using the EZ DNA Methylation Gold Kit (Zymo Research) and used for microarray-based DNA methylation analysis on the HumanMethylation850 BeadChip (Illumina, Inc.), according to the manufacturer's instructions. Beadchip images were scanned on the iScan system and the data quality was assessed using the minfi (version 1.20.2) package[35] using default analysis settings.

DNA methylation data analysis

Illumina Infinium HumanMethylation850 BeadChip fluorescent data (>850,000 CpG sites) were imported and transformed to methylated (M) and unmethylated (U) signal by minfi package[35]. CpG probes were quality-checked and filtered using the following criteria: (i) probes that failed in at least 5% samples were removed, (ii) probes with bead count < 3 in at least 5% of samples were removed, (iii) probes targeting SNP sites were removed, and (iv) probes that aligned to multiple locations were removed as described[36]. We further removed the probes for the sex chromosomes. One sample (102920-001-17, moDC differentiation sample from donor 4 on day 2) did not pass the quality check and was removed from the subsequent analysis. Approximately 558,000 CpG sites located in six regions (TSS1500, TSS200, 5'UTR, 1stExon, Exon boundaries and 3'UTR) remained after the quality checks. The intra-array data normalization for the bias introduced by two types of Infinium probes was performed by Beta-mixture quantile normalization (BMIQ) method in ChAMP (version 2.6.0) package[37]. The DNA methylation level of each CpG was depicted by the ratio of methylated (M) signal relative to the sum of both methylated and unmethylated (U) signal:

$$\beta = \frac{M}{M + U + 100}$$

We studied the alterations of DNA methylation considering: i) individual CpG sites, ii) region of the CpG site (including 1500 base pairs before TSS or TSS1500, TSS200, 5'UTR, 1st Exon, Exon boundaries and 3'UTR), and iii) proximal genes. To find the differentially methylated CpGs (DMPs) of moDC or of CXCL4 moDC associated with time, a linear regression model with two variables (donor and time) was fitted at each probe. We analyzed DMPs separately for differentiation and stimulation experiments. CpG sites with time-associated FDR corrected p-value <0.05 were considered DMPs. Similarly, DMPs between moDCs and CXCL moDCs were identified using a linear regression model with three variables (donor, time and condition). To obtain region-specific β-values, we calculated the average β-values using all probes that mapped to the same region (including TSS1500, TSS200, 5'UTR, 1stExon, ExonBnd and 3'UTR38) for a given gene. We then applied the same regression models to find differentially methylated regions (DMRs). If any of the regions around the gene were significantly altered, we considered that the gene was differentially methylated (DMGs).

Multidimensional scaling (MDS) analysis

Transcriptional data (VSD) and DNA methylation data (β) were utilized to visualize the differences of cells during differentiation and polyI:C stimulation. The Euclidean distances between samples were calculated based on VSD or β. Multidimensional scaling was performed using these distances in R (cmdscale function from stats package) to project (visualized using ggplot2 package) the high dimensional transcriptional or DNA methylation data onto two dimensions. MDS plots were generated using the DEGs or DMGs.

Comparison of gene expression and DNA methylation

To compare the relationship between expression and methylation data, we analyzed the two-layered data from genes that were both differentially expressed and methylated. We calculated Spearman correlation coefficients (for **Fig. 3a**, and **S4b-d**) between the expression (VSD) and methylation (β values) data for the genes using the cor function in R. To ensure paired analysis, we removed the corresponding expression profiles for the sample which failed the DNA methylation quality checks. Thus, we performed all correlation-based analysis using 64 pairs of samples. To study the global relationship between gene expression and DNA methylation, contour plots were constructed for paired expression (VSD) and methylation (β values) data using geom_density2d function in R (**Fig. S4f** and **g**). For **Fig. S4f** we used the paired data from all the genes, while for **Fig. S4g** we used the paired data from all the genes that were both differentially expressed and differentially methylated. We further analyzed the relationship between the paired expression (VSD) and methylation (β values) data using linear regression models and by fitting smoothing curves using generalized additive model (GAM).

Pathway enrichment analysis

Pathway enrichment analysis, for DEGs, DMGs or module genes, was performed using hypergeometric test in ReactomePA package[39]. The compareCluster function in the ReactomePA package (with parameters fun="enrichPathway", pAdjustMethod = "fdr", and pvalueCutoff = 0.05) was used to compare and plot the pathways enriched in different sets of genes.

CIITA-silencing in monocytes

Freshly purified monocytes were cultured in medium without antibiotics at a density of $2x10^6$ cells/ml. Transfection mix was prepared with 40nM of Silencer® pre-designed siRNA against human CIITA (targeting exon 3 and 4; siCIITA) or the SilencerTM Negative Control No.1 (siControl) (Life technologies), Lipofectamine 2000 and Plus Reagent (both from Invitrogen), diluted in Opti-MEM® I Reduced-Serum Medium (Life Technologies). After 5 hours, transfected cells were washed with culture medium and were differentiated into moDCs as described above.

Fibroblast cultures

Dermal fibroblasts (DF) were isolated from healthy skin biopsies. Skin biopsies were obtained from unused material after cosmetic surgery from anonymous donors who had given prior informed consent to use the biopsies for research. The use of this material is exempted from ethical review processes. DF were isolated using the Whole Skin Dissociation Kit (MiltenyiBiotec) following the manufacturer's instructions, cultured in DMEM medium (Life Technologies) supplemented with 10% (v/v) FBS, and 1% (v/v) antibiotics (used for experiments between passages 4 and 5). Prior to the treatment, DF were cultured O/N with DMEM medium containing 1% FBS. Supernatants collected from moDCs and CXCL4 moDCs stimulated with polyI:C for 24 hours were added to the DF for 24 hours. Medium and polyI:C were also added to the DF as controls (data not shown).

Real-time quantitative PCR

Purified RNA was retro-transcribed with iScript Reverse Transcriptase Kit (Bio-Rad). Gene expression was measured by Real-Time quantitative-PCR (RT-qPCR) on the QuantStudio 12k flex system using SybrSelect Mastermix (Life Technologies). To calculate the ratio between the expression of a gene of interest and housekeeping genes (mean between *RPL32* and *RPL13A* for moDCs cultures; RPL13A for the fibroblasts cultures), we used either the 2-DCt or the 2-DDCt method. Primer sequences are listed in the online **Table S2**.

Cytokine production measurement

To validate secreted targets at the protein level, we collected cell-free supernatants after moDC and CXCL4 moDCs differentiation (day 6) and after 24 hour stimulation with polyI:C (day 8) from the same 5 HDs that were used for RNA sequencing and DNA methylation profiling. Cytokine measurements were assessed using Luminex assay as previously described8 at the MultiPlex Core Facility of the Laboratory of Translational Immunology (University Medical Center Utrecht). Data were acquired using Bio-Rad FlexMap3D system and the Xponent 4.2 software, and analyzed using Bio-Plex Manager (version 6.1).

Flow cytometry

Cells were first incubated with Fixable Viability Dye eFluor780 (eBioscience) in PBS to exclude dead cells and were further treated with 10% (v/v) mouse serum (Fitzgerald). Next, cells were stained with the following anti-human fluorochrome-conjugated mAbs: CD14 (clone M5E2), CD86 (clone IT2.2) and CLEC10A (H037G3) obtained from BioLegend, CD1a (clone HI149) and LAMP1/ CD107a (clone H4A3) obtained from BD. Cells were acquired on the LSR Fortessa (BD) and data was analyzed using the FlowJo software (version 7.6.5; Tree Star. Inc.).

Western blot

Cells were washed with PBS and lysed in Laemmli buffer. Protein concentration was quantified using the Pierce BCA Protein Assay Kit (Thermo Scientific) according to the manufacture's protocol. Equal amounts of protein from different lysates were separated by electrophoresis on a 4-12% Bis-Tris SDS NuPAGE gels (Invitrogen) and transferred to a PVDF membrane (Millipore). After blocking the membranes with Tris-buffered saline (pH 8) containing 0.05% Tween-20 and 4% milk (Bio-Rad) for 1 hour at room temperature (RT), the membranes were probed with the antibodies recognizing FN1 (Abcam) and tubulin (Sigma-Aldrich) O/N at 4oC. Afterwards, membranes were washed and incubated for 1 hour at RT with the secondary anti-rabbit or anti-mouse antibodies, both HRP-conjugated (Dako). Protein detection was assessed using a ChemiDoc MP System (Bio-Rad). Protein visualization and densitometry analysis of band intensity were performed using the Image Lab software (version 5.1, Bio-Rad). We calculated the ratio between the expression of FN1 and tubulin to determine the relative expression of FN1 in different conditions.

Confocal microscopy

As an alternative way to validate the expression and production of FN1, we performed microscopy analyses as described before[8], with minor modifications. For the differentiation of moDCs, we used Nunc® Lab-Tek® II chamber slides (Thermo

Scientific) pre-coated with 0.01% (v/v) poly-L-lysine (Sigma-Aldrich) in sterile water. After differentiation, cells were incubated with fixation/permeabilization solution (eBioscience) supplemented with 5% (v/v) normal goat serum (Cell Signaling) for 30 minutes at RT, followed by two washes with permeabilization buffer (eBioscience). Cells were incubated for 1 hour with primary antibody recognizing FN1 (Abcam). After washing twice, cells were incubated with secondary antibody Alexa 594 anti-rabbit (Life Technologies) and phalloidin-labeled FITC (ENZO) for 1 hour. Cells were washed and incubated with Hoechst 33342 (1 µM; Invitrogen) for 15 minutes. Next, cells were washed with permeabilization buffer twice, and at last washed with 1% (w/v) BSA and 0.1% (v/v) sodium azide (NaN_3; Sigma-Aldrich) in PBS. Mowiol (Sigma-Aldrich) was used to mount the dry slides and coverslips. Image acquisition was performed on a LSM710 (Zeiss) confocal microscope using the Zen2009 (Zeiss Enhanced Navigation) acquisition software. Confocal images were obtained with the objective 63x 1.40 oil and analyzed using the ImageJ software.

RegEnrich pipeline

We developed a data driven pipeline (RegEnrich) to integrate CXCL4 specific transcriptional and DNA methylation signatures and to predict the key TFs driving the differential transcriptional profile of CXCL4 moDCs compared to moDCs (**Fig. 3b-e**, and **4a-b**). RegEnrich pipeline involves three steps: 1) construction of data-driven networks; 2) deducing genes of interest; and 3) enrichment of transcriptional factors or regulators (henceforth called "*TF*"). The aim of RegEnrich pipeline is to rank TFs based on their differential expression and the enrichment of their own downstream targets in a given gene set. RegEnrich pipeline can be made available upon request from the authors.

Co-expression/co-methylation network construction

For co-expression network, VSD data of all DEGs were used to construct a co-expression network by R package WGCNA (version 1.51)[19] as described in https://labs.genetics.ucla.edu/horvath/CoexpressionNetwork. Briefly, we used unsigned correlations and a soft thresholding power of 6 to construct networks with scale free topology. We calculated the adjacency matrix which was further used to calculate Topological overlap matrix (TOM) to identify modules of co-expressed genes. Modules were identified using cutreeDynamic function with the minimum module size of 30. Modules were further merged if the Pearson correlation of their eigengene was <0.25. Using this methodology, we obtained 27 co-expression modules (**Fig. S5a**). Nodes (genes) and edges (connections of genes) in each module were exported by exportNetworkToCytoscape function (threshold >=0.02).

To build co-methylation network, we first assigned a unique β value to a given gene of a sample by setting priority to four regions: TSS200>TSS1500>5'UTR>1stExon as described in Jiao *et al*.[38]. If for a gene TSS200 region is differentially methylated (DM), we considered the β value of TSS200 as the methylation level of this gene. Similarly, for a gene without DM TSS200 but with DM TSS1500, β value of TSS1500 region was used, and so on. Then these regions, representing corresponding genes, were used to build co-methylation networks using the methodology described for the co-expression network. To achieve topological scale-free networks, standard parameters were set to a soft thresholding power of 12, "unsigned" network, minimum module size of 30, merged module threshold < 0.25, and an exporting network threshold of 0.02. In total, 10 modules were reserved in the end (**Fig. S5b**).

Integration of co-expression and co-methylation network

Spearman correlation coefficients were calculated using the co-expression and co-methylation module eigengenes to integrate the two networks (**Fig. S5c**). We calculated the number of genes shared between co-expression and co-methylation modules and two-tailed fisher exact test was used to evaluate the significance of each overlap (**Fig. 3c**). Pearson correlation coefficients were used to relate gene modules to sample traits i.e., CXCL4+/-, time and polyI:C+/- (**Fig. 3c**).

Gene regulatory network (GRN) construction based on random forest (RF) algorithm

To obtain potential transcription (co-)factor/regulators (TF) for each gene in a data-driven manner, we constructed a TF-target GRN using random forest machine learning algorithm (modified from[40, 41] and is part of RegEnrich package developed by us; see below). This TF-target GRN is a directed network of two types of components: a) TFs and b) their potential targets. Here targets might not necessarily be direct downstream targets that the TFs might bind to, rather the genes that are inferred to be directly/indirectly regulated by the TFs based on the transcriptional data. The construction of TF-target GRN consisted of four steps. First, the VST normalized data from 17,709 DEGs (same genes in co-expression network), including 1,172 differentially expressed TFs (**Table S9**), were selected for the analyses. Second, we removed all the target genes that are expressed in less than 10 samples. Third, for every target gene, a random forest model was built to predict its expression based on TF expression (the parameters are: K = "sqrt", nb.trees = 1000, importance.measure = "IncNodePurity"). As a last step, models with low performance (MSE < 0.5) were removed to achieve a robust TF-target GRN.

TF enrichment analysis

In this study, TF enrichment analyses were performed on two data-driven networks, a co-expression network and a GRN network. For the co-expression network, we ranked the edges between TFs and their potential targets based on the edge weight. Top 5% edges were then selected and were considered for further analyses. This resulted in 1,037,689 TF-target connections. Similarly for the GRN network, we used top 5% of edges (688,559 TF-target connections). One-tailed hypergeometric test was used to calculate the enrichment p-values (P_ε) for each TF in a given set of genes (here genes differential between CXCL4 moDCs and moDCs). Those TFs that exhibited significant differential expression ($P_o < 0.05$) and had significant enrichment ($P_\varepsilon < 0.05$) were considered as key TFs. In other words, TFs that were differentially expressed along with their own targets were considered to be enriched in a given gene set. The overall scores of TFs were calculated by:

$score = norm(-log\ (P_\varepsilon)) + norm(-log(P_o))$, where $\text{norm}(x) = \frac{\text{x-min (r)}}{\text{max (r) - min(r)}}$.

Cytoscape 3.4 (www.cytoscape.org) was used to visualize the networks. In TF-TF networks, we only plot the edges connecting the enriched key TFs in both co-expression and GRN network. For better visualization, only TFs with |log2(fold change)| > 0.6 were shown (**Fig. 4a**, **b**, **S7a** and **b**).

Data availability: RNAseq count matrices and BAM files have been deposited in the National Center for Biotechnology Information's Gene Expression Omnibus under accession number GSE115488. Raw and processed DNA methylation data has been deposited in the National Center for Biotechnology Information's Gene Expression Omnibus under accession number GSE115201.

References

1. Rinkevich, Y. *et al.* Skin fibrosis. Identification and isolation of a dermal lineage with intrinsic fibrogenic potential. *Science* **348**, aaa2151 (2015).
2. Zeisberg, M. & Kalluri, R. Cellular mechanisms of tissue fibrosis. 1. Common and organ-specific mechanisms associated with tissue fibrosis. *Am. J. Physiol. Cell Physiol.* **304**, C216-225 (2013).
3. Wick, G. *et al.* The immunology of fibrosis: innate and adaptive responses. *Trends Immunol.* **31**, 110-119 (2010).
4. Levine, S.P. & Wohl, H. Human platelet factor 4: Purification and characterization by affinity chromatography. Purification of human platelet factor 4. *J. Biol. Chem.* **251**, 324-328 (1976).
5. van Bon, L. *et al.* Proteome-wide analysis and CXCL4 as a biomarker in systemic sclerosis. *N. Engl. J. Med.* **370**, 433-443 (2014).
6. Schaffner, A., Rhyn, P., Schoedon, G. & Schaer, D.J. Regulated expression of platelet factor 4 in human monocytes - role of PARs as a quantitatively important monocyte activation pathway. *J. Leukoc. Biol.* **78**, 202-209 (2005).
7. Affandi, A.J. *et al.* CXCL4 is a novel inducer of human Th17 cells and correlates with IL-17 and IL-22 in psoriatic arthritis. *Eur. J. Immunol.* **48**, 522-531 (2018).
8. Silva-Cardoso, S.C. *et al.* CXCL4 exposure potentiates TLR-driven polarization of human monocyte-derived dendritic cells and increases stimulation of T cells. *J. Immunol.* **199**, 253-262 (2017).
9. Scheuerer, B. *et al.* The CXC-chemokine platelet factor 4 promotes monocyte survival and induces monocyte differentiation into macrophages. *Blood* **95**, 1158-1166 (2000).
10. Schinnerling, K., Garcia-Gonzalez, P. & Aguillon, J.C. Gene expression profiling of human monocyte-derived dendritic cells - searching for molecular regulators of tolerogenicity. *Front. Immunol.* **6**, 528 (2015).
11. Gleissner, C.A., Shaked, I., Little, K.M. & Ley, K. CXC chemokine ligand 4 induces a unique transcriptome in monocyte-derived macrophages. *J. Immunol.* **184**, 4810-4818 (2010).
12. Vento-Tormo, R. *et al.* IL-4 orchestrates STAT6-mediated DNA demethylation leading to dendritic cell differentiation. *Genome Biol.* **17**, 4 (2016).
13. Saeed, S. *et al.* Epigenetic programming of monocyte-to-macrophage differentiation and trained innate immunity. *Science* **345** (2014).
14. Zhang, X. *et al.* DNA methylation dynamics during ex vivo differentiation and maturation of human dendritic cells. *Epigenet. Chromatin* **7** (2014).
15. Broen, J.C., Radstake, T.R. & Rossato, M. The role of genetics and epigenetics in the pathogenesis of systemic sclerosis. *Nat. Rev. Rheumatol.* **10**, 671-681 (2014).
16. Altorok, N., Tsou, P.S., Coit, P., Khanna, D. & Sawalha, A.H. Genome-wide DNA methylation analysis in dermal fibroblasts from patients with diffuse and limited systemic sclerosis reveals common and subset-specific DNA methylation aberrancies. *Ann. Rheum. Dis.* **74**, 1612-1620 (2015).
17. Ramirez, R.N. *et al.* Dynamic gene regulatory networks of human myeloid differentiation. *Cell Syst.* **4**, 416-429 (2017).
18. Goode, D.K. *et al.* Dynamic gene regulatory networks drive hematopoietic specification and differentiation. *Dev. Cell* **36**, 572-587 (2016).
19. Langfelder, P. & Horvath, S. WGCNA: an R package for weighted correlation network analysis. *BMC Bioinformatics* **9**, 559 (2008).
20. Langfelder, P., Luo, R., Oldham, M.C. & Horvath, S. Is my network module preserved and reproducible? *PLoS Comp. Biol.* **7** (2011).

21. Landsverk, O.J.B., Ottesen, A.H., Berg-Larsen, A., Appel, S. & Bakke, O. Differential regulation of MHC II and invariant chain expression during maturation of monocyte-derived dendritic cells. *J. Leukoc. Biol.* **91**, 729-737 (2012).
22. Massague, J. TGF beta signalling in context. *Nat. Rev. Mol. Cell Biol.* **13**, 616-630 (2012).
23. Xue, M. & Jackson, C.J. Extracellular matrix reorganization during wound healing and its impact on abnormal scarring. *Adv. Wound Care (New Rochelle)* **4**, 119-136 (2015).
24. van Bon, L. *et al.* Low heme oxygenase-1 levels in patients with systemic sclerosis are associated with an altered Toll-like receptor response: another role for CXCL4? *Rheumatology* **55**, 2066-2073 (2016).
25. Hwaiz, R., Rahman, M., Zhang, E.M. & Thorlacius, H. Platelet secretion of CXCL4 is Rac1-dependent and regulates neutrophil infiltration and tissue damage in septic lung damage. *Br. J. Pharmacol.* **172**, 5347-5359 (2015).
26. Yeo, L. *et al.* Expression of chemokines CXCL4 and CXCL7 by synovial macrophages defines an early stage of rheumatoid arthritis. *Ann. Rheum. Dis.* **75**, 763-771 (2016).
27. Cheng, S.C. *et al.* mTOR- and HIF-1α–mediated aerobic glycolysis as metabolic basis for trained immunity. *Science* **345** (2014).
28. Mourits, V.P., Wijkmans, J.C., Joosten, L.A. & Netea, M.G. Trained immunity as a novel therapeutic strategy. *Curr. Opin. Pharmacol.* **41**, 52-58 (2018).
29. Bekkering, S. *et al.* Oxidized low-density lipoprotein induces long-term proinflammatory cytokine production and foam cell formation via epigenetic reprogramming of monocytes. *Thrombosis* **34**, 1731-1738 (2014).
30. Crisan, T.O. *et al.* Soluble uric acid primes TLR-induced proinflammatory cytokine production by human primary cells via inhibition of IL-1Ra. *Ann. Rheum. Dis.* **75**, 755-762 (2016).
31. LeRoy, E.C. Increased collagen synthesis by scleroderma skin fibroblasts in vitro: a possible defect in the regulation or activation of the scleroderma fibroblast. *J. Clin. Invest.* **54**, 880-889 (1974).
32. van Bon, L. *et al.* Proteomic analysis of plasma identifies the Toll-like receptor agonists S100A8/A9 as a novel possible marker for systemic sclerosis phenotype. *Ann. Rheum. Dis.* **73**, 1585-1589 (2014).
33. Anders, S., Pyl, P.T. & Huber, W. HTSeq--a Python framework to work with high-throughput sequencing data. *Bioinformatics* **31**, 166-169 (2015).
34. Love, M.I., Huber, W. & Anders, S. Moderated estimation of fold change and dispersion for RNA-seq data with DESeq2. *Genome Biol.* **15** (2014).
35. Aryee, M.J. *et al.* Minfi: a flexible and comprehensive Bioconductor package for the analysis of Infinium DNA methylation microarrays. *Bioinformatics* **30**, 1363-1369 (2014).
36. Nordlund, J. *et al.* Genome-wide signatures of differential DNA methylation in pediatric acute lymphoblastic leukemia. *Genome Biol* **14**, r105 (2013).
37. Morris, T.J. *et al.* ChAMP: 450k Chip Analysis Methylation Pipeline. *Bioinformatics* **30**, 428-430 (2014).
38. Jiao, Y., Widschwendter, M. & Teschendorff, A.E. A systems-level integrative framework for genome-wide DNA methylation and gene expression data identifies differential gene expression modules under epigenetic control. *Bioinformatics* **30**, 2360-2366 (2014).
39. Yu, G.C. & He, Q.Y. ReactomePA: an R/Bioconductor package for reactome pathway analysis and visualization. *Mol. Biosyst.* **12**, 477-479 (2016).
40. Huynh-Thu, V.A., Irrthum, A., Wehenkel, L. & Geurts, P. Inferring Regulatory Networks from Expression Data Using Tree-Based Methods. *PLoS One* **5** (2010).
41. Walley, J.W. *et al.* Integration of omic networks in a developmental atlas of maize. *Science* **353**, 814-818 (2016).

Acknowledgments: We thank Dr. Kris Reedquist and Prof. Linde Meyaard for their critical comments, Dr. Marzia Rossato for discussions about RNAseq and other members of our lab for the fruitful discussions. Funding: SCSC was supported by Portuguese FCT No.SFRH/BD/89643/2012; WT was supported by China Scholarship Council (CSC) No.201606300050; AP was supported by Netherlands Organisation for Scientific Research (NWO) grant number: 016.Veni.178.027; TRDJR was supported by ERC starting grant (CIRCUMVENT) and Arthritis foundation grant.

Author contributions: Conceptualization (TRDJR, MB, SCSC, WT, AP on the conceptualization SCSC), Methodology (SCSC, BG, MC, WT, CA, APL, CPJB), Formal Analysis (WT, AD, AP), Resources (TRDJR), Writing original draft (SCSC, WT, AP, TRDJR), Writing reviewing and editing (SCSC, WT, CA, APL, CPJB, AD, JL, WM, EH, RJB, MB, AP, TRDJR), Visualization (WT, SCSC, AP), Supervision (TRDJR, MB, AP), Project Administration (TRDJR), Funding Acquisition (TRDJR, AP).

Supplementary Materials

Supplementary figures

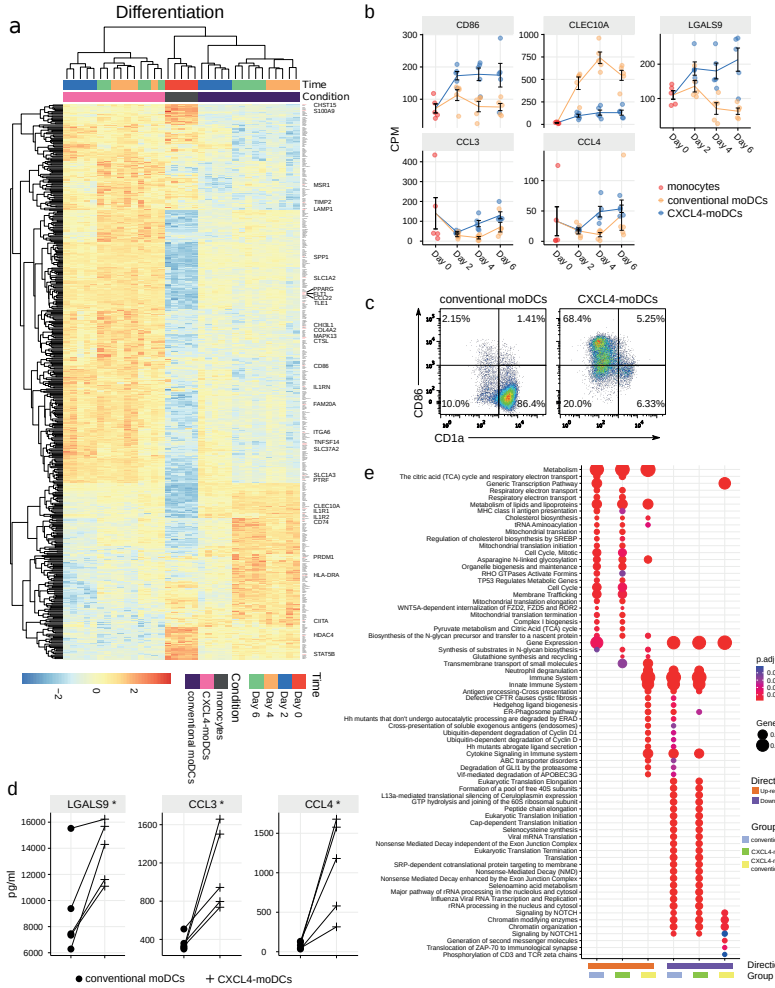

Fig. S1. Differentially expressed genes during differentiation. (a) Heatmap showing normalized expression (VSD) of top 500 DEGs between CXCL4 moDCs and moDCs during their differentiation (day 0 to day 6). Heatmap color schemes are based on z-scores. Hierarchical clustering dendrograms were calculated using Euclidean distance. **(b)** Gene expression profiles for example genes from top 500 DEGs that were further validated at the protein level. Data are shown as mean of count per million (CPM) ± SEM. **(c)** Flow cytometry dot plot showing expression of CD86 and CD1a. Representative data from 5 HDs are shown. **(d)** Cytokine production of selected example proteins measured by Luminex using cell-free supernatants collected on day 6. Each symbol represents an individual donor; lines connect the same donor. **(e)** Pathway enrichment analysis for the genes which were significantly up- and down-regulated during differentiation, as shown in **Fig. 1b**. Up to 30 most significant pathways (FDR adjusted $p < 0.05$) were shown for each set of genes. The size of the circle depicts the gene ratio of DEGs in the pathway to the total number of DEGs in each set of genes. Circle color represents FDR adjusted p values. The full lists of pathways are available in **Table S5**. Paired two-sided Student's *t*-test; * $P<0.05$.

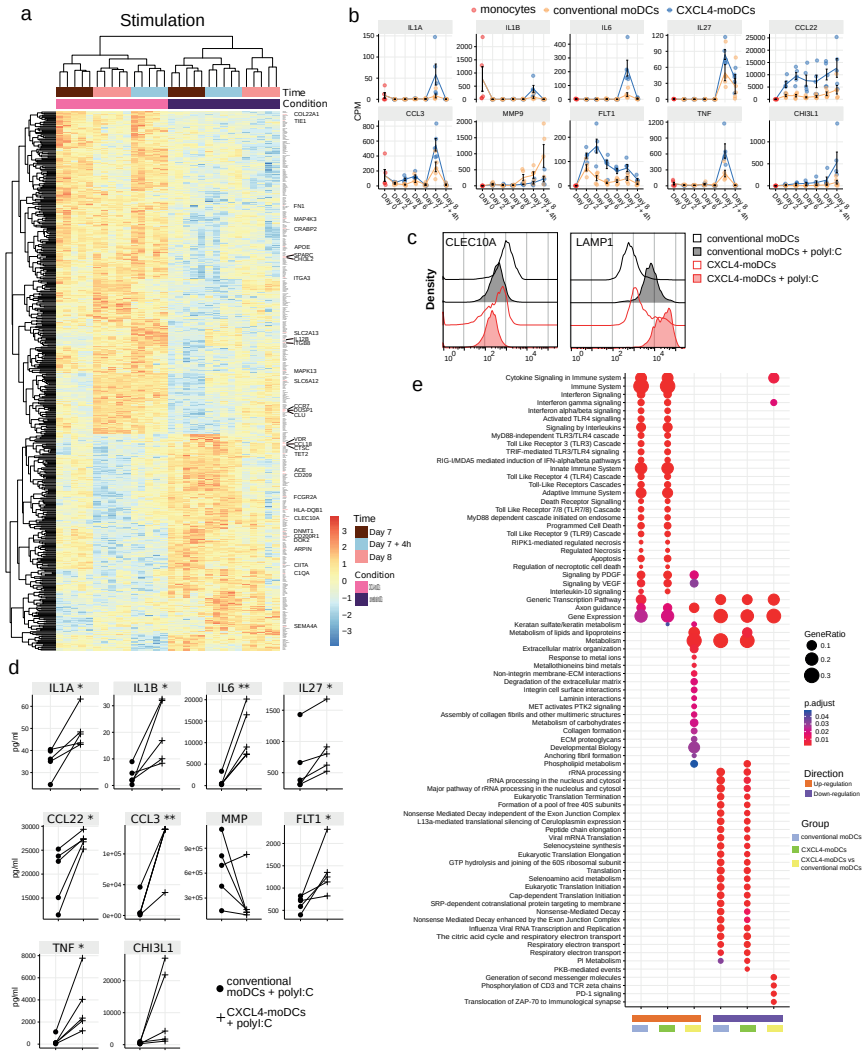

Fig. S2. Differentially expressed genes upon polyI:C stimulation. (a) Heatmap same as Fig. S1 for top 500 DEGs between CXCL4 moDCs and moDCs upon polyI:C stimulation (day 7 to day 8). **(b)** Gene expression profiles for example genes from top 500 DEGs that were further validated on protein level. Data are shown as mean±SEM. **(c)** Flow cytometry analysis showing the relative expression of CLEC10A and LAMP1 between CXCL4 moDCs and moDCs, unstimulated and stimulated with polyI:C for 24 hours (on day 8). Representative data from 5 HDs are shown. **(d)** Cytokine production was measured by Luminex on cell-free supernatants after 24 hours stimulation with polyI:C (day 8). Each symbol represents an individual donor; lines connect the same donor. **(e)** Pathway enrichment analysis for the genes that were significantly up- and down-regulated upon polyI:C stimulation, shown in **Fig. 1c**. Up to 30 most significant pathways (FDR adjusted $p < 0.05$) were shown for each set of genes. The size of the circle depicts the gene ratio of DEGs in the pathway to the total number of DEGs in each set of genes. Circle color represents FDR adjusted p values. The full lists of pathways are available in **Table S6**. Paired two-sided Student's *t*-test; * $P<0.05$, ** $P < 0.01$.

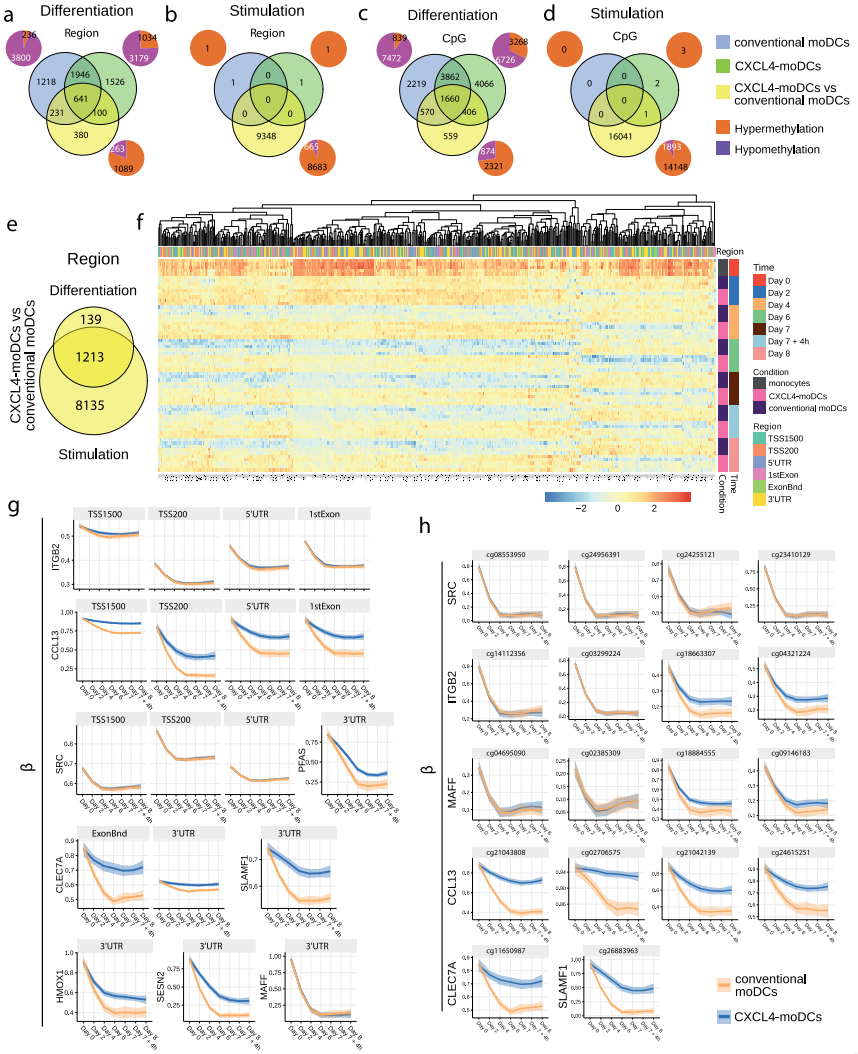

Fig. S3. Dynamics of DNA methylation on region and CpG levels. (a) Venn diagram shows the overlaps of differentially methylated regions (DMRs) and CpG sites **(c)** during differentiation of: monocytes into moDCs (blue); monocytes into CXCL4 moDCs (green), and DMRs between moDCs and CXCL4 moDCs (yellow). (**b**) Venn diagram showing DMRs and CpG sites **(d)** in moDC (blue), CXCL4 moDCs (green) and DMR/CpG between moDCs and CXCL4 moDCs (yellow) after polyI:C stimulation. In **(a-d)** pie charts represent the number of hyper-methylated regions (orange) and hypo-methylated regions (magenta). **(e)** Venn diagram showing the overlap of DMRs during differentiation (yellow circle in panel **a**) and upon polyI:C stimulation (yellow circle in panel **b**). **(f)** Heatmap reporting top 500 regions in overlapping DMRs in panel **d**. **(g)** Temporal methylation patterns of selected regions and CpG sites **(h)** found to be differential in different comparisons. Lines represent mean of β values and shades represent 95% confidence interval.

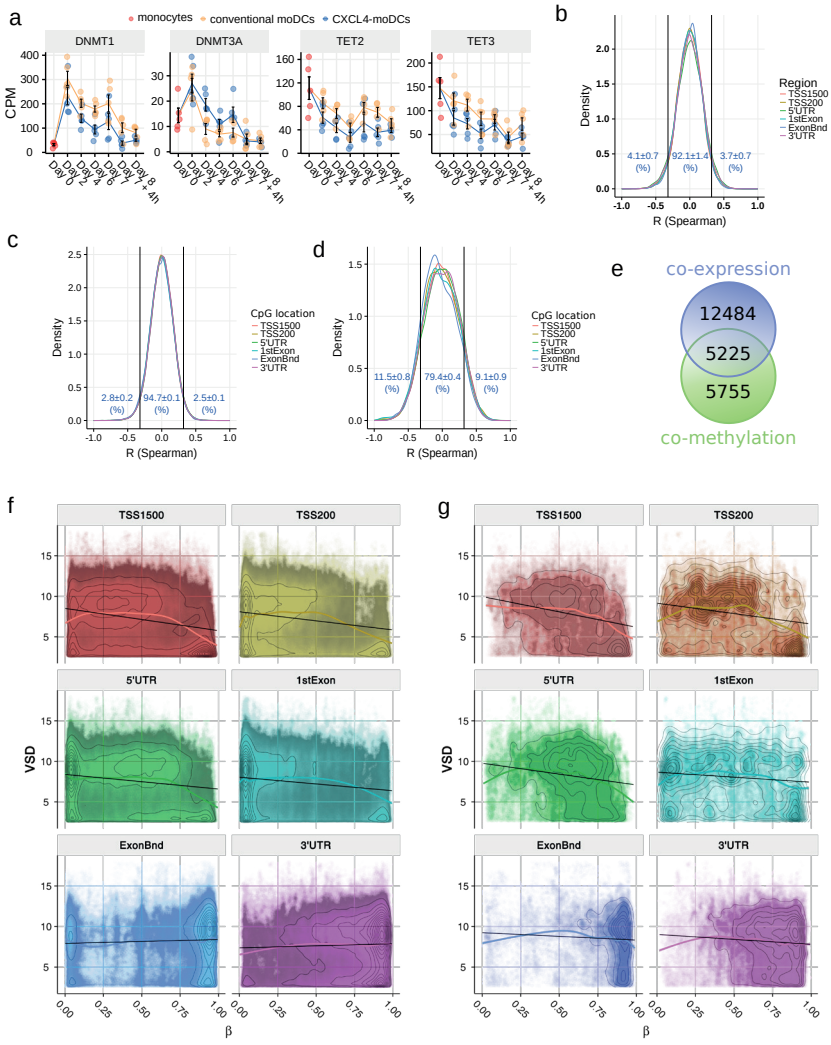

Fig. S4. Comparison of transcriptome and DNA methylome. (a) Gene expression profile alterations of DNA methyltransferases and DNA demethylases. Data are shown as mean±SEM. **(b)** The distribution of Spearman correlation coefficients between the methylation levels of all regions (including the regions that are not differentially methylated) and the corresponding gene expression. **(c)** The distribution of Spearman correlation coefficients between the methylation levels of all CpG sites (including the CpGs that are not differentially methylated) and the corresponding gene expression. **(d)** The distribution of Spearman correlation coefficients between the methylation levels of differentially methylated CpGs and the corresponding gene expression. In (**b** to **d**) the cut-offs (two vertical lines at R = ±0.32) indicate significant correlation coefficients ($P < 0.01$). Overlap between differentially expressed genes (DEGs) and differentially methylated genes (DMGs) during differentiation and upon polyI:C stimulation. A gene is considered differentially methylated if there is at least one region within this gene that is differentially methylated. **(e)** Venn diagram shows the overlapping genes between DEGs and DMGs in all comparisons which were used for further analysis. **(f)** Contour plots show global comparison of β values (x-axis) and VSD values (y-axis) for all the genes. **(g)** Contour plots show global comparison of β values (x-axis) and VSD values (y-axis) for genes that are differentially expressed and methylated. The black straight lines were obtained by fitting a linear regression model and the smoothing curves were obtained by fitting a non-linear model (see Methods).

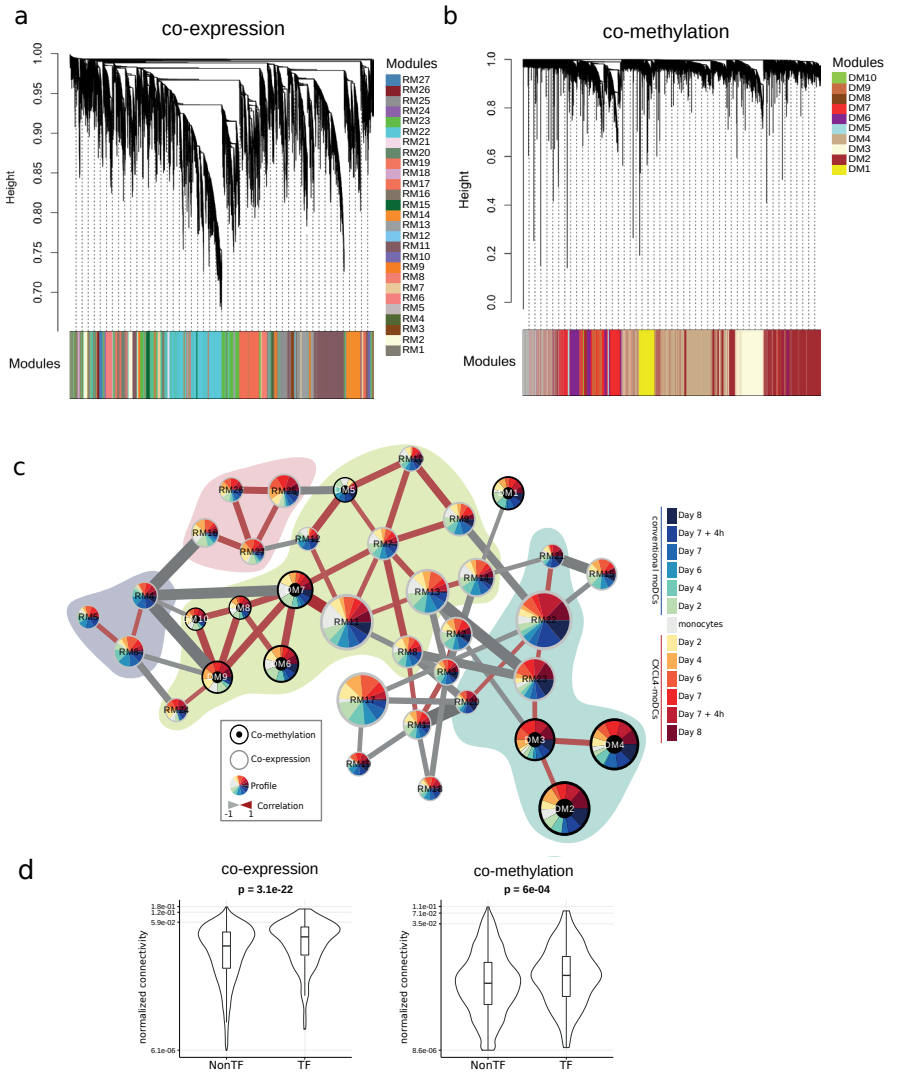

Fig. S5. Modules of co-expression and co-methylation networks. Hierarchical clustering dendrogram of genes generated using topological overlap matrix (TOM) obtained from **(a)** gene expression or **(b)** methylation data. The co-expression and co-methylation modules were obtained using WGCNA package and are shown with different colors independently. **(c)** Network of co-expression and co-methylation modules based on the correlation of module eigengenes. Each circle (node) represents either co-expression or co-methylation module. Co-methylation modules are denoted as a node with a black circle in the middle, while the other nodes denote co-expression modules. The size of each node depicts the number of genes within that module. Different time and conditions are represented by the colors shown in the legend. The colored pie chart within each node represents the eigengene profile of that module. The edges (lines between two nodes) represent spearman correlation coefficient (ρ) of eigengenes between two modules. The thickness of edge depicts the absolute value of ρ and edges with absolute value of ρ<0.65 are not shown. Colored shades in the background depict strongly positively correlated modules. **(d)** Violin/box plots comparing the connectivity, normalized by the total connectivity in the corresponding module, for transcription (co-)factors (TF) and other genes (NonTF) in the co-expression (left) and co-methylation (right) networks.

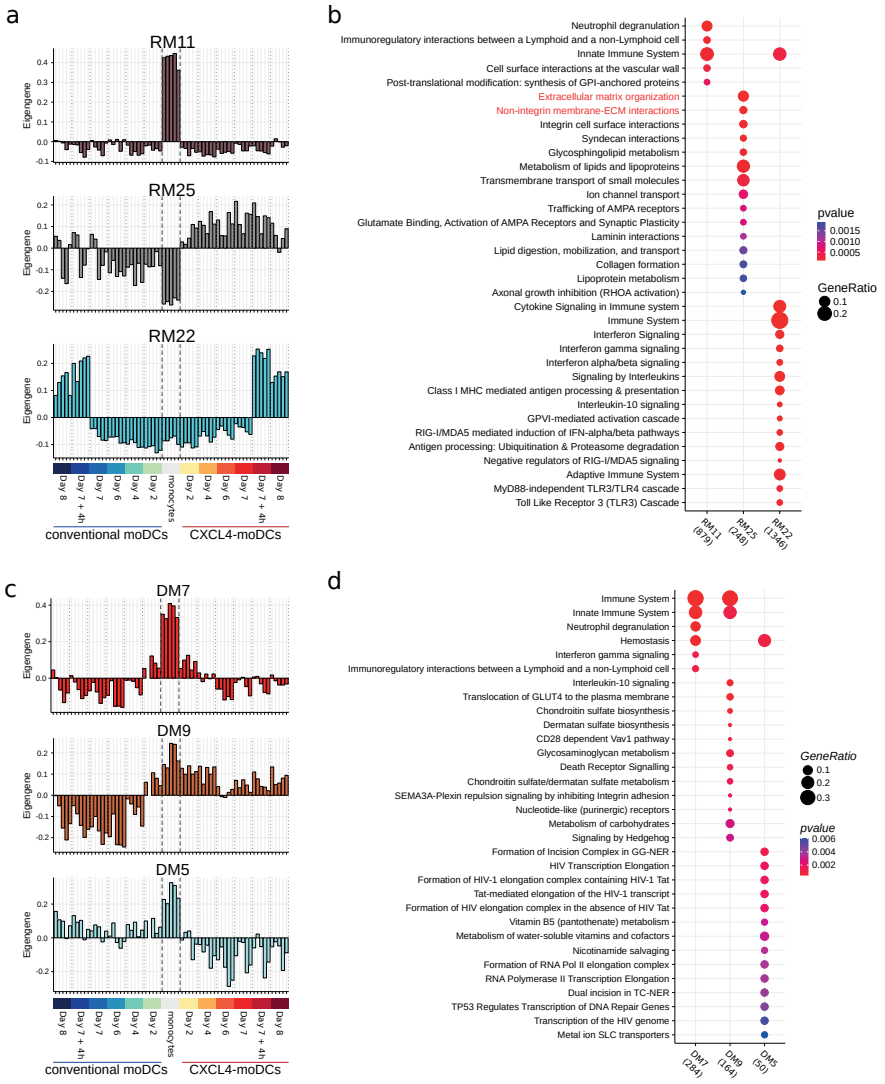

Fig. S6. Characteristics of co-expression and co-methylation modules. **(a)** Bar charts show the eigengene of representative co-expression modules. **(b)** Pathway enrichment analyses for the modules shown in **(a)**. **(c)** Bar charts of the eigengene of representative co-mehtylation modules. **(d)** Enriched pathways analysis for the modules shown in **(c)**. In **(b)** and **(c)** the size of the circle depicts the gene ratio of DEGs in the pathway to the total number of DEGs in each set of genes; the colors of the circle represent FDR adjusted p values. In brackets, below the graph, we show the number of genes in each module. The full lists of pathways are available in **Table S8**.

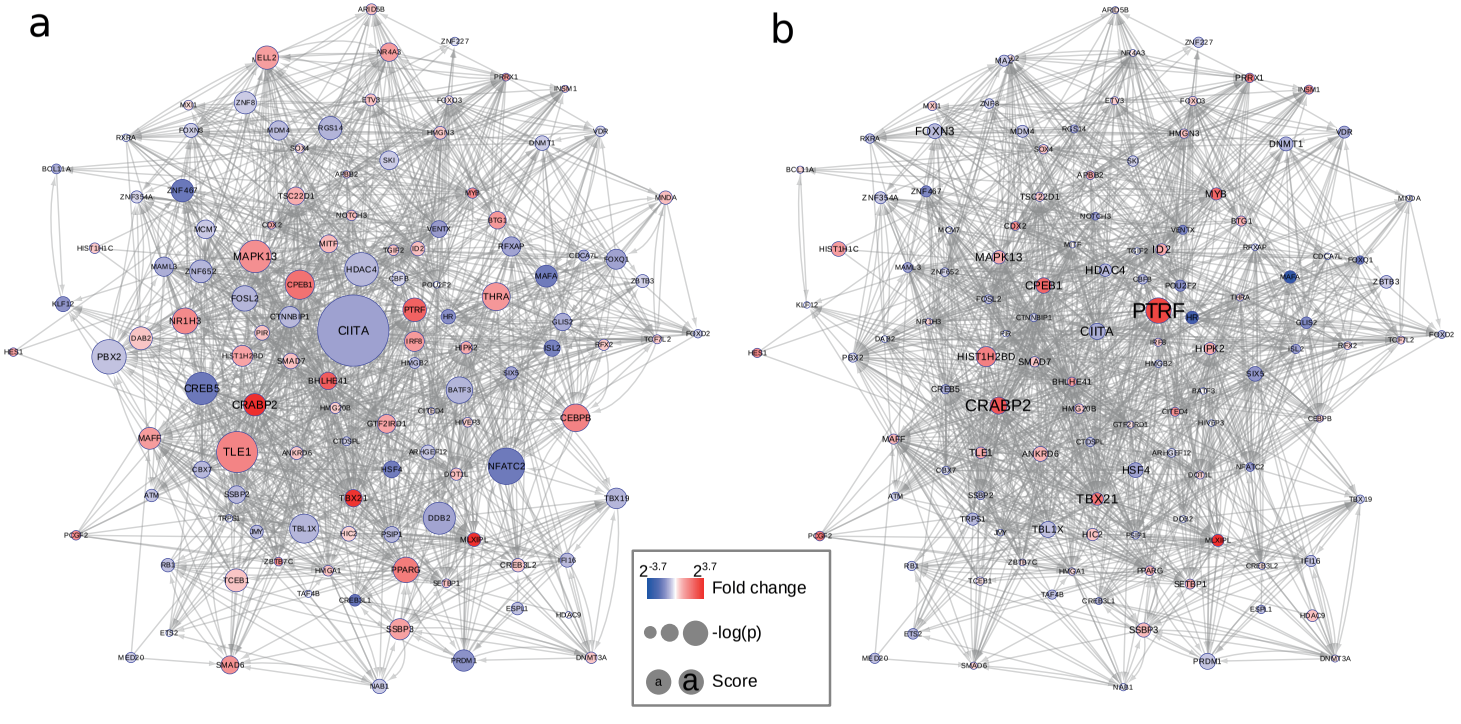
a
b
MAPK13
CIITA
CREB5
CRABP2
TLE1
PBX2
MAFF
CEBPB
NFATC2
TBX21
PPARG
HDAC4
CPEB1
PTRF
THRA
MAFA
FOSL2
NR1H3
FOXN3
HIST1H2BD
SMAD7
BHLHE41
HSP4
TBL1X
DNMT1
MYB
2-3.7
23.7
Fold change
-log(p)
Score

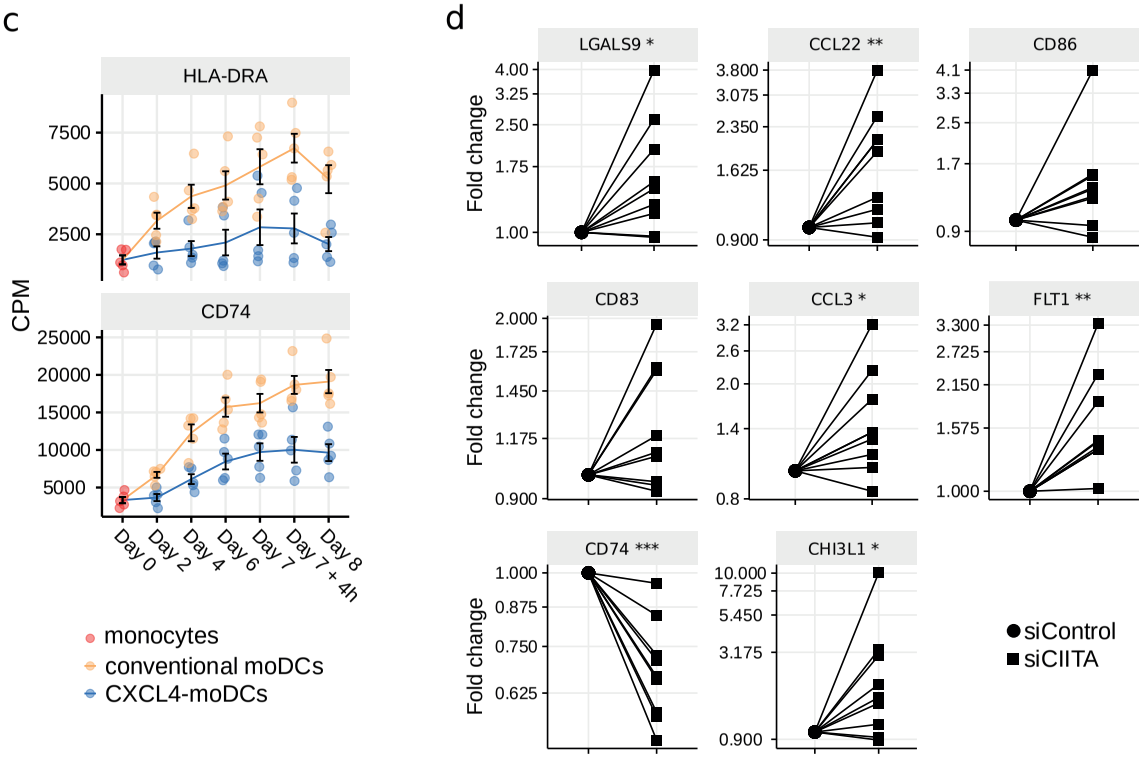

Fig. S7. Enriched transcription regulators obtained using random forest based gene regulatory network. Enriched transcription regulator networks **(a)** during differentiation and **(b)** upon stimulation. Red indicates up- regulation and blue indicates down-regulation of TFs in CXCL4 moDCs compared to moDCs. Circle size shows ($-\log_{10}(p)$) obtained using differential expression analysis. Text size represents the overall score of TF enrichment obtained from RegEnrich (see Methods). Edges (lines) were obtained from top 5% edges in gene regulatory network inferred by random forest. To make the networks comparable same scales and parameters were used. **(c)** Gene expression profile of DEGs downstream to CIITA regulation. **(d)** After transfection of monocytes with Silencer negative control siRNA (siControl) and Silencer CIITA siRNA (siCIITA), cells were differentiated into moDCs for 6 days. On day 6, inflammatory and co-stimulatory genes were analyzed by qPCR. (Data are normalized by the mean expression of *RPL32* and *RPL13A*; fold change relative to siControl). Each symbol represents an individual moDC donor; lines connect the same donor. Paired two-sided Student's *t*-test. * P <0.05, ** P < 0.01, *** P < 0.001.

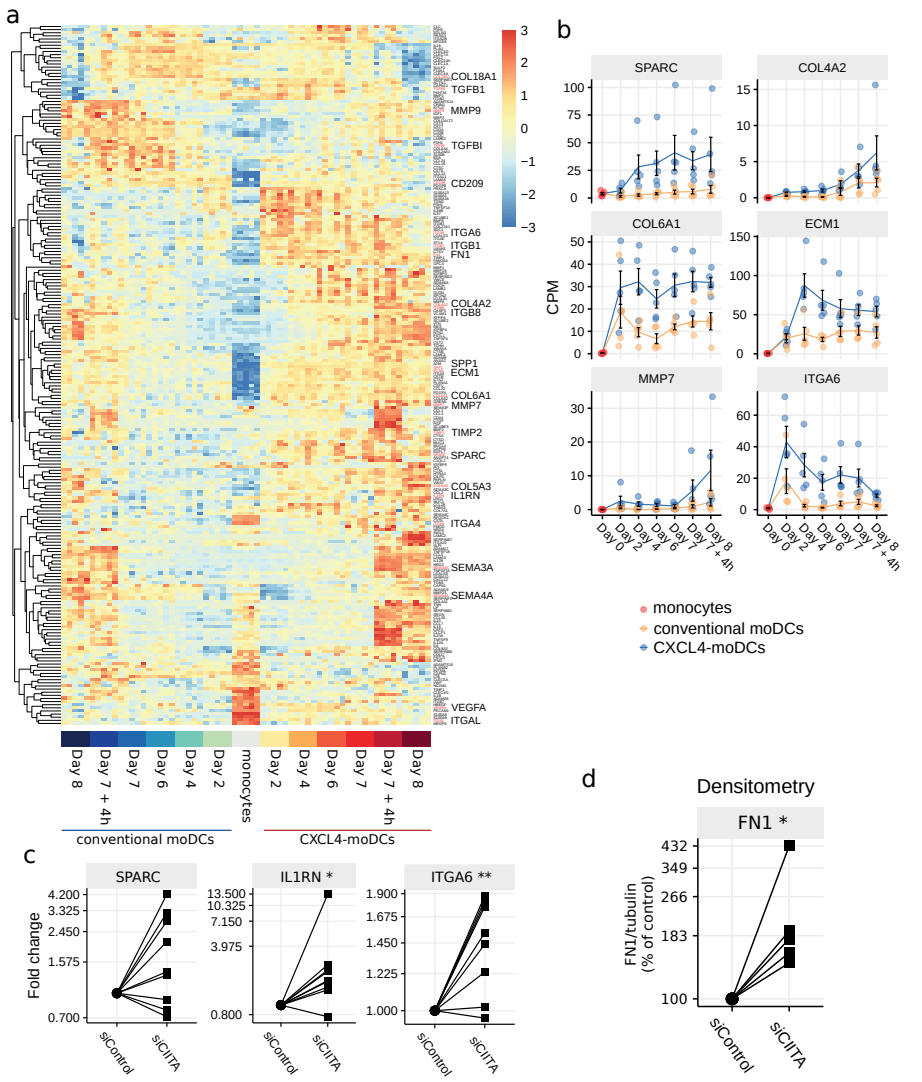

Fig. S8. Identification of genes implicated in ECM remodeling. (a) Heatmap showing differentially expressed genes that play a role in ECM remodeling, identified from pathway enrichment analysis (**Fig. S1b** and **Fig. S2b**), and CXCL4 responsive co-expression modules (**Fig. S5b**). Each column represents a sample and the colors on the bottom denote different time and conditions. The color schemes in the heatmap are shown as z-scores. **(b)** Expression profiles of example genes implicated in ECM remodeling. Data are shown as mean±SEM. **(c)** After transfection of monocytes with Silencer negative control siRNA (siControl) and Silencer CIITA siRNA (siCIITA), cells were differentiated into moDCs for 6 days. Genes involved in ECM remodeling/fibrosis analyzed by qPCR on day 6. Data are normalized by the mean expression of RPL32 and RPL13A; fold change relative to siControl. **(d)** Fibronectin (FN1) and tubulin expression measured by western blot on day 6. Signal intensity of 5 independent experiments was quantified by densitometry analysis. To determine the relative expression of FN1 between siControl and siCIITA, the ratio between the expression of FN1 and tubulin was first calculated. In panels **(c)** and **(d)** each symbol represents an individual moDC donor; lines connect the same donor. Paired two-sided Student's *t*-test. * P <0.05, ** P < 0.01, *** P < 0.001.

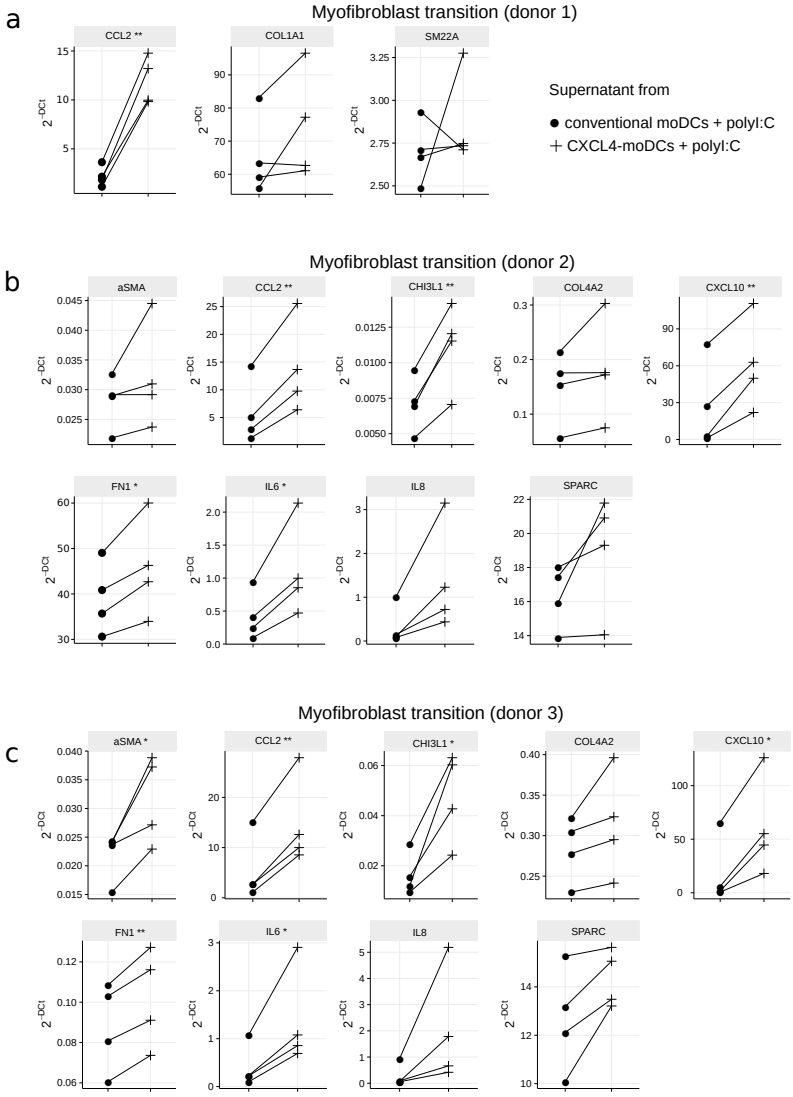

Fig. S9. Gene expression analysis of healthy myofibroblasts after exposure to cell-free supernatants from CXCL4 moDCs and moDCs. CXCL4 moDCs and moDCs on day 7 were stimulated with polyI:C for 24 hours. Cell-free supernatants were added to healthy myofibroblasts for 24 hours. Inflammatory and fibrotic gene expression was analyzed by qPCR. Each symbol represents an individual moDC donor (n=4). Lines connect the same moDC donors. **(a)** shows the gene expression for the first fibroblast donor. The remaining measured genes are shown in **Fig. 5h**. The gene expression for the **(b)** second and **(c)** third independent fibroblast donors. Paired two-sided Student's *t*-test. * P <0.05, ** P < 0.01, *** P < 0.001.

Supplementary Tables

In request, complete version of all Supplementary tables will be available online in https://bitbucket.org/systemsimmunology/cxcl4_modcs/downloads/CXCL4_moDC_Tables.zip

Table S1. Number of differently expressed genes (DEGs) and differently methylated genes (DMGs).

		Differentiation (I)			Stimulation with polyI:C (ii)		
		mono to conventional moDCs	mono to CXCL4-moDCs	CXCL4-moDC VS conventional moDCs	conventional moDCs	CXCL4-moDCs	CXCL4-moDC VS conventional moDCs
Gene transcription	**Total DEG**	13192	13110	5775	7767	8949	2397
	Upregulated	6350	6390	3091	4161	4551	1325
	Downregulated	6842	6720	2684	3606	4398	1072
DNA methylation	**Total DMG**	2804	2930	1065	1	1	5944
	Hypermethylated	206	810	863	1	1	5493
	Hypomethylated	2617	2156	207	0	0	529

Show are the comparisons between: **1**. monocytes (day 0) and moDCs (day2, 4 and 6); **2**. monocytes (day 0) and CXCL4-moDCs (day2, 4 and 6); **3**. moDCs (day2, 4 and 6) and CXCL4-moDCs (day2, 4 and 6); **4**. unstimulated and polyI:C stimulated (4h and 24h) moDCs; **5**. unstimulated and polyI:C stimulated (4h and 24h) CXCL4-moDCs; **6**. polyI:C stimulated (4h and 24h) moDCs and CXCL4-moDCs.

Table S2. Sequences of primers used for RT-qPCR analysis.

Gene	Forward	Reverse
CIITA	CCTGCTGTTCGGGACCTAAA	GGATCCGCACCAGTTTGG
IRF8	CGACGCGCACCATTCA	GCTTGCCCCCATAGTAGAAGCT
HLA DR	CGATCACCAATGTACCTCCA	ACTTGCGGAAAAGGTGGTCT
CD74	ATGCACCTGCTCCAGAATG	TTTCGGTGGAGCGTCAGT
CD83	TCCTGAGCTGCGCCTACAG	AAGTCCACATCTTCGGAGCAA
CD86	GAGTGAACAGACCAAGAAAAGAGAA	AAAAACACGCTGGGCTTCATC
FLT1 / VEGFR1	GAAGCAACAGTCAATGGGCA	GCGTGGTGTGCTTATTTGGA
FN1	CTGGCCGAAAATACATTGTAAA	CCACAGTCGGGTCAGGAG
SPARC	GCGGAAAATCCCTGCCAGAA	GGCAGGAAGAGTCGAAGGTC
αSMA	CCGACCGAATGCAGAAGGA	ACAGAGTATTTGCGCTCCGAA
Sm22a/TAGLN	CTCATGCCATAGGAAGGACC	GTCCGAACCCAGACACAAGT
CHI3L1	GGAGTGGAATGATGTGACGC	CCATCCTCCGACAGACAAGA
MCP1/CCL2	TCTGTGCCTGCTGCTCATAG	GGGCATTGATTGCATCTGGC
MIP1α/CCL3	TGCTCAGAATCATGCAGGTCT	GCAGCAAGTGATGCAGAGAAC
CCL22	CCTGACCCCTCTAACCCATC	GGGTTTAAGCAGGGGAATCG
IL8	GCTCTGTGTGAAGGTGCAGT	CCAGACAGAGCTCTCTTCCA
IL6	GACAGCCACTCACCTCTTCA	CCTCTTTGCTGCTTTCACAC
CXCL10	TGAAATTATTCCTGCAAGCCAA	CAGACATCTCTTCTCACCCTTCTTT
RPL32	AGGGTTCGTAGAAGATTCAAGG	GGA AAC ATT GTG AGC GAT CTC
RPL13A	CCTGGAGGAGAAGAGGAAAGAGA	TTGAGGACCTCTGTGTATTTGTCAA
GAPDH	ATCTTCTTTTGCGTCGCCAG	TTCCCCATGGTGTCTGAGC
LAGLS9	CCGAGGAGAGGAAGACACAC	CCCGTTCACCATCACCTTGA
C0L1A1	CCAGAAGAACTGGTACATCAGCA	CGCCATACTCGAACTGGAAT
C0L4A2	CCTGAAGGCACAGCTAACCA	TGCTGTTGTCTCGTCTGTCC

Table S3. List of top 50 most differently expressed genes (DEGs) displayed in Table S1 based on adjusted p-values from differential expression analysis during differentiation of moDCs and CXCL4-moDCs, and stimulation with polyI:C (4h and 24h).

Differentiation (I)

Comparison Monocytes (day 0) and moDCs (day 2, 4, 6)			
Gene name	base mean	log2 Fold Change	adjusted p-value
ARHGAP10	3199,181	4,440	0
BST1	866,058	-5,735	0
ITPRIPL1	1699,258	7,676	5.4723E-318
IRS2	2449,516	-5,155	5.5521E-312
TPPP3	125,097	-9,353	2.3634E-311
DUSP1	21910,749	-4,167	7,618E-307
CD209	16556,918	7,073	8,133E-288
FAM65B	1412,944	-6,678	1,127E-269
RAB37	238,441	-7,900	3,086E-264
DGKD	1157,419	-2,952	6,373E-256
CACNA2D3	69,026	-10,494	1,242E-251
RRP1B	5435,467	3,696	8,199E-243
AC074289.1	103,417	-7,873	6,1E-236
HOMER2	4744,110	6,697	3,855E-232
ARHGAP24	135,032	-7,873	4,813E-215
TSC22D3	2712,979	-5,687	9,331E-215
CD14	6555,649	-7,373	1,126E-210
CLEC4E	431,965	-8,576	7,224E-209
EMR1	417,186	-6,252	5,724E-208
ZBTB16	59,719	-7,951	1,337E-200
S100Z	66,629	-8,859	8,221E-195
RP11-383H13.1	551,089	7,151	1,174E-188
SPATA6	114,862	-3,706	2,376E-184
PTPRO	3351,272	5,328	1,281E-183
SMARCD3	611,710	-4,924	1,45E-183
BMF	1019,230	-1,801	1,779E-183
CDKN2D	445,290	-5,181	1,779E-183
CDH2	1206,433	9,129	1,05E-182
RASGRP2	751,218	-3,957	8,641E-182
OLIG1	214,587	-10,554	4,409E-180
RBP7	191,043	-7,367	5,473E-180
RP11-389C8.2	3382,098	6,444	4,402E-174
MPEG1	13837,060	-4,410	5,359E-174
DTNA	1410,808	5,376	2,642E-173
CCDC149	258,831	-4,403	3,223E-172
CD1B	10796,871	8,324	3,264E-168
CDKN1C	180,018	-6,567	6,835E-168
NLRP1	2724,889	-3,560	2,82E-166
VNN3	108,421	-9,566	3,322E-164
DENND3	1298,852	-3,918	3,701E-164
SELL	3368,299	-7,926	8,508E-164
S100A9	15982,512	-8,810	1,248E-162
HPSE	641,751	-8,286	1,176E-161
BTBD11	137,508	-7,212	4,877E-159
CSF3R	8578,833	-5,929	1,782E-158
SLC11A1	4071,236	-7,296	2,999E-156
GNG2	821,408	-3,589	4,499E-156
FBXL5	2941,129	-1,931	3,247E-155
MCUR1	1503,155	3,426	3,244E-153
PELI1	1232,299	-3,564	1,032E-152

Comparison Monocytes (day 0) and CXCL4-moDCs (day 2, 4, 6)			
Gene name	base mean	log2 Fold Change	adjusted p-value
ARHGAP10	2572,102	4,311	0
CD244	383,045	-12,993	0
PID1	427,015	-15,540	0
RAB37	233,353	-10,253	0
GLT1D1	495,361	-8,614	2,5113E-307
TPPP3	122,765	-13,737	4,1004E-300
DUSP1	21744,356	-3,918	1,9996E-283
F5	924,321	-10,127	4,5765E-272
RBP7	187,843	-8,341	2,5704E-269
HPSE	628,429	-10,396	1,342E-254
FAM65B	1372,525	-8,034	6,6587E-252
AC074289.1	101,319	-8,726	2,7335E-248
NCAPH	2155,517	9,026	4,4238E-247
EMR3	108,583	-10,159	5,1815E-246
S100A12	929,522	-14,278	5,3533E-245
PLBD1	4050,456	-3,082	6,3843E-225
TSC22D3	2654,340	-6,349	1,326E-222
IRAK3	2082,367	-4,827	7,4868E-221
PADI4	665,536	-9,674	5,3694E-220
POU2F2	2390,482	-3,770	8,7825E-213
DTNA	1083,875	5,339	2,4972E-211
RP11-383H13.1	515,768	7,160	1,2357E-209
CACNA2D3	67,949	-9,493	2,2754E-208
GALNT12	3681,960	8,805	9,2712E-207
VNN3	106,012	-13,530	2,3876E-199
CEACAM4	119,865	-6,445	5,6532E-197
HOMER2	3816,410	6,564	5,5756E-193
DGKD	1048,473	-3,553	3,9031E-189
VNN2	918,541	-7,308	1,2257E-187
RAP1GAP	2307,886	8,681	2,2329E-186
SIRPB2	958,259	-3,827	1,6021E-185
KLF11	1364,470	-1,989	3,4157E-181
ITPRIPL1	997,267	7,060	2,0815E-179
C10orf54	10619,245	-3,737	5,9381E-178
CDKN2D	425,581	-6,189	9,181E-174
MTMR3	1757,644	-2,032	1,7578E-171
TMEM45B	523,355	6,873	1,7578E-171
AOAH	3333,684	-2,229	1,4802E-170
CCDC109B	304,221	-4,043	3,7854E-169
CCDC88C	971,709	-4,573	4,1961E-169
BCAR3	1436,164	8,322	4,6346E-168
KSR1	805,878	-3,921	1,2891E-167
ABCG2	691,553	7,565	6,908E-167
FOS	39195,297	-4,623	1,0213E-166
GAS7	4944,943	-2,456	2,0711E-164
PPAP2B	1944,550	8,720	1,9007E-163
PELI2	526,884	-4,065	3,1184E-160
RP11-389C8.2	2784,001	6,643	2,4723E-157
SERPINA1	8874,123	-4,708	4,2825E-157
BIN2	2678,702	-2,209	1,905E-156

Comparison moDCs (day 2, 4, 6) and CXCL4-moDCs (day 2, 4, 6)			
Gene name	base mean	log2 Fold Change	adjusted p-value
CIITA	10723,298	-1,201	5,99E-48
MTUS1	402,881	2,044	1,94E-35
BCL2A1	170,672	3,223	6,04E-34
FAIM	87,527	2,056	4,35E-33
SH3RF3	187,489	3,005	4,92E-33
GM2A	37883,442	1,868	1,78E-32
SPP1	14162,392	2,931	2,7E-30
RRAGD	1418,681	1,600	3,26E-30
WFS1	1289,004	1,653	4,03E-30
CDH2	1059,927	-1,967	4,81E-30
GIPR	68,205	-3,360	5,76E-30
EPB41L1	829,552	3,014	7,34E-29
ROR1-AS1	436,890	3,482	7,71E-29
TIFAB	960,464	-1,952	9,51E-29
LGALS3	12430,084	1,201	9,66E-29
PDE3B	877,182	1,966	2,01E-28
TRAF3IP2	81,792	2,528	3,52E-28
STIP1	4328,369	0,797	4,11E-27
GPD1	172,493	3,301	1,43E-26
RP11-876N24.3	422,362	-1,563	1,43E-26
MYRF	506,627	-2,397	3,58E-26
PTPN22	366,777	1,417	4,36E-26
MESDC2	1298,254	0,817	5,64E-26
TMEM117	272,804	1,557	6,27E-26
FAR2	1079,717	3,602	1,59E-25
TMEM140	260,882	1,583	1,63E-25
ASAH1	6478,534	0,963	2,54E-25
CACNA1G	184,035	3,290	4,48E-25
APOC1	464,852	2,744	4,68E-25
FABP5P7	84,321	1,619	8,6E-25
MCEMP1	179,635	3,929	9,19E-25
AQP9	4532,746	2,587	2,29E-24
NCEH1	2010,570	1,679	3E-24
GSTO1	1732,291	0,909	7,84E-24
ABCG2	602,837	2,354	1,09E-23
CHST11	5864,770	1,120	1,57E-23
TLE1	620,494	1,757	2,09E-23
CSTB	14658,356	1,142	7,05E-23
MANEAL	149,367	1,997	7,45E-23
APLP2	9752,578	0,901	7,71E-23
ADAM19	3370,329	-1,698	8,28E-23
ZC3H12D	324,576	-1,691	9,45E-23
ANKS6	348,516	2,039	3,73E-22
IL1RN	15286,593	2,173	3,9E-22
PDGFA	210,132	1,769	1,1E-21
SIGLEC15	150,611	1,730	1,27E-21
GGT5	1350,501	-2,450	1,71E-21
ARPIN	1609,191	-1,200	2,22E-21
MAN2A2	3872,273	-1,108	3,88E-21
MREG	3072,592	1,247	4,68E-21

Table S3. List of top 50 most differently expressed genes (DEGs) displayed in Table S1 based on adjusted p-values from differential expression analysis during differentiation of moDCs and CXCL4-moDCs, and stimulation with polyI:C (4h and 24h).

Stimulation (II)

Comparison moDCs and stimulated moDCs

Gene name	base mean	log2 Fold Change	adjusted p-value
CMPK2	8491,171	6,265	2,6406E-73
OASL	16974,144	7,644	5,1938E-69
IFIT5	1911,562	3,405	3,1765E-66
ZC3HAV1	17890,277	0,061	3,8455E-65
DTX3L	10246,308	3,206	1,2551E-63
EIF2AK2	8034,554	3,193	1,6707E-63
TRIM56	2909,654	1,715	4,1161E-62
HELZ2	14999,569	4,047	6,9492E-59
XAF1	7121,754	3,781	2,4265E-56
MX1	32692,328	6,776	7,2399E-54
IFIT2	60504,053	8,576	1,8763E-53
IFIT3	42831,404	7,715	2,318E-52
APOL6	9812,664	2,548	4,1228E-52
HERC6	2520,984	4,708	5,3859E-52
PARP9	6767,803	4,058	2,3715E-51
DDX58	16606,275	4,363	2,0185E-50
PARP14	20488,368	3,173	5,2354E-50
USP18	1702,240	6,973	6,6091E-49
GCH1	4001,673	5,953	8,1675E-47
USP42	623,879	0,963	2,5804E-46
IFIH1	12158,567	4,169	5,2964E-46
AIM2	443,240	5,739	1,3046E-45
DDX60	2641,185	3,357	2,1274E-44
OAS2	23995,041	5,636	2,6286E-44
APOL2	3142,483	2,441	5,8558E-44
MX2	14357,474	5,582	8,8465E-44
CFB	854,444	5,968	3,7569E-42
LAG3	1868,546	9,736	3,7895E-40
GBP5	10913,705	5,156	1,6542E-39
NT5C3A	2390,988	5,298	7,4021E-39
IFITM2	1432,826	4,635	1,2252E-38
IFI44	3382,313	4,462	2,0199E-38
RNF213	45083,230	2,355	2,246E-38
FUT4	1534,392	2,458	3,7391E-38
ADAR	18336,266	1,998	7,7546E-38
TRIM21	2534,072	2,324	1,4908E-37
PELI1	3297,061	2,207	1,4908E-37
IFI35	3013,030	4,103	1,5755E-37
GBP1	21232,379	5,483	1,028E-36
HIST1H2AC	502,505	3,597	1,5913E-36
HESX1	397,608	7,396	2,0816E-36
TRIM25	6628,572	2,046	3,8379E-36
IL15RA	1469,948	6,171	2,9721E-35
OAS3	28790,393	5,268	1,4089E-34
CXCL9	49933,816	11,305	4,9859E-34
GBP1P1	323,308	10,084	6,7925E-34
C9orf139	287,374	0,367	7,8767E-34
CTD-2521M24.9	534,132	2,594	9,6396E-33
IFITM1	2221,404	9,295	1,278E-32
C19orf66	2185,297	2,594	1,6344E-32

Comparison CXCL4-moDCs and stimulated CXCL4-moDCs

Gene name	base mean	log2 Fold Change	adjusted p-value
ZC3HAV1	14901,620	0,376	3,2458E-121
USP18	1772,704	5,616	7,1999E-104
CCL3L3	3378,351	0,930	7,1999E-104
FOXF1	110,487	5,737	1,98287E-94
OASL	15763,674	7,300	5,01025E-90
TNF	10493,048	1,358	2,04221E-89
GCH1	4765,393	6,227	2,72826E-88
ZNFX1	21916,358	2,594	3,88164E-84
DNAAF1	1022,876	6,346	2,22553E-79
CCL5	55155,413	9,654	3,1357E-79
IL27	1806,575	12,937	6,12291E-79
NEURL3	1154,004	8,365	1,54672E-78
TRIM21	2082,985	2,326	9,75401E-78
IL6	3606,660	10,398	1,21297E-75
PARP14	20805,268	2,693	1,19649E-71
RIPK2	2529,752	2,348	2,45089E-71
BRIP1	1352,986	4,700	3,9063E-71
GBP1	22067,337	5,282	1,34246E-70
SLC38A5	984,067	9,534	1,67839E-69
NT5C3A	2478,945	5,393	3,64994E-69
DHX58	4558,831	4,026	3,80293E-69
SERPINB9	10590,892	3,218	4,61756E-68
IFIH1	12574,178	4,303	6,7826E-68
XBP1	4119,704	-0,155	3,1787E-67
CCL4L1	5252,558	0,463	1,32352E-65
CCL4	8806,152	1,217	1,19647E-64
TAP1	15332,901	3,555	7,88224E-64
NFKBIZ	1604,954	3,002	1,5101E-63
CLCF1	2038,387	3,047	6,33665E-63
ETV7	660,465	7,618	1,25152E-62
GBP1P1	299,752	8,458	1,25152E-62
HELZ2	14757,446	4,400	1,83737E-62
DCP1A	2556,836	1,999	1,51372E-61
ISG20	5691,933	6,981	2,44882E-61
CCL3	9062,494	0,647	7,0813E-61
HES4	619,636	8,593	1,1584E-60
PDGFRL	597,734	9,391	4,51041E-60
OAS3	25750,058	4,652	1,01231E-59
SEMA3D	48,071	-2,322	8,53357E-58
ADAR	16793,894	2,038	3,71475E-57
MAP3K8	2127,676	2,150	1,01507E-56
ISG15	23124,582	7,983	1,7426E-56
IFITM1	1639,782	9,478	2,26352E-56
B4GALT5	5754,189	2,210	3,59618E-56
GBP5	10236,485	5,224	9,47036E-56
IFIT3	37554,172	6,727	1,18315E-55
RAPGEF2	8100,374	1,063	2,02477E-55
DTX3L	8221,639	2,995	3,12618E-55
BST2	4287,165	3,272	1,39025E-53
IFIT2	45896,534	7,186	1,43436E-53

Comparison stimulated moDCs and stimulated CXCL4-moDCs

Gene name	base mean	log2 Fold Change	adjusted p-value
GALNT12	1092,540	2,205	1,08E-55
TIFAB	1826,675	-2,791	1,36E-22
TJP1	323,097	1,833	3,56E-21
LILRA2	322,920	2,833	4,61E-20
HIST1H2BC	60,456	2,060	1,9E-19
TGM2	6413,758	2,700	1,32E-18
ANKS6	102,337	1,719	3,73E-18
SLC1A2	1095,401	2,640	1,7E-17
HLA-DQA1	31213,055	-1,588	2,12E-16
ROR1-AS1	323,255	2,933	7,68E-16
AFAP1L2	55,660	3,131	8,58E-16
HLA-DQB1	18867,328	-1,525	2,24E-15
CYP27B1	1637,879	2,755	3,42E-15
ASTN2	210,078	3,217	4,34E-15
FAR2	95,147	3,463	2,67E-14
CLSTN3	206,258	3,090	2,67E-14
S100A16	11,098	3,193	4,34E-14
TRAF3IP2	189,281	1,828	4,92E-14
AQP9	4828,172	2,466	5,66E-14
IFNLR1	336,700	2,641	6,87E-14
SORT1	3040,499	1,200	1,27E-13
APLP2	8826,405	0,967	1,7E-13
BEX1	16,491	4,400	3,33E-13
PTRF	550,303	3,011	3,51E-13
GFRA2	199,868	-6,666	5,65E-13
BCL2A1	1477,519	2,151	2,52E-12
LDHB	1071,227	0,622	3,94E-12
GFPT2	63,895	3,307	3,94E-12
CST2	46,720	3,439	6,99E-12
TIE1	230,575	2,773	7,11E-12
KIAA1244	31,195	2,848	1E-11
PLD4	539,367	3,037	1,54E-11
EPS8	253,956	1,320	2,7E-11
HLA-DPA1	91528,517	-1,200	3,1E-11
CTTN	390,707	1,759	3,42E-11
PODXL	479,854	1,498	4,9E-11
IGHE	34,340	2,592	5,25E-11
LIX1L	671,182	-0,622	6,27E-11
HLA-DRB1	75376,482	-1,304	7,84E-11
RP11-118B22.4	16,278	2,925	8,83E-11
AHRR	2379,618	-1,171	1,27E-10
ENHO	275,956	3,216	1,57E-10
OVOL1	78,105	3,653	1,81E-10
ITGA6	420,862	2,266	2,21E-10
RNASE1	4625,363	-2,834	2,94E-10
CLEC4G	227,586	-3,402	3,18E-10
SERPINF1	255,815	-1,830	3,26E-10
NUP210	795,493	1,486	3,73E-10
RP11-91K9.1	9,312	4,451	3,73E-10
DCSTAMP	927,526	1,816	5,06E-10

Table S4. List of top 50 most differently methylated regions (DMRs) displayed in Table S1 based on adjusted p-values from differential methylation analysis during differentiation of moDCs and CXCL4-moDCs, and stimulation with polyI:C (4h and 24h).

Differentiation (I)

Comparison Monocytes (day 0) and moDCs (day 2, 4, 6)

Gene name	Region	delta beta	adjusted p-value
AC068570.1	TSS200	-0,5825761	8,05749E-08
ZNF365	3'UTR	-0,2119406	1,4234E-07
RP11-7F17.7	TSS1500	-0,402659	1,4234E-07
TM4SF19	5'UTR	-0,3508595	1,51577E-07
MIR4435-1HG	TSS200	-0,6326897	1,51577E-07
MIR21	5'UTR	-0,381074	1,55912E-07
TM4SF19	1stExon	-0,4650081	1,55912E-07
HEATR5A	ExonBnd	-0,6375986	1,69504E-07
TMEM144	3'UTR	-0,2609753	1,69504E-07
TRAJ31	TSS1500	-0,2724725	2,32978E-07
LINC01389	TSS1500	-0,1858677	2,32978E-07
RNU6-539P	TSS200	-0,6942954	2,32978E-07
TM4SF19	TSS200	-0,3368456	2,32978E-07
PDCD11	3'UTR	-0,3741932	2,32978E-07
LINC00152	TSS200	-0,4924534	2,32978E-07
PIGR	ExonBnd	-0,8369119	2,32978E-07
TTLL4	3'UTR	-0,515664	2,59457E-07
SESN2	3'UTR	-0,7618135	2,68896E-07
RP11-275I4.2	5'UTR	-0,2724829	2,68896E-07
PIGR	TSS1500	-0,1152385	2,68896E-07
RP11-661D19.3	1stExon	-0,4590115	2,6972E-07
CASP10	ExonBnd	-0,4448008	3,02157E-07
VMP1	3'UTR	-0,3114108	3,02157E-07
UPP1	5'UTR	-0,1189615	3,13822E-07
SLFN12L	1stExon	-0,164253	3,77898E-07
HMOX1	3'UTR	-0,4954423	3,84587E-07
CTB-113P19.1	TSS200	-0,4222587	4,57808E-07
CCL13	TSS200	-0,6444222	4,95049E-07
LRRC8A	TSS200	-0,1083781	5,03573E-07
CMTM6	3'UTR	-0,1401123	5,40635E-07
RP11-383G10.5	TSS1500	-0,3171621	5,64421E-07
SPEN	1stExon	-0,2111134	5,71281E-07
SIK3-IT1	TSS200	-0,409855	6,14168E-07
KIAA1683	TSS200	-0,1489672	6,14168E-07
LINC00607	1stExon	-0,1644618	6,14168E-07
RP11-83B20.1	TSS1500	-0,277612	6,14168E-07
RNU6-1254P	TSS1500	-0,8268091	6,36332E-07
TPRG1-AS1	3'UTR	-0,1608365	6,36332E-07
CASP7	5'UTR	-0,072365	6,36332E-07
TTLL3	ExonBnd	-0,6104625	6,36332E-07
ARHGEF17	3'UTR	-0,5311052	6,36332E-07
GPT	TSS200	-0,4371365	7,04282E-07
A2M	1stExon	-0,334983	7,04282E-07
SLFN12L	5'UTR	-0,1530438	7,40505E-07
KIF3B	3'UTR	-0,4924473	8,1151E-07
SRC	TSS200	-0,1509214	8,1151E-07
Y_RNA	TSS1500	-0,3772051	8,24636E-07
CTC-537E7.3	TSS200	-0,4257598	8,45735E-07
RP11-661D19.3	3'UTR	-0,150289	9,1068E-07
RP11-661D19.3	TSS1500	-0,2426949	9,1068E-07

Comparison Monocytes (day 0) and CXCL4-moDCs (day 2, 4, 6)

Gene name	Region	delta beta	adjusted p-value
NAGPA	TSS1500	-0,0690611	1,15362E-07
PPP1R16B	TSS1500	0,08964009	1,15362E-07
RP13-631K18.2	TSS1500	-0,5620356	1,15362E-07
AP000695.6	TSS1500	-0,1658102	1,15362E-07
KIAA1683	TSS200	-0,1302923	1,20789E-07
LINC00152	TSS200	-0,4919342	1,20789E-07
RP11-7F17.7	TSS1500	-0,41854	1,50534E-07
TM4SF19	1stExon	-0,55044	1,94105E-07
NCAPH	5'UTR	-0,104388	1,94105E-07
TM4SF19	5'UTR	-0,4203628	1,94105E-07
KIF3B	3'UTR	-0,4608204	1,94105E-07
ARPC4-TTLL3	ExonBnd	-0,1940313	1,94105E-07
THOC6	TSS1500	-0,1541161	1,94105E-07
MIR4435-1HG	TSS200	-0,6507557	1,94105E-07
RP11-394B2.6	TSS1500	-0,3188323	1,94105E-07
UPP1	5'UTR	-0,1189088	2,04213E-07
LIPA	ExonBnd	-0,321982	2,06177E-07
TM4SF19	TSS200	-0,3969872	2,06177E-07
PFAS	3'UTR	-0,4611342	2,30179E-07
CTSH	TSS200	-0,1263983	2,30179E-07
SNORA71B	TSS1500	-0,4031552	2,30179E-07
SRC	TSS200	-0,1513724	2,30179E-07
AC147651.4	TSS1500	-0,1969036	2,30179E-07
ZNF365	3'UTR	-0,2441646	2,35142E-07
PIGR	TSS1500	-0,1177447	2,35142E-07
PIGR	ExonBnd	-0,8614962	2,71869E-07
Y_RNA	TSS1500	-0,4274653	2,79629E-07
MIR21	TSS1500	-0,2214486	2,79629E-07
TTLL3	ExonBnd	-0,6994396	2,79629E-07
LINC00885	5'UTR	-0,1519336	2,79629E-07
LINC01271	TSS200	-0,2591337	2,97762E-07
ATP13A3	1stExon	-0,2620233	3,01381E-07
CTC-527H23.2	TSS200	-0,6860035	3,09653E-07
AC008440.5	TSS200	-0,3048931	3,31041E-07
RP11-383G10.5	TSS1500	-0,235203	3,31041E-07
NAGPA	1stExon	-0,082998	3,31041E-07
RP11-353N14.3	TSS1500	-0,1419076	3,31041E-07
RP11-7F17.7	TSS200	-0,5849474	3,31041E-07
CCR1	5'UTR	-0,1929012	3,31041E-07
C10orf71	5'UTR	-0,0600204	3,31041E-07
LINC00607	1stExon	-0,1957185	3,32894E-07
TMEM144	3'UTR	-0,2499338	3,69724E-07
LINC01226	TSS200	-0,4530739	3,73127E-07
RNU6-539P	TSS200	-0,5362817	3,76282E-07
NAGPA	ExonBnd	-0,1444314	3,76282E-07
SMPDL3B	1stExon	0,06255111	3,76282E-07
CTD-2135D7.5	3'UTR	-0,1883969	3,76282E-07
RP11-661D19.3	TSS1500	-0,2391143	3,76282E-07
HS1BP3-IT1	TSS1500	-0,2423823	3,79923E-07
ZBTB48	1stExon	-0,0820685	3,95823E-07

Comparison moDCs (day 2, 4, 6) and CXCL4-moDCs (day 2, 4, 6)

Gene name	Region	delta beta	adjusted p-value
ACSL1	1stExon	-0,086301	4,06355E-06
RP11-513G19.1	TSS200	-0,1944051	8,85071E-06
WFDC21P	TSS1500	0,10768578	8,85071E-06
LA16c-380H5.2	TSS1500	-0,106275	9,45384E-06
AC011747.3	TSS1500	0,10198475	9,45384E-06
MCL1	3'UTR	-0,080071	9,45384E-06
SLAMF1	3'UTR	0,0994807	9,45384E-06
RP4-530I15.9	3'UTR	-0,0305053	1,06432E-05
C2orf80	TSS200	0,07094491	1,06432E-05
MIR1250	TSS200	-0,1283163	1,06432E-05
CD300C	TSS1500	0,07182702	1,06432E-05
SLC51B	TSS1500	-0,1578718	1,19511E-05
PLIN4	3'UTR	-0,0857758	1,5866E-05
DNASE1L3	TSS200	0,10757416	1,99554E-05
WBP2	3'UTR	0,19920241	1,99671E-05
TNFRSF10B	TSS1500	0,0357548	2,55675E-05
LINC01226	TSS200	-0,2175723	2,6996E-05
CCL13	TSS1500	0,13253999	2,6996E-05
TTLL4	3'UTR	0,12878658	2,74947E-05
PSTPIP2	3'UTR	0,01835699	2,74947E-05
TNF	TSS1500	0,10806579	2,74947E-05
SESN2	3'UTR	0,23484883	2,74947E-05
PELP1	ExonBnd	0,15891744	2,74947E-05
RP11-753D20.1	3'UTR	0,04536762	3,20907E-05
IPO4	ExonBnd	0,03554921	3,47776E-05
CASP8AP2	5'UTR	0,04852801	3,47776E-05
CASP10	ExonBnd	0,16154932	3,47776E-05
CCL13	1stExon	0,22444855	3,47776E-05
CCL13	5'UTR	0,22444855	3,47776E-05
Y_RNA	TSS1500	0,17922615	3,64217E-05
CCL13	TSS200	0,23797136	3,82784E-05
RP11-513G19.1	5'UTR	-0,0267436	4,0612E-05
SNAI3	TSS1500	-0,1070075	4,49012E-05
HCAR1	5'UTR	0,10937015	4,49012E-05
SNORA67	TSS1500	0,08689472	4,49012E-05
SPEN	1stExon	0,05567964	4,49012E-05
HEATR5A	1stExon	0,05070568	4,49012E-05
C2orf80	5'UTR	0,03705897	4,49012E-05
METTL12	3'UTR	0,09148735	4,49012E-05
KCNJ15	1stExon	0,03957571	4,49012E-05
RP5-1050D4.4	TSS1500	0,06134553	5,09994E-05
PLEK	TSS1500	-0,0479118	5,09994E-05
CCL22	1stExon	-0,2717516	5,14898E-05
AC092687.4	TSS200	0,16972239	5,53265E-05
IFNGR2	3'UTR	-0,0177459	6,52998E-05
RP11-57H14.4	5'UTR	0,04089019	7,32037E-05
WFDC21P	TSS200	0,16077419	7,32037E-05
DPP9	5'UTR	0,18776066	7,32745E-05
PSD3	5'UTR	0,01438148	7,32745E-05
Z99756.1	TSS1500	-0,0633369	7,32745E-05

Table S4. List of top 50 most differently methylated regions (DMRs) displayed in Table S1 based on adjusted p-values from differential methylation analysis during differentiation of moDCs and CXCL4-moDCs, and stimulation with polyI:C (4h and 24h).

Stimulation (II)

Comparison moDCs and stimulated moDCs			
Gene name	Region	delta beta	adjusted p-value
TUBA3C	3'UTR	0,02627326	0,00816869 8

Comparison CXCL4-moDCs and stimulated CXCL4-moDCs			
Gene name	Region	delta beta	adjusted p-value
RP11-278A23.1	TSS200	0,01896943	0,013444122

Comparison stimulated moDCs and stimulated CXCL4-moDCs			
Gene name	Region	delta beta	adjusted p-value
CHID1	TSS200	0,06799817	1,68326E-14
CHID1	TSS1500	0,05261383	1,68326E-14
CLEC10A	ExonBnd	0,22043262	1,68326E-14
RP11-202G18.1	TSS1500	0,24150129	1,68326E-14
CLEC10A	TSS200	0,11027306	2,93253E-14
RP11-513G19.1	TSS200	-0,1865267	4,64899E-13
CLEC10A	5'UTR	0,1452135	5,19488E-13
CCL13	TSS1500	0,12529487	5,19488E-13
RNU6-792P	TSS1500	0,30781876	1,31117E-12
HCAR1	5'UTR	0,109385	2,22307E-12
WBP2	3'UTR	0,18361766	2,22307E-12
MFSD6	1stExon	0,0878349	2,36554E-12
PELP1	ExonBnd	0,15187185	4,15657E-12
LINC01132	TSS200	0,12705351	4,22867E-12
PQLC1	TSS1500	0,02735322	4,22867E-12
CLEC10A	3'UTR	0,06957422	4,22867E-12
CLEC10A	1stExon	0,13149035	4,38856E-12
RP11-181G12.4	3'UTR	0,03259799	8,97759E-12
HCAR1	1stExon	0,08764445	1,10725E-11
ACIN1	ExonBnd	-0,1727122	1,86874E-11
CCL13	1stExon	0,22561592	2,11215E-11
CCL13	5'UTR	0,22561592	2,11215E-11
CETP	TSS1500	0,06998165	2,2575E-11
GNMT	3'UTR	0,15184469	2,28361E-11
LA16c-380H5.2	TSS1500	-0,0864493	2,88679E-11
PELP1	TSS200	0,03811858	3,28348E-11
MFSD6	TSS1500	0,03041055	3,66112E-11
LINC01226	TSS200	-0,2338216	4,2352E-11
PLAU	1stExon	0,08759248	4,2352E-11
RNASE1	ExonBnd	0,14051859	4,5525E-11
RGL1	ExonBnd	0,07225006	4,56721E-11
TRAJ31	TSS1500	0,12348737	4,56721E-11
MPZL3	3'UTR	0,08406633	4,77851E-11
CD38	1stExon	0,07126088	5,48893E-11
ASGR2	TSS1500	0,03205242	5,48893E-11
PDGFB	3'UTR	0,04991457	6,2704E-11
MYADM	3'UTR	0,09173503	7,03173E-11
DNASE1L3	1stExon	0,18670472	7,03173E-11
RP11-20G13.2	TSS200	-0,2562082	7,51875E-11
SLAMF1	3'UTR	0,09636984	7,56008E-11
EGOT	TSS1500	0,0485708	8,4447E-11
ABCA6	1stExon	0,13681803	8,4447E-11
GPR97	1stExon	0,16072609	9,33747E-11
FCRL6	TSS200	0,08517108	9,75963E-11
DPP9	5'UTR	0,17439138	9,75963E-11
GPT	TSS200	0,08587356	1,00156E-10
SLC25A12	TSS200	0,05824089	1,06141E-10
KCNJ15	TSS200	0,03989612	1,07208E-10
GNAT2	1stExon	0,04980113	1,07288E-10
GNAT2	5'UTR	0,04980113	1,07288E-10

Table S5. List of top 25 most significantly enriched pathways (adjusted p-value < 0.05) for the differently expressed genes (DEGs) either upregulated or downregulated during differentiation. Gene # - number of genes matching the annotated Reactome pathway.

Differentiation (I)

	Comparison monocytes and moDCs			
	ID Reactome pathway	Description	adjusted p-value	Gene #
Upregulated	R-HSA-1430728	Metabolism	3,1942E-08	765
	R-HSA-1428517	The citric acid (TCA) cycle and respiratory electron transport	5,8232E-08	90
	R-HSA-212436	Generic Transcription Pathway	9,5843E-08	335
	R-HSA-6111105	Respiratory electron transport	1,8023E-07	60
	R-HSA-163200	Respiratory electron transport, ATP synthesis by chemiosmotic coupling, and heat production by uncoupling proteins.	3,0591E-06	67
	R-HSA-556833	Metabolism of lipids and lipoproteins	5,9656E-06	307
	R-HSA-2132295	MHC class II antigen presentation	5,9656E-06	64
	R-HSA-191273	Cholesterol biosynthesis	0,00010654	19
	R-HSA-379724	tRNA Aminoacylation	0,00071932	28
	R-HSA-5368287	Mitochondrial translation	0,00097307	48
	R-HSA-1655829	Regulation of cholesterol biosynthesis by SREBP (SREBF)	0,00097307	32
	R-HSA-5368286	Mitochondrial translation initiation	0,00109608	45
	R-HSA-69278	Cell Cycle, Mitotic	0,00130274	199
	R-HSA-446203	Asparagine N-linked glycosylation	0,00130274	123
	R-HSA-1852241	Organelle biogenesis and maintenance	0,00136546	140
	R-HSA-5663220	RHO GTPases Activate Formins	0,00155052	62
	R-HSA-5628897	TP53 Regulates Metabolic Genes	0,00224856	43
	R-HSA-1640170	Cell Cycle	0,00224856	232
	R-HSA-199991	Membrane Trafficking	0,00224856	231
	R-HSA-5389840	Mitochondrial translation elongation	0,00232526	44
	R-HSA-453274	Mitotic G2-G2/M phases	0,00232526	84
	R-HSA-196780	Biotin transport and metabolism	0,00232526	10
	R-HSA-69275	G2/M Transition	0,00257951	83
	R-HSA-5653656	Vesicle-mediated transport	0,00258727	243
	R-HSA-5140745	WNT5A-dependent internalization of FZD2, FZD5 and ROR2	0,00310773	11
Downregulated	R-HSA-156842	Eukaryotic Translation Elongation	8,5342E-28	79
	R-HSA-72689	Formation of a pool of free 40S subunits	8,5342E-28	84
	R-HSA-156827	L13a-mediated translational silencing of Ceruloplasmin expression	8,5342E-28	90
	R-HSA-72706	GTP hydrolysis and joining of the 60S ribosomal subunit	8,5342E-28	90
	R-HSA-156902	Peptide chain elongation	2,1416E-27	76
	R-HSA-72613	Eukaryotic Translation Initiation	3,0632E-26	92
	R-HSA-72737	Cap-dependent Translation Initiation	3,0632E-26	92
	R-HSA-2408557	Selenocysteine synthesis	7,127E-26	76
	R-HSA-192823	Viral mRNA Translation	1,77E-25	74
	R-HSA-168256	Immune System	1,5609E-24	742
	R-HSA-168249	Innate Immune System	2,3103E-24	493
	R-HSA-975956	Nonsense Mediated Decay (NMD) independent of the Exon Junction Comple	5,599E-24	76
	R-HSA-72764	Eukaryotic Translation Termination	1,5309E-23	74
	R-HSA-72766	Translation	2,3428E-23	105
	R-HSA-1799339	SRP-dependent cotranslational protein targeting to membrane	1,977E-22	82
	R-HSA-927802	Nonsense-Mediated Decay (NMD)	3,4336E-22	84
	R-HSA-975957	Nonsense Mediated Decay (NMD) enhanced by the Exon Junction Complex (	3,4336E-22	84
	R-HSA-6798695	Neutrophil degranulation	1,2954E-20	222
	R-HSA-2408522	Selenoamino acid metabolism	6,6896E-20	82
	R-HSA-6791226	Major pathway of rRNA processing in the nucleolus and cytosol	4,5247E-19	106
	R-HSA-168273	Influenza Viral RNA Transcription and Replication	1,2014E-17	85
	R-HSA-8868773	rRNA processing in the nucleus and cytosol	2,0173E-17	108
	R-HSA-72312	rRNA processing	2,2922E-16	110
	R-HSA-168254	Influenza Infection	3,5052E-16	91
	R-HSA-168255	Influenza Life Cycle	2,8795E-15	85

	Comparison monocytes and CXCL4-moDCs			
	ID Reactome pathway	Description	adjusted p-value	Gene #
Upregulated	R-HSA-1430728	Metabolism	6,5378E-18	833
	R-HSA-1428517	The citric acid (TCA) cycle and respiratory electron transport	8,3971E-13	101
	R-HSA-556833	Metabolism of lipids and lipoproteins	9,9148E-12	340
	R-HSA-163200	Respiratory electron transport, ATP synthesis by chemiosmotic coupling, and heat production by uncoupling proteins.	1E-09	75
	R-HSA-6111105	Respiratory electron transport	1,9127E-09	64
	R-HSA-5368287	Mitochondrial translation initiation	5,3313E-06	51
	R-HSA-5368286	Mitochondrial translation	5,3313E-06	54
	R-HSA-446203	Asparagine N-linked glycosylation	1,1204E-05	134
	R-HSA-5389840	Mitochondrial translation elongation	2,1733E-05	50
	R-HSA-5419276	Mitochondrial translation termination	3,7587E-05	49
	R-HSA-379724	tRNA Aminoacylation	0,00022453	29
	R-HSA-446193	Biosynthesis of the N-glycan precursor (dolichol lipid-linked oligosaccharide, LLO) and transfer to a nascent protein	0,00035847	43
	R-HSA-71406	Pyruvate metabolism and Citric Acid (TCA) cycle	0,0005956	30
	R-HSA-191273	Cholesterol biosynthesis	0,000667	18
	R-HSA-6799198	Complex I biogenesis	0,00093909	33
	R-HSA-1852241	Organelle biogenesis and maintenance	0,00093909	143
	R-HSA-5628897	TP53 Regulates Metabolic Genes	0,00169012	44
	R-HSA-446203	Synthesis of substrates in N-glycan biosythesis	0,00450547	34
	R-HSA-5140745	WNT5A-dependent internalization of FZD2, FZD5 and ROR2	0,00508519	11
	R-HSA-174403	Glutathione synthesis and recycling	0,00608939	12
	R-HSA-199991	Membrane Trafficking	0,00626159	232
	R-HSA-5663205	RHO GTPases Activate WASPs and WAVEs	0,00648504	22
	R-HSA-1655829	Regulation of cholesterol biosynthesis by SREBP (SREBF)	0,00730082	30
	R-HSA-390466	Folding of actin by CCT/TiC	0,00788372	9
	R-HSA-5653656	Vesicle-mediated transport	0,00788372	244
Downregulated	R-HSA-72681	Formation of a pool of free 40S subunits	3,511E-31	85
	R-HSA-156827	L13a-mediated translational silencing of Ceruloplasmin expression	3,511E-31	91
	R-HSA-156902	Peptide chain elongation	1,1236E-30	77
	R-HSA-156842	Eukaryotic Translation Elongation	1,1947E-30	79
	R-HSA-72706	GTP hydrolysis and joining of the 60S ribosomal subunit	1,4633E-30	90
	R-HSA-2408557	Selenocysteine synthesis	3,7841E-29	77
	R-HSA-72613	Eukaryotic Translation Initiation	5,6921E-29	92
	R-HSA-72737	Cap-dependent Translation Initiation	5,6921E-29	92
	R-HSA-192823	Viral mRNA Translation	7,8296E-29	75
	R-HSA-72764	Eukaryotic Translation Termination	1,1738E-26	75
	R-HSA-975957	Nonsense Mediated Decay (NMD) independent of the Exon Junction Co	3,4099E-26	76
	R-HSA-1799339	SRP-dependent cotranslational protein targeting to membrane	1,1075E-24	82
	R-HSA-72766	Translation	1,1585E-24	103
	R-HSA-927802	Nonsense-Mediated Decay (NMD)	1,1766E-23	83
	R-HSA-975957	Nonsense Mediated Decay (NMD) enhanced by the Exon Junction Com	1,1766E-23	83
	R-HSA-2408522	Selenoamino acid metabolism	2,723E-21	81
	R-HSA-168256	Immune System	3,4493E-19	675
	R-HSA-6791226	Major pathway of rRNA processing in the nucleolus and cytosol	3,7468E-19	102
	R-HSA-168273	Influenza Viral RNA Transcription and Replication	3,8739E-19	84
	R-HSA-8868773	rRNA processing in the nucleus and cytosol	7,8589E-19	106
	R-HSA-168249	Innate Immune System	1,6851E-18	444
	R-HSA-72312	rRNA processing	2,0372E-18	109
	R-HSA-168255	Influenza Life Cycle	9,6965E-17	84
	R-HSA-6798695	Neutrophil degranulation	2,5521E-16	200
	R-HSA-168254	Influenza Infection	5,73E-16	87

	Comparison moDCs and CXCL4-moDCs			
	ID Reactome pathway	Description	adjusted p-value	Gene #
Upregulated	R-HSA-1430728	Metabolism	1,7381E-14	464
	R-HSA-6798695	Neutrophil degranulation	3,8255E-13	143
	R-HSA-556833	Metabolism of lipids and lipoproteins	9,211E-08	189
	R-HSA-168256	Immune System	1,3541E-07	420
	R-HSA-168249	Innate Immune System	1,4448E-06	270
	R-HSA-1236975	Antigen processing-Cross presentation	1,4448E-06	39
	R-HSA-5678895	Defective CFTR causes cystic fibrosis	3,8769E-06	28
	R-HSA-5358346	Hedgehog ligand biogenesis	0,00000614	29
	R-HSA-382551	Transmembrane transport of small molecules	8,1494E-06	156
	R-HSA-1236974	ER-Phagosome pathway	8,6694E-06	33
	R-HSA-5362768	Hh mutants that don't undergo autocatalytic processing are degraded by ERAD	8,6694E-06	26
	R-HSA-1236978	Cross-presentation of soluble exogenous antigens (endosomes	8,6694E-06	24
	R-HSA-69229	Ubiquitin-dependent degradation of Cyclin D1	1,1806E-05	24
	R-HSA-75815	Ubiquitin-dependent degradation of Cyclin D	1,1806E-05	24
	R-HSA-5387390	Hh mutants abrogate ligand secretion	1,5998E-05	26
	R-HSA-1280215	Cytokine Signaling in Immune system	1,8033E-05	167
	R-HSA-446203	Asparagine N-linked glycosylation	2,1079E-05	80
	R-HSA-561984	ABC transporter disorders	2,4146E-05	28
	R-HSA-5610780	Degradation of GLI1 by the proteasome	2,773E-05	26
	R-HSA-180585	Vif-mediated degradation of APOBEC3G	3,0205E-05	24
	R-HSA-351202	Metabolism of polyamines	4,3808E-05	32
	R-HSA-71387	Metabolism of carbohydrates	5,902E-05	77
	R-HSA-211733		9,9502E-05	22
	R-HSA-1234176	ulation of activated PAK-2p34 by proteasome mediated degrad	0,00012956	26
	R-HSA-350562	Regulation of ornithine decarboxylase (ODC)	0,00013063	22
Downregulated	R-HSA-212436	Generic Transcription Pathway	1,9561E-24	203
	R-HSA-74160	Gene Expression	3,3172E-12	303
	R-HSA-157118	Signaling by NOTCH	0,00380239	29
	R-HSA-3247509	Chromatin modifying enzymes	0,00380239	55
	R-HSA-4839726	Chromatin organization	0,00380239	55
	R-HSA-202433	Generation of second messenger molecules	0,00526001	13
	R-HSA-202430	Translocation of ZAP-70 to Immunological synapse	0,01444696	9
	R-HSA-202427	Phosphorylation of CD3 and TCR zeta chains	0,04962925	9
	R-HSA-1980143	Signaling by NOTCH1	0,04962925	19

Table S6. List of top 25 most significantly enriched pathways (adjusted p-value < 0.05) for the differently expressed genes (DEGs) either upregulated or downregulated upon stimulation. Gene # - number of genes matching the annotated Reactome pathway.

Stimulation (II)

	Comparison moDCs and stimulated moDCs				Comparison CXCL4-moDCs and stimulated CXCL4-moDCs				Comparison stimulated moDCs and stimulated CXCL4-moDCs			
	ID Reactome pathway	Description	adjusted p-value	Gene #	ID Reactome pathway	Description	adjusted p-value	Gene #	ID Reactome pathway	Description	adjusted p-value	Gene #
Upregulated	R-HSA-1280215	Cytokine Signaling in Immune system	1,40784E-28	268	R-HSA-1280215	Cytokine Signaling in Immune system	1,7784E-33	297	R-HSA-556833	Metabolism of lipids and lipoproteins	0,00047598	90
	R-HSA-168256	Immune System	8,69271E-27	574	R-HSA-168256	Immune System	4,6781E-26	617	R-HSA-422475	Axon guidance	0,00071424	68
	R-HSA-913531	Interferon Signaling	9,40642E-22	99	R-HSA-913531	Interferon Signaling	2,5481E-22	105	R-HSA-1430728	Metabolism	0,00143659	192
	R-HSA-877300	Interferon gamma signaling	6,96043E-17	56	R-HSA-877300	Interferon gamma signaling	3,5287E-18	60	R-HSA-1474244	Extracellular matrix organization	0,00458176	40
	R-HSA-909733	Interferon alpha/beta signaling	2,94642E-14	43	R-HSA-449147	Signaling by Interleukins	1,97E-13	183	R-HSA-5660526	Response to metal ions	0,00529293	6
	R-HSA-166054	Activated TLR4 signalling	1,21823E-09	53	R-HSA-909733	Interferon alpha/beta signaling	9,6429E-13	43	R-HSA-5661231	Metallothioneins bind metals	0,00529293	6
	R-HSA-449147	Signaling by Interleukins	2,76707E-09	158	R-HSA-5357801	Programmed Cell Death	2,6996E-10	76	R-HSA-3000171	Non-integrin membrane-ECM interactions	0,00941874	14
	R-HSA-166166	MyD88-independent TLR3/TLR4 cascade	3,17684E-09	47	R-HSA-109581	Apoptosis	2,5108E-09	73	R-HSA-186797	Signaling by PDGF	0,01815033	45
	R-HSA-168164	Toll Like Receptor 3 (TLR3) Cascade	3,17684E-09	47	R-HSA-166166	MyD88-independent TLR3/TLR4 cascade	6,0807E-09	49	R-HSA-1474228	Degradation of the extracellular matrix	0,01815033	22
	R-HSA-937061	TRIF-mediated TLR3/TLR4 signaling	3,17684E-09	47	R-HSA-168164	Toll Like Receptor 3 (TLR3) Cascade	6,0807E-09	49	R-HSA-216083	Integrin cell surface interactions	0,01815033	16
	R-HSA-168928	RIG-I/MDA5 mediated induction of IFN-alpha/beta pathways	1,82445E-08	41	R-HSA-937061	TRIF-mediated TLR3/TLR4 signaling	6,0807E-09	49	R-HSA-1638074	Keratan sulfate/keratin metabolism	0,01815033	9
	R-HSA-168249	Innate Immune System	6,02856E-08	318	R-HSA-166054	Activated TLR4 signalling	7,7057E-09	54	R-HSA-3000157	Laminin interactions	0,01815033	9
	R-HSA-166016	Toll Like Receptor 4 (TLR4) Cascade	1,07816E-07	53	R-HSA-168249	Innate Immune System	4,8655E-08	345	R-HSA-8874081	MET activates PTK2 signaling	0,01815033	9
	R-HSA-168898	Toll-Like Receptors Cascades	5,11243E-07	59	R-HSA-5213460	RIPK1-mediated regulated necrosis	7,2275E-08	17	R-HSA-2022090	Assembly of collagen fibrils and other multimeric structures	0,01895851	13
	R-HSA-1280218	Adaptive Immune System	2,03639E-06	214	R-HSA-5218859	Regulated Necrosis	7,2275E-08	17	R-HSA-71387	Metabolism of carbohydrates	0,02114424	36
	R-HSA-73887	Death Receptor Signalling	5,54739E-06	26	R-HSA-1280218	Adaptive Immune System	7,7882E-08	238	R-HSA-1474290	Collagen formation	0,02522869	16
	R-HSA-168181	Toll Like Receptor 7/8 (TLR7/8) Cascade	6,33334E-06	39	R-HSA-166016	Toll Like Receptor 4 (TLR4) Cascade	2,9992E-07	55	R-HSA-3000178	ECM proteoglycans	0,02902079	14
	R-HSA-975155	MyD88 dependent cascade initiated on endosome	6,33334E-06	39	R-HSA-73887	Death Receptor Signalling	2,9992E-07	29	R-HSA-1266738	Developmental Biology	0,02902079	100
	R-HSA-5357801	Programmed Cell Death	6,78957E-06	61	R-HSA-6783783	Interleukin-10 signaling	8,3245E-07	28	R-HSA-2214320	Anchoring fibril formation	0,03143644	6
	R-HSA-168138	Toll Like Receptor 9 (TLR9) Cascade	6,78957E-06	40	R-HSA-5675482	Regulation of necroptotic cell death	9,7517E-07	15	R-HSA-194138	Signaling by VEGF	0,03143644	39
	R-HSA-3247509	Chromatin modifying enzymes	1,86068E-05	85	R-HSA-2454202	Fc epsilon receptor (FCERI) signaling	2,601E-06	119	R-HSA-1630316	Glycosaminoglycan metabolism	0,03207698	19
	R-HSA-4839726	Chromatin organization	1,86068E-05	85	R-HSA-168928	RIG-I/MDA5 mediated induction of IFN-alpha/beta pathways	2,6937E-06	39	R-HSA-111465	Apoptotic cleavage of cellular proteins	0,04118232	9
	R-HSA-975138	TRAF6 mediated induction of NFkB and MAP kinases upon TLR7/8 or 9 activation	2,67848E-05	37	R-HSA-6785807	Interleukin-4 and 13 signaling	3,9724E-06	47	R-HSA-2172127	DAP12 interactions	0,04204841	41
	R-HSA-3214847	HATs acetylate histones	2,67848E-05	51	R-HSA-168181	Toll Like Receptor 7/8 (TLR7/8) Cascade	6,5169E-06	41	R-HSA-1483257	Phospholipid metabolism	0,04825269	26
	R-HSA-1640170	Cell Cycle	2,67848E-05	164	R-HSA-975155	MyD88 dependent cascade initiated on endosome	6,5169E-06	41				
Downregulated	R-HSA-72312	rRNA processing	1,45974E-18	94	R-HSA-1428517	The citric acid (TCA) cycle and respiratory electron transport	1,3737E-08	74	R-HSA-212436	Generic Transcription Pathway	3,1443E-05	85
	R-HSA-8868773	rRNA processing in the nucleus and cytosol	3,06912E-18	90	R-HSA-1430728	Metabolism	1,3737E-08	564	R-HSA-74160	Gene Expression	4,0961E-05	148
	R-HSA-6791226	Major pathway of rRNA processing in the nucleolus and cytosol	3,45802E-18	86	R-HSA-163200	Respiratory electron transport, ATP synthesis by chemiosmotic coupling, and heat production by uncoupling proteins.	4,5692E-07	56	R-HSA-202433	Generation of second messenger molecules	0,00024906	11
	R-HSA-72764	Eukaryotic Translation Termination	1,76251E-17	57	R-HSA-611105	Respiratory electron transport	2,5943E-05	45	R-HSA-202427	Phosphorylation of CD3 and TCR zeta chains	0,00026414	9
	R-HSA-72689	Formation of a pool of free 40S subunits	3,77456E-17	60	R-HSA-156827	L13a-mediated translational silencing of Ceruloplasmin expression	0,00020773	48	R-HSA-389948	PD-1 signaling	0,00033046	9
	R-HSA-975956	Nonsense Mediated Decay (NMD) independent of the Exon Junction Complex (EJC)	8,89413E-17	57	R-HSA-72689	Formation of a pool of free 40S subunits	0,00026445	44	R-HSA-202430	Translocation of ZAP-70 to Immunological synapse	0,00055203	8
	R-HSA-156827	L13a-mediated translational silencing of Ceruloplasmin expression	1,61095E-16	63	R-HSA-212436	Generic Transcription Pathway	0,00033982	233	R-HSA-1280215	Cytokine Signaling in Immune system	0,00655416	67
	R-HSA-156902	Peptide chain elongation	1,61095E-16	54	R-HSA-72706	GTP hydrolysis and joining of the 60S ribosomal subunit	0,00034181	47	R-HSA-877300	Interferon gamma signaling	0,01754232	15
	R-HSA-192823	Viral mRNA Translation	1,61095E-16	54	R-HSA-72613	Eukaryotic Translation Initiation	0,00036989	49				
	R-HSA-2408557	Selenocysteine synthesis	1,62735E-16	55	R-HSA-72737	Cap-dependent Translation Initiation	0,00036989	49				
	R-HSA-156842	Eukaryotic Translation Elongation	2,84557E-16	55	R-HSA-72766	Translation	0,00049219	59				
	R-HSA-72706	GTP hydrolysis and joining of the 60S ribosomal subunit	5,592E-16	62	R-HSA-1799339	SRP-dependent cotranslational protein targeting to membrane	0,00065491	45				
	R-HSA-72766	Translation	6,21144E-16	76	R-HSA-74160	Gene Expression	0,00070963	447				
	R-HSA-2408522	Selenoamino acid metabolism	7,92201E-16	63	R-HSA-192823	Viral mRNA Translation	0,00070999	38				
	R-HSA-72613	Eukaryotic Translation Initiation	1,10598E-15	64	R-HSA-1483257	Phospholipid metabolism	0,00083865	69				
	R-HSA-72737	Cap-dependent Translation Initiation	1,10598E-15	64	R-HSA-1483255	PI Metabolism	0,0010141	33				
	R-HSA-74160	Gene Expression	6,07936E-15	443	R-HSA-168273	Influenza Viral RNA Transcription and Replication	0,0010141	50				
	R-HSA-1799339	SRP-dependent cotranslational protein targeting to membrane	1,04914E-14	59	R-HSA-109703	PKB-mediated events	0,0010141	21				
	R-HSA-927802	Nonsense-Mediated Decay (NMD)	1,16222E-13	59	R-HSA-2408522	Selenoamino acid metabolism	0,0010141	46				
	R-HSA-975957	Nonsense Mediated Decay (NMD) enhanced by the Exon Junction Complex (EJC)	1,16222E-13	59	R-HSA-2408557	Selenocysteine synthesis	0,0011587	38				
	R-HSA-168273	Influenza Viral RNA Transcription and Replication	4,23631E-13	63	R-HSA-156902	Peptide chain elongation	0,0011587	37				
	R-HSA-168255	Influenza Life Cycle	1,0418E-12	65	R-HSA-168255	Influenza Life Cycle	0,0011587	52				
	R-HSA-168254	Influenza Infection	4,87418E-12	67	R-HSA-6799198	Complex I biogenesis	0,0011587	26				
	R-HSA-71291	Metabolism of amino acids and derivatives	6,24238E-11	118	R-HSA-975956	Nonsense Mediated Decay (NMD) independent of the Exon Junction (	0,0011587	39				
	R-HSA-1430728	Metabolism	4,15036E-09	482	R-HSA-156842	Eukaryotic Translation Elongation	0,00120587	38				

Table S7. List of significantly enriched pathways (adjusted p-value < 0.05) for the differently expressed genes (DEGs) overlapping from the comparisons between: 1. moDCs and CXCL4-moDCs (day 2, 4, 6) during differentiation, 2. stimulated moDCs and stimulated CXCL4-moDCs (polyI:C 4h and 24h). Gene # - number of genes matching the pathway annotated.

ID Reactome pathway	Description	adjusted p-value	Gene #
R-HSA-202433	Generation of second messenger molecules	0,015718	11
R-HSA-877300	Interferon gamma signaling	0,015718	20
R-HSA-202430	Translocation of ZAP-70 to Immunological synapse	0,015785	8
R-HSA-5660526	Response to metal ions	0,015785	6
R-HSA-5661231	Metallothioneins bind metals	0,015785	6
R-HSA-556833	Metabolism of lipids and lipoproteins	0,015785	93
R-HSA-202427	Phosphorylation of CD3 and TCR zeta chains	0,025556	8
R-HSA-168256	Immune System	0,025556	208
R-HSA-389948	PD-1 signaling	0,029926	8
R-HSA-168249	Innate Immune System	0,034765	134
R-HSA-174403	Glutathione synthesis and recycling	0,064187	6
R-HSA-373755	Semaphorin interactions	0,064187	14
R-HSA-109582	Hemostasis	0,064187	73
R-HSA-164952	The role of Nef in HIV-1 replication and disease pathogenesis	0,104892	8
R-HSA-422475	Axon guidance	0,104892	65
R-HSA-1280215	Cytokine Signaling in Immune system	0,107355	82
R-HSA-2142691	Synthesis of Leukotrienes (LT) and Eoxins (EX)	0,127141	7
R-HSA-399719	Trafficking of AMPA receptors	0,127217	8
R-HSA-399721	Glutamate Binding, Activation of AMPA Receptors and Synaptic Plasticity	0,127217	8
R-HSA-1474290	Collagen formation	0,127217	16
R-HSA-2132295	MHC class II antigen presentation	0,134047	19
R-HSA-1650814	Collagen biosynthesis and modifying enzymes	0,139483	13
R-HSA-388841	Costimulation by the CD28 family	0,139483	13
R-HSA-4085001	Sialic acid metabolism	0,151171	8
R-HSA-216083	Integrin cell surface interactions	0,151171	15
R-HSA-76005	Response to elevated platelet cytosolic Ca2+	0,156699	20
R-HSA-2022090	Assembly of collagen fibrils and other multimeric structures	0,156805	12
R-HSA-6783783	Interleukin-10 signaling	0,16942	10
R-HSA-114608	Platelet degranulation	0,191733	19
R-HSA-419812	Calcitonin-like ligand receptors	0,191733	4
R-HSA-77286	mitochondrial fatty acid beta-oxidation of saturated fatty acids	0,191733	4
R-HSA-419037	NCAM1 interactions	0,191733	9
R-HSA-164938	diates down modulation of cell surface receptors by recruiting them to clathrin ac	0,191733	6
R-HSA-77289	Mitochondrial Fatty Acid Beta-Oxidation	0,191733	6
R-HSA-6798695	Neutrophil degranulation	0,191733	54

Table S8. List of significantly enriched pathways (adjusted p-value < 0.05) for co-expression and co-methylation modules. Gene # - number of genes matching the pathway annotated.

Co-expression modules

Co-expression modules	Module ID	ID Reactome pathway	Description	adjusted p-value	Gene #
lightpink4	RM11	R-HSA-6798695	Neutrophil degranulation	6,25E-08	77
		R-HSA-198933	Immunoregulatory interactions between a Lymphoid and a non-Lymphoid cell	4,31E-05	26
		R-HSA-168249	Innate Immune System	0,000103	147
		R-HSA-202733	Cell surface interactions at the vascular wall	0,000216	25
		R-HSA-163125	Post-translational modification: synthesis of GPI-anchored proteins	0,000595	18
grey60	RM25	R-HSA-1474244	Extracellular matrix organization	9,15E-07	23
		R-HSA-3000171	Non-integrin membrane-ECM interactions	2,07E-05	9
		R-HSA-216083	Integrin cell surface interactions	4,81E-05	10
		R-HSA-3000170	Syndecan interactions	5,53E-05	6
		R-HSA-1660662	Glycosphingolipid metabolism	9,06E-05	7
		R-HSA-556833	Metabolism of lipids and lipoproteins	0,000105	37
		R-HSA-382551	Transmembrane transport of small molecules	0,000219	32
		R-HSA-983712	Ion channel transport	0,000645	14
		R-HSA-399719	Trafficking of AMPA receptors	0,000798	5
		R-HSA-399721	Glutamate Binding, Activation of AMPA Receptors and Synaptic Plasticity	0,000798	5
		R-HSA-3000157	Laminin interactions	0,001071	5
		R-HSA-73923	Lipid digestion, mobilization, and transport	0,001515	9
		R-HSA-1474290	Collagen formation	0,001783	8
		R-HSA-174824	Lipoprotein metabolism	0,001835	7
		R-HSA-193634	Axonal growth inhibition (RHOA activation)	0,001982	3
		R-HSA-5660526	Response to metal ions	0,001982	3
		R-HSA-5661231	Metallothioneins bind metals	0,001982	3
		R-HSA-2187338	Visual phototransduction	0,002485	8
		R-HSA-3000178	ECM proteoglycans	0,002497	7
		R-HSA-193697	p75NTR regulates axonogenesis	0,002596	3
		R-HSA-936837	Ion transport by P-type ATPases	0,002629	6
		R-HSA-210991	Basigin interactions	0,003747	4
		R-HSA-917937	Iron uptake and transport	0,003954	5
		R-HSA-354192	Integrin alphaIIb beta3 signaling	0,00429	4
		R-HSA-428157	Sphingolipid metabolism	0,005275	7
		R-HSA-917977	Transferrin endocytosis and recycling	0,00553	4
		R-HSA-372708	p130Cas linkage to MAPK signaling for integrins	0,006154	3
		R-HSA-2022928	HS-GAG biosynthesis	0,006231	4
		R-HSA-1474228	Degradation of the extracellular matrix	0,007398	9
		R-HSA-8874081	MET activates PTK2 signaling	0,007805	4
		R-HSA-1793185	Chondroitin sulfate/dermatan sulfate metabolism	0,008099	5
		R-HSA-1638091	Heparan sulfate/heparin (HS-GAG) metabolism	0,010229	5
		R-HSA-1280215	Cytokine Signaling in Immune system	1,65E-21	192
		R-HSA-168256	Immune System	3,49E-17	399
		R-HSA-913531	Interferon Signaling	3,13E-15	69
		R-HSA-877300	Interferon gamma signaling	4,25E-12	39
		R-HSA-909733	Interferon alpha/beta signaling	5E-09	28
		R-HSA-449147	Signaling by Interleukins	1,97E-08	114
		R-HSA-983169	Class I MHC mediated antigen processing & presentation	4,87E-07	83
		R-HSA-6783783	Interleukin-10 signaling	5,63E-06	19
		R-HSA-114604	GPVI-mediated activation cascade	1,38E-05	20
		R-HSA-168928	RIG-I/MDA5 mediated induction of IFN-alpha/beta pathways	1,5E-05	26
		R-HSA-983168	Antigen processing: Ubiquitination & Proteasome degradation	1,92E-05	67
		R-HSA-936440	Negative regulators of RIG-I/MDA5 signaling	9,27E-05	14
		R-HSA-1280218	Adaptive Immune System	9,82E-05	146
		R-HSA-166166	MyD88-independent TLR3/TLR4 cascade	0,000122	27
		R-HSA-168164	Toll Like Receptor 3 (TLR3) Cascade	0,000122	27
		R-HSA-937061	TRIF-mediated TLR3/TLR4 signaling	0,000122	27
		R-HSA-166054	Activated TLR4 signalling	0,000127	30
		R-HSA-389356	CD28 co-stimulation	0,000141	13
		R-HSA-166520	Signalling by NGF	0,000173	91
		R-HSA-168249	Innate Immune System	0,000245	210
		R-HSA-1433557	Signaling by SCF-KIT	0,000296	67
		R-HSA-6783589	Interleukin-6 family signaling	0,000325	11
		R-HSA-1834949	Cytosolic sensors of pathogen-associated DNA	0,000377	20
		R-HSA-918233	TRAF3-dependent IRF activation pathway	0,00041	8

cyan	RM22	R-HSA-73887	Death Receptor Signalling	0,000423	16
		R-HSA-166016	Toll Like Receptor 4 (TLR4) Cascade	0,000482	31
		R-HSA-73980	RNA Polymerase III Transcription Termination	0,000491	10
		R-HSA-168181	Toll Like Receptor 7/8 (TLR7/8) Cascade	0,000689	24
		R-HSA-975155	MyD88 dependent cascade initiated on endosome	0,000689	24
		R-HSA-877312	Regulation of IFNG signaling	0,000962	7
		R-HSA-186763	Downstream signal transduction	0,001092	67
		R-HSA-2454202	Fc epsilon receptor (FCERI) signaling	0,00116	70
		R-HSA-975138	TRAF6 mediated induction of NFkB and MAP kinases upon TLR7/8 or 9 activation	0,001201	23
		R-HSA-8875555	MET activates RAP1 and RAC1	0,001278	6
		R-HSA-168138	Toll Like Receptor 9 (TLR9) Cascade	0,001307	24
		R-HSA-5668541	TNFR2 non-canonical NF-kB pathway	0,001404	25
		R-HSA-1169408	ISG15 antiviral mechanism	0,001443	20
		R-HSA-1169410	Antiviral mechanism by IFN-stimulated genes	0,001443	20
		R-HSA-6806834	Signaling by MET	0,001613	21
		R-HSA-194138	Signaling by VEGF	0,001613	64
		R-HSA-73780	RNA Polymerase III Chain Elongation	0,001675	8
		R-HSA-76066	RNA Polymerase III Transcription Initiation From Type 2 Promoter	0,002004	10
		R-HSA-74158	RNA Polymerase III Transcription	0,002022	13
		R-HSA-749476	RNA Polymerase III Abortive And Retractive Initiation	0,002022	13
		R-HSA-168643	Nucleotide-binding domain, leucine rich repeat containing receptor (NLR) signaling pathways	0,002075	15
		R-HSA-168142	Toll Like Receptor 10 (TLR10) Cascade	0,002226	21
		R-HSA-168176	Toll Like Receptor 5 (TLR5) Cascade	0,002226	21
		R-HSA-975871	MyD88 cascade initiated on plasma membrane	0,002226	21
		R-HSA-389359	CD28 dependent Vav1 pathway	0,002274	6
		R-HSA-186797	Signaling by PDGF	0,002352	70
		R-HSA-6788467	IL-6-type cytokine receptor ligand interactions	0,002475	8
		R-HSA-109581	Apoptosis	0,002614	36
		R-HSA-5669034	TNFs bind their physiological receptors	0,002705	10
		R-HSA-76061	RNA Polymerase III Transcription Initiation From Type 1 Promote	0,002705	10
		R-HSA-933542	TRAF6 mediated NF-kB activation	0,003141	9
		R-HSA-187037	NGF signalling via TRKA from the plasma membrane	0,003279	70
		R-HSA-512988	Interleukin-3, 5 and GM-CSF signaling	0,003336	52
		R-HSA-5357801	Programmed Cell Death	0,003539	36
		R-HSA-4420097	VEGFA-VEGFR2 Pathway	0,003656	61
		R-HSA-3134963	DEx/H-box helicases activate type I IFN and inflammatory cytokines production	0,003759	6
		R-HSA-933543	NF-kB activation through FADD/RIP-1 pathway mediated by caspase-8 and -10	0,003759	6
		R-HSA-140534	Ligand-dependent caspase activation	0,003814	7
		R-HSA-6785807	Interleukin-4 and 13 signaling	0,00415	25
		R-HSA-166058	MyD88:Mal cascade initiated on plasma membrane	0,004876	22
		R-HSA-168188	Toll Like Receptor TLR6:TLR2 Cascade	0,004876	22
		R-HSA-76002	Platelet activation, signaling and aggregation	0,004879	52
		R-HSA-389357	CD28 dependent PI3K/Akt signaling	0,00494	8
		R-HSA-193692	Regulated proteolysis of p75NTR	0,005439	5
		R-HSA-2465910	MASTL Facilitates Mitotic Progression	0,005439	5
		R-HSA-168898	Toll-Like Receptors Cascades	0,006002	32
		R-HSA-177929	Signaling by EGFR	0,006141	65
		R-HSA-5689896	Ovarian tumor domain proteases	0,006169	11
		R-HSA-76046	RNA Polymerase III Transcription Initiation	0,006169	11
		R-HSA-168179	Toll Like Receptor TLR1:TLR2 Cascade	0,00718	22
		R-HSA-181438	Toll Like Receptor 2 (TLR2) Cascade	0,00718	22
		R-HSA-392451	G beta:gamma signalling through PI3Kgamma	0,007226	13
		R-HSA-5357769	Caspase activation via extrinsic apoptotic signalling pathway	0,007381	9
		R-HSA-453274	Mitotic G2-G2/M phases	0,007784	38
		R-HSA-5683057	MAPK family signaling cascades	0,008313	53
		R-HSA-2424491	DAP12 signaling	0,008462	63
		R-HSA-6811440	Retrograde transport at the Trans-Golgi-Network	0,008685	13
		R-HSA-3371378	Regulation by c-FLIP	0,008906	5
		R-HSA-5218900	CASP8 activity is inhibited	0,008906	5
		R-HSA-69416	Dimerization of procaspase-8	0,008906	5
		R-HSA-76071	RNA Polymerase III Transcription Initiation From Type 3 Promoter	0,009485	9
		R-HSA-195253	Degradation of beta-catenin by the destruction complex	0,009677	19
		R-HSA-1236974	ER-Phagosome pathway	0,011015	19
		R-HSA-69275	G2/M Transition	0,011105	37
		R-HSA-451927	Interleukin-2 signaling	0,011334	48
		R-HSA-1251985	Nuclear signaling by ERBB4	0,011675	8
		R-HSA-1606322	ZBP1(DAI) mediated induction of type I IFNs	0,011675	8
		R-HSA-983170	Antigen Presentation: Folding, assembly and peptide loading of class I MHC	0,011675	8
		R-HSA-933541	TRAF6 mediated IRF7 activation	0,011914	10
		R-HSA-187687	Signalling to ERKs	0,012129	48

		R-HSA-397795	G-protein beta:gamma signalling	0,01229	13
		R-HSA-446652	Interleukin-1 signaling	0,013157	12
		R-HSA-2730905	Role of LAT2/NTAL/LAB on calcium mobilization	0,013851	27
		R-HSA-169893	Prolonged ERK activation events	0,013927	46
		R-HSA-1168372	Downstream signaling events of B Cell Receptor (BCR)	0,014073	37
		R-HSA-1810476	RIP-mediated NFkB activation via ZBP1	0,014237	7
		R-HSA-2028269	Signaling by Hippo	0,014237	7
		R-HSA-2428924	IGF1R signaling cascade	0,014829	53
		R-HSA-2428928	IRS-related events triggered by IGF1R	0,014829	53
		R-HSA-74160	Gene Expression	0,015333	267
		R-HSA-2404192	Signaling by Type 1 Insulin-like Growth Factor 1 Receptor (IGF1R)	0,015759	53
		R-HSA-6804756	Regulation of TP53 Activity through Phosphorylation	0,016063	20
		R-HSA-450294	MAP kinase activation in TLR cascade	0,016352	15
		R-HSA-388841	Costimulation by the CD28 family	0,016972	16
		R-HSA-912526	Interleukin receptor SHC signaling	0,01699	46
		R-HSA-622312	Inflammasomes	0,017074	6
		R-HSA-2172127	DAP12 interactions	0,017744	63
		R-HSA-1236975	Antigen processing-Cross presentation	0,017959	21
		R-HSA-5633007	Regulation of TP53 Activity	0,018097	31
		R-HSA-389513	CTLA4 inhibitory signaling	0,018575	7
		R-HSA-69273	Cyclin A/B1 associated events during G2/M transition	0,018575	7
		R-HSA-912631	Regulation of signaling by CBL	0,018575	7
		R-HSA-5663202	Diseases of signal transduction	0,018713	63
		R-HSA-170968	Frs2-mediated activation	0,018811	45
		R-HSA-69206	G1/S Transition	0,019315	24
		R-HSA-69656	Cyclin A:Cdk2-associated events at S phase entry	0,019331	16
		R-HSA-72306	tRNA processing	0,019807	22
		R-HSA-75893	TNF signaling	0,019902	11
		R-HSA-193704	p75 NTR receptor-mediated signalling	0,019968	21
		R-HSA-5684996	MAPK1/MAPK3 signaling	0,02006	45
		R-HSA-74751	Insulin receptor signalling cascade	0,020769	52
		R-HSA-1660499	Synthesis of PIPs at the plasma membrane	0,021577	12
		R-HSA-5357905	Regulation of TNFR1 signaling	0,02259	9
		R-HSA-2586552	Signaling by Leptin	0,022756	45
		R-HSA-5675482	Regulation of necroptotic cell death	0,022838	6
		R-HSA-936964	Activation of IRF3/IRF7 mediated by TBK1/IKK epsilon	0,022838	6
		R-HSA-8875878	MET promotes cell motility	0,023493	11

Co-Methylation modules

Co-methylation modules	Module ID	ID Reactome pathway	Description	adjusted p-value	Gene #
red	DM7	R-HSA-168256	Immune System	6,46E-09	100
		R-HSA-168249	Innate Immune System	6,84E-06	62
		R-HSA-6798695	Neutrophil degranulation	3,08E-05	30
		R-HSA-109582	Hemostasis	0,000185	34
		R-HSA-877300	Interferon gamma signaling	0,001042	9
		R-HSA-198933	Immunoregulatory interactions between a Lymphoid and a non-Lymphoid cell	0,001055	11
sienna3	DM9	R-HSA-6783783	Interleukin-10 signaling	0,000119	6
		R-HSA-168256	Immune System	0,000153	54
		R-HSA-1445148	Translocation of GLUT4 to the plasma membrane	0,000299	7
		R-HSA-2022870	Chondroitin sulfate biosynthesis	0,000365	4
		R-HSA-2022923	Dermatan sulfate biosynthesis	0,000599	3
		R-HSA-389359	CD28 dependent Vav1 pathway	0,000789	3
		R-HSA-1630316	Glycosaminoglycan metabolism	0,000902	8
		R-HSA-168249	Innate Immune System	0,00102	35
		R-HSA-73887	Death Receptor Signalling	0,001153	5
		R-HSA-1793185	Chondroitin sulfate/dermatan sulfate metabolism	0,001379	5
		R-HSA-399955	SEMA3A-Plexin repulsion signaling by inhibiting Integrin adhesi	0,001575	3
		R-HSA-418038	Nucleotide-like (purinergic) receptors	0,001916	3
		R-HSA-71387	Metabolism of carbohydrates	0,002757	12
		R-HSA-5358351	Signaling by Hedgehog	0,002971	8
		R-HSA-109582	Hemostasis	0,000886	10
		R-HSA-5696395	Formation of Incision Complex in GG-NER	0,001165	3
		R-HSA-167169	HIV Transcription Elongation	0,001704	3
		R-HSA-167200	Formation of HIV-1 elongation complex containing HIV-1 Tat	0,001704	3
		R-HSA-167246	Tat-mediated elongation of the HIV-1 transcript	0,001704	3
		R-HSA-167152	Formation of HIV elongation complex in the absence of HIV Tat	0,001913	3
		R-HSA-199220	Vitamin B5 (pantothenate) metabolism	0,003009	2
		R-HSA-196849	Metabolism of water-soluble vitamins and cofactors	0,003114	4
		R-HSA-197264	Nicotinamide salvaging	0,003375	2
		R-HSA-112382	Formation of RNA Pol II elongation complex	0,003661	3
		R-HSA-75955	RNA Polymerase II Transcription Elongation	0,003661	3
		R-HSA-6782135	Dual incision in TC-NER	0,003994	3
		R-HSA-6796648	TP53 Regulates Transcription of DNA Repair Genes	0,004526	3

paleturquoise	DM5	R-HSA-167172	Transcription of the HIV genome	0,00593	3
		R-HSA-425410	Metal ion SLC transporters	0,006475	2
		R-HSA-6781827	Transcription-Coupled Nucleotide Excision Repair (TC-NER)	0,006603	3
		R-HSA-73857	RNA Polymerase II Transcription	0,007144	4
		R-HSA-167160	RNA Pol II CTD phosphorylation and interaction with CE during HIV infection	0,007529	2
		R-HSA-210991	Basigin interactions	0,007529	2
		R-HSA-77075	RNA Pol II CTD phosphorylation and interaction with CE	0,007529	2
		R-HSA-5696399	Global Genome Nucleotide Excision Repair (GG-NER)	0,008082	3
		R-HSA-674695	RNA Polymerase II Pre-transcription Events	0,008614	3
		R-HSA-72086	mRNA Capping	0,008655	2
		R-HSA-196807	Nicotinate metabolism	0,009244	2
		R-HSA-73772	RNA Polymerase I Promoter Escape	0,009851	2
		R-HSA-196854	Metabolism of vitamins and cofactors	0,010361	4
		R-HSA-73863	RNA Polymerase I Transcription Termination	0,011117	2
		R-HSA-113418	Formation of the Early Elongation Complex	0,011776	2
		R-HSA-167158	Formation of the HIV-1 Early Elongation Complex	0,011776	2
		R-HSA-5694530	Cargo concentration in the ER	0,011776	2
		R-HSA-425366	Transport of glucose and other sugars, bile salts and organic acids, metal ions and amine compounds	0,014702	3
		R-HSA-5696400	Dual Incision in GG-NER	0,016845	2
		R-HSA-5696398	Nucleotide Excision Repair	0,017021	3
		R-HSA-983168	Antigen processing: Ubiquitination & Proteasome degradation	0,017089	5
		R-HSA-5362517	Signaling by Retinoic Acid	0,018436	2
		R-HSA-73894	DNA Repair	0,018866	5
		R-HSA-167161	HIV Transcription Initiation	0,0218	2
		R-HSA-167162	RNA Polymerase II HIV Promoter Escape	0,0218	2
		R-HSA-73776	RNA Polymerase II Promoter Escape	0,0218	2
		R-HSA-73779	RNA Polymerase II Transcription Pre-Initiation And Promoter Op	0,0218	2
		R-HSA-75953	RNA Polymerase II Transcription Initiation	0,0218	2
		R-HSA-76042	RNA Polymerase II Transcription Initiation And Promoter Clearar	0,0218	2
		R-HSA-1989781	PPARA activates gene expression	0,022242	3
		R-HSA-73762	RNA Polymerase I Transcription Initiation	0,022678	2
		R-HSA-400206	Regulation of lipid metabolism by Peroxisome proliferator-activated receptor alpha (PPARalpha)	0,02367	3
		R-HSA-114608	Platelet degranulation	0,024157	3
		R-HSA-383280	Nuclear Receptor transcription pathway	0,025399	2
		R-HSA-162906	HIV Infection	0,026615	4
		R-HSA-76005	Response to elevated platelet cytosolic Ca2+	0,026671	3
		R-HSA-6781823	Formation of TC-NER Pre-Incision Complex	0,028245	2
		R-HSA-162599	Late Phase of HIV Life Cycle	0,028781	3
		R-HSA-202733	Cell surface interactions at the vascular wall	0,028781	3
		R-HSA-180585	Vif-mediated degradation of APOBEC3G	0,029221	2

Chapter 5

CXCL4 suppresses tolerogenic immune signature of monocyte-derived dendritic cells

Authors: Sandra C. Silva-Cardoso[1,2#]; Weiyang Tao[1,2#]; Beatriz Malvar Fernández[1,2]; Marianne Boes[1,3]; Timothy R.D.J. Radstake[1,2*]; Aridaman Pandit[1,2*]

Affiliations:

[1] Laboratory of Translational Immunology, University Medical Center Utrecht, the Netherlands

[2] Department of Rheumatology & Clinical Immunology, University Medical Center Utrecht, the Netherlands

[3] Department of Pediatrics, University Medical Center Utrecht, the Netherlands

[#*]Authors equally contributed

Submitted

Abstract

Dendritic cells (DCs) are immune sentinels that play a crucial role in inducing peripheral tolerance and immune response. Molecules resulting of cell damage, microbial products, and cytokines can modulate DCs towards tolerogenic or immunogenic responses. Therefore, disturbance of DC function contributes to autoimmunity. CXCL4 is a chemokine that modulates DC functions and has been implicated in several autoimmune diseases such as systemic sclerosis (SSc). Previously we showed that differentiation of monocyte-derived dendritic cells (moDCs) in the presence of CXCL4 promotes cell maturation by increasing the expression of activation molecules, sensitization to TLR-mediated stimulation, and potentiated activation of inflammatory responses by T-cells. Here we investigated the effect of CXCL4 on established markers of DC immunogenicity and tolerogenicity using RNA sequencing and DNA methylomics. CXCL4 impaired the transcriptional expression of tolerogenic genes, and induced the expression of immunogenic markers. We investigated in detail the complement component C1q, a robust tolerogenic marker, for which the reduced levels are associated with autoimmune disease development. CXCL4 epigenetically modified promotors of C1q genes and repressed expression of C1q genes. Thus, CXCL4 suppresses a tolerogenic DC phenotype thereby boosting immunogenic responses, and elucidates C1q as a critical factor in CXCL4-driven autoimmune diseases such as SSc.

Keywords: CXCL4, monocyte-derived dendritic cells, C1q, immunogenicity, tolerogenecity, RNA sequencing, DNA methylation, epigenetics

Abbreviations: moDC, monocyte-derived dendritic cells;

Introduction

Dendritic cells (DCs) are pivotal antigen-presenting cells (APCs) that bridge the innate and adaptive immune systems, thus playing a crucial role in the activation of immune responses and immunological tolerance [1]. On one hand, immature DCs upon recognition of apoptotic cells or damage-associated molecular patterns (DAMPs) are able to uptake, process, and present antigen-derived peptides on major histocompatibility complex (MHC). Migration of these incompletely matured DCs to draining lymph nodes promotes anergy, elimination of self-reactive T-cells or generation of regulatory T-cells (Tregs), and drives immune tolerance. On the other hand, DCs that encounter inflammatory cytokines or pathogen-associated molecular patterns (PAMPs) acquire a mature phenotype and migrate to lymphoid organs resulting in T-cell activation, and drive immunogenic responses. The control of tolerogenic and immunogenic responses by DCs involves intensive transcriptional and epigenetic reprograming, including DNA methylation.

Modulating the function of DCs become an active area in immunological and translational research. Several protocols have been proposed for the generation of tolerogenic and immunogenic DCs and established multiple candidate biomarkers that characterizes their function [2]–[4]. Among others, C1q was established as a regulatory marker of DCs as it is consistently overexpressed on tolerogenic DCs generated via distinct protocols [5],[6].

C1q is the first component of the classical pathway of complement system and its deficiency is associated with autoimmune conditions, both in mouse models and in humans [7],[8]. C1q also functions as an opsonin that enables the detection and phagocytosis of PAMPs and apoptotic cell fragments either directly, or indirectly via binding to secreted antibodies and C-reactive protein (CRP). Immature DCs and macrophages are able to secrete high levels of C1q in contrast to monocytes, mature DCs and T-cells [9],[10].

CXCL4 is a chemokine abundantly produced by activated platelets [11] and immune cells [12]–[15]. CXCL4 participates in several physiological processes and is implicated in autoimmune diseases such as systemic sclerosis (SSc) [13],[16]. We and others have shown that CXCL4 modulates immune responses of monocytes, DCs, macrophages and T-cells [17]–[22]. We showed that differentiation of moDCs in the presence of CXCL4 (CXCL4-moDCs), results in immunogenic DC phenotype characterized by increased expression of activation molecules, potentiated T-cell activation, and augmented response to TLR triggering [22]. Here, we investigated how CXCL4 controls the transcriptional programming of DCs regarding immunogenicity and tolerogenicity markers, and studied in detail C1q genes as they are the most consistent marker for tolerogenic DC.

Results and discussion

CXCL4 up-regulates immunogenic and down-regulates tolerogenic markers

Previously, we showed that exposure to CXCL4 drives moDCs to a semi-mature phenotype and function [22]. Here we performed RNA sequencing analysis to investigate how CXCL4 exposure affects tolerogenic and immunogenic signatures. We observed that genes associated with immunogenic DC responses such as CD86, CD83, HLA-A, CCR7, CCL17, FSCN1, LAMP3, SOD2, CD40 and ICAM1 were up-regulated on CXCL4-moDCs. Interestingly, the expression of colony stimulating factor 1 receptor (CSF1R), which is down-regulated in inflammatory DCs [23], was also found to be down-regulated on CXCL4-moDCs (Fig. 1A, 1C). However, CD80, a co-stimulatory molecule associated with response to stimuli, was not differentially expressed between moDCs and CXCL4-moDCs (Supporting Information Fig. 1A).

We found that genes associated with DC tolerogenicity such as IL10, SLAMF1, SMAD3, FZD2, F13A1, STAB1, CTSC, FCGR2B, CD37 and GILZ (TSC22D3) were significantly down-regulated by CXCL4 (Fig. 1B, 1C, Supporting Information Fig. 1B). NAMPT and THBS1, previously implicated in tolerogenic responses [6],[24],[25], were not differential between moDCs and CXCL4-moDCs (Supporting Information Fig. 1B). Thus, CXCL4 induces immunogenic DC phenotype by up-regulating specific (but not all) genes involved in the maturation of moDCs and down-regulates genes associated with tolerogenicity.

CXCL4 dramatically suppresses C1q genes

C1q is critical for maintaining immune tolerance. Binding of C1q to PAMPs and apoptotic cell fragments results in the initiation of the complement system cascade and cell activation. Primary C1q deficiency in humans [26] and C1q knockout mice [27] have been shown to result in autoimmune conditions such as systemic lupus erythematosus (SLE). Moreover, C1q has been consistently shown to be up-regulated on tolerogenic DCs [2]–[4]. We found that CXCL4 down-regulates the expression of all three C1q genes (*C1QA*, *C1QB* and *C1QC*) and diminished their protein expression (Fig. 2A, 2B). Additionally, CXCL4-moDCs released lower amounts of C1q in comparison to moDCs (Fig. 2 C).

Decrease C1q expression may reflect immunogenic phenotype of CXCL4-moDCs

We further investigated whether CXCL4 simultaneously dysregulates the expression of immunogenic and tolerogenic genes, including *C1Q*. We found that C1q genes negatively correlated with immunogenic genes (Fig. 2D), and positively correlated

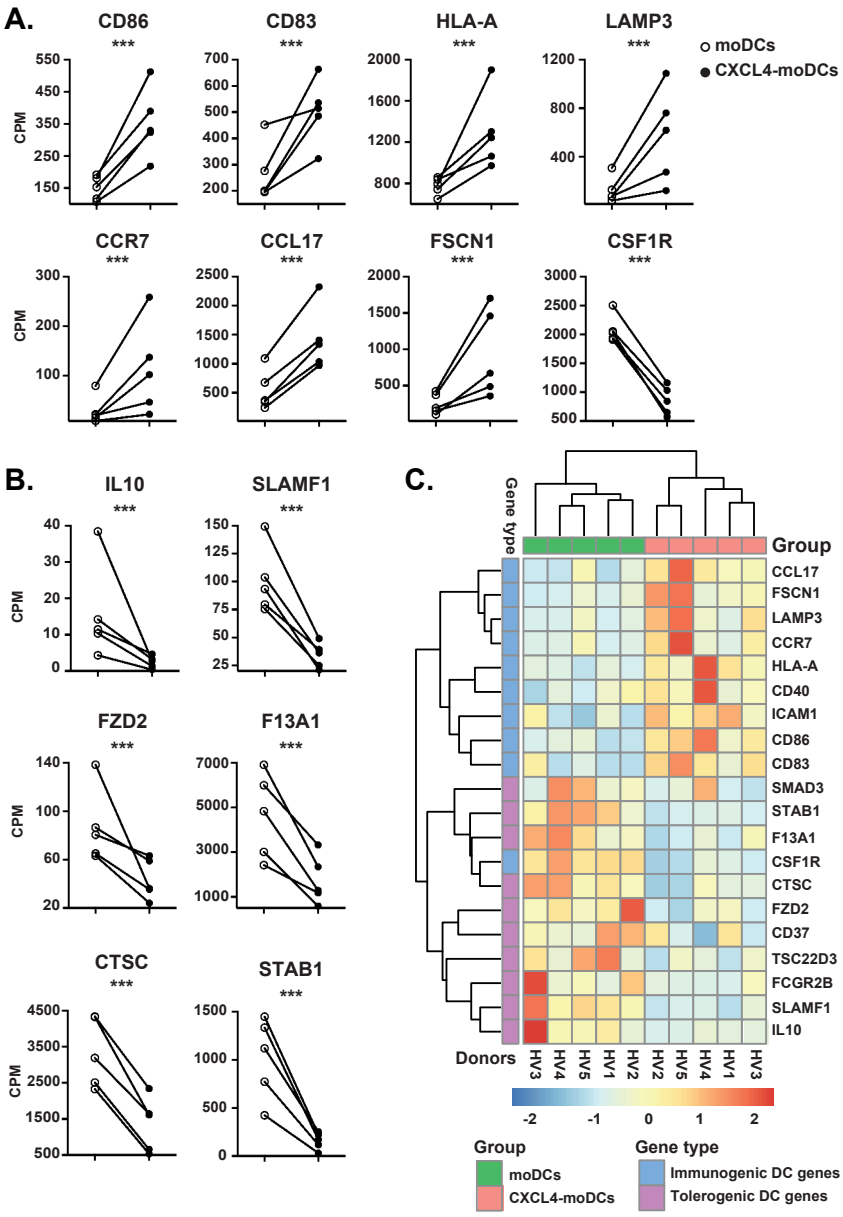

Figure 1. CXCL4 drives dramatic up-regulation of immunogenic signature and down-regulation of tolerogenic markers. RNA sequencing was performed on day 6 of differentiated moDCs and CXCL4-moDCs. Gene expression analysis of (A) immunogenic and (B) tolerogenic associated molecules shown in count per million (CPM). Lines connect samples of individual HV. (n=5 HV, n=5 per group). Likelihood ratio test. ***P<0.005. (C) Heat map showing immunogenic and tolerogenic gene signatures . The colour scheme represente gene expression and is shown as Z-scores. Data shown for 5 HV, all from independent experiments.

with the other tolerogenic genes. In fact, *C1QA*, *C1QB* and *C1QC* genes exhibited the strongest negative correlation with most of the immunogenic markers (Fig. 2D).

CXCL4 leads to dramatic hypermethylation of C1q and other tolerogenic genes

Changes in DNA methylation have been associated with aberrant gene expression and autoimmune disorders [28]. To assess whether CXCL4 exposure epigenetically affects C1q genes, we performed DNA methylation analyses. We found that CXCL4 induced hypermethylation in the promoter regions (TSS200, TSS1500) of all 3 C1q (*C1QA*, *C1QB*, *C1QC*) genes and in the gene body (1st Exon, 5'UTR) of *C1QB* and *C1QC* genes (Fig. 3A, 3B, 3C). All these hypermethylated regions were strongly negative correlated with the corresponding gene's expression (Fig. 3D, 3E, 3F). Additionally, we showed that CXCL4 drives hypermethylation of individual CpGs across the *C1QA (cg15399505)*, *C1QB* (cg002155182, cg01577837, cg10103528, cg14041976, cg24931346 and cg04097715) and *C1QC* (cg12775742 and cg17104151) genes, and exhibits strong negative correlated with the corresponding gene's expression (Supporting Information Fig. 2A, 2B, 2C).

Other genes associated with tolerogenic responses including IL10, SLAMF1, STAB1, and CTSC were hypermethylated in CXCL4-moDCs and exhibited negative correlations between RNA expression and DNA methylation levels (Supporting Information Fig.3). However, it was not the same case for other tolerogenic genes (F13A1, STAB1 and SMAD3) (Supporting Information Fig.4). Interestingly, no immunogenic gene exhibited significant negative correlation between RNA expression and DNA methylation levels (Supporting Information Fig.4). Thus, CXCL4 mediates epigenetic modifications and transcriptional suppression of tolerogenic markers (especially C1q) to tip the balance between immunogenic and tolerogenic DCs.

Concluding Remarks

The orchestration of innate and adaptive immune responses by DCs in response to danger signals modulates both tolerogenic and immunogenic responses, and is critical to prevent the development of autoimmune conditions. Corroborating with the literature and our previous findings, we showed that exposure to CXCL4 during moDC differentiation leads to an amplified immunogenic response [20],[22].

C1q has been consistently proposed as a tolerogenic DC marker [2]–[4]. Inflammatory triggers were shown to diminish C1q production during DC maturation [9]. Here, we revealed for the first time that CXCL4 exposure down-regulates the expression of gene associated with tolerogenic responses, especially C1q, on moDCs. We further showed that CXCL4 drives hypermethylation of multiple tolerogenic genes, and strikingly, we found strong negative correlation between the

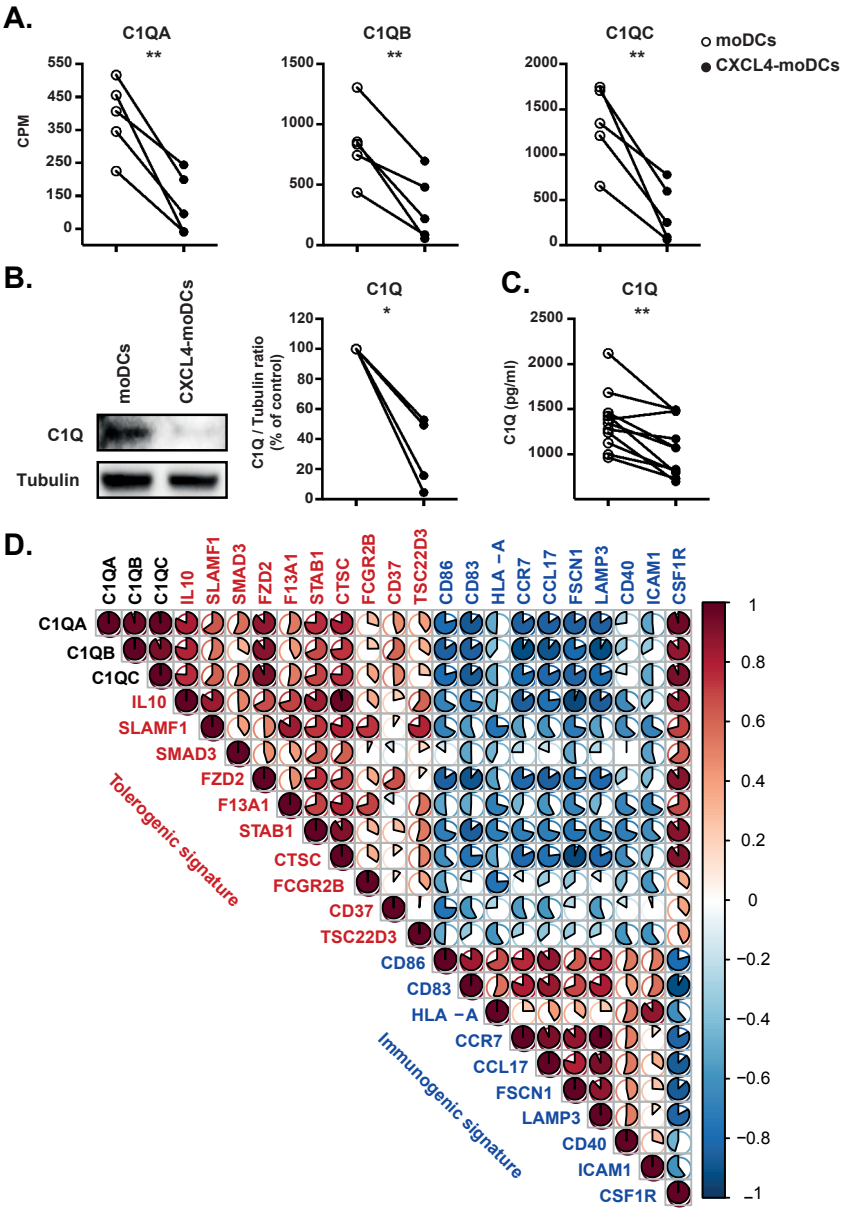

Figure 2. C1q expression and production dramatically diminishes in the presence of CXCL4. RNA sequencing was performed on day 6 of differentiated moDCs and CXCL4-moDCs. (A) Expression of *C1QA*, *C1QB* and *C1QC* genes on moDCs and CXCL4-moDCs. (n=5 HV, n=5 per group). Likelihood ratio test. $^{**}P<0.01$ (B) Western blot analysis of C1q and tubulin. Representative blot of 4 HV is shown (4 independent experiments, n=4 per group). On the right, we show the quantification for 4 HV. Paired *t*-test. $^{*}P<0.05$; (C) Measurement of soluble C1q by Elisa (n=11, 8 independent experiments). Paired *t*-test. $^{**}P<0.005$; (D) Pearson correlation analysis between the expression of *C1QA*, *C1QB* and *C1QC* genes (black text) and tolerogenic (red text) or immunogenic (blue text) signature genes. Colour scheme gradient and pie graphs represent the correlation coefficients between comparisons. Data shown for 5 HV, all from independent experiments.

RNA expression and DNA methylation levels of C1q genes. Thus, our data suggests that CXCL4-driven immunogenic DC phenotype is accompanied by down-regulation of tolerogenic genes such as C1q, and may contribute to the break of tolerance in inflammatory conditions, resulting in the development of autoimmune disorders.

Materials and Methods

Generation of moDCs and preparation of RNA and DNA samples

Differentiation of moDCs was implemented as described before [22]. DNA and RNA were extracted from moDCs and CXCL4-moDCs on day6 upon differentiation. Cells were lysed in RLTplus buffer (Qiagen) containing 1% (v/v) β-mercapto-ethanol (Sigma). DNA and RNA were purified using an Allprep Universal Kit (Qiagen) accordingly to manufacturer's instructions, and quantified using Qubit dsDNA HS Assay Kit and Qubit RNA HS Assay Kit, and measured using Qubit 2.0 fluorimeter (Invitrogen).

RNA sequencing and analysis

RNA-seq library was prepared using 100ng total RNA by the TruSeq kit (Illumina). The RNA-seq library was prepared using TruSeq kit (Illumina) and the library products were sequenced on an Illumina NextSeq 500 sequencer (25 million clean single-end reads of 75 bp) at Utrecht Sequencing Facility UMC Utrecht. Reads were aligned to Ensembl human genome (GrCh38, v79; http://www.ensembl.org), using STAR aligner with the default parameters [29] and were counted using HTSeq package [30]. Likelihood ratio test (LRT) was performed to obtain differentially expressed genes using the DESeq2 (1.8.2) R/Bioconductor package, and genes with FDR adjusted p-value < 0.05 were considered to be differentially expressed. [31]. The raw read counts were normalized in each sample to count per million (CPM).

DNA methylation analysis

HumanMethylation850-BeadChip-based DNA methylation profiling (Illumina, Inc.) was performed according to the manufacturer's instructions at the GenomeScan (GenomeScan B.V., Leiden, The Netherlands). The CpG data obtained was quality checked and normalized using Beta-mixture quantile normalization (BMIQ) method in ChAMP (version 2.6.0) package [32]. The results of global integration of RNA-seq and DNA methylation are part of another manuscript (manuscript under review).

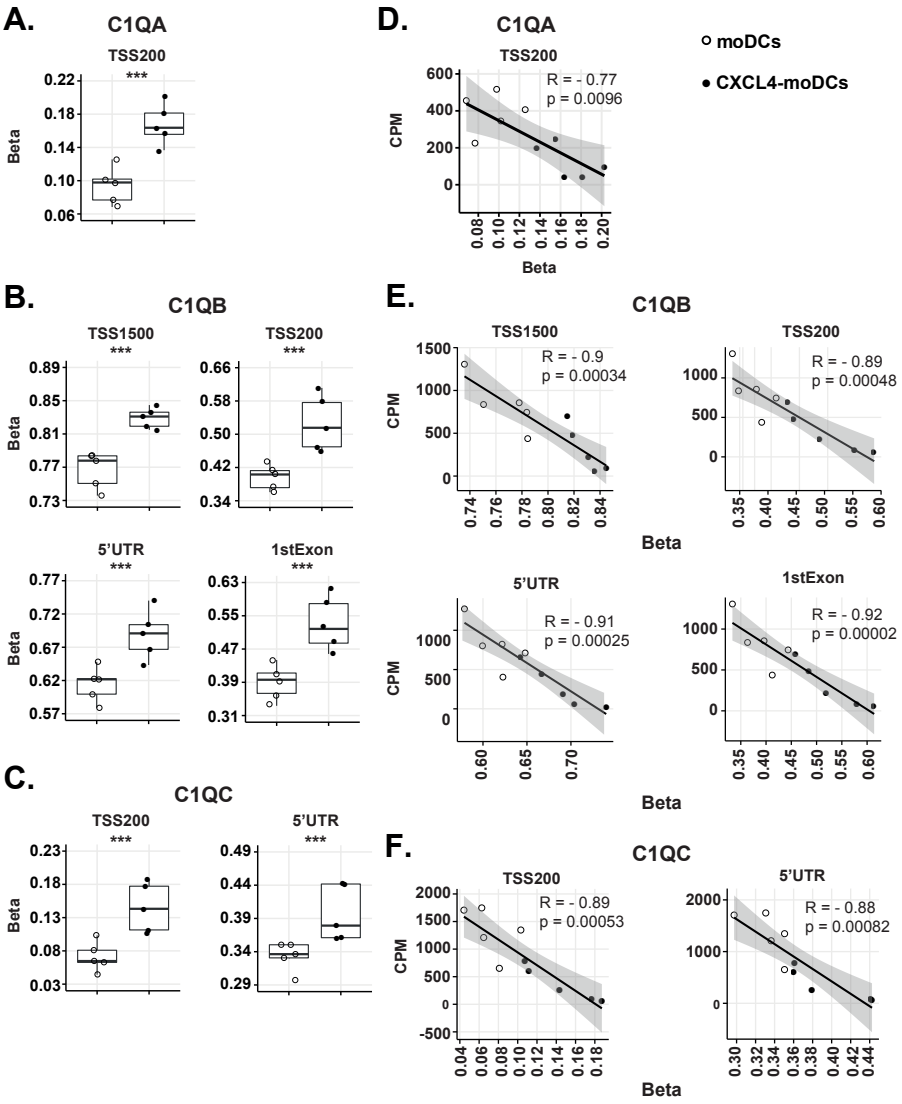

Figure 3. CXCL4 exposure during moDC differentiation associates with strong hypermethylation of C1q. DNA methylation analysis were performed on day 6 of differentiated moDCs and CXCL4-moDCs. (A) DNA methylation analysis between moDCs and CXCL4-moDCs on day 6 of differentiation. (n=5 HV, n=5 per group). Likelihood ratio test. ***$P<0.005$. (B) Correlation between differently methylated (A) *C1QA*, (B) *C1QB,* (C) *C1QC* regions (1500 and 200 bp upstream of the transcription start site (TSS); 5'untranslated region (UTR), and 1st exon) and their corresponding gene expression, respectively. "R" represents Pearson correlation and "p" represents p-value calculated by *t* test. Data shown for 5 HV, all from independent experiments.

Cytokine quantification by ELISA

Secreted C1q was quantified by ELISA accordingly to the manufacturer's instructions (Human C1q ELISA Kit, Cat# E-EL-H0803, Elabscience) and measured on CLARIOstar micro-plate reader (BMG LABTECH) set to 450 nm.

Western blot

Cell lysates were resolved on 4-12% Bis-Tris SDS NuPAGE gels (Invitrogen). After blocking the membranes were probed overnight at 4°C with the Abs for C1q (PA5-29586, Invitrogen) and alpha-tubulin (Sigma, T9026). Membranes were extensively washed and incubated with secondary swine anti-rabbit and goat anti-mouse HRP-conjugated Ab (Dako) for 1 hour at RT. The ratio between the levels of C1q and tubulin were calculated to determine the relative expression of C1q.

Statistical analysis

GraphPad Prism software (version 7) was used for statistical analysis of protein validation. Paired Student *t* test were used and significance was defined as *p*-value ≤ 0.05.

Data availability

RNAseq data has been deposited in NCBI's Gene Expression Omnibus (accession number: GSE115488). DNA methylation data has been deposited in NCBI's Gene Expression Omnibus (accession number: GSE115201).

Acknowledgments

This work was supported by a PhD grant from the Portuguese Fundação para a Ciência e a Tecnologia (SFRH/BD/89643/2012) (to S.C.S.C.); China Scholarship Council (CSC) No.201606300050 (to W.T.); Netherlands Organisation for Scientific Research (NWO) grant number: 016.Veni.178.027 (to A.P); ERC Starting grant, a grant from the Dutch Arthritis Foundation and Pre-Seed grant Dutch Association of Science (NWO) (to T.R.D.J.R.).

References

1. Hubo M, Trinschek B, Kryczanowsky F, Tuettenberg A, Steinbrink K, Jonuleit H. Costimulatory molecules on immunogenic versus tolerogenic human dendritic cells. Front. Immunol. 2013; 4.
2. Schinnerling K, García-González P, Aguillón JC. Gene expression profiling of human monocyte-derived dendritic cells - Searching for molecular regulators of tolerogenicity. Front. Immunol. 2015; 6.
3. Navarro-Barriuso J, Mansilla MJ, Martínez-Cáceres EM. Searching for the transcriptomic signature of immune tolerance induction-biomarkers of safety and functionality for tolerogenic dendritic cells and regulatory macrophages. Front. Immunol. 2018; 9.
4. Gordon JR, Ma Y, Churchman L, Gordon SA, Dawicki W. Regulatory dendritic cells for immunotherapy in immunologic diseases. Front. Immunol. 2014; 5.
5. Zimmer A, Bouley J, Le Mignon M, Pliquet E, Horiot S, Turfkruyer M, Baron-Bodo V, et al. A regulatory dendritic cell signature correlates with the clinical efficacy of allergen-specific sublingual immunotherapy. J. Allergy Clin. Immunol. 2012; 129:1020–1030.
6. Torres-Aguilar H, Aguilar-Ruiz SR, González-Pérez G, Munguía R, Bajaña S, Meraz-Ríos MA, Sánchez-Torres C. Tolerogenic Dendritic Cells Generated with Different Immunosuppressive Cytokines Induce Antigen-Specific Anergy and Regulatory Properties in Memory CD4+ T Cells. J. Immunol. 2010; 184:1765–1775.
7. Ling GS, Crawford G, Buang N, Bartok I, Tian K, Thielens NM, Bally I, et al. C1q restrains autoimmunity and viral infection by regulating CD8+ T cell metabolism. Science 2018; 360:558–563.
8. Schaller M, Bigler C, Danner D, Ditzel HJ, Trendelenburg M. Autoantibodies against C1q in Systemic Lupus Erythematosus Are Antigen-Driven. J. Immunol. 2009; 183:8225–8231.
9. Castellano G, Woltman AM, Nauta AJ, Roos A, Trouw LA, Seelen MA, Schena FP, et al. Maturation of dendritic cells abrogates C1q production in vivo and in vitro. Blood 2004; 103:3813–3820.
10. Colten HR, Perlmutter RC, Schlessinger DH, Cole FS. Regulation of Complement Protein Biosynthesis in Mononuclear Phagocytes. In: ; 2008:141–154.
11. Levine SP, Wohl H. Human platelet factor 4: Purification and Characterization by affinity chromatography. Purification of human platelet factor 4. J. Biol. Chem. 1976; 251:324–328.
12. Maier M, Geiger E V, Henrich D, Bendt C, Wutzler S, Lehnert M, Marzi I. Platelet factor 4 is highly upregulated in dendritic cells after severe trauma. Mol. Med. 2009; 15:384–91.
13. van Bon L, Affandi AJ, Broen J, Christmann RB, Marijnissen RJ, Stawski L, Farina G, et al. Proteome-wide analysis and CXCL4 as a biomarker in systemic sclerosis. N. Engl. J. Med. 2014; 370:433–43.
14. Schaffner A, Rhyn P, Schoedon G, Schaer DJ. Regulated expression of platelet factor 4 in human monocytes--role of PARs as a quantitatively important monocyte activation pathway. J. Leukoc. Biol. 2005; 78:202–9.
15. Lasagni L, Grepin R, Mazzinghi B, Lazzeri E, Meini C, Sagrinati C, Liotta F, et al. PF-4/CXCL4 and CXCL4L1 exhibit distinct subcellular localization and a differentially regulated mechanism of secretion. Blood. 2007; 109:4127–34.
16. Vandercappellen J, Van Damme J, Struyf S. The role of the CXC chemokines platelet factor-4 (CXCL4/PF-4) and its variant (CXCL4L1/PF-4var) in inflammation, angiogenesis and cancer. Cytokine Growth Factor Rev. 2011; 22:1–18.
17. Affandi AJ, Silva-Cardoso SC, Garcia S, Leijten EFA, van Kempen TS, Marut W, van Roon JAG, et al. CXCL4 is a novel inducer of human Th17 cells and correlates with IL-17 and IL-22 in psoriatic arthritis. Eur. J. Immunol. 2018; 48:522–531.

18. Scheuerer B, Ernst M, Dürrbaum-landmann I, Fleischer J, Grage-griebenow E, Brandt E, Flad H-D, et al. The CXC-chemokine platelet factor 4 promotes monocyte survival and induces monocyte differentiation into macrophages. Blood. 2000; 95:1158–1166.
19. Gleissner CA, Shaked I, Little KM, Ley K. CXC Chemokine Ligand 4 Induces a Unique Transcriptome in Monocyte-Derived Macrophages. J. Immunol. 2010; 184:4810–4818.
20. Xia C-Q, Kao K-J. Effect of CXC chemokine platelet factor 4 on differentiation and function of monocyte-derived dendritic cells. Int. Immunol. 2003; 15:1007–1015.
21. Gouwy M, Ruytinx P, Radice E, Claudi F, Van Raemdonck K, Bonecchi R, Locati M, et al. CXCL4 and CXCL4L1 Differentially Affect Monocyte Survival and Dendritic Cell Differentiation and Phagocytosis. PLoS One. 2016; 11:e0166006.
22. Silva-Cardoso SC, Affandi AJ, Spel L, Cossu M, van Roon JAG, Boes M, Radstake TRDJ. CXCL4 Exposure Potentiates TLR-Driven Polarization of Human Monocyte-Derived Dendritic Cells and Increases Stimulation of T Cells. J. Immunol. 2017; 199:253–262.
23. Riepsaame J, van Oudenaren A, den Broeder BJH, van IJcken WFJ, Pothof J, Leenen PJM. MicroRNA-Mediated Down-Regulation of M-CSF Receptor Contributes to Maturation of Mouse Monocyte-Derived Dendritic Cells. Front. Immunol. 2013; 4.
24. Perrier P, Martinez FO, Locati M, Bianchi G, Nebuloni M, Vago G, Bazzoni F, et al. Distinct transcriptional programs activated by interleukin-10 with or without lipopolysaccharide in dendritic cells: induction of the B cell-activating chemokine, CXC chemokine ligand 13. J. Immunol. 2004; 172:7031–42.
25. Ferreira GB, Van Etten E, Lage K, Hansen DA, Moreau Y, Workman CT, Waer M, et al. Proteome analysis demonstrates profound alterations in human dendritic cell nature by TX527, an analogue of vitamin D. Proteomics. 2009; 9:3752–3764.
26. Walport MJ, Davies KA, Botto M. C1q Deficiencies and C1q in Autoimmunity C1q and Systemic Lupus Erythematosus. Immunobiology. 1998; 199:265–285.
27. Botto M, Dell'Agnola C, Bygrave AE, Thompson EM, Cook HT, Petry F, Loos M, et al. Homozygous C1q deficiency causes glomerulonephritis associated with multiple apoptotic bodies. Nat. Genet. 1998; 19:56–59.
28. Wang X, Lei D, Ding J, Liu S, Tao L, Zhang F, Peng J, et al. A DNA-Methylated Sight on Autoimmune Inflammation Network across RA, pSS, and SLE. J. Immunol. Res. 2018; 2018:1–13.
29. Dobin A, Davis CA, Schlesinger F, Drenkow J, Zaleski C, Jha S, Batut P, et al. STAR: Ultrafast universal RNA-seq aligner. Bioinformatics. 2013; 29:15–21.
30. Anders S, Pyl PT, Huber W. HTSeq-A Python framework to work with high-throughput sequencing data. Bioinformatics. 2015; 31:166–169.
31. Love MI, Huber W, Anders S. Moderated estimation of fold change and dispersion for RNA-seq data with DESeq2. Genome Biol. 2014; 15:550.
32. Morris TJ, Butcher LM, Feber A, Teschendorff AE, Chakravarthy AR, Wojdacz TK, Beck S. ChAMP: 450k Chip Analysis Methylation Pipeline. Bioinformatics. 2014; 30:428–430.

Supporting Information

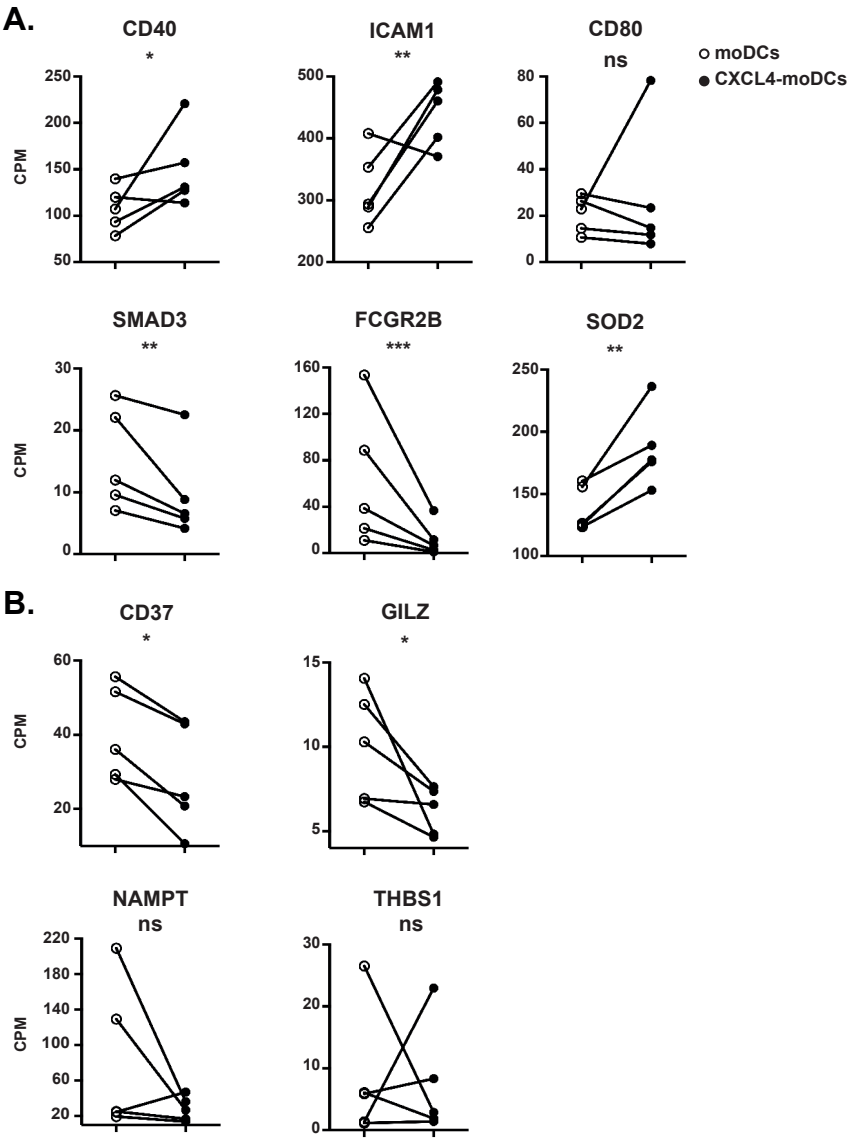

Figure S1. Exposure to CXCL4 during moDC differentiation leads to up-regulation of immunogenic and down-regulation of tolerogenic markers on moDCs. RNA sequencing was performed on day 6 of differentiated moDCs and CXCL4-moDCs. Gene expression analysis of (A) immunogenic and (B) tolerogenic associated molecules in count per million (CPM). Lines connect samples of individual HV; Likelihood ratio test. $^{*}P<0.05$; $^{**}P<0.01$. Data shown for 5 HV, all from independent experiments.

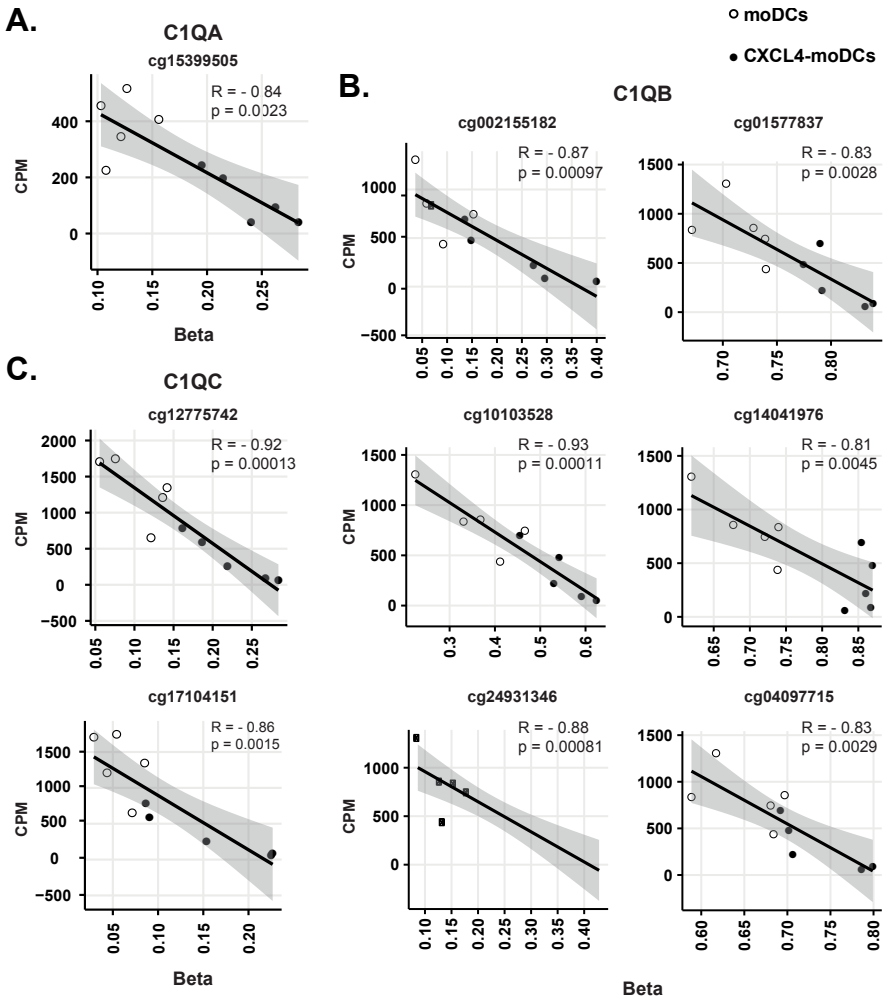

Figure S2. CXCL4 associates with strong hypermethylation of C1q CpGs. RNA sequencing and DNA methylation profiling were performed on day 6 of differentiated moDCs and CXCL4-moDCs. (A) Correlation between differently methylated *C1QA, C1QB, C1QC* CpGs and their corresponding gene expression, respectively**.** "R" represents Pearson correlation and "p" p value calculated by *t* test. Data shown for 5 HV, all from independent experiments.

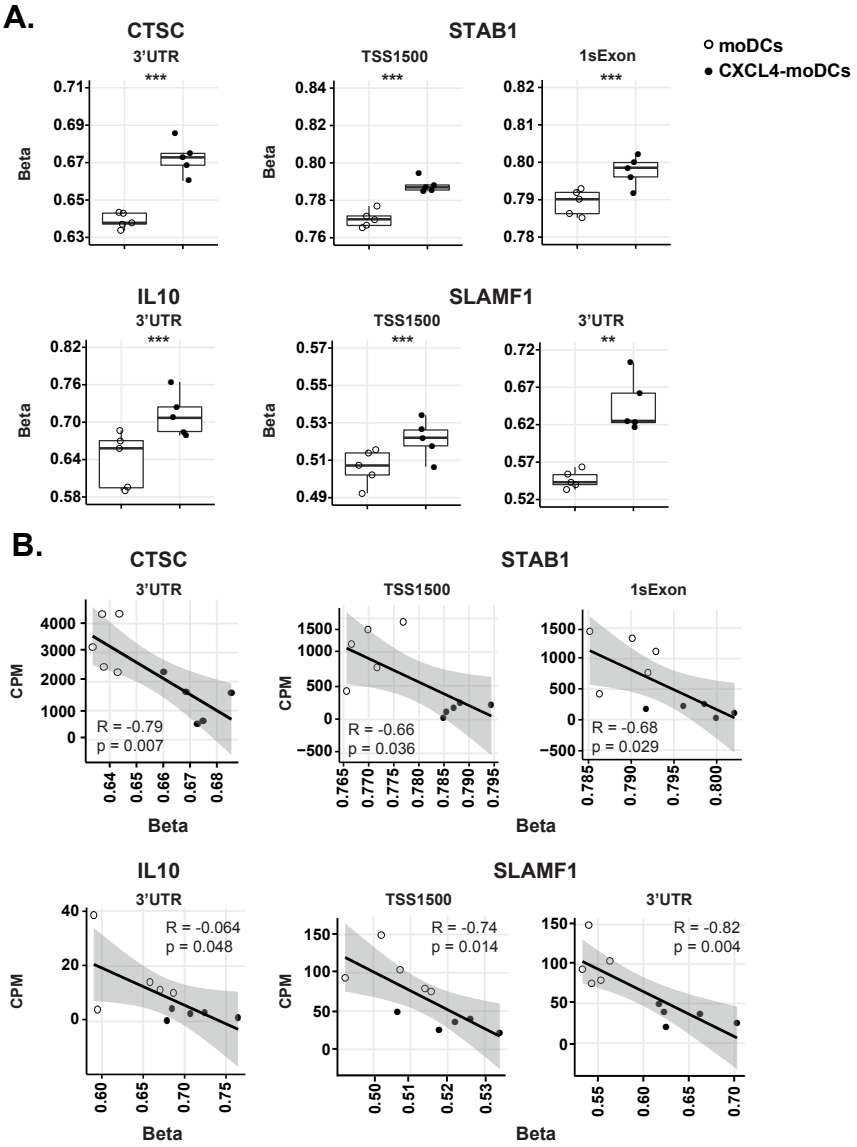

Figure S3. Down-regulation of particular tolerogenic markers by CXCL4 is associated with strong hypermethylation. RNA sequencing and DNA methylation profiling were performed on day 6 of differentiated moDCs and CXCL4-moDCs. (A) DNA methylation levels between moDCs and CXCL4-moDCs. Likelihood ratio test. $^{**}P<0.01$; $^{***}P<0.005$. (B) Correlation between differently methylated regions (1500 upstream of the transcription start site (TSS); 1st exon and 3'UTR) and their corresponding gene expression, respectively. "R" represents Pearson correlation and "p" p value calculated by *t* test. Data shown for 5 HV, all from independent experiments.

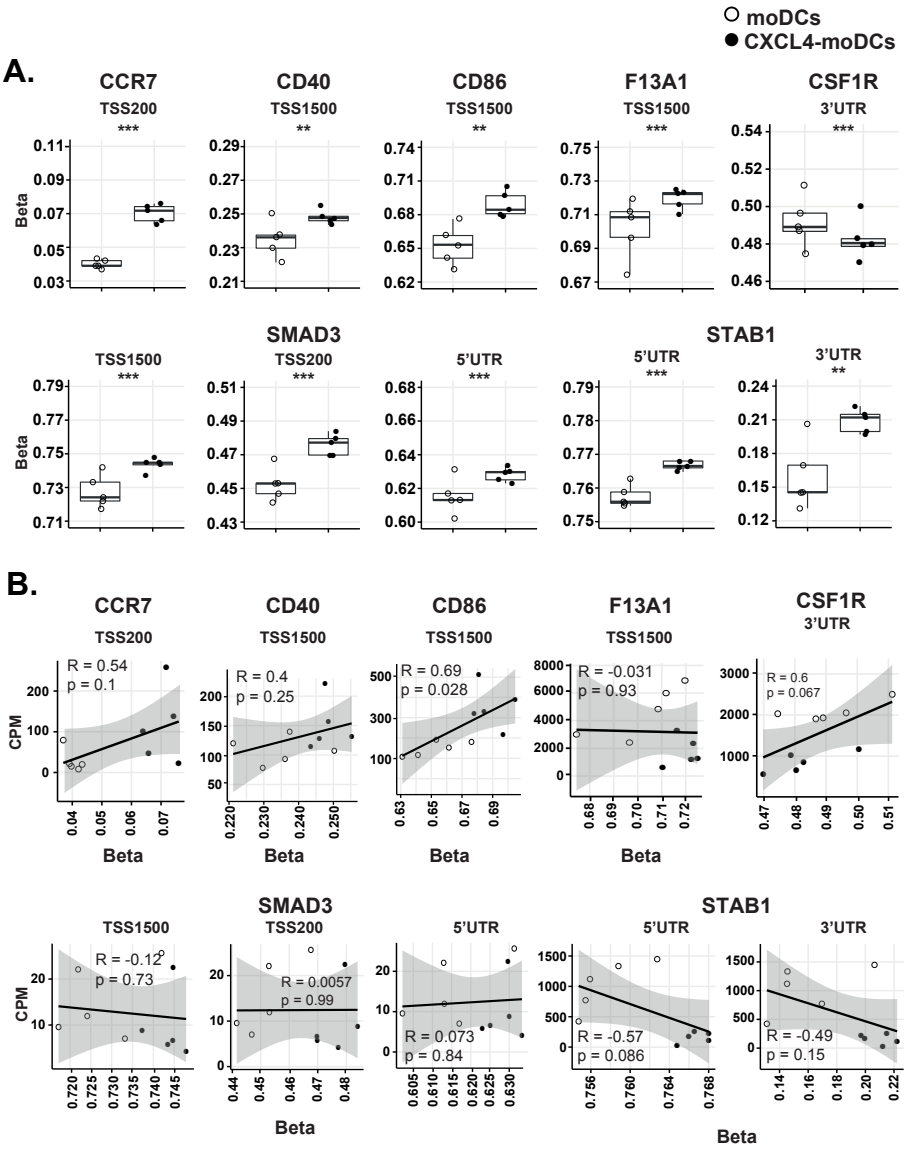

Figure S4. Effects of CXCL4 exposure on DNA methylation of immunogenic and tolerogenic markers. RNA sequencing and DNA methylation profiling were performed on day 6 of differentiated moDCs and CXCL4-moDCs. (A) DNA methylation analysis between moDCs and CXCL4-moDCs. Likelihood ratio test. $^{**}P<0.01$; $^{***}P<0.005$. (B) Correlation between differently methylated regions (1500 upstream of the transcription start site (TSS); 1st exon and 3'UTR) and their corresponding gene expression, respectively. "R" represents Pearson correlation and "p" p value calculated by *t* test. Data shown for 5 HV, all from independent experiments.

Chapter 6

CXCL4 is a driver of cytokine mRNA stability in monocyte-derived dendritic cells

Sandra C. Silva-Cardoso[a,b], Cornelis P.J. Bekker[a,b]; †Marianne Boes[a,c]; Timothy R.D.J. Radstake[a,b,#*]; Chiara Angiolilli[a,b,#]

Affiliations:

[a] Laboratory of Translational Immunology, University Medical Center Utrecht, the Netherlands

[b] Department of Rheumatology & Clinical Immunology, University Medical Center Utrecht, the Netherlands

[c] Department of Pediatrics, University Medical Center Utrecht, the Netherlands

[#] Authors contributed equally

Mol Immunol. 2019; 114:524-534 doi: 10.1016/j.molimm.2019.09.004

Abstract

The chemokine CXCL4 has been implicated in several immune diseases. Exposure of monocyte-derived dendritic cells (moDCs) to CXCL4 potentiates the production of inflammatory cytokines in the presence of TLR3 or TLR7/8 agonists. Here we investigated the transcriptional and post-transcriptional events underlying the augmented inflammatory responses in CXCL4-moDCs. Our results indicate that CXCL4-moDCs display an increased expression and secretion of IL-12, IL-23, IL-6 and TNF upon TLR3 activation. Analysis of the cytokine transcripts for the presence of AU-rich elements (ARE), motifs necessary for ARE-mediated mRNA decay, revealed that all these cytokine transcripts are, at least *in silico*, possibly regulated at the level of mRNA stability. *In vitro* assays confirmed that mRNA stability of *IL6* and *TNF*, but not *IL12B* and *IL23A,* is increased in CXCL4-moDCs. We next screened the expression of ARE-binding proteins (ARE-BPs) and found that TLR stimulation of CXCL4-moDCs induced tristetraprolin (TTP or ZFP36). Increased TTP mRNA expression was found to be a consequence of TTP phospho-mediated inactivation, which over time causes the protein to degrade its own mRNA. Concomitantly with TTP inactivation, we observed increased MAPK p38 signalling, upstream of TTP, in stimulated CXCL4-moDCs. P38 inhibition restored TTP activation and subsequently reduced the production of inflammatory cytokines. Finally, TTP knockdown in moDCs resulted in an increased production of *IL6* and *TNF* after TLR stimulation. Overall, our study shows that the pro-inflammatory phenotype of CXCL4-moDCs relies in part on enhanced cytokine mRNA stability dictated by TTP inactivation.

Keywords: monocyte-derived dendritic cells, CXCL4, cytokines, mRNA stability, TTP

Abbreviations: moDC, monocyte-derived dendritic cells; polyI:C, poly Inosinic-polycytidylic acid; ARE, AU-rich elements; ARE-BPs, ARE-binding proteins

1. Introduction

CXCL4 is a chemokine produced by activated platelets and immune cells involved in pathological conditions such as cancer (Aivado et al., 2007), infections (Schwartzkopff et al., 2009; Srivastava et al., 2008) and inflammatory diseases like systemic sclerosis (SSc), rheumatoid arthritis (RA) and psoriatic arthritis (PsA), among others (Affandi et al., 2018b; Ah Kioon et al., 2018; Patsouras et al., 2015; van Bon et al., 2014; Yeo et al., 2016). CXCL4 plays a determinant role in distinct physiological processes such as in hematopoiesis (Han et al., 1990), angiogenesis (Maione et al., 1990), coagulation (Dehmer et al., 1995) and modulation of immune responses. For instance, exposure of monocytes to CXCL4 prevents apoptosis, induces the production of TNF and reactive oxygen species (ROS) and promotes monocyte differentiation into a unique macrophage-like phenotype (Gleissner et al., 2010; Scheuerer et al., 2000). In addition, we and others have shown that CXCL4 also modulates T-cell activation and regulates both the phenotype and the TLR-mediated innate responses of dendritic cells (DCs) (Affandi et al., 2018b; Fleischer et al., 2002; Fricke et al., 2004; Gouwy et al., 2016; Silva-Cardoso et al., 2017; Xia and Kao, 2003).

DCs are professional antigen-presenting cells (APCs) playing a crucial role in the maintenance of peripheral tolerance and bridging innate and adaptive immune responses. External- and self-dangerous molecules activate DCs downstream inflammatory signalling pathways which, when unresolved, can result in cytokine storm and autoimmunity. Immune regulatory positive and negative feedback mechanisms are therefore crucial to control inflammatory responses, prevent tissue damage and restore immune homeostasis. In DCs, as well as in other immune and non-immune cells, a tight control of inflammation starts at the transcriptional level. However, post-transcriptional regulation of cytokine mRNA stability is a determining factor for final cytokine abundance (Barreau et al., 2005; Stoecklin and Anderson, 2007). In fact, disturbances in mRNA regulatory processes are notoriously associated with pathological manifestations, such as chronic inflammation and cancer (Brooks et al., 2002; Huang et al., 2016; Khabar, 2010; Seko et al., 2006; Zhang et al., 2013).

mRNA decay mediated by adenosine uridine (AU)-rich elements (AREs) is one of the best described mechanisms of mRNA regulation in mammalian cells. ARE motifs are found in the three prime untranslated region (3'UTR) of many short-lived inflammatory and oncogenic mRNAs. AREs conventionally act as mRNA destabilizing factors, however the interaction of AREs with *trans*-acting ARE-binding proteins (ARE-BPs) ultimately determines mRNA degradation or stabilization (Barreau et al., 2005; Carpenter et al., 2014; Stoecklin et al., 2004). Tristetrapolin (TTP or *ZFP36*), TTP family members BRF1 (*ZFP36L1*) and BRF2 (*ZFP36L2*), AU-rich binding factor-1 (AUF1 or *HNRNPD*), KH-type splicing regulatory protein (*KHSRP*), Hu

antigen R (HuR, or *ELAVL1*), T-Cell-Restricted Intracellular Antigen 1 (*TIA1*) and TIA1-related protein (TIAR or *TIAL1*) are examples of well characterized ARE-BPs. Among ARE-BPs, TTP is a critical regulator of DC maturation and DC-mediated activation of T-cell responses (Emmons et al., 2008) and it is implicated in the regulation of inflammatory cytokines, including TNF, IL-6, IL-12 and IL-23 (Brooks and Blackshear, 2013; Bros et al., 2010; Carballo et al., 1998; Molle et al., 2013; Tudor et al., 2009). TTP expression is influenced by transcriptional events, as well as by negative feedback loop mechanisms that lead to TTP mRNA degradation following the interaction of TTP protein with its own mRNA (Kratochvill et al., 2011; Ross et al., 2015; Tiedje et al., 2016). At the same time, TTP is tightly controlled by MAPK signalling pathways, which promote TTP phosphorylation and subsequent inactivation (Brooks and Blackshear, 2013; Kratochvill et al., 2011; Sandler and Stoecklin, 2008). Multiple studies have shown that deregulated expression and activity of TTP are associated with aberrant inflammatory conditions. Mice whose myeloid cells lack TTP manifest exacerbated inflammation in response to LPS exposure and septic shock (Kratochvill et al., 2011; Qiu et al., 2012). Moreover, constitutive TTP knockout mice spontaneously manifest a severe autoimmune syndrome characterized by the erosion of peripheral joints and TNF overproduction, features analogously observed in RA patients (Taylor et al., 1996). Conversely, genetic modifications in mice either enhancing TTP endogenous levels (Patial et al., 2016) or ensuring constitutive TTP activation (Ross et al., 2017) were shown beneficial in dampening inflammation and preventing arthritis progression. While drugs directly reverting TTP activation status are currently unavailable, understanding when and which mRNA stability mechanisms play a role in inflammatory and autoimmune settings is a recent challenge in biomedical research (Patial and Blackshear, 2016; Ross et al., 2017) and a necessary condition for the discovery of new targets aimed at therapeutic intervention.

Earlier studies, inclusive ours, have supported the established association of CXCL4 with inflammation and autoimmunity (Affandi et al., 2018b; Patsouras et al., 2015; van Bon et al., 2014; Yeo et al., 2016). Furthermore, we identified a role of CXCL4 in sensitizing monocyte-derived dendritic cells (moDCs) to aberrant TLR-mediated TNF and IL-12 production (Affandi et al., 2018b; Silva-Cardoso et al., 2017). Here, we investigated whether deregulation of TTP expression and cytokine mRNA stability could underlie the aberrant inflammatory phenotype of CXCL4-moDCs.

2. Materials and Methods

2.1 Monocyte isolation and moDC differentiation

Monocyte isolation and moDC differentiation were performed as described previously (Silva-Cardoso et al., 2017). Peripheral blood mononuclear cells (PBMCs) were isolated from the blood of healthy volunteers that was collected in accordance with institutional ethical approval. After the isolation of PBMCs by density-gradient centrifugation over FicollPaque™ Plus (GE Healthcare), monocytes were purified using anti-CD14 magnetic beads, based on positive isolation by autoMACS Pro Separator-assisted cell sorting (MiltenyiBiotec). For moDC differentiation, monocytes were cultured at a density of $1x10^6$ cells/ml using the medium RPMI 1640 with GlutaMAX (Life Technologies), supplemented with 10% (v/v) heat-inactivated FCS (Biowest) and 1% (v/v) antibiotics (penicillin and streptomycin) (both form Life Technologies), for 6 days at 37ºC in the presence of 5% CO_2. Recombinant human IL-4 (500 U/ml; R&D**)** and GM-CSF (800 U/ml; R&D) were added to the medium on day 0 and day 3. Recombinant human CXCL4 (10 µg/ml; PeproTech) was added on day 0 and day 3 to differentiate CXCL4-moDCs.

2.2 moDC treatment and stimulation

After the differentiation of moDCs and CXCL4-moDCs, cells were left overnight in medium supplemented with FCS and antibiotics. When indicated, cells were pre-treated or not with 10µM p38 inhibitor (SB202190; Sigma-Aldrich), MEK1/2-ERK inhibitor (U0126; Calbiochem) and JNK inhibitor (SP600125; Bio Connect) 30 minutes prior to stimulation with polyI:C (25ug/ml; Invitrogen) for 2 or 8 hours.

For mRNA stability analysis, moDCs and CXCL4-moDCs were stimulated with polyI:C for 2 hours, followed by actinomycin D (ActD) (5ug/ml; Sigma-Aldrich) treatment. Cells were harvested at 0, 2, 4 and 6 hours after treatment.

2.3 RNA purification and real-time quantitative PCR

RNA was purified using the RNeasy Micro Kit (Qiagen) and reverse-transcribed with SuperScript® Reverse Transcriptase Kit (Invitrogen) according to the manufacturer's protocols. Real-Time quantitative-PCRs (RT-qPCR) were performed on the QuantStudio 12k flex system using SYBR Select Master Mix (Life Technologies). For each time point analysed, the difference between the expression of a gene of interest and housekeeping gene (*RPL32*) was calculated by using either the $2^{-\Delta Ct}$ or the $2^{-\Delta\Delta Ct}$ methods. Sequences of the primers are listed in Table 1.

Table 1. Sequences of primers used for qPCR analysis.

Gene	Forward primer	Reverse primer
RPL32	AGGGTTCGTAGAAGATTCAAGG	GGAAACATTGTGAGCGATCTC
IL12B	TGCCGTTCACAAGCTCAAGT	TGGGTCAGGTTTGATGATGTCC
PT IL12B	TCATCTGCCGCAAAAATGCC	TTTGAGGGCCTGCTCACCTA
IL23A	CAACAGTCAGTTCTGCTTGC	GAAGGCTCCCCTGTGAAAAT
PT IL23A	AGCCTTCTCTGCTCCCTGATA	ATCCTCCACGCCCCTACTT
TNF	CCCATGTTGTAGCAAACCCT	TGAGGTACAGGCCCTCTGAT
PT TNF	TCAGGATCATCTTCTCGAACC	GAGTCCTTCTCACATTGTCTC
IL6	GACAGCCACTCACCTCTTCA	CCTCTTTGCTGCTTTCACAC
PT IL6	ACATCCTCGACGGCATCTCAG	CCCAGCAAAGACCTCCTAATG
AUF1	TTTGTTGGTGGCCTTTCTCC	ATTCCACCTCACCAAAACCAC
BRF1	ATGCAAGGGTAACAAGATGCTC	CACTGCCTTTCTGTCCAGC
BRF2	TCCAGAAACATGTCGACCAC	AGGGATTTCTCTGTCTTGCAC
KHSRP	CTTACAAAGTGCAGCAAGCC	AGATCCGTACTCATTCCGGT
HuR	AAGCCTGTTCAGCAGCATTG	CCAAGCTGTGTCCTGCTACT
TIAL1	GGAGTAGATCAATCACCTTCTGCTG	ATCCGGCTTGGTTAGGAGGA
TIA1	GATGCCCGAGTGGTAAAAGAC	CCCATCTGTTGAATGGCGTTT
TTP	CTGCCATCTACGAGAGCCT	ACTCAGTCCCTCCATGGTC
PT TTP	GCCATCTACGAGGTGAGTCC	AGTTTGCGGCGCTAGAGAG

2.4 Primers design

Primers were designed with Primer-BLAST (Ye et al., 2012). FASTA sequences retrieved from GRCh38 Primary Assembly (TNF, NC_000006.12; IL6, NC_000007.14; IL12B NC_000005.10; IL23A, NC_000012.12; TTP, NC_000019.10) were used as template for the design of primers recognizing primary transcripts. FASTA sequences from protein-coding transcripts (IL6, NM_000600.5; TNF, NM_000594.4; IL12B, NM_002187.2; IL23A NM_016584.3; TTP, NM_003407.4) were used as template for the design of primers recognizing mature mRNA.

2.5 Cytokine quantification by Luminex

Supernatants were collected after 8 hours stimulation with polyI:C and cytokine measurements were assessed by Luminex technology as described before (de Jager et al., 2005) at the MultiPlex Core Facility of the Laboratory of Translational Immunology in the University Medical Center of Utrecht.

2.6 Western blot

MoDCs and CXCL4-moDCs were left unstimulated or stimulated with polyI:C (25ug/ml) for 15 minutes, 30 minutes, 1 or 2 hours. When indicated, prior to stimulation, cells were pre-treated with the p38 inhibitor SB202190. Cells were lysed in Laemmli's buffer and protein concentration was quantified using a BCA Protein Assay Kit (Pierce, Thermo Scientific) according to the manufacture's protocol. Equal amounts of protein lysate were mixed with loading buffer and boiled at 95°C for 5 minutes, and separated by electrophoresis on a 4-12% Bis-Tris SDS NuPAGE gels (Invitrogen). Alternatively, samples were ran on 10% SDS-PAGE gels for 5 hours at constant 70 V for better separation of immune-reactive bands ranging between 26 and 55 kDa. Gels were transferred to a PVDF membrane (Millipore). The membranes were blocked with Tris-buffered saline (pH 8) containing 0.05% Tween-20 and 4% milk (Bio-Rad) for 1 hour at room temperature (RT) and probed overnight at 4°C with antibodies for total p38 and phospho-p38; ERK and phospho-ERK; TTP and histone 3 (H3) (all from Cell signaling) or tubulin (Sigma-Aldrich). After washing, membranes were incubated for 1 hour at RT with the secondary anti-rabbit HRP-conjugated Ab (Dako). Protein detection was assessed using a ChemiDoc MP System (Bio-Rad). For protein visualization and densitometry analysis, the Image Lab software (version 5.1, Bio-Rad) was used. The ratio between the levels of the protein of interest and H3 or tubulin was calculated to determine relative expression.

2.7 Lambda phosphatase treatment

CXCL4-moDCs were lysed in non-denaturing lysis buffer (10mM Tris HCl pH 8.0, 10mM NaCl, 1% NP-40). Protein lysates were supplemented with 10X NEBuffer for Protein MetalloPhosphatases (PMP) and 10 mM MnCl2 (New England Biolabs). Cell lysates were incubated on ice for 30 min, after which supernatants were centrifuged at 4 °C for 10 min (10.000g) and collected. Supernatants were incubated with 1000 units of lambda (λ) phosphatase (New England Biolabs) at 30 °C for 30 min, after which loading buffer was added to the protein lysate. Samples were boiled at 95 °C for 5 min, and further processed for immunoblotting as described above.

2.8 siRNA transfection

On day 6 of differentiation, moDCs were transfected for 4 hours with 20nM control non-targeting siRNA (siCtrl) or specific siRNA targeting TTP (siTTP), using DharmaFECT1 (all from Dharmacon). Transfection reagents were replaced with complete cell culture medium, and cells were left resting overnight. Cells were stimulated with polyI:C for 8 hours for gene expression analysis.

2.9 Analysis of AU rich motifs

3'UTR sequences for *IL-12B* (ENST00000231228.2), *IL-23A* (ENST00000228534.5), *IL-6* (ENST00000404625.5) and *TNF* (ENST00000449264.2) were retrieved from UCSC Genome Browser. ARE sequences in the 3'UTR of the same transcripts were obtained from AREsite2 database (Fallmann et al., 2016) and mapped by making use of a customized C# application made with Unity3D which identifies specific ARE sequences in the 3'UTR and outputs an image assigning different colours to the ARE family motifs.

3.0 Statistical analysis

Data analyses and graphs were performed using GraphPad Prism software (version 7). Data are represented as mean ±SD. To compare two groups the paired *t* test was used or one-way analysis of variance (ANOVA) was applied when more than two groups were compared. The significance was defined as $p \leq 0.05$. Statistical significance indicated as * for $p<0.05$; ** for $p<0.01$; *** for $p<0.001$; **** for $p<0.00013$.

Results

3.1 Cytokines induced in CXCL4-moDCs display ARE sequences in their 3'UTR

Previously, we have shown that exposure of moDCs to CXCL4 (CXCL4-moDCs) during differentiation results in aberrant IL-12 and TNF production after TLR3 (polyI:C) and TLR7/8 (CL075 and R848) triggering (Silva-Cardoso et al., 2017). In this study we used the same cell culture model to differentiate moDCs in the presence of CXCL4 for 6 days, and further stimulated the cells for 8 hours with polyI:C. We confirmed that stimulated CXCL4-moDCs secrete increased levels of IL-12 and TNF in comparison to moDCs, and additionally found that IL-6 and IL-23 are also strongly produced by CXCL4-moDCs (Fig.1A). No differences in the expression of these inflammatory cytokines were found between unstimulated moDCs and CXCL4-moDCs (Supplementary Fig S1). As these inflammatory cytokines have been reported to be regulated at the level of mRNA stability (Carballo et al., 1998; Molle et al., 2013; Tudor et al., 2009), we screened the 3'UTR regions of their transcripts for the presence of AU-rich motifs, which constitute necessary sites for ARE-mediated mRNA decay (Fig.1B) (Fallmann et al., 2016). All cytokine transcripts displayed at least one AUUUA pentamer and one WWWUUUWWW nonamer motif, preferential binding sites for ARE-BPs (Fig.1C-D) (Barreau et al., 2005; Kratochvill et al., 2011). Thus, based on the presence of ARE motifs, we hypothesized that the mRNA of these cytokines could be stabilized in stimulated CXCL4-moDCs.

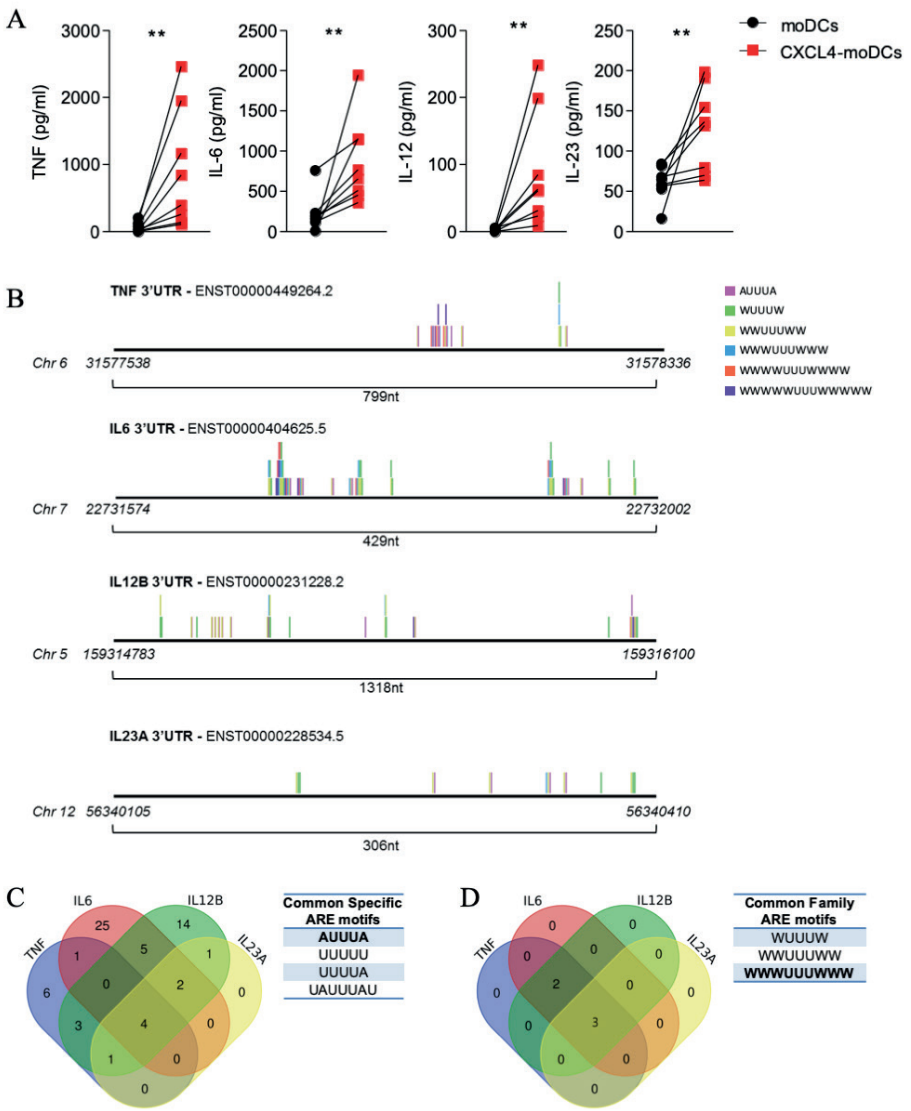

Figure 1. Cytokines induced in CXCL4-moDCs display enriched ARE sequences. (A) Monocyte-derived dendritic cells (moDCs) were differentiated in the absence or presence of CXCL4 (CXCL4-moDCs) for 6 days. Cytokine production was measured by Luminex after 8 hours stimulation with polyI:C. Lines connect individual donors. (N=8); Wilcoxon matched-pairs signed rank test. (B) ARE sequences in *IL12B*, *IL23A*, *IL6* and *TNF* protein-coding transcripts were obtained from AREsite2 database and mapped in the 3'UTR of the respective transcripts. In the figure, specific ARE sequences are illustrated and coloured based on their belonging to defined ARE family motifs. W indicates either A (adenine) or U (uracil) nucleotide. (C-D) Specific AREs (C) and family ARE motifs (D) retrieved from (B) were overlapped in Venn-Diagram, and common sequences are shown in the table.

3.2 Enhanced cytokine production by CXCL4-moDCs relies on both transcriptional and post-transcriptional regulation

Given the presence of ARE motifs in *IL6*, *TNF*, *IL12B* and *IL23A* transcripts, we next hypothesized that the protein induction observed in stimulated CXCL4-moDCs would be a consequence of post-transcriptional, rather than transcriptional, regulation. To test our hypothesis, we designed primers specifically recognizing the unspliced 'primary' transcript or the spliced 'mature' transcript of all 4 cytokines (Fig.2A and Supplementary Fig S2). In fact, while primary transcript expression reflects transcriptional regulation, the expression of mature transcripts is sensitive to mRNA degradation (Scherrer, 2018). Analyses of the mature/primary ratios revealed that the mature transcript expression of *IL6* and *TNF*, but not *IL-12B* and *IL-23A,* was significantly higher in stimulated CXCL4-moDCs at early time points (Fig.2A and Supplementary Fig S3A), suggesting mRNA stabilization of *IL6* and *TNF* transcripts. In order to validate these results, we made use of an alternative assay using actinomycin D (ActD), a transcriptional inhibitor, to determine mRNA stability. In line with previous reports (Loupasakis et al., 2017; Paschoud et al., 2006), the mRNA of *IL-6* and *TNF* quickly decayed after 2 hours ActD treatment. However, in CXCL4-moDCs, *IL6* and *TNF* transcripts retained higher stability at later time points (4 and 6 hours ActD treatment) in comparison to conventional moDCs (Fig.2B). The expression of *IL12B* and *IL23A* was intrinsically stable, in agreement with previous studies (O'Neil et al., 2017) and showed slow mRNA decay rates in both moDCs and CXCL4-moDCs (Fig.2B and Supplementary Fig S3B). These results indicate that stimulated CXCL4-moDCs display an enhanced production of IL-6 and TNF, which is explained by their post-transcriptional regulation (enhanced mRNA stability). On the contrary, the increased expression of IL-12 and IL-23 observed in these cells is dependent on transcriptional regulatory mechanisms.

3.3 TTP expression and activity are altered in CXCL4-moDCs

Several ARE-BPs have been shown to play a crucial role on mRNA stability regulation. Thus, we analysed the expression of well characterized ARE-BPs retaining either destabilizing or stabilizing properties (Carpenter et al., 2014). We found a strong induction of TTP mature transcript expression by CXCL4-moDCs after 2 hours stimulation with polyI:C, in comparison to conventional moDCs (Fig.3A). No differences were found for all the other analysed ARE-BPs (BRF1, BRF2, AUF1, KHSRP, TIA, TIAL1 and HuR) (Fig.3A). We confirmed that TTP was induced at the protein level in polyI:C stimulated CXCL4-moDCs (Fig.3B). However, given the mRNA-degrading properties of this ARE-BP, we hypothesized that the increased TTP expression observed by Western blot would be a consequence of TTP phosphorylation. In fact, MAPK-induced TTP phosphorylation, besides making TTP protein inactive,

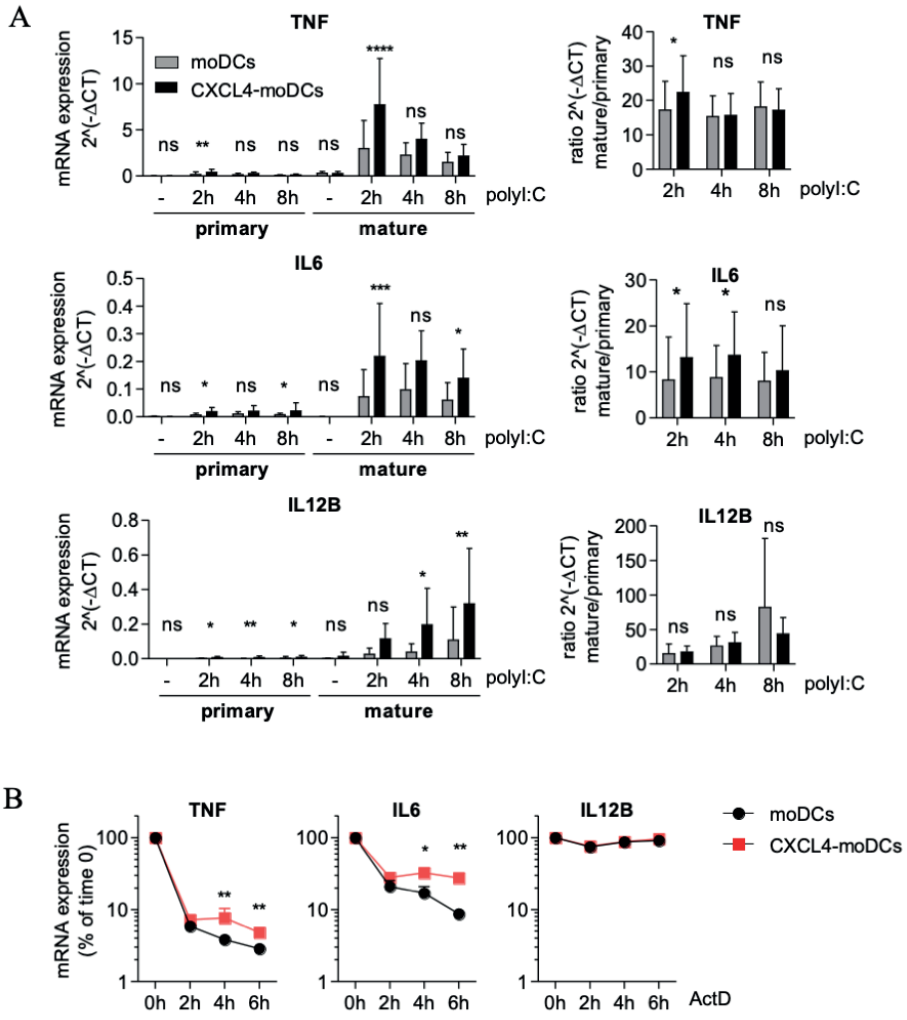

Figure 2. Increased cytokine production by CXCL4-moDCs relies on both transcriptional and post-transcriptional regulation. (A) Primers for *IL6*, *TNF* and *IL12B* were designed in a way to amplify either intron-exon regions or exon-exon regions, allowing the detection of primary and mature transcripts, respectively. MoDCs and CXCL4-moDCs were left unstimulated (-) or stimulated for 2, 4 and 8 hours with polyI:C. Gene expression of primary and mature transcripts of inflammatory cytokines is represented as relative expression levels for both primary and mature transcripts (2^-ΔCT), while ratios were calculated according to the formula: 2^-ΔCT mature transcript/2^-ΔCT primary transcript. (N=8); One-way ANOVA followed by Fisher's LSD test. (B) MoDCs and CXCL4 moDCs were stimulated with polyI:C for 2 hours, and further treated with actinomycin D (ActD) for the indicated time points, followed by gene expression analysis. (N=10); Wilcoxon matched-pairs signed rank test.

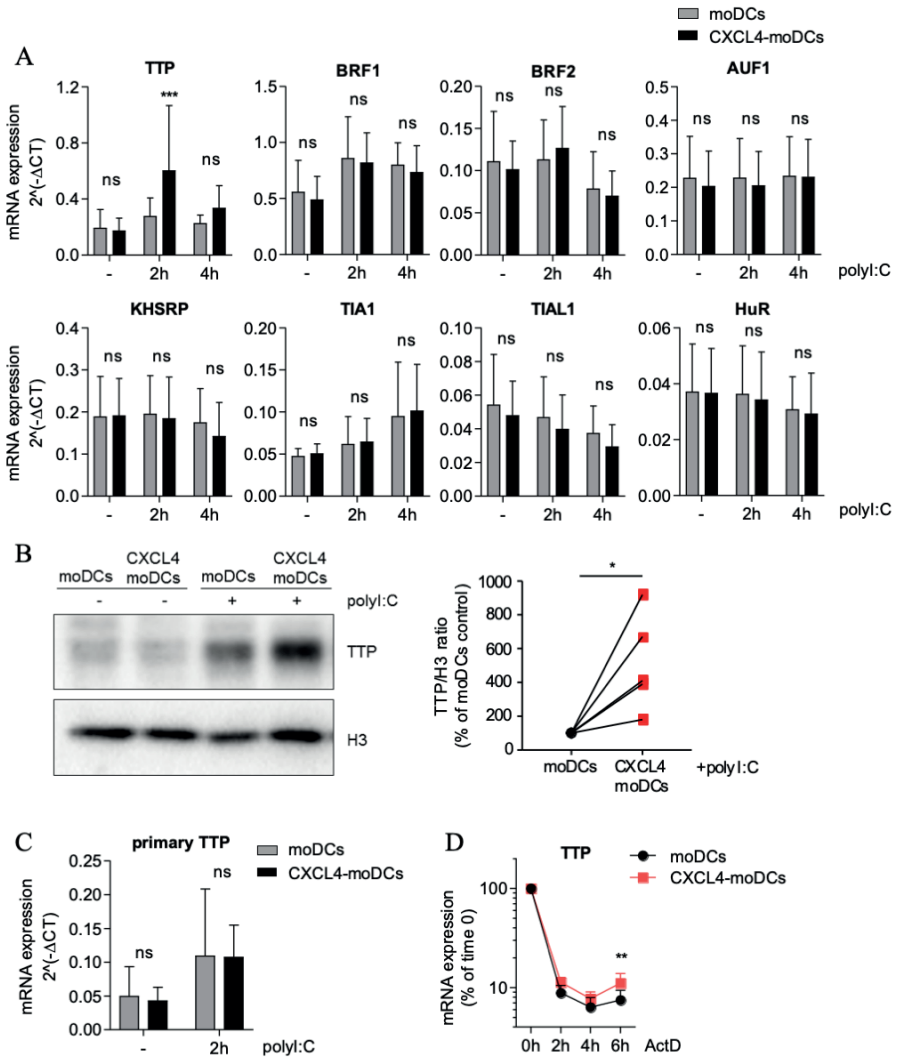

Figure 3. TTP expression and activity are altered in CXCL4-moDCs. (A) MoDCs and CXCL4-moDCs were stimulated with polyI:C for the indicated time points and ARE-BPs expression was analysed by qPCR. Data are represented as relative expression levels. (N=9); One-way ANOVA followed by Fisher's LSD test (B) TTP protein induction was analysed by Western blot after stimulating moDCs and CXCL4-moDCs for 2 hours with polyI:C. Densitometry analysis indicates the signal intensity of TTP expression normalized to control Histone 3 (H3). Lines connect individual donors. (N=5); Paired *t* test. (C) TTP primary transcript expression upon 2 hours stimulation with polyI:C was analysed by qPCR. (N=6); One-way ANOVA followed by Fisher's LSD test (D) MoDCs and CXCL4-moDCs were stimulated with polyI:C for 2 hours. Cells were treated with ActD for the indicated time points and TTP mature transcript was analysed by qPCR. (N=10); Wilcoxon matched-pairs signed rank test.

also prevents it from being processed for proteasomal degradation (Brooks and Blackshear, 2013; Deleault et al., 2008). Improved resolving for TTP protein by Western Blot allowed the identification of two immune-reactive bands of to 45 and 47 kDa (Angiolilli et al., 2018a). ActD treatment inhibited de novo TTP protein synthesis, leading to the reduction of the lower immune-reactive band, but it did not affect the higher phosphorylated band (Supplementary Fig S4A). Furthermore, treatment of the protein lysates with lamda phosphatase (λ-phosphatase) reduced the expression of the higher, but not the lower, band (Supplementary Fig S4B). In line with these results, and provided that active TTP destabilizes its own mRNA (Patial et al., 2016), we found that the induced TTP mRNA expression observed in stimulated CXCL4-moDCs was a consequence of increased TTP mRNA stability (Fig.3D), but not transcription (Fig.3C). Overall, our findings indicate that the increased mRNA expression of TTP in stimulated CXCL4-moDCs reflects TTP phospho-mediated inactivation.

3.4 Aberrant cytokine production by CXCL4-moDCs is dependent on MAPK p38 activation

TTP phosphorylation and consequent inactivation is a result of MAPK p38 activation upon inflammatory triggering (Carballo et al., 2001; Mahtani et al., 2001; Stoecklin et al., 2004; Tudor et al., 2009). Thus, we investigated whether stimulated CXCL4-moDCs would also display a perturbed MAPK signalling as compared to moDCs. We found that stimulation of CXCL4-moDCs with polyI:C for 30 and 60 minutes was followed by an increased phosphorylation of p38 (Fig.4A). Treatment of CXCL4-moDCs with p38 inhibitor (p38i) SB202190 prior to polyI:C stimulation significantly reduced the protein expression of IL-6 and TNF, but also IL-12 and IL-23 (Fig.4B). However, while affecting mature *IL6* and *TNF* expression, p38i effects on IL-12 and IL-23 production were mostly linked to the suppression of their primary transcripts, as the mature/primary ratio of *IL12B* and *IL23A* expression was not significantly altered by p38i treatment (Fig.4C and Supplementary Fig S5). Furthermore, while MEK/ERK, but not JNK, inhibition also resulted in a modest suppression of IL-6 and TNF production (Supplementary Fig S6A-B), ERK signalling was not found potentiated in stimulated CXCL4-moDCs (Supplementary Fig S6C). Overall, these results suggest that p38 is the predominant MAPK driving inflammatory activation in stimulated CXCL4-moDCs and that p38 inhibition uniformly reduces cytokine expression. However the mechanisms underlying p38i effects could be dependent on either control of cytokine mRNA stability (in case of *IL6* and *TNF*) or transcriptional regulation (in case of *IL12B* and *IL23A*).

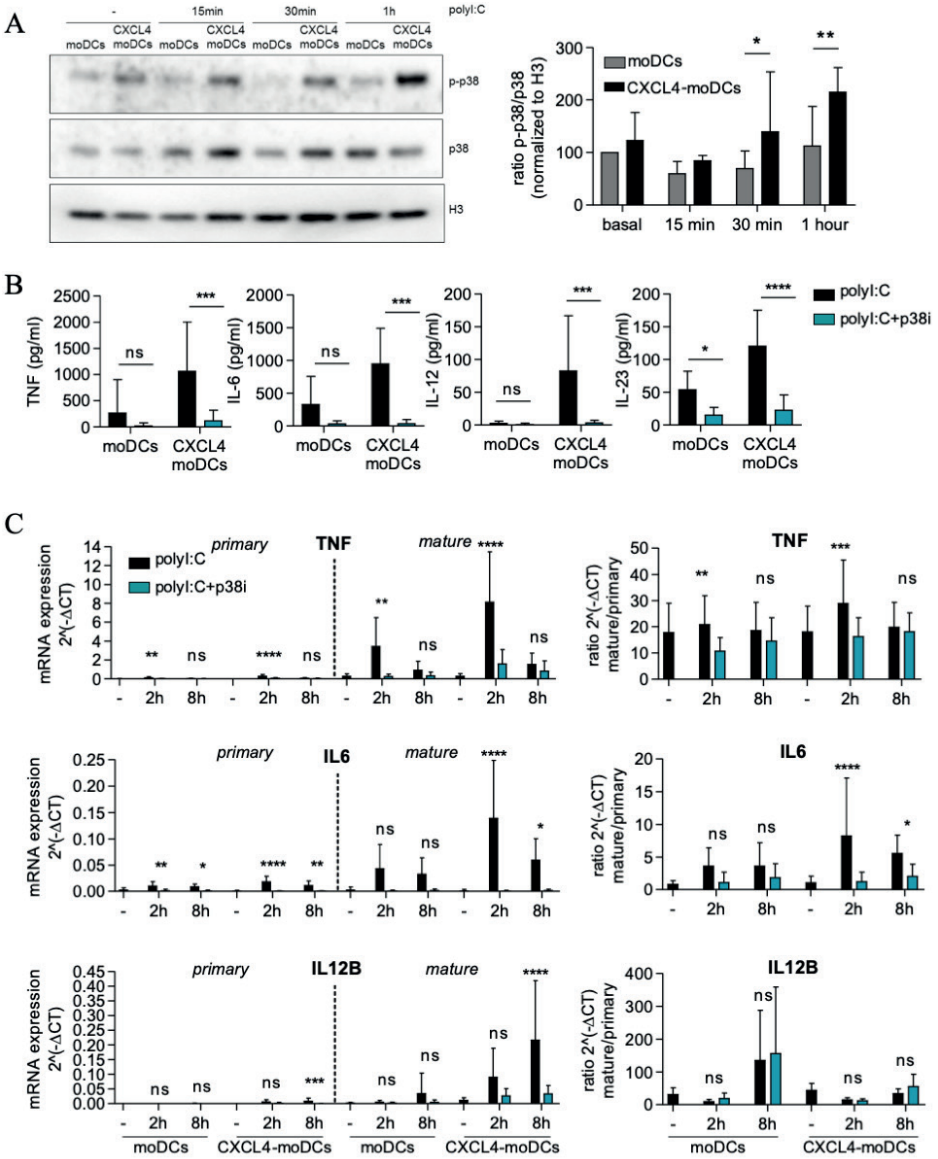

Figure 4. Amplified activation of MAPK p38 in CXCL4-moDCs contributes to increased cytokine production.

(A) MoDCs and CXCL4-moDCs were stimulated with polyI:C for the indicated time points. Phosphorylated p38 (p-p38), total p38 (p38) and H3 expression were measured by Western blot. Densitometry analysis indicates the signal intensity of p-p38/p38 ratio normalized to control H3. (N=5); One-way ANOVA followed by Fisher's LSD test (B) Prior to polyI:C stimulation for 8 hours, moDCs and CXCL4-moDCs were pre-treated with the p38 inhibitor SB202190 and cytokine production was measured by Luminex. (N=9); One-way ANOVA followed by Fisher's LSD test (C) Cells were pre-treated as in (B), further stimulated for 2 and 8 hours with polyI:C and processed for qPCR analysis. Gene expression of primary and mature transcripts of inflammatory cytokines is represented as relative expression levels for both primary and mature transcripts (2^-ΔCT), while ratios were calculated according to the formula: 2^-ΔCT mature transcript/2^-ΔCT primary transcript. (N=6); One-way ANOVA followed by Fisher's LSD test.

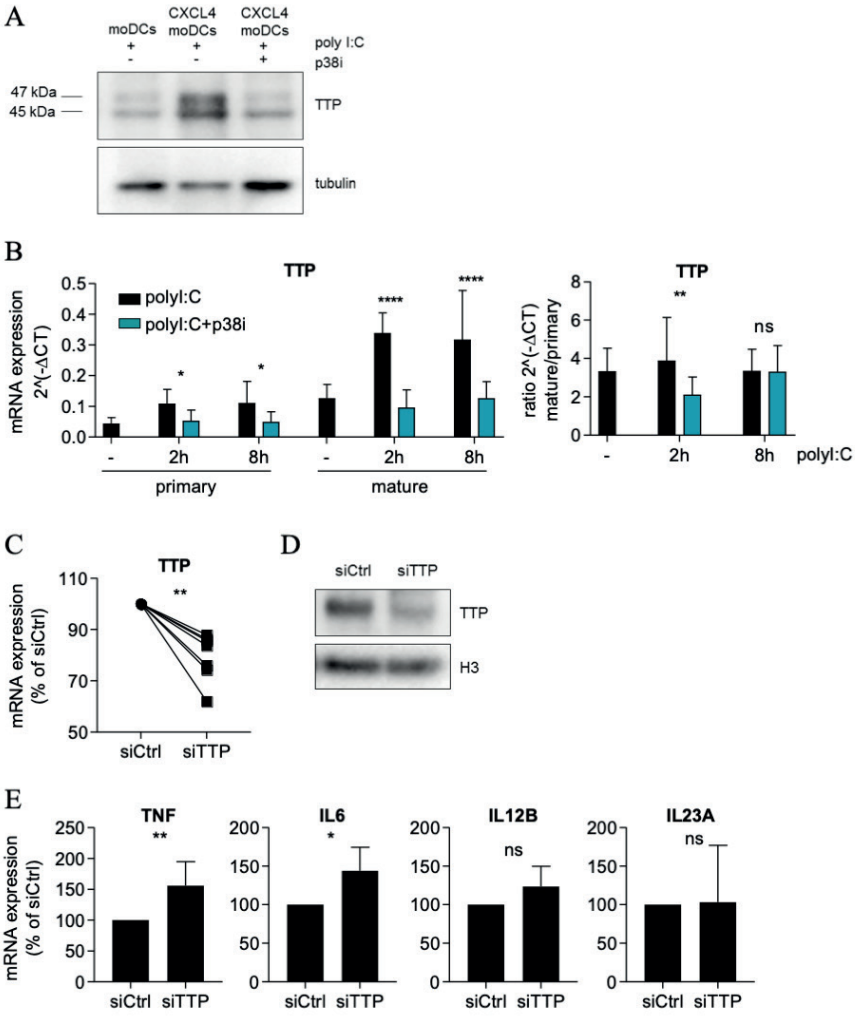

Figure 5. Suppression of TTP activity or expression leads to increased cytokine production. (A) Prior to polyI:C stimulation for 2 hours, CXCL4-moDCs were pre-treated or not with the p38i SB202190. TTP and Tubulin expression were measured by Western blot. (N=3). (B) Cells were pre-treated as in (A) and stimulated for 2 and 8 hours with polyI:C. TTP primary and mature transcripts were analysed by qPCR. Data are represented as relative expression levels for both primary and mature TTP transcripts (2^-ΔCT), while ratio is calculated as 2^-ΔCT mature transcript/ 2^-ΔCT primary transcript. (N=6); One-way ANOVA followed by Fisher's LSD test (C-E) moDCs were transfected with either control non-targeting siRNA (siCtrl) or with specific siRNA targeting TTP (siTTP). In (C), knockdown efficiency was determined by qPCR. Data are represented as fold change mRNA expression compared to siCtrl condition. (N=7); Paired *t* test. In (D), transfected moDCs were stimulated with polyI:C for 2 hours, and knockdown efficiency was confirmed by Western blot. (N=4). In (E), transfected moDCs were stimulated with polyI:C for 8 hours and cytokine expression was analysed by qPCR. (N=6) Paired *t* test.

3.5 Suppression of TTP expression or activity leads to increased cytokine production.

To further assess the phosphorylation status of TTP in CXCL4-moDCs, we pre-treated cells with p38i before stimulation with polyI:C. In the presence of p38 inhibitor, the higher immune-reactive band corresponding to phosphorylated TTP was reduced in CXCL4-moDCs (Fig.5A). As expected, treatment with p38i led to decreased TTP mature transcript after 2 hours polyI:C stimulation (Fig.5B), a possible consequence of the restored TTP activity which also causes TTP mRNA degradation. Conversely, neither ERK or JNK inhibition reduced TTP expression (Supplementary Fig S7). These results suggest that, in CXCL4-moDCs, polyI:C stimulation mediates the aberrant activation of MAPK p38 signalling and the inactivation of TTP, the latter contributing to the increase mRNA stability of inflammatory cytokines. Interference of this pathway by the use of a p38i leads to restored activation of TTP function and consequent cytokine and TTP mRNA degradation. To further confirm the role of TTP on the regulation of cytokine production by moDCs, we performed TTP silencing by siRNA. TTP knockdown was confirmed at the mRNA (Fig.5C) and protein level (Fig.5D). While not reporting changes in cell viability after TTP silencing (Supplementary Fig S8), we observed that *IL6* and *TNF* mRNA expression was boosted in TTP knockout moDCs upon polyI:C stimulation (Fig.5E). In contrast, the expression of *IL-12B* and *IL-23A* was not significantly affected after TTP silencing. Altogether, our results indicate that *TNF* and *IL6* expression in CXCL4-moDCs is regulated at the post-transcriptional level and relies on TTP inactivation.

4. Discussion

CXCL4 is a chemokine which is massively released by activated platelets, as well as immune cells, under pathological conditions (Affandi et al., 2018a; Angiolilli et al., 2018b; Fox et al., 2018). Increased levels of CXCL4 were detected in individuals with chronic autoimmune diseases, both in circulation and at the site of inflammation (Affandi et al., 2018b; Patsouras et al., 2015; van Bon et al., 2014; Yeo et al., 2016). Furthermore, we and others have previously shown that during the differentiation of monocytes into DCs (moDCs) the prolonged exposure to CXCL4, a condition that mimics chronic inflammatory status, is able to significantly affect DCs phenotype and activation (Fricke et al., 2004; Silva-Cardoso et al., 2017; Xia and Kao, 2003). Specifically, we reported that CXCL4-moDCs produce higher levels of TNF and IL-12 cytokines after stimulation with polyI:C, a TLR3 agonist (Silva-Cardoso et al., 2017).. Here we show that IL-6 and IL-23, two cytokines notoriously produced by DCs and playing a central role in autoimmune conditions (Abdel-Magied et al., 2016; Komura

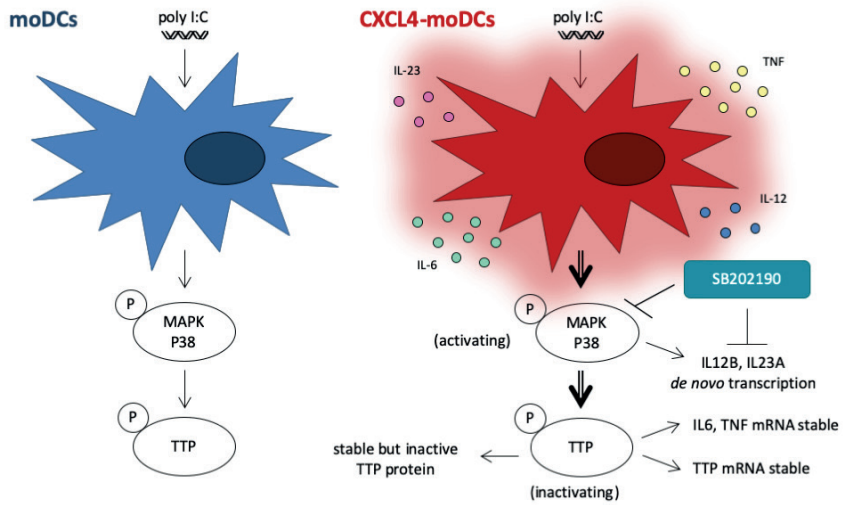

Figure 6. Schematic overview of proposed mechanism.
Conventional monocyte differentiation in the presence of IL-4 and GM-CSF generates monocyte-derived dendritic cells (moDCs). In our study we added CXCL4 during moDCs differentiation to generate CXCL4-moDCs. Compared to conventional moDCs, polyI:C stimulation of CXCL4-moDCs leads to abnormal phospho(P)-mediated activation of MAPK p38 signalling, which in turn mediates the phospho-mediated inactivation of TTP. When inactive, TTP does not degrade its target mRNAs, including its own mRNA. In our study we observe that the expression of *IL6* and *TNF* transcripts is increased in moDCs lacking TTP, a model mimicking TTP inactivation observed in CXCL4-moDCs. In line with this model, p38 inhibition suppresses not only IL-6 and TNF, but also IL-12 and IL-23, production possibly via mRNA stability-independent mechanisms.

et al., 2008; Lee et al., 2004; Nakayama et al., 2017; Schmidt et al., 2005), are also upregulated in CXCL4-moDCs upon stimulation, in comparison to conventional moDCs. As these inflammatory cytokines have been reported to be regulated at the level of mRNA stability (Carballo et al., 1998; Molle et al., 2013; Tudor et al., 2009), and given that ARE sequences in the 3'UTR play a determinant role in mRNA regulation (Barreau et al., 2005; Carpenter et al., 2014; Stoecklin and Anderson, 2007), we hypothesized that these cytokines could all be subject to post-transcriptional events, explaining their higher production in stimulated CXCL4-moDCs. However, our assays used to define mRNA stability (Angiolilli et al., 2018a; Smallie et al., 2015) indicated that *IL6* and *TNF*, but not *IL12B* and *IL23A*, transcripts are stabilized in TLR3-triggered CXCL4 moDCs. Although *IL12B* and *IL23A* mRNA can both be physically recognized by ARE-BPs (Molle et al., 2013; Qian et al., 2011; Sedlyarov et al., 2016), more studies indicated no effects of ARE-BPs on *IL12B* mRNA stability (Jalonen et al., 2006; Molle et al., 2013; O'Neil et al., 2017), and rather hinted for transcriptional

mechanisms of regulation mediated by inhibition of NF-κB nuclear translocation (Gu et al., 2013). Additionally, interaction of ARE-BPs with target ARE-containing mRNAs is dictated by different parameters, such as cellular activation status, and different accessibility and adaptability of mRNA binding motifs (Garcia-Maurino et al., 2017; Ripin et al., 2019). Thus, it is plausible that in our experimental settings *IL23A* mRNA is not sufficiently affected by mRNA decay due to missing molecular counterparts or structural mRNA components that are instead present in other cells, or induced upon different stimulations. In line with this hypothesis, we also observed that TTP knockdown in moDCs failed to upregulate *IL12B* and *IL23A* mRNA expression upon poly:IC stimulation, while it potentiated *TNF* and *IL6* mRNA expression. Even though the use of primary cells in our study did not allow us to confirm a direct interaction between TTP and the target cytokines (data not shown), TTP binding to *TNF* and *IL6* has been previously confirmed in a variety of human and murine cells upon different experimental conditions (Patino et al., 2006; Shi et al., 2012; Tiedje et al., 2016; Zhao et al., 2011). Furthermore, ARE sequences in the 3'UTR region of *TNF* and *IL6* mRNAs are highly similar within mammalian species, suggesting a highly conserved mechanism of mRNA degradation for these cytokines (Carrick et al., 2004; Paschoud et al., 2006). Thus, in our experimental model, we could speculate that the mRNA stabilization of *TNF* and *IL6* mRNA in CXCL4-moDCs is likely a direct consequence of TTP inactivation, which results in the reduced binding of TTP to its target mRNAs.

Binding of ARE-BPs to AREs plays a determinant role in mRNA degradation. Among several ARE-BPs, TTP plays a pivotal role in cytokine regulation, by both guiding cytokine mRNA for degradation or preventing translation (Brooks and Blackshear, 2013). Carballo et al. had first described that LPS stimulation of macrophages derived from TTP knockout mice results in increased *TNF* mRNA and protein production (Carballo et al., 1997; Carballo et al., 1998). Also, it has been shown that TTP on one hand regulates DC maturation and cytokine production in response to TLR agonists and on the other hand regulates DC-mediated activation of T-cell responses (Emmons et al., 2008; Molle et al., 2013). In this work, expression analysis of several ARE-BPs showed that TTP is significantly and selectively upregulated in stimulated CXCL4-moDCs, as compared to the other ARE-BPs. While it has been previously shown that TTP regulates the expression of ARE- and non-ARE- enriched genes with a critical function for DC maturation and activation (Emmons et al., 2008), it is worth mentioning that inflammatory triggers, besides enhancing cytokine production, typically induce TTP mRNA expression. Despite counterintuitive, given the mRNA degrading properties of this ARE-BP (Brooks and Blackshear, 2013), higher TTP levels are explained by the impaired activity of TTP protein upon inflammatory conditions, which also renders TTP less efficient in degrading its own mRNA (Patial et al., 2016). For instance, stimulation of RA FLS with IL-1β leads to increased phospho-

inactive TTP protein levels, higher TTP mRNA expression and subsequent increased production of IL6 and CXCL8 (Angiolilli et al., 2018a). Similarly, in LPS-stimulated murine macrophages, induced expression of TTP is coupled to increased *IL23A* mRNA stability (Qian et al., 2011). High expression of TTP by macrophages and fibroblasts has also been found in the inflamed synovial tissue of RA patients, and reflected higher p38 activation in these sites (Ross et al., 2017). Overall our results indicate that induced, but phospho-inactive TTP in CXCL4-moDCs fails to degrade *TNF* and *IL6* mRNA. Additionally, our data indicate for the first time that inactivation of TTP function is one of the mechanisms by which CXCL4 controls cytokine production. In the longer term, this could explain the inflammatory and autoimmune features of the diseases where CXCL4 has been implicated.

MAPK play an important function in inflammation and tissue damage by regulating cytokines at the post-transcriptional level, promoting mRNA stability and increasing protein translation (Kratochvill et al., 2011; Mahtani et al., 2001; Ross et al., 2015; Stoecklin et al., 2004). Specifically, MAPK p38 and downstream kinase MAPK-activated protein kinase 2 (MK2) regulate the activity of several ARE-BPs, including TTP (Mahtani et al., 2001; Tiedje et al., 2016). MK2 mediates Ser-52 and Ser-178 phosphorylation of TTP, simultaneously inhibiting TTP activity and promoting its binding to 14-3-3 proteins, which prevent its degradation by the proteasome complex (Chrestensen et al., 2004; Stoecklin et al., 2004; Tiedje et al., 2016). In keeping with the need for therapeutic drugs able to prevent, or inhibit, inflammatory cytokine production, several immunomodulatory inhibitors have emerged in the last decades. Given the pleiotropic role of MAPK p38 in the regulation of transcriptional and mRNA-stabilizing events which control cytokine production (Arthur and Ley, 2013), compounds affecting p38 activity have been extensively investigated in experimental and clinical settings (Cohen et al., 2009; Salgado et al., 2014). Although p38 inhibitors have proven therapeutic potential in different experimental models of autoimmune diseases, including arthritis (Mihara et al., 2008), colitis (Li et al., 2013) and systemic sclerosis (Matsushita et al., 2017), their effects on the suppression of inflammatory parameters was shown to be only transient, possibly explaining their moderate effects in clinical trials. While 'the unexpected failure' of p38 inhibitors has not been completely understood, recent work elucidated how p38 acts as a pro- but also anti-inflammatory protein depending on the cell context and on the presence of co-stimulatory signalling (Jones et al., 2018; Raza et al., 2017). Thus, investigation of p38 inhibitors in combination therapies, and the development of second-generation inhibitors able to boost anti-inflammatory properties of p38, while preventing its pro-inflammatory effects, remains a current need.

Our study shows for the first time that TLR3-mediated activation of CXCL4-moDCs leads to transcriptional and post-transcriptional events that underlie the enhanced

inflammatory cytokine production in these cells (Fig.6). Future investigations aimed at systematically assessing CXCL4 contribution to immune processes will possibly help discerning the role of CXCL4 in health and disease.

Acknowledgments

S.C. was supported by a PhD grant from the Portuguese Fundação para a Ciência e a Tecnologia (SFRH/BD/89643/2012); T.R.D.J.R. was funded by an ERC Starting grant, a grant from the Dutch Arthritis Foundation and Pre-Seed grant Dutch Association of Science (NWO).

We thank the Multiplex Core Facility of the Laboratory of Translational Immunology (University Medical Center Utrecht) for performing the cytokine measurement.

References

Abdel-Magied, R.A., Kamel, S.R., Said, A.F., Ali, H.M., Abdel Gawad, E.A., Moussa, M.M., 2016. Serum interleukin-6 in systemic sclerosis and its correlation with disease parameters and cardiopulmonary involvement. Sarcoidosis Vasc Diffuse Lung Dis 33, 321-330.

Affandi, A.J., Carvalheiro, T., Radstake, T., Marut, W., 2018a. Dendritic cells in systemic sclerosis: Advances from human and mice studies. Immunol Lett 195, 18-29.

Affandi, A.J., Silva-Cardoso, S.C., Garcia, S., Leijten, E.F.A., van Kempen, T.S., Marut, W., van Roon, J.A.G., Radstake, T., 2018b. CXCL4 is a novel inducer of human Th17 cells and correlates with IL-17 and IL-22 in psoriatic arthritis. Eur J Immunol 48, 522-531.

Ah Kioon, M.D., Tripodo, C., Fernandez, D., Kirou, K.A., Spiera, R.F., Crow, M.K., Gordon, J.K., Barrat, F.J., 2018. Plasmacytoid dendritic cells promote systemic sclerosis with a key role for TLR8. Sci Transl Med 10.

Aivado, M., Spentzos, D., Germing, U., Alterovitz, G., Meng, X.Y., Grall, F., Giagounidis, A.A., Klement, G., Steidl, U., Otu, H.H., Czibere, A., Prall, W.C., Iking-Konert, C., Shayne, M., Ramoni, M.F., Gattermann, N., Haas, R., Mitsiades, C.S., Fung, E.T., Libermann, T.A., 2007. Serum proteome profiling detects myelodysplastic syndromes and identifies CXC chemokine ligands 4 and 7 as markers for advanced disease. Proc Natl Acad Sci U S A 104, 1307-1312.

Angiolilli, C., Kabala, P.A., Grabiec, A.M., Rossato, M., Lai, W.S., Fossati, G., Mascagni, P., Steinkuhler, C., Blackshear, P.J., Reedquist, K.A., Baeten, D.L., Radstake, T., 2018a. Control of cytokine mRNA degradation by the histone deacetylase inhibitor ITF2357 in rheumatoid arthritis fibroblast-like synoviocytes: beyond transcriptional regulation. Arthritis Res Ther 20, 148.

Angiolilli, C., Marut, W., van der Kroef, M., Chouri, E., Reedquist, K.A., Radstake, T., 2018b. New insights into the genetics and epigenetics of systemic sclerosis. Nat Rev Rheumatol 14, 657-673.

Arthur, J.S., Ley, S.C., 2013. Mitogen-activated protein kinases in innate immunity. Nat Rev Immunol 13, 679-692.

Barreau, C., Paillard, L., Osborne, H.B., 2005. AU-rich elements and associated factors: are there unifying principles? Nucleic Acids Res 33, 7138-7150.

Brooks, S.A., Blackshear, P.J., 2013. Tristetraprolin (TTP): interactions with mRNA and proteins, and current thoughts on mechanisms of action. Biochim Biophys Acta 1829, 666-679.

Brooks, S.A., Connolly, J.E., Diegel, R.J., Fava, R.A., Rigby, W.F., 2002. Analysis of the function, expression, and subcellular distribution of human tristetraprolin. Arthritis Rheum 46, 1362-1370.

Bros, M., Wiechmann, N., Besche, V., Art, J., Pautz, A., Grabbe, S., Kleinert, H., Reske-Kunz, A.B., 2010. The RNA binding protein tristetraprolin influences the activation state of murine dendritic cells. Mol Immunol 47, 1161-1170.

Carballo, E., Cao, H., Lai, W.S., Kennington, E.A., Campbell, D., Blackshear, P.J., 2001. Decreased sensitivity of tristetraprolin-deficient cells to p38 inhibitors suggests the involvement of tristetraprolin in the p38 signaling pathway. J Biol Chem 276, 42580-42587.

Carballo, E., Gilkeson, G.S., Blackshear, P.J., 1997. Bone marrow transplantation reproduces the tristetraprolin-deficiency syndrome in recombination activating gene-2 (-/-) mice. Evidence that monocyte/macrophage progenitors may be responsible for TNFalpha overproduction. J Clin Invest 100, 986-995.

Carballo, E., Lai, W.S., Blackshear, P.J., 1998. Feedback inhibition of macrophage tumor necrosis factor-alpha production by tristetraprolin. Science 281, 1001-1005.

Carpenter, S., Ricci, E.P., Mercier, B.C., Moore, M.J., Fitzgerald, K.A., 2014. Post-transcriptional regulation of gene expression in innate immunity. Nat Rev Immunol 14, 361-376.

Carrick, D.M., Lai, W.S., Blackshear, P.J., 2004. The tandem CCCH zinc finger protein tristetraprolin and its relevance to cytokine mRNA turnover and arthritis. Arthritis Res Ther 6, 248-264.

Chrestensen, C.A., Schroeder, M.J., Shabanowitz, J., Hunt, D.F., Pelo, J.W., Worthington, M.T., Sturgill, T.W., 2004. MAPKAP kinase 2 phosphorylates tristetraprolin on in vivo sites including Ser178, a site required for 14-3-3 binding. J Biol Chem 279, 10176-10184.

Cohen, S.B., Cheng, T.T., Chindalore, V., Damjanov, N., Burgos-Vargas, R., Delora, P., Zimany, K., Travers, H., Caulfield, J.P., 2009. Evaluation of the efficacy and safety of pamapimod, a p38 MAP kinase inhibitor, in a double-blind, methotrexate-controlled study of patients with active rheumatoid arthritis. Arthritis Rheum 60, 335-344.

de Jager, W., Prakken, B.J., Bijlsma, J.W., Kuis, W., Rijkers, G.T., 2005. Improved multiplex immunoassay performance in human plasma and synovial fluid following removal of interfering heterophilic antibodies. J Immunol Methods 300, 124-135.

Dehmer, G.J., Fisher, M., Tate, D.A., Teo, S., Bonnem, E.M., 1995. Reversal of heparin anticoagulation by recombinant platelet factor 4 in humans. Circulation 91, 2188-2194.

Deleault, K.M., Skinner, S.J., Brooks, S.A., 2008. Tristetraprolin regulates TNF TNF-alpha mRNA stability via a proteasome dependent mechanism involving the combined action of the ERK and p38 pathways. Mol Immunol 45, 13-24.

Emmons, J., Townley-Tilson, W.H., Deleault, K.M., Skinner, S.J., Gross, R.H., Whitfield, M.L., Brooks, S.A., 2008. Identification of TTP mRNA targets in human dendritic cells reveals TTP as a critical regulator of dendritic cell maturation. RNA 14, 888-902.

Fallmann, J., Sedlyarov, V., Tanzer, A., Kovarik, P., Hofacker, I.L., 2016. AREsite2: an enhanced database for the comprehensive investigation of AU/GU/U-rich elements. Nucleic Acids Res 44, D90-95.

Fleischer, J., Grage-Griebenow, E., Kasper, B., Heine, H., Ernst, M., Brandt, E., Flad, H.D., Petersen, F., 2002. Platelet factor 4 inhibits proliferation and cytokine release of activated human T cells. J Immunol 169, 770-777.

Fox, J.M., Kausar, F., Day, A., Osborne, M., Hussain, K., Mueller, A., Lin, J., Tsuchiya, T., Kanegasaki, S., Pease, J.E., 2018. CXCL4/Platelet Factor 4 is an agonist of CCR1 and drives human monocyte migration. Sci Rep 8, 9466.

Fricke, I., Mitchell, D., Petersen, F., Bohle, A., Bulfone-Paus, S., Brandau, S., 2004. Platelet factor 4 in conjunction with IL-4 directs differentiation of human monocytes into specialized antigen-presenting cells. FASEB J 18, 1588-1590.

Garcia-Maurino, S.M., Rivero-Rodriguez, F., Velazquez-Cruz, A., Hernandez-Vellisca, M., Diaz-Quintana, A., De la Rosa, M.A., Diaz-Moreno, I., 2017. RNA Binding Protein Regulation and Cross-Talk in the Control of AU-rich mRNA Fate. Front Mol Biosci 4, 71.

Gleissner, C.A., Shaked, I., Little, K.M., Ley, K., 2010. CXC chemokine ligand 4 induces a unique transcriptome in monocyte-derived macrophages. J Immunol 184, 4810-4818.

Gouwy, M., Ruytinx, P., Radice, E., Claudi, F., Van Raemdonck, K., Bonecchi, R., Locati, M., Struyf, S., 2016. CXCL4 and CXCL4L1 Differentially Affect Monocyte Survival and Dendritic Cell Differentiation and Phagocytosis. PLoS One 11, e0166006.

Gu, L., Ning, H., Qian, X., Huang, Q., Hou, R., Almourani, R., Fu, M., Blackshear, P.J., Liu, J., 2013. Suppression of IL-12 production by tristetraprolin through blocking NF-kcyB nuclear translocation. J Immunol 191, 3922-3930.

Han, Z.C., Sensebe, L., Abgrall, J.F., Briere, J., 1990. Platelet factor 4 inhibits human megakaryocytopoiesis in vitro. Blood 75, 1234-1239.

Huang, L., Yu, Z., Zhang, Z., Ma, W., Song, S., Huang, G., 2016. Interaction with Pyruvate Kinase M2 Destabilizes Tristetraprolin by Proteasome Degradation and Regulates Cell Proliferation in Breast Cancer. Sci Rep 6, 22449.

Jalonen, U., Nieminen, R., Vuolteenaho, K., Kankaanranta, H., Moilanen, E., 2006. Down-regulation of tristetraprolin expression results in enhanced IL-12 and MIP-2 production and reduced MIP-3alpha synthesis in activated macrophages. Mediators Inflamm 2006, 40691.

Jones, D.S., Jenney, A.P., Joughin, B.A., Sorger, P.K., Lauffenburger, D.A., 2018. Inflammatory but not mitogenic contexts prime synovial fibroblasts for compensatory signaling responses to p38 inhibition. Sci Signal 11.

Khabar, K.S., 2010. Post-transcriptional control during chronic inflammation and cancer: a focus on AU-rich elements. Cell Mol Life Sci 67, 2937-2955.

Komura, K., Fujimoto, M., Hasegawa, M., Ogawa, F., Hara, T., Muroi, E., Takehara, K., Sato, S., 2008. Increased serum interleukin 23 in patients with systemic sclerosis. J Rheumatol 35, 120-125.

Kratochvill, F., Machacek, C., Vogl, C., Ebner, F., Sedlyarov, V., Gruber, A.R., Hartweger, H., Vielnascher, R., Karaghiosoff, M., Rulicke, T., Muller, M., Hofacker, I., Lang, R., Kovarik, P., 2011. Tristetraprolin-driven regulatory circuit controls quality and timing of mRNA decay in inflammation. Mol Syst Biol 7, 560.

Lee, E., Trepicchio, W.L., Oestreicher, J.L., Pittman, D., Wang, F., Chamian, F., Dhodapkar, M., Krueger, J.G., 2004. Increased expression of interleukin 23 p19 and p40 in lesional skin of patients with psoriasis vulgaris. J Exp Med 199, 125-130.

Li, Y.Y., Yuece, B., Cao, H.M., Lin, H.X., Lv, S., Chen, J.C., Ochs, S., Sibaev, A., Deindl, E., Schaefer, C., Storr, M., 2013. Inhibition of p38/Mk2 signaling pathway improves the anti-inflammatory effect of WIN55 on mouse experimental colitis. Lab Invest 93, 322-333.

Loupasakis, K., Kuo, D., Sokhi, U.K., Sohn, C., Syracuse, B., Giannopoulou, E.G., Park, S.H., Kang, H., Ratsch, G., Ivashkiv, L.B., Kalliolias, G.D., 2017. Tumor Necrosis Factor dynamically regulates the mRNA stabilome in rheumatoid arthritis fibroblast-like synoviocytes. PLoS One 12, e0179762.

Mahtani, K.R., Brook, M., Dean, J.L., Sully, G., Saklatvala, J., Clark, A.R., 2001. Mitogen-activated protein kinase p38 controls the expression and posttranslational modification of tristetraprolin, a regulator of tumor necrosis factor alpha mRNA stability. Mol Cell Biol 21, 6461-6469.

Maione, T.E., Gray, G.S., Petro, J., Hunt, A.J., Donner, A.L., Bauer, S.I., Carson, H.F., Sharpe, R.J., 1990. Inhibition of angiogenesis by recombinant human platelet factor-4 and related peptides. Science 247, 77-79.

Matsushita, T., Date, M., Kano, M., Mizumaki, K., Tennichi, M., Kobayashi, T., Hamaguchi, Y., Hasegawa, M., Fujimoto, M., Takehara, K., 2017. Blockade of p38 Mitogen-Activated Protein Kinase Inhibits Murine Sclerodermatous Chronic Graft-versus-Host Disease. Am J Pathol 187, 841-850.

Mihara, K., Almansa, C., Smeets, R.L., Loomans, E.E., Dulos, J., Vink, P.M., Rooseboom, M., Kreutzer, H., Cavalcanti, F., Boots, A.M., Nelissen, R.L., 2008. A potent and selective p38 inhibitor protects against bone damage in murine collagen-induced arthritis: a comparison with neutralization of mouse TNFalpha. Br J Pharmacol 154, 153-164.

Molle, C., Zhang, T., Ysebrant de Lendonck, L., Gueydan, C., Andrianne, M., Sherer, F., Van Simaeys, G., Blackshear, P.J., Leo, O., Goriely, S., 2013. Tristetraprolin regulation of interleukin 23 mRNA stability prevents a spontaneous inflammatory disease. J Exp Med 210, 1675-1684.

Nakayama, W., Jinnin, M., Tomizawa, Y., Nakamura, K., Kudo, H., Inoue, K., Makino, K., Honda, N., Kajihara, I., Fukushima, S., Ihn, H., 2017. Dysregulated interleukin-23 signalling contributes to the increased collagen production in scleroderma fibroblasts via balancing microRNA expression. Rheumatology (Oxford) 56, 145-155.

O'Neil, J.D., Ross, E.A., Ridley, M.L., Ding, Q., Tang, T., Rosner, D.R., Crowley, T., Malhi, D., Dean, J.L., Smallie, T., Buckley, C.D., Clark, A.R., 2017. Gain-of-Function Mutation of Tristetraprolin Impairs Negative Feedback Control of Macrophages In Vitro yet Has Overwhelmingly Anti-Inflammatory Consequences In Vivo. Mol Cell Biol 37.

Paschoud, S., Dogar, A.M., Kuntz, C., Grisoni-Neupert, B., Richman, L., Kuhn, L.C., 2006. Destabilization of interleukin-6 mRNA requires a putative RNA stem-loop structure, an AU-rich element, and the RNA-binding protein AUF1. Mol Cell Biol 26, 8228-8241.

Patial, S., Blackshear, P.J., 2016. Tristetraprolin as a Therapeutic Target in Inflammatory Disease. Trends Pharmacol Sci 37, 811-821.

Patial, S., Curtis, A.D., 2nd, Lai, W.S., Stumpo, D.J., Hill, G.D., Flake, G.P., Mannie, M.D., Blackshear, P.J., 2016. Enhanced stability of tristetraprolin mRNA protects mice against immune-mediated inflammatory pathologies. Proc Natl Acad Sci U S A 113, 1865-1870.

Patino, W.D., Kang, J.G., Matoba, S., Mian, O.Y., Gochuico, B.R., Hwang, P.M., 2006. Atherosclerotic plaque macrophage transcriptional regulators are expressed in blood and modulated by tristetraprolin. Circ Res 98, 1282-1289.

Patsouras, M.D., Sikara, M.P., Grika, E.P., Moutsopoulos, H.M., Tzioufas, A.G., Vlachoyiannopoulos, P.G., 2015. Elevated expression of platelet-derived chemokines in patients with antiphospholipid syndrome. J Autoimmun 65, 30-37.

Qian, X., Ning, H., Zhang, J., Hoft, D.F., Stumpo, D.J., Blackshear, P.J., Liu, J., 2011. Posttranscriptional regulation of IL-23 expression by IFN-gamma through tristetraprolin. J Immunol 186, 6454-6464.

Qiu, L.Q., Stumpo, D.J., Blackshear, P.J., 2012. Myeloid-specific tristetraprolin deficiency in mice results in extreme lipopolysaccharide sensitivity in an otherwise minimal phenotype. J Immunol 188, 5150-5159.

Raza, A., Crothers, J.W., McGill, M.M., Mawe, G.M., Teuscher, C., Krementsov, D.N., 2017. Anti-inflammatory roles of p38alpha MAPK in macrophages are context dependent and require IL-10. J Leukoc Biol 102, 1219-1227.

Ripin, N., Boudet, J., Duszczyk, M.M., Hinniger, A., Faller, M., Krepl, M., Gadi, A., Schneider, R.J., Sponer, J., Meisner-Kober, N.C., Allain, F.H., 2019. Molecular basis for AU-rich element recognition and dimerization by the HuR C-terminal RRM. Proc Natl Acad Sci U S A 116, 2935-2944.

Ross, E.A., Naylor, A.J., O'Neil, J.D., Crowley, T., Ridley, M.L., Crowe, J., Smallie, T., Tang, T.J., Turner, J.D., Norling, L.V., Dominguez, S., Perlman, H., Verrills, N.M., Kollias, G., Vitek, M.P., Filer, A., Buckley, C.D., Dean, J.L., Clark, A.R., 2017. Treatment of inflammatory arthritis via targeting of tristetraprolin, a master regulator of pro-inflammatory gene expression. Ann Rheum Dis 76, 612-619.

Ross, E.A., Smallie, T., Ding, Q., O'Neil, J.D., Cunliffe, H.E., Tang, T., Rosner, D.R., Klevernic, I., Morrice, N.A., Monaco, C., Cunningham, A.F., Buckley, C.D., Saklatvala, J., Dean, J.L., Clark, A.R., 2015. Dominant Suppression of Inflammation via Targeted Mutation of the mRNA Destabilizing Protein Tristetraprolin. J Immunol 195, 265-276.

Salgado, E., Maneiro, J.R., Carmona, L., Gomez-Reino, J.J., 2014. Safety profile of protein kinase inhibitors in rheumatoid arthritis: systematic review and meta-analysis. Ann Rheum Dis 73, 871-882.

Sandler, H., Stoecklin, G., 2008. Control of mRNA decay by phosphorylation of tristetraprolin. Biochem Soc Trans 36, 491-496.

Scherrer, K., 2018. Primary transcripts: From the discovery of RNA processing to current concepts of gene expression - Review. Exp Cell Res 373, 1-33.

Scheuerer, B., Ernst, M., Durrbaum-Landmann, I., Fleischer, J., Grage-Griebenow, E., Brandt, E., Flad, H.D., Petersen, F., 2000. The CXC-chemokine platelet factor 4 promotes monocyte survival and induces monocyte differentiation into macrophages. Blood 95, 1158-1166.

Schmidt, C., Giese, T., Ludwig, B., Mueller-Molaian, I., Marth, T., Zeuzem, S., Meuer, S.C., Stallmach, A., 2005. Expression of interleukin-12-related cytokine transcripts in inflammatory bowel disease: elevated interleukin-23p19 and interleukin-27p28 in Crohn's disease but not in ulcerative colitis. Inflamm Bowel Dis 11, 16-23.

Schwartzkopff, F., Grimm, T.A., Lankford, C.S., Fields, K., Wang, J., Brandt, E., Clouse, K.A., 2009. Platelet factor 4 (CXCL4) facilitates human macrophage infection with HIV-1 and potentiates virus replication. Innate Immun 15, 368-379.

Sedlyarov, V., Fallmann, J., Ebner, F., Huemer, J., Sneezum, L., Ivin, M., Kreiner, K., Tanzer, A., Vogl, C., Hofacker, I., Kovarik, P., 2016. Tristetraprolin binding site atlas in the macrophage transcriptome reveals a switch for inflammation resolution. Mol Syst Biol 12, 868.

Seko, Y., Cole, S., Kasprzak, W., Shapiro, B.A., Ragheb, J.A., 2006. The role of cytokine mRNA stability in the pathogenesis of autoimmune disease. Autoimmun Rev 5, 299-305.

Shi, J.X., Su, X., Xu, J., Zhang, W.Y., Shi, Y., 2012. HuR post-transcriptionally regulates TNF-alpha-induced IL-6 expression in human pulmonary microvascular endothelial cells mainly via tristetraprolin. Respir Physiol Neurobiol 181, 154-161.

Silva-Cardoso, S.C., Affandi, A.J., Spel, L., Cossu, M., van Roon, J.A.G., Boes, M., Radstake, T., 2017. CXCL4 Exposure Potentiates TLR-Driven Polarization of Human Monocyte-Derived Dendritic Cells and Increases Stimulation of T Cells. J Immunol 199, 253-262.

Smallie, T., Ross, E.A., Ammit, A.J., Cunliffe, H.E., Tang, T., Rosner, D.R., Ridley, M.L., Buckley, C.D., Saklatvala, J., Dean, J.L., Clark, A.R., 2015. Dual-Specificity Phosphatase 1 and Tristetraprolin Cooperate To Regulate Macrophage Responses to Lipopolysaccharide. J Immunol 195, 277-288.

Srivastava, K., Cockburn, I.A., Swaim, A., Thompson, L.E., Tripathi, A., Fletcher, C.A., Shirk, E.M., Sun, H., Kowalska, M.A., Fox-Talbot, K., Sullivan, D., Zavala, F., Morrell, C.N., 2008. Platelet factor 4 mediates inflammation in experimental cerebral malaria. Cell Host Microbe 4, 179-187.

Stoecklin, G., Anderson, P., 2007. In a tight spot: ARE-mRNAs at processing bodies. Genes Dev 21, 627-631.

Stoecklin, G., Stubbs, T., Kedersha, N., Wax, S., Rigby, W.F., Blackwell, T.K., Anderson, P., 2004. MK2-induced tristetraprolin:14-3-3 complexes prevent stress granule association and ARE-mRNA decay. EMBO J 23, 1313-1324.

Taylor, G.A., Carballo, E., Lee, D.M., Lai, W.S., Thompson, M.J., Patel, D.D., Schenkman, D.I., Gilkeson, G.S., Broxmeyer, H.E., Haynes, B.F., Blackshear, P.J., 1996. A pathogenetic role for TNF alpha in the syndrome of cachexia, arthritis, and autoimmunity resulting from tristetraprolin (TTP) deficiency. Immunity 4, 445-454.

Tiedje, C., Diaz-Munoz, M.D., Trulley, P., Ahlfors, H., Laass, K., Blackshear, P.J., Turner, M., Gaestel, M., 2016. The RNA-binding protein TTP is a global post-transcriptional regulator of feedback control in inflammation. Nucleic Acids Res 44, 7418-7440.

Tudor, C., Marchese, F.P., Hitti, E., Aubareda, A., Rawlinson, L., Gaestel, M., Blackshear, P.J., Clark, A.R., Saklatvala, J., Dean, J.L., 2009. The p38 MAPK pathway inhibits tristetraprolin-directed decay of interleukin-10 and pro-inflammatory mediator mRNAs in murine macrophages. FEBS Lett 583, 1933-1938.

van Bon, L., Affandi, A.J., Broen, J., Christmann, R.B., Marijnissen, R.J., Stawski, L., Farina, G.A., Stifano, G., Mathes, A.L., Cossu, M., York, M., Collins, C., Wenink, M., Huijbens, R., Hesselstrand, R., Saxne, T., DiMarzio, M., Wuttge, D., Agarwal, S.K., Reveille, J.D., Assassi, S., Mayes, M., Deng, Y., Drenth, J.P., de Graaf, J., den Heijer, M., Kallenberg, C.G., Bijl, M., Loof, A., van den Berg, W.B., Joosten, L.A., Smith, V., de Keyser, F., Scorza, R., Lunardi, C., van Riel, P.L., Vonk, M., van Heerde, W., Meller, S., Homey, B., Beretta, L., Roest, M., Trojanowska, M., Lafyatis, R., Radstake, T.R., 2014. Proteome-wide analysis and CXCL4 as a biomarker in systemic sclerosis. N Engl J Med 370, 433-443.

Xia, C.Q., Kao, K.J., 2003. Effect of CXC chemokine platelet factor 4 on differentiation and function of monocyte-derived dendritic cells. Int Immunol 15, 1007-1015.

Yeo, L., Adlard, N., Biehl, M., Juarez, M., Smallie, T., Snow, M., Buckley, C.D., Raza, K., Filer, A., Scheel-Toellner, D., 2016. Expression of chemokines CXCL4 and CXCL7 by synovial macrophages defines an early stage of rheumatoid arthritis. Ann Rheum Dis 75, 763-771.

Zhang, H., Taylor, W.R., Joseph, G., Caracciolo, V., Gonzales, D.M., Sidell, N., Seli, E., Blackshear, P.J., Kallen, C.B., 2013. mRNA-binding protein ZFP36 is expressed in atherosclerotic lesions and reduces inflammation in aortic endothelial cells. Arterioscler Thromb Vasc Biol 33, 1212-1220.

Zhao, W., Liu, M., D'Silva, N.J., Kirkwood, K.L., 2011. Tristetraprolin regulates interleukin-6 expression through p38 MAPK-dependent affinity changes with mRNA 3' untranslated region. J Interferon Cytokine Res 31, 629-637.

Supplementary Figures

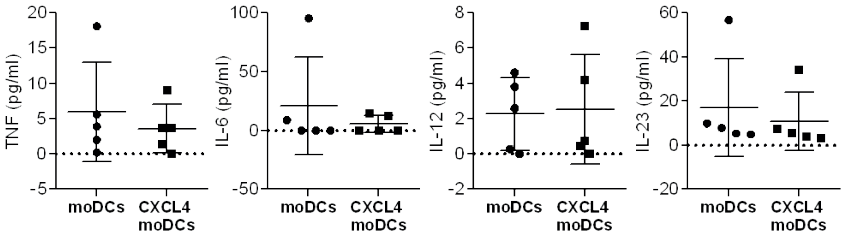

Fig. S1: Monocyte-derived dendritic cells (moDCs) were differentiated in the absence or presence of CXCL4 (CXCL4-moDCs) for 6 days. Cytokine production was measured by Luminex. (N=5).

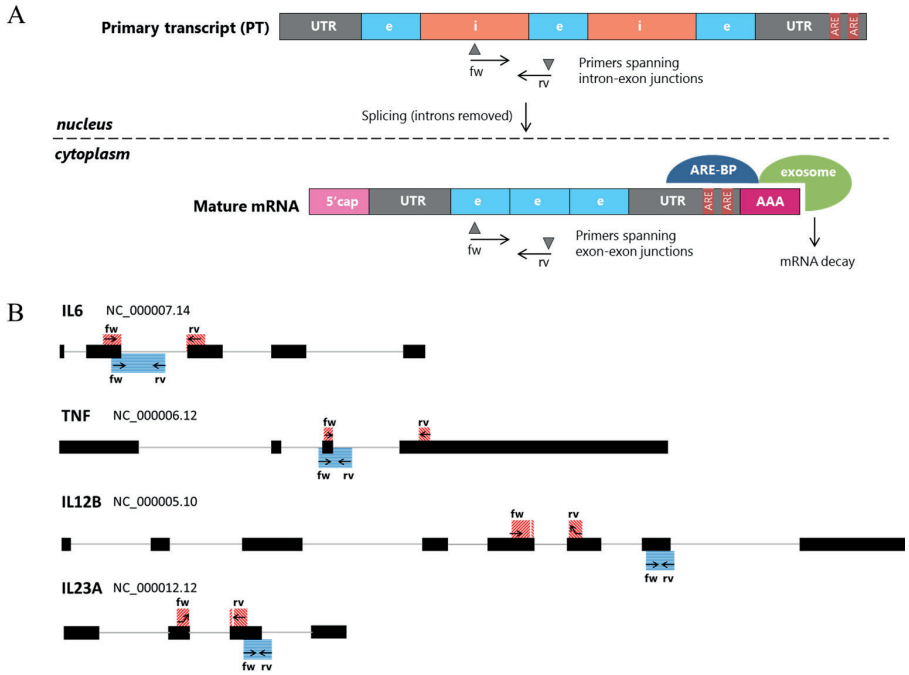

Fig. S2: (A) A simplified representation for primer design strategy is shown. Primers amplifying intron-exon regions are used to detect primary (PT) transcripts located in the nucleus. Conversely, primers spanning exon-exon regions allow the detection of mature mRNA located in the cytoplasm. Mature mRNA, when containing ARE sequences in the 3'UTR, is subject to recognition of ARE-binding proteins which favor the recruitment of the exosome complex and prime mRNA decay from the 3'poly(A) tail. e=exon; i=intron; AAA= poly(A) tail; UTR= untranslated region; ARE= AU-rich elements; ARE-BP= ARE-binding proteins; 5'cap=Five-prime cap; fw=forward primer; rv=reverse primer.
(B) Sets of primers used in this study were designed to amplify either intron-exon or exon-exon regions of *IL6, TNF, IL12B* and *IL23A* transcripts. In the scheme, exons (black) and the amplified regions obtained from primers recognizing primary transcript (blue) or mature transcript (red) are shown. NC number refers to the NCBI Genomic Reference Sequence (GRCh38 Assembly) for each gene.

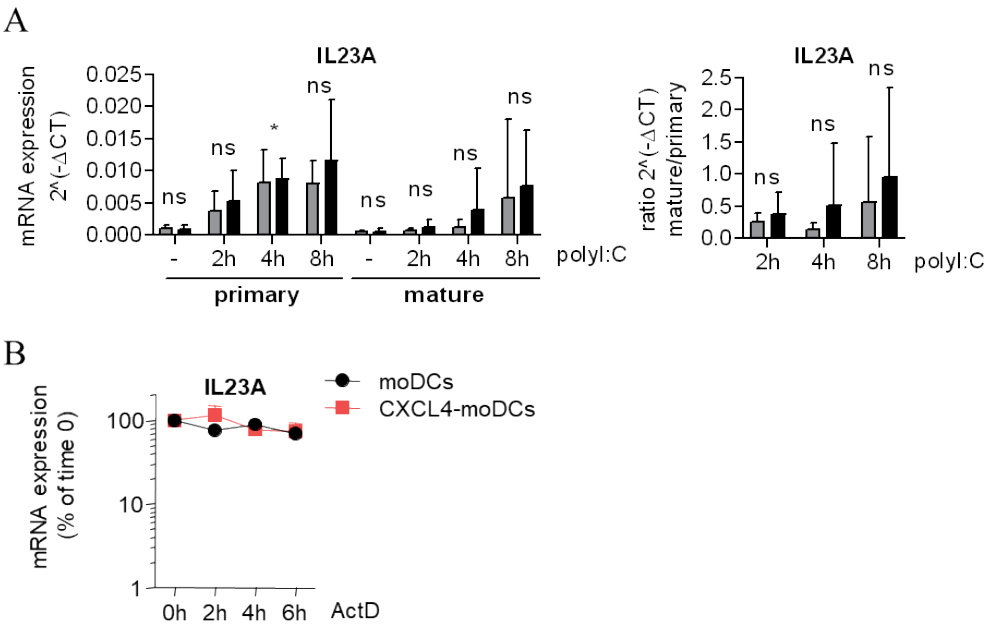

Fig. S3: (A) MoDCs and CXCL4-moDCs were left unstimulated (-) or stimulated for 2, 4 and 8 hours with polyI:C. Gene expression of primary and mature transcripts of IL23A is represented as relative expression levels for both primary and mature transcripts (2^-ΔCT), while ratios were calculated according to the formula: 2^-ΔCT mature transcript/2^-ΔCT primary transcript. (N=8); One-way ANOVA followed by Fisher's LSD test. (B) MoDCs and CXCL4 moDCs were stimulated with polyI:C for 2 hours, and further treated with actinomycin D (ActD) for the indicated time points, followed by gene expression analysis. (N=10); Wilcoxon matched-pairs signed rank test.

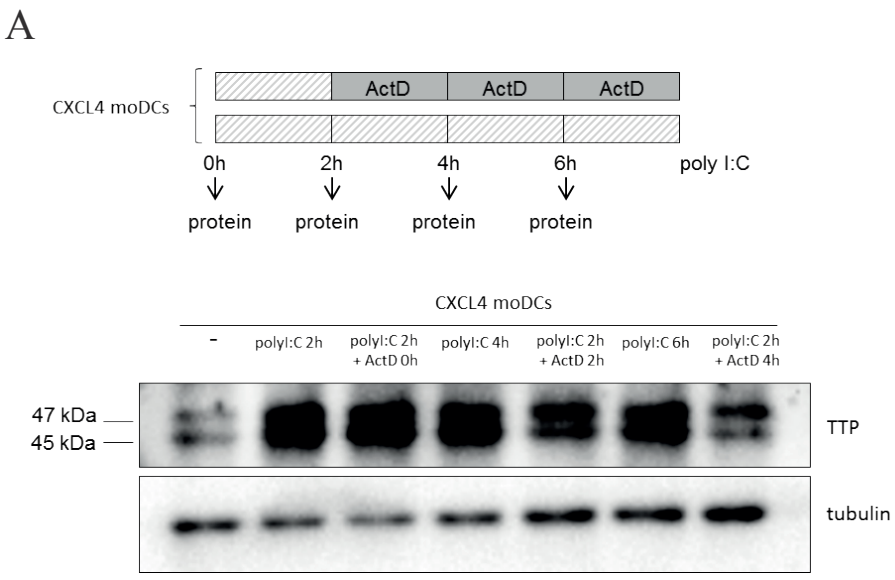

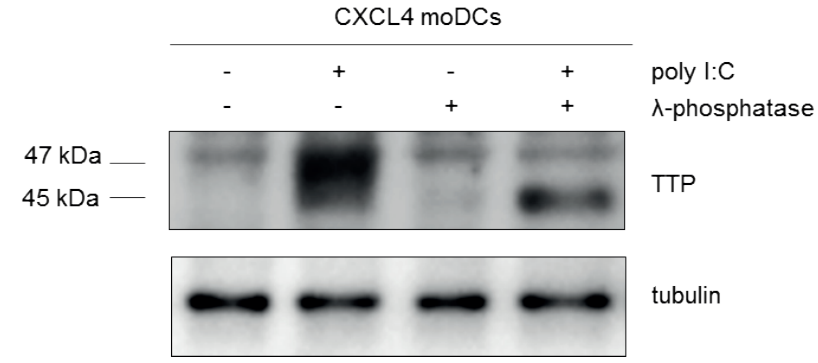

Fig. S4: (A) CXCL4-moDCs were either stimulated with polyI:C for 2, 4 and 6 hours, or stimulated with polyI:C for 2 hours and further treated with actinomycin D (ActD). Cells were lysed in protein lysis buffer and samples processed for Western-Blot (N=1). (B) CXCL4-moDCs were either left unstimulated or stimulated with polyI:C for 2 hours. Protein lysates were either left untreated or treated with lambda phosphatase (λ-phosphatase) for 30 min, and samples processed for Western-Blot (N=1).

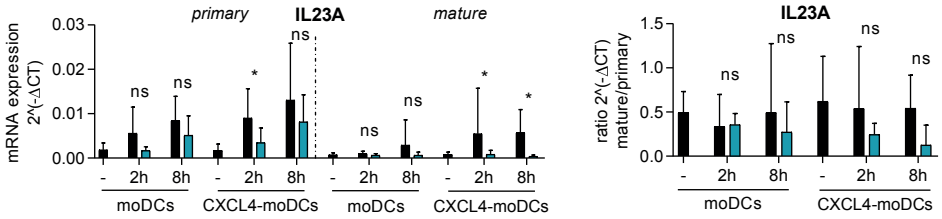

Fig. S5: Prior to polyI:C stimulation for 8 hours, moDCs and CXCL4-moDCs were pre-treated with the p38 inhibitor SB202190 and further stimulated for 2 and 8 hours with polyI:C and processed for qPCR analysis. Gene expression of primary and mature transcripts of inflammatory cytokines is represented as relative expression levels for both primary and mature transcripts (2^-ΔCT), while ratios were calculated according to the formula: 2^-ΔCT mature transcript/2^-ΔCT primary transcript. (N=6); One-way ANOVA followed by Fisher's LSD test.

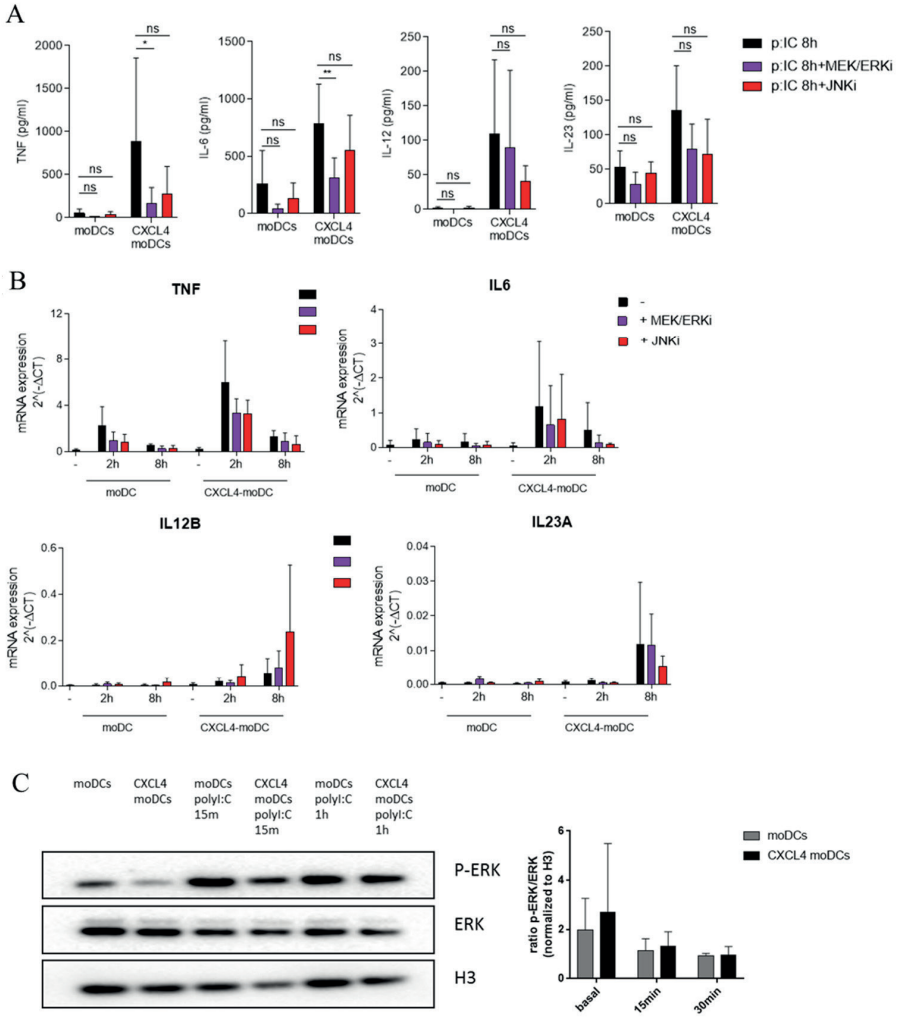

Fig. S6: (A-C) moDCs and CXCL4-moDCs were either left untreated or treated with MEK/ERK inhibitor (U0126) or JNK inhibitor (SP600125) prior to stimulation with polyI:C for different time points. In (A), cells were stimulated with polyI:C for 8 hours, supernatant was collected and cytokine production was measured by Luminex (N=6), One-way ANOVA followed by Fisher's LSD test. In (B), cells were stimulated with either 2 or 8 hours polyI:C, and gene expression assessed by qPCR (N=3). In (C), cells were stimulated with either 15 minutes or 1 hour, and protein lysates processed for Western-blot. Densitometry analysis indicates the signal intensity of (p)ERK/ERK ratio normalized to control H3 (N=3).

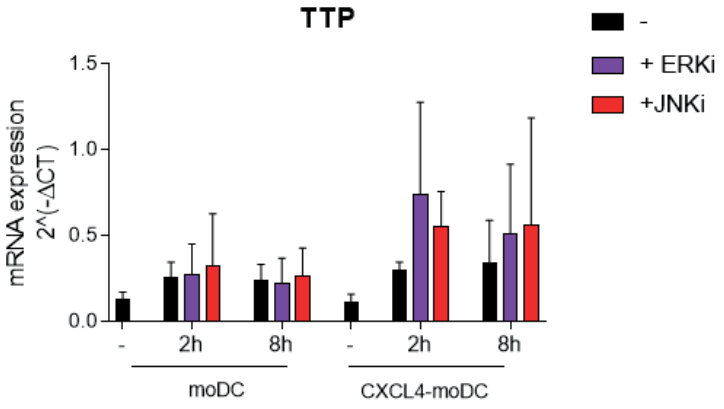

Fig. S7: moDCs and CXCL4-moDCs were either left untreated or treated with MEK/ERK inhibitor (U0126) or JNK inhibitor (SP600125) prior to stimulation with polyI:C for 2 or 8 hours, and gene expression assessed by qPCR (N=3).

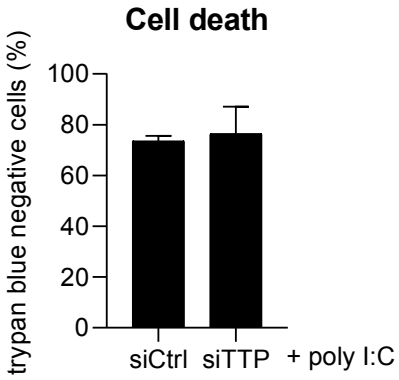

Fig. S8: moDCs were transfected with either control non-targeting siRNA (siCtrl) or with specific siRNA targeting TTP (siTTP). Cell viability was assessed by trypan blue staining, and represented as percentage of total live cells (N=2).

Chapter 7

General Discussion

Immune mediators such as cytokines and chemokines play a dual role in physiological and pathological conditions. CXCL4 is a chemokine released by activated platelets and immune cells, and plays a critical role in biological processes such as hematopoiesis, coagulation and immune regulation [1]. Our group found, for the first time, increased levels of CXCL4 in circulation and skin of patients with systemic sclerosis (SSc)[2]. Later studies have validated the implication of CXCL4 in the pathogenesis of SSc[3–6] and in other inflammatory diseases such as psoriasis, rheumatoid arthritis (RA) and atherosclerosis [7–9].

Interestingly, increased frequency and activation of platelets (the major source of CXCL4) are implicated in aberrant inflammatory and fibrotic responses associated with SSc [2,3,10–13]. Enhanced platelet activation and aggregation in SSc patients contributes to increased pro-coagulation, extensive cytoskeletal remodelling and mobilization of intracellular calcium. In turn, these inflammatory and fibrotic responses enhance the release of platelet factors, which forms a positive feedback loop that promote platelet activation [11,14,15].

While it has been established that both innate and adaptive immune systems are compromised in SSc[4,16–21], the contribution of CXCL4 to these immune aberrations remains poorly investigated.

In this thesis, we investigated the effects of CXCL4 exposure on immune responses by monocyte-derived dendritic cells (moDCs), an *in vitro* model of inflammatory DCs. Additionally, we explored the underlying molecular mechanisms implicated in the reprogramming of moDC phenotype and function by CXCL4.

CXCL4 primes inflammatory innate and adaptive immune responses

Changes in DC frequencies and augmented pro-inflammatory responses were implicated in the pathology of SSc[2,13]. Previously our group showed that *in vitro* triggering of DCs from SSc patients with TLR agonists results in amplified production of inflammatory cytokines and type-I interferon (IFN-I) [2,18]. Therefore, in **Chapter 2** we studied how CXCL4 affects the phenotype and TLR-mediated responses by human moDCs. Xia and colleagues were the first ones looking at the role of human purified CXCL4 on differentiation and function of moDCs [22]. In line with their observations, we observed that exposure to CXCL4 throughout the differentiation dramatically modifies the conventional morphology of moDCs to an irregular shape, formation of long dendrites and extremely adherent cellular clusters, suggesting a mature phenotype. Also, phenotypic characterization by flow cytometry showed that CXCL4-moDCs expressed higher levels of activation molecules, but no production

of inflammatory cytokines in the absence of TLR-stimulation. We revealed for the first time that stimulation of CXCL4-moDCs with the endosomal TLR agonists polyI:C (TLR3), CL075 (TLR8) or R848 (TLR7/8), results in amplified expression of maturation molecules and production of pro-inflammatory cytokines.

Thus, we suggest that circulating CXCL4 contribute to impaired DC phenotype and function, and prime cells to produce aberrant levels of inflammatory cytokines upon endossomal TLR triggering, as previously observed in cells from SSc patients[18,23–25]. DCs play a key role in bridging innate and adaptive immune responses, through the instruction of inflammatory mediators. The pivotal role of T-cells in autoimmune conditions is well established. Indeed, disturbed frequency and augmented pro-fibrotic cytokine production, especially Th2 and Th17 cytokines, are associated with disease activity and fibrosis in patients with SSc [20,21,26–31]. Interestingly, DCs found in inflammatory tissues are potent inducers of T-cell activation, which includes Th17-mediated responses [32].

In **Chapter 2** and **3** we investigated the role of CXCL4 in the activation and skewing of T-cells**.** We showed that CXCL4-moDCs potentiate the activation and the inflammatory cytokine production by autologous $CD4^+$ and $CD8^+$ T-cells, and antigen (Ag) specific $CD8^+$ T-cells (**Chapter 2**). Remarkably, exposure to CXCL4 induced the production of Th17 cytokines directly by CD3/CD28 activated $CD4^+$T-cells, and by $CD4^+$ T-cells in co-culture with myeloid DCs (mDCs), monocytes or CXCL4-moDCs (**Chapter 3**). Moreover, we found increased levels of CXCL4 in plasma from patients with psoriatic arthritis (PsA), a Th17-driven disease. A strong correlation was found between CXCL4 and IL-17 or IL-22 in PsA synovial fluid (**Chapter 3**). Thus, we hypothesize that CXCL4 plays a critical role in driving inflammatory T-cell responses and in skewing Th17 differentiation. This hypothesis is supported by a previous study showing that in autologous co-culture, platelets increased anti-CD3/CD28-induced IL-17 production by $CD4^+$T-cells [33]. However, the effects of CXCL4 in the regulation of T-cells remains debatable due to the contrasting results reported in human and mice[34–37], distinct methodologies used to induce the activation of T-cells (anti-CD3/CD28, APCs, Ag) and the different subsets of T-cells studied[38–40].

Altogether, we showed that CXCL4 plays a critical role in priming aberrant inflammatory responses on DCs and T-cells, which have been implicated in the pathogenesis of autoimmune diseases where CXCL4 is implicated.

CXCL4-mediated regulation at the transcriptional and epigenetic levels

Rather few studies have extensively explored the role of CXCL4 in monocyte-derived cells, especially moDCs. Overall, it was reported that CXCL4 strictly changes the differentiation and function of immune and non-immune cells[22,41–43], although the underlying molecular mechanisms remain poorly investigated [44,45].

Differentiation and maturation of moDCs is followed by dramatic changes at the transcriptomic and epigenetic level [46]. Environmental disturbances in the immune micro milieu play a critical role in epigenetic modifications, for instance at the DNA methylation level. These modifications ultimately result in the regulation of inflammatory gene expression and were associated with infection and autoimmune diseases [47,48].

To gain insights into the molecular mechanisms that underlie the effects of CXCL4 exposure on moDCs, in **Chapter 4** we performed transcriptomic and DNA methylation analyses of 65 paired longitudinal samples throughout differentiation and polyI:C stimulation of moDCs and CXCL4-moDCs. Remarkably, we observed that CXCL4 exposure drives extensive transcriptional and epigenetic remodelling of moDC phenotype and function. We identified key immune (TLR-signalling) and non-immune (e.g. metabolism, ECM remodelling) associated pathways modulated by CXCL4 during the differentiation and stimulation of moDCs. Remarkably, we validated the overexpression or down-regulation of several inflammatory (e.g. CCL3, IL6) and fibrotic mediators, such as fibronectin (FN1) and TGFβ on the protein level, bringing forward the implication of inflammatory DCs in inflammatory and fibrotic disorders.

Additionally, we investigated whether secreted mediators by CXCL4-moDCs contribute to induce and maintain the positive loop of inflammatory and fibrotic responses by fibroblasts, an important cell subset implicated in the pathology of SSc [49]. Fibroblasts serve pivotal roles in ECM remodelling, wound healing, angiogenesis and inflammation. However, uncontrolled activation of fibroblasts results in pathological fibrotic and inflammatory responses that promote cancer progression or fibrotic-mediated diseases. Strikingly, we observed that co-culture of fibroblasts with cell-free supernatants from stimulated CXCL4-moDCs, induced myofibroblast transition and increased expression of inflammatory (e.g. IL8, IL6) and fibrotic mediators (e.g. FN1, αSMA), which are implicated in the pathogenesis of SSc.

Overall, we showed that CXCL4 drives inflammatory and fibrotic responses both directly in moDCs and indirectly in dermal fibroblasts. Thus, we propose a novel role for inflammatory DCs in promoting and sustaining pro-fibrotic conditions.

Interestingly, also DNA methylation analysis revealed that CXCL4 drives considerable changes (mostly hypermethylation) of genes associated with immune responses and ECM remodelling. Surprisingly, in contrary to the findings on the transcriptomic level, polyI:C stimulation of moDCs and CXCL4-moDCs did not induce changes on DNA methylation. Although, more than 5000 genes were found differently methylated between polyI:C stimulated moDCs and CXCL4-moDCs. Our results are supported by the findings of Vento-Tormo et al., showing that changes in DNA methylation occur mostly during moDC differentiation, but not after LPS stimulation [46]. Thus, we hypothesize that CXCL4-driven inflammatory and fibrotic responses are epigenetically imprinted during moDC differentiation.

In support, we observed dynamic changes in the transcription of the DNA methyltransferases (DNMT1, DNMT3A) and DNA demethylases (TET2, TET3), which indicate possible mechanisms contributing for the more pronounced loss in DNA methylation driven by the exposure to CXCL4. In fact, epigenetic aberrancies, including those occurring at the DNA methylation level, have been implicated in the pathology of SSc [50–52]. Despite the accumulating evidences showing that alterations in DNA methylation cause aberrant gene expression and influence the development or progression of autoimmune disorders, the complete understanding on the underling mechanisms remain debatable. [46,47,53].

In our experimental setting, we observed lack of correlation between DNA methylation and RNA expression at the level of differently expressed genes between moDCs and CXCL4-moDCs. However, we observed both positive and negative correlations between DNA methylation and RNA expression levels when we analysed the overall genome. Moreover, we developed a new methodology, named RegEnrich, to identify the underlying complexity and interconnectivity of signalling pathways reprogrammed by CXCL4. For this purpose, genes were clustered into distinct modules based on their co-expression or co-methylation patterns. CXCL4-correlated modules were associated predominantly with ECM organization, metabolic reprogramming, Ag processing and cytokine signalling. Still, we found very low overlap between CXCL4-moDC specific co-expression and co-methylation modules, suggesting that in these experimental settings, DNA methylation has little influence on CXCL4-mediated transcriptional changes.

There is increasing evidence that DNA methylation levels are quickly disturbed in response to environmental signals [54–57]. Also, Pacis and colleagues have shown that stimulation of moDCs with *Mycobacterium tuberculosis* (MTB) results in dramatic transcriptomic changes, which in certain conditions gene expression activation preceded detectable DNA methylation changes[47]. Thus, we hypothesize that these processes may contribute for the poor correlation between DNA methylation and RNA expression levels for CXCL4-signature genes analysed in our experimental time-course.

Besides the epigenetic programming, transcription regulators play a critical regulatory function in modulating their downstream target genes. Gene regulatory network analysis revealed that CXCL4 modulate key transcription regulators such as CIITA (class II major histocompatibility complex transactivator) and IRF8 (interferon regulatory factor 8), among others. To mimic the down-regulation of CIITA on CXCL4-moDCs, siRNA-mediated knockdown of CIITA resulted on upregulation of inflammatory and ECM remodelling genes, such as FN1.

The transcriptional co-activator CIITA is the master regulator of MHC-II genes [58]. CIITA impairment is associated with diminished MHC gene expression and susceptibility to autoimmune diseases such as Type II bare lymphocyte syndrome, RA and cancer[59–61]. Interestingly, interferon γ (IFN-γ), which plays a pivotal role in the development and severity of autoimmune diseases [62,63], induces up-regulation of CIITA. In turn, CIITA mediates IFN-γ- induced repression of collagen (*COL1A2*) transcription [64–67]. These represent critical mechanisms that control inflammation, development of scars and fibrosis.

Furthermore, triggering of immature moDCs with distinct stimuli results in rapid reduction in the synthesis of CIITA mRNA and protein. This is accompanied by transcriptional silencing of MHC-II mRNA, while the expression of cell surface molecules remain increased during the maturation of DC [68]. In line with previous reports, we hypothesize that CXCL4-mediated activation of moDCs results in up-regulation of MHC-II protein expression of cell surface and down-regulation of MHC-II mRNA expression as a consequence of CXCL4-driven transcriptional silencing of CIITA. Moreover, we propose that silencing of CIITA is also directly or indirectly associated to up-regulation of molecules involved in inflammatory and fibrotic responses. Further research on the implication of CIITA in the pathogenesis of SSc will provide new insights on possible therapeutic avenues.

Altogether, we underscored CXCL4-downstream signalling pathways on moDCs and the pivotal contribution of transcriptional regulators such as CIITA on CXCL4-mediated reprogramming of moDC function.

Impairment of tolerogenic signature – molecular marks that define DCs exposed to CXCL4

DC immune function strictly depends on the local micro milieu and inflammatory stimuli, which ultimately defines their activation state. Thus, tissue resident immature DCs acquire immunogenic properties, which promote immune responses, or tolerogenic properties, which contribute to the maintenance of peripheral tolerance [69]. In turn, several protocols have been optimized for the *in vitro* generation

of DCs with either immunogenic or tolerogenic functions, and candidate molecules that are associated with their functions have been characterized [70–72]. In line with our previous results, in **Chapter 5** we showed that exposure of moDCs to CXCL4 amplified the expression of several activation and co-stimulatory molecules involved in inflammatory responses. However, molecules associated with tolerogenic DC function were abrogated. Interestingly, we showed that CXCL4 dramatically down-regulated the expression and production of C1q, a DC regulatory marker [73,74]. These findings are in line with previous observations showing that *in vivo* and *in vitro* stimulation of DCs with inflammatory triggers abrogates C1q production [75].

C1q is the first component of the classical complement pathway and plays a critical function as an opsonin involved in the recognition and phagocytosis of PAMPs and apoptotic cell fragments[76,77]. C1q deficiency in human and mice is associated with infections and autoimmune conditions, such as Systemic Lupus Erythematosus [78–80].

Additionally, we investigated whether CXCL4 epigenetically modulated molecules associated with immunogenic and tolerogenic functions. Several tolerogenic genes, inclusively C1q, were hypermethylated in CXCL4-moDCs, and we found strong negative correlation between their mRNA expression and DNA methylation levels. Particularly, the significantly up-regulated immunogenic markers between moDCs and CXCL4-moDCs were also hypermethylated, thus not displaying negative correlation between mRNA expression and DNA methylation levels. Therefore, on one hand we hypothesize that CXCL4-mediated transcriptional repression of C1q, among other tolerogenic markers, may be explained by epigenetic regulatory mechanisms, such as strong hypermethylation observed on CXCL4-moDCs. On the other hand, alternative transcriptional and epigenetic mechanisms of regulation may be implicated in the CXCL4-reprograming of immunogenic marks. Prospectively, we reveal C1q a potential biomarker associated with CXCL4-driven autoimmune conditions. Future research should further investigate the implication of CXCL4-mediated impairment of C1q in the pathogenesis of SSc.

CXCL4 regulation of cytokine production at the post-transcriptional level

In Chapter 2 we described for the first time that CXCL4 potentiates the production of inflammatory cytokines in moDCs upon stimulation with polyI:C, a TLR3 agonist. Multiple studies reported that inflammatory cytokines are regulated at the transcriptional level, but also at post-transcriptional level through mechanisms that control, for instance, mRNA stability[81–84]. The regulation of mRNA stability is crucial to control cytokine production during inflammatory responses[85,86]. In **Chapter 6** we

explored the transcriptional and post-transcriptional mechanisms underlying the aberrant production of pro-inflammatory cytokines in stimulated CXCL4-moDCs. We found that the enhanced production of IL-6 and TNF, but not IL-12 and IL-23, was a consequence of enhanced cytokine mRNA stability. Based on this evidence, we investigated whether CXCL4-signaling affects *trans*-acting AU-rich element binding proteins (ARE-BPs), which are crucial players in the regulation of mRNA stability. We observed that IL-6 and TNF mRNA stabilization was a result of the inactivation of the RNA-binding protein tristetraprolin (TTP). In line with these findings, siRNA-mediated knockdown of TTP, used to mimic TTP inactivation, resulted in enhanced *IL6* and *TNF* expression in polyI:C-stimulated moDCs, however it failed to upregulate *IL12B* and *IL23A*. Thus, in our investigation setting, aberrant production of IL-12 and IL-23 by CXCL4-moDCs is majorly mediated by transcriptional regulatory mechanisms. Supporting our observations, several studies showed that deregulated expression and activity of TTP are associated with aberrant inflammatory conditions. Indeed, TTP play a key role in the regulation of adenosine uridine (AU)-rich elements (ARE)- and non-ARE- enriched genes with a critical function for DC maturation in response to TLR agonists [87]. In addition, human and mice studies reported the implication of disturbed TTP function in aberrant inflammatory responses and the contribution to autoimmune conditions[88–92].

Mitogen-activated protein kinases (MAPKs) play a critical role in inflammation and tissue damage by regulating cytokines at the post-transcriptional level [88,93,94]. Inclusively, TTP is regulated by MAPK signaling pathways, which promote TTP phosphorylation and subsequent inactivation [84,88,95]. We observed that p38 inhibition restores TTP function and decreases cytokine production in CXCL4-moDCs. Thus, we hypothesize that MAPK-p38 signalling plays a key function in CXCL4-induced cytokine production upon polyI:C stimulation in moDCs, and mediates TTP phosphorylation.

Disturbances in mRNA regulation are implicated in chronic inflammation and cancer [96–100]. Our results highlight the critical role of CXCL4 on post-transcriptional regulation of cytokine mRNA stability, and provide new insights on the mechanisms that contribute to the development of CXCL4-mediated autoimmune conditions. Thus, we could possibly suggest future investigations on the contribution of mRNA stability regulation in the pathology of SSc.

Conclusion and future perspectives

CXCL4 is implicated in the modulation of immune cell responses and is associated with several autoimmune conditions. However the underlying mechanisms by which CXCL4 contribute to aberrant inflammatory and fibrotic responses remains under

investigation. Altogether, we propose CXCL4 as disease-associated endogenous ligand that promotes DC trained immunity by inducing the sensitization of cells to pursue fast and strong innate and adaptive immune responses. Additionally, our results provide new evidences on how CXCL4 amplifies pro-inflammatory and pro-fibrotic responses observed in autoimmune diseases where CXCL4 has been implicated, such as SSc and PsA. Thus, we propose a novel function for CXCL4-derived inflammatory DCs in promoting aberrant inflammatory and pro-fibrotic responses, alongside with monocytes, macrophages and fibroblasts, which are also implicated in the pathogenesis of SSc[49,101,102]. We identified and validated for the first time CXCL4-downstream pathways and master regulators on moDCs that may represent potential targets for therapeutic intervention. Due to the critical role of CXCL4 in biological processes such as coagulation and wound healing, research efforts in this regard will allow to target key molecules downstream to CXCL4 signalling that possible represent a more effective strategy. Due to the differences on the CXCL4 receptor among the immune and non-immune cells, upcoming research on therapeutic targets should explore the combination of therapies targeting directly CXCL4, the receptor of CXCL4 and master inflammatory and fibrotic regulatory genes downstream to CXCL4 signalling.

In future studies, to complement our transcriptome and DNA methylation analysis, it would be of high interest to investigate the effects of CXCL4 on microRNAs, long non-coding RNAs (lncRNAs) and histone modifications, which are also epigenetic mechanisms implicated in gene regulation. Ideally, the future validation of our findings in mice models and patients would bring strength to our results.

References

1. Vandercappellen, J., Van Damme, J. & Struyf, S. The role of the CXC chemokines platelet factor-4 (CXCL4/PF-4) and its variant (CXCL4L1/PF-4var) in inflammation, angiogenesis and cancer. *Cytokine Growth Factor Rev.* **22,** 1–18 (2011).
2. van Bon, L. *et al.* Proteome-wide analysis and CXCL4 as a biomarker in systemic sclerosis. *N. Engl. J. Med.* **370,** 433–43 (2014).
3. Kioon, M. D. A. *et al.* Plasmacytoid dendritic cells promote systemic sclerosis with a key role for TLR8. *Sci. Transl. Med.* **10,** (2018).
4. Lande, R. *et al.* CXCL4 assembles DNA into liquid crystalline complexes to amplify TLR9-mediated interferon-α production in systemic sclerosis. *Nat. Commun.* **10,** (2019).
5. Volkmann, E. R. *et al.* Changes in plasma CXCL4 levels are associated with improvements in lung function in patients receiving immunosuppressive therapy for systemic sclerosis-related interstitial lung disease. *Arthritis Res. Ther.* **18,** (2016).
6. Haddon, D. J. *et al.* Proteomic analysis of sera from individuals with diffuse cutaneous systemic sclerosis reveals a multianalyte signature associated with clinical improvement during imatinib mesylate treatment. *J. Rheumatol.* **44,** 631–638 (2017).
7. Tamagawa-Mineoka, R., Katoh, N., Ueda, E., Masuda, K. & Kishimoto, S. Elevated Platelet Activation in Patients with Atopic Dermatitis and Psoriasis: Increased Plasma Levels of β-Thromboglobulin and Platelet Factor 4. *Allergol. Int.* **57,** 391–396 (2008).
8. Yeo, L. *et al.* Expression of chemokines CXCL4 and CXCL7 by synovial macrophages defines an early stage of rheumatoid arthritis. *Ann. Rheum. Dis.* **75,** 763–71 (2016).
9. Pitsilos, S. *et al.* Platelet factor 4 localization in carotid atherosclerotic plaques: correlation with clinical parameters. *Thromb. Haemost.* **90,** 1112–1120 (2003).
10. Agache, I., Radoi, M. & Duca, L. Platelet activation in patients with systemic scleroderma--pattern and significance. *Rom. J. Intern. Med.* **45,** 183–191 (2007).
11. Ramirez, G. a *et al.* The role of platelets in the pathogenesis of systemic sclerosis. *Front. Immunol.* **3,** 160 (2012).
12. Affandi, A. J., Carvalheiro, T., Radstake, T. R. D. J. & Marut, W. Dendritic cells in systemic sclerosis: Advances from human and mice studies. *Immunology Letters* **195,** 18–29 (2018).
13. Rossato, M. *et al.* Association of MicroRNA-618 Expression With Altered Frequency and Activation of Plasmacytoid Dendritic Cells in Patients With Systemic Sclerosis. *Arthritis Rheumatol.* **69,** 1891–1902 (2017).
14. Chiang, T. M., Takayama, H. & Postlethwaite, A. E. Increase in platelet non-integrin type I collagen receptor in patients with systemic sclerosis. *Thromb. Res.* **117,** 299–306 (2006).
15. Postlethwaite, A. E. & Chiang, T. M. Platelet contributions to the pathogenesis of systemic sclerosis. *Current Opinion in Rheumatology* **19,** 574–579 (2007).
16. Ciechomska, M. *et al.* Toll-like receptor-mediated, enhanced production of profibrotic TIMP-1 in monocytes from patients with systemic sclerosis: role of serum factors. *Ann Rheum Dis* **72,** 1382–1389 (2013).
17. Broen, J. C. a *et al.* A rare polymorphism in the gene for Toll-like receptor 2 is associated with systemic sclerosis phenotype and increases the production of inflammatory mediators. *Arthritis Rheum.* **64,** 264–71 (2012).
18. Van Bon, L. *et al.* Distinct evolution of TLR-mediated dendritic cell cytokine secretion in patients with limited and diffuse cutaneous systemic sclerosis. *Ann. Rheum. Dis.* **69,** 1539–1547 (2010).

19. Van Lieshout, A. W. T. *et al.* Enhanced interleukin-10 production by dendritic cells upon stimulation with Toll-like receptor 4 agonists in systemic sclerosis that is possibly implicated in CCL18 secretion. *Scand. J. Rheumatol.* **38,** 282–290 (2009).
20. Kurasawa, K. *et al.* Increased interleukin-17 production in patients with systemic sclerosis. *Arthritis Rheum.* **43,** 2455–2463 (2000).
21. O'Reilly, S., Hügle, T. & Van Laar, J. M. T cells in systemic sclerosis: A reappraisal. *Rheumatology (United Kingdom)* **51,** 1540–1549 (2012).
22. Xia, C.-Q. & Kao, K.-J. Effect of CXC chemokine platelet factor 4 on differentiation and function of monocyte-derived dendritic cells. *Int. Immunol.* **15,** 1007–1015 (2003).
23. Van Bon, L. *et al.* Proteomic analysis of plasma identifies the Toll-like receptor agonists S100A8/A9 as a novel possible marker for systemic sclerosis phenotype. *Ann. Rheum. Dis.* **73,** 1585–1589 (2014).
24. Farina, G. A. *et al.* Poly(I:C) drives type i IFN- and TGFB-mediated inflammation and dermal fibrosis simulating altered gene expression in systemic sclerosis. *J. Invest. Dermatol.* **130,** 2583–2593 (2010).
25. Agarwal, S. K. *et al.* Toll-like receptor 3 upregulation by type I interferon in healthy and scleroderma dermal fibroblasts. *Arthritis Res. Ther.* **13,** R3 (2011).
26. Parel, Y. *et al.* Presence of CD4+CD8+ double-positive T cells with very high interleukin-4 production potential in lesional skin of patients with systemic sclerosis. *Arthritis Rheum.* **56,** 3459–3467 (2007).
27. Li, G. *et al.* Skin-Resident Effector Memory CD8+CD28– T Cells Exhibit a Profibrotic Phenotype in Patients with Systemic Sclerosis. *J. Invest. Dermatol.* **137,** 1042–1050 (2017).
28. Fuschiotti, P., Larregina, A. T., Ho, J., Feghali-Bostwick, C. & Medsger, T. A. Interleukin-13-producing CD8+ T cells mediate dermal fibrosis in patients with systemic sclerosis. *Arthritis Rheum.* **65,** 236–246 (2013).
29. Mavalia, C. *et al.* Type 2 helper T-cell predominance and high CD30 expression in systemic sclerosis. *Am. J. Pathol.* **151,** 1751–8 (1997).
30. Yang, X., Yang, J., Xing, X., Wan, L. & Li, M. Increased frequency of Th17 cells in systemic sclerosis is related to disease activity and collagen overproduction. *Arthritis Res. Ther.* **16,** (2014).
31. Radstake, T. R. D. J. *et al.* The pronounced Th17 profile in systemic sclerosis (SSc) together with intracellular expression of TGF?? and IFN?? distinguishes SSc phenotypes. *PLoS One* **4,** (2009).
32. Segura, E. *et al.* Human Inflammatory Dendritic Cells Induce Th17 Cell Differentiation. *Immunity* **38,** 336–348 (2013).
33. Gerdes, N. *et al.* Platelets regulate CD4+ T-cell differentiation via multiple chemokines in humans. *Thromb. Haemost.* **106,** 353–362 (2011).
34. Annunziato, F., Cosmi, L., Liotta, F., Maggi, E. & Romagnani, S. Human Th17 cells: Are they different from murine Th17 cells? *Eur. J. Immunol.* **39,** 637–640 (2009).
35. Fang, S. *et al.* Platelet Factor 4 Inhibits IL-17/Stat3 Pathway via Upregulation of SOCS3 Expression in Melanoma. *Inflammation* **37,** 1744–1750 (2014).
36. Shi, G. *et al.* Platelet factor 4 limits Th17 differentiation and cardiac allograft rejection. *J. Clin. Invest.* **124,** 543–552 (2014).
37. Noster, R. *et al.* IL-17 and GM-CSF expression are antagonistically regulated by human T helper cells. *Sci. Transl. Med.* **6,** (2014).
38. Fleischer, J. *et al.* Platelet Factor 4 Inhibits Proliferation and Cytokine Release of Activated Human T Cells. *J. Immunol.* **169,** 770–777 (2002).
39. Romagnani, P. *et al.* CXCR3-mediated opposite effects of CXCL10 and CXCL4 on TH1 or TH2 cytokine production. *J. Allergy Clin. Immunol.* **116,** 1372–1379 (2005).

40. Liu, C. Y. *et al.* Platelet factor 4 differentially modulates CD4+CD25+ (regulatory) versus CD4+CD25- (nonregulatory) T cells. *J. Immunol.* **174,** 2680–2686 (2005).
41. Fricke, I. *et al.* Platelet factor 4 in conjunction with IL-4 directs differentiation of human monocytes into specialized antigen-presenting cells. *FASEB J.* **18,** 1588–90 (2004).
42. Scheuerer, B. *et al.* The CXC-chemokine platelet factor 4 promotes monocyte survival and induces monocyte differentiation into macrophages. *Blood* **95,** 1158–1166 (2000).
43. Gouwy, M. *et al.* CXCL4 and CXCL4L1 Differentially Affect Monocyte Survival and Dendritic Cell Differentiation and Phagocytosis. *PLoS One* **11,** e0166006 (2016).
44. Kasper, B., Brandt, E., Brandau, S. & Petersen, F. Platelet Factor 4 (CXC Chemokine Ligand 4) Differentially Regulates Respiratory Burst, Survival, and Cytokine Expression of Human monocyes by Using Distinct Signaling Pathways. *J. Immunol.* **179,** 2584–2591 (2007).
45. Gleissner, C. A., Shaked, I., Little, K. M. & Ley, K. CXC Chemokine Ligand 4 Induces a Unique Transcriptome in Monocyte-Derived Macrophages. *J. Immunol.* **184,** 4810–4818 (2010).
46. Vento-Tormo, R. *et al.* IL-4 orchestrates STAT6-mediated DNA demethylation leading to dendritic cell differentiation. *Genome Biol.* **17,** (2016).
47. Pacis, A. *et al.* Bacterial infection remodels the DNA methylation landscape of human dendritic cells. *Genome Res.* **25,** 1801–1811 (2015).
48. Wang, X. *et al.* A DNA-Methylated Sight on Autoimmune Inflammation Network across RA, pSS, and SLE. *J. Immunol. Res.* **2018,** 1–13 (2018).
49. Kendall, R. T. & Feghali-Bostwick, C. A. Fibroblasts in fibrosis: Novel roles and mediators. *Frontiers in Pharmacology* **5 MAY,** (2014).
50. Altorok, N., Tsou, P. S., Coit, P., Khanna, D. & Sawalha, A. H. Genome-wide DNA methylation analysis in dermal fibroblasts from patients with diffuse and limited systemic sclerosis reveals common and subset-specific DNA methylation aberrancies. *Ann. Rheum. Dis.* **74,** 1612–1620 (2015).
51. Hattori, M. *et al.* Global DNA hypomethylation and hypoxia-induced expression of the ten eleven translocation (TET) family, TET1, in scleroderma fibroblasts. *Exp. Dermatol.* **24,** 841–846 (2015).
52. Lei, W. *et al.* Abnormal DNA methylation in CD4+ T cells from patients with systemic lupus erythematosus, systemic sclerosis, and dermatomyositis. *Scand. J. Rheumatol.* **38,** 369–374 (2009).
53. Moarii, M., Boeva, V., Vert, J. P. & Reyal, F. Changes in correlation between promoter methylation and gene expression in cancer. *BMC Genomics* **16,** (2015).
54. Klug, M. *et al.* Active DNA demethylation in human postmitotic cells correlates with activating histone modifications, but not transcription levels. *Genome Biol.* **11,** (2010).
55. Guo, J. U. *et al.* Neuronal activity modifies the DNA methylation landscape in the adult brain. *Nat. Neurosci.* **14,** 1345–1351 (2011).
56. Dowen, R. H. *et al.* Widespread dynamic DNA methylation in response to biotic stress. *Proc. Natl. Acad. Sci. U. S. A.* **109,** E2183-91 (2012).
57. Marr, A. K. *et al.* Leishmania donovani Infection Causes Distinct Epigenetic DNA Methylation Changes in Host Macrophages. *PLoS Pathog.* **10,** (2014).
58. Devaiah, B. N. & Singer, D. S. CIITA and its dual roles in MHC gene transcription. *Front. Immunol.* **4,** (2013).
59. Steimle, V., Otten, L. A., Zufferey, M. & Mach, B. Complementation cloning of an MHC class II transactivator mutated in hereditary MHC class II deficiency (or bare lymphocyte syndrome). *Cell* **75,** 135–146 (1993).
60. Vora, A. R. *et al.* An immunohistochemical study of altered immunomodulatory molecule expression in head and neck squamous cell carcinoma. *Br. J. Cancer* **76,** 836–844 (1997).

61. Swanberg, M. *et al.* MHC2TA is associated with differential MHC molecule expression and susceptibility to rheumatoid arthritis, multiple sclerosis and myocardial infarction. *Nat. Genet.* **37,** 486–494 (2005).
62. Hu, X. & Ivashkiv, L. B. Cross-regulation of Signaling Pathways by Interferon-γ: Implications for Immune Responses and Autoimmune Diseases. *Immunity* **31,** 539–550 (2009).
63. Pollard, K. M., Cauvi, D. M., Toomey, C. B., Morris, K. V & Kono, D. H. Interferon-γ and systemic autoimmunity. *Discov. Med.* **16,** 123–31 (2013).
64. Xu, Y., Wang, L., Butticè, G., Sengupta, P. K. & Smith, B. D. Major histocompatibility class II transactivator (CIITA) mediates repression of collagen (COL1A2) transcription by interferon γ (IFN-γ). *J. Biol. Chem.* **279,** 41319–41332 (2004).
65. Xu, Y. *et al.* Collagen and major histocompatibility class II expression in mesenchymal cells from CIITA hypomorphic mice. *Mol. Immunol.* **44,** 1709–1721 (2007).
66. Zhu, X.-S. & Ting, J. P.-Y. A 36-Amino-Acid Region of CIITA Is an Effective Inhibitor of CBP: Novel Mechanism of Gamma Interferon-Mediated Suppression of Collagen 2(I) and Other Promoters. *Mol. Cell. Biol.* **21,** 7078–7088 (2001).
67. Sengupta, P. K., Fargo, J. & Smith, B. D. The RFX family interacts at the collagen (COL1A2) start site and represses transcription. *J. Biol. Chem.* **277,** 24926–24937 (2002).
68. Landmann, S. *et al.* Maturation of Dendritic Cells Is Accompanied by Rapid Transcriptional Silencing of Class II Transactivator (Ciita) Expression. *J. Exp. Med.* **194,** 379–392 (2002).
69. Lewis, K. L. & Reizis, B. Dendritic cells: Arbiters of immunity and immunological tolerance. *Cold Spring Harb. Perspect. Biol.* **4,** (2012).
70. Schinnerling, K., García-González, P. & Aguillón, J. C. Gene expression profiling of human monocyte-derived dendritic cells - Searching for molecular regulators of tolerogenicity. *Frontiers in Immunology* **6,** (2015).
71. Navarro-Barriuso, J., Mansilla, M. J. & Martínez-Cáceres, E. M. Searching for the transcriptomic signature of immune tolerance induction-biomarkers of safety and functionality for tolerogenic dendritic cells and regulatory macrophages. *Frontiers in Immunology* **9,** (2018).
72. Gordon, J. R., Ma, Y., Churchman, L., Gordon, S. A. & Dawicki, W. Regulatory dendritic cells for immunotherapy in immunologic diseases. *Frontiers in Immunology* **5,** (2014).
73. Zimmer, A. *et al.* A regulatory dendritic cell signature correlates with the clinical efficacy of allergen-specific sublingual immunotherapy. *J. Allergy Clin. Immunol.* **129,** 1020–1030 (2012).
74. Torres-Aguilar, H. *et al.* Tolerogenic Dendritic Cells Generated with Different Immunosuppressive Cytokines Induce Antigen-Specific Anergy and Regulatory Properties in Memory CD4 + T Cells . *J. Immunol.* **184,** 1765–1775 (2010).
75. Castellano, G. *et al.* Maturation of dendritic cells abrogates C1q production in vivo and in vitro. *Blood* **103,** 3813–3820 (2004).
76. Taylor, P. R. *et al.* A Hierarchical Role for Classical Pathway Complement Proteins in the Clearance of Apoptotic Cells in Vivo. *J. Exp. Med.* **192,** 359–366 (2000).
77. Ogden, C. A. *et al.* C1q and Mannose Binding Lectin Engagement of Cell Surface Calreticulin and Cd91 Initiates Macropinocytosis and Uptake of Apoptotic Cells. *J. Exp. Med.* **194,** 781–796 (2001).
78. Ling, G. S. *et al.* C1q restrains autoimmunity and viral infection by regulating CD8+ T cell metabolism. *Science (80-.).* **360,** 558–563 (2018).
79. Schaller, M., Bigler, C., Danner, D., Ditzel, H. J. & Trendelenburg, M. Autoantibodies against C1q in Systemic Lupus Erythematosus Are Antigen-Driven. *J. Immunol.* **183,** 8225–8231 (2009).
80. Botto, M. *et al.* Homozygous C1q deficiency causes glomerulonephritis associated with multiple apoptotic bodies. *Nat. Genet.* **19,** 56–59 (1998).

81. Carballo, E. Feedback Inhibition of Macrophage Tumor Necrosis Factor-Production by Tristetraprolin. *Science (80-.).* **281,** 1001–1005 (1998).
82. Molle, C. *et al.* Tristetraprolin regulation of interleukin 23 mRNA stability prevents a spontaneous inflammatory disease. *J. Exp. Med.* **210,** 1675–1684 (2013).
83. Tudor, C. *et al.* The p38 MAPK pathway inhibits tristetraprolin-directed decay of interleukin-10 and pro-inflammatory mediator mRNAs in murine macrophages. *FEBS Lett.* **583,** 1933–1938 (2009).
84. Brooks, S. A. & Blackshear, P. J. Tristetraprolin (TTP): Interactions with mRNA and proteins, and current thoughts on mechanisms of action. *Biochimica et Biophysica Acta - Gene Regulatory Mechanisms* **1829,** 666–679 (2013).
85. Barreau, C., Paillard, L. & Osborne, H. B. AU-rich elements and associated factors: Are there unifying principles? *Nucleic Acids Research* **33,** 7138–7150 (2005).
86. Stoecklin, G. & Anderson, P. In a tight spot: ARE-mRNAs at processing bodies. *Genes and Development* **21,** 627–631 (2007).
87. Emmons, J. *et al.* Identification of TTP mRNA targets in human dendritic cells reveals TTP as a critical regulator of dendritic cell maturation. *RNA* **14,** 888–902 (2008).
88. Kratochvill, F. *et al.* Tristetraprolin-driven regulatory circuit controls quality and timing of mRNA decay in inflammation. *Mol. Syst. Biol.* **7,** (2011).
89. Qiu, L.-Q., Stumpo, D. J. & Blackshear, P. J. Myeloid-Specific Tristetraprolin Deficiency in Mice Results in Extreme Lipopolysaccharide Sensitivity in an Otherwise Minimal Phenotype. *J. Immunol.* **188,** 5150–5159 (2012).
90. Angiolilli, C. *et al.* Control of cytokine mRNA degradation by the histone deacetylase inhibitor ITF2357 in rheumatoid arthritis fibroblast-like synoviocytes: Beyond transcriptional regulation. *Arthritis Res. Ther.* **20,** (2018).
91. Qian, X. *et al.* Posttranscriptional Regulation of IL-23 Expression by IFN- through Tristetraprolin. *J. Immunol.* **186,** 6454–6464 (2011).
92. Ross, E. A. *et al.* Treatment of inflammatory arthritis via targeting of tristetraprolin, a master regulator of pro-inflammatory gene expression. *Ann. Rheum. Dis.* **76,** 612–619 (2017).
93. Mahtani, K. R. *et al.* Mitogen-Activated Protein Kinase p38 Controls the Expression and Posttranslational Modification of Tristetraprolin, a Regulator of Tumor Necrosis Factor Alpha mRNA Stability. *Mol. Cell. Biol.* **21,** 6461–6469 (2002).
94. Ross, E. A. *et al.* Dominant Suppression of Inflammation via Targeted Mutation of the mRNA Destabilizing Protein Tristetraprolin. *J. Immunol.* **195,** 265–276 (2015).
95. Sandler, H. & Stoecklin, G. Control of mRNA decay by phosphorylation of tristetraprolin. *Biochem. Soc. Trans.* **36,** 491–496 (2008).
96. Brooks, S. A., Connolly, J. E., Diegel, R. J., Fava, R. A. & Rigby, W. F. C. Analysis of the function, expression, and subcellular distribution of human tristetraprolin. *Arthritis Rheum.* **46,** 1362–1370 (2002).
97. Huang, L. *et al.* Interaction with Pyruvate Kinase M2 Destabilizes Tristetraprolin by Proteasome Degradation and Regulates Cell Proliferation in Breast Cancer. *Sci. Rep.* **6,** (2016).
98. Khabar, K. S. A. Post-transcriptional control during chronic inflammation and cancer: A focus on AU-rich elements. *Cellular and Molecular Life Sciences* **67,** 2937–2955 (2010).
99. Seko, Y., Cole, S., Kasprzak, W., Shapiro, B. A. & Ragheb, J. A. The role of cytokine mRNA stability in the pathogenesis of autoimmune disease. *Autoimmunity Reviews* **5,** 299–305 (2006).
100. Zhang, H. *et al.* MRNA-binding protein ZFP36 is expressed in atherosclerotic lesions and reduces inflammation in aortic endothelial cells. *Arterioscler. Thromb. Vasc. Biol.* **33,** 1212–1220 (2013).
101. Higashi-Kuwata, N. *et al.* Characterization of monocyte/macrophage subsets in the skin and peripheral blood derived from patients with systemic sclerosis. *Arthritis Res. Ther.* **12,** (2010).
102. Ishikawa, O. & Ishikawa, H. Macrophage infiltration in the skin of patients with systemic sclerosis. *J. Rheumatol.* **19,** 1202–1206 (1992).

7

Appendix

English summary
Nederlandse samenvatting
Acknowledgments
Curriculum vitae
List of publications

A

English Summary

CXCL4 (also known as platelet factor 4, PF4) is a chemokine involved in physiological processes that include blood coagulation, inhibition of haematopoiesis and reprogramming of the immune responses. High levels of CXCL4, both in circulation and within inflammatory tissues, were previously associated with multiple autoimmune diseases such as Rheumatoid Arthritis (RA) and Sjögren's Syndrome (SS). Importantly, our group identified CXCL4 as a biomarker of Systemic Sclerosis (SSc).

SSc is an heterogeneous disorder characterised by several hallmarks, including vasculopathy, immune cell dysfunction, antibodies production and aberrant deposition of extracellular matrix components (ECM), such as fibronectin. Among the different immune cell subsets that may contribute to SSc pathology, dendritic cells (DCs) were shown to display exacerbated TLR-mediated responses in SSc patients. Also, DC infiltrates were observed in SSc fibrotic tissues, along with T-cells typically displaying a Th2 and Th17 phenotype.

The aim of this PhD thesis was to clarify the role of CXCL4 in steering immune responses, and to unravel the molecular mechanisms modulated by CXCL4 that contribute to chronic inflammatory and fibrotic aberrant responses in SSc. The identification of CXCL4-modulated targets is a necessary step for the development of therapeutic strategies aimed at diseases where CXCL4 is implicated.

CXCL4 potentiate innate and adaptive immune responses

CXCL4 modulates DC and T-cell phenotype and function. In **Chapter 2** we elucidated the role of CXCL4 in steering innate and adaptive immune responses in human DCs derived from monocytes (moDCs). We showed that CXCL4 drives the up-regulation of co-stimulatory and maturation molecules in moDCs, which we used as a model of inflammatory DCs. Additionally, we observed for the first time that exposure of moDCs to CXCL4 during differentiation primes cells to aberrant production of pro-inflammatory cytokines upon TLR3 (polyI:C) or TLR7/8 (R848 and CL075) triggering. Moreover, we showed that CXCL4-moDCs potentiate the activation of autologous $CD4^+$ and $CD8^+$ T-cell responses, as well as antigen specific $CD8^+$ T-cell inflammatory responses.

High levels of CXCL4 have been associated with Th17-associated inflammatory diseases, such as RA, psoriasis and SSc. Thus, in **Chapter 3,** we investigated the role of CXCL4 in T-cell activation and skewing Th17 differentiation. We showed that CXCL4 promotes the activation of $CD4^+$ T-cells towards IL17-producing cells, either upon

CD3/CD28 stimulation or in co-culture experiments with monocytes, myeloid DCs (mDCs) and CXCL4-moDCs. In order to elucidate how CXCL4 levels associate with IL-17 production in psoriatic arthritis (PsA), a Th17-mediated disease, we measured CXCL4 and IL-17 levels in plasma and synovial fluid from PsA patients. We found that CXCL4 is increased in the circulation of PsA patients, and CXCL4 levels strongly correlate with IL-17 levels in synovial fluid.

CXCL4-driven immunogenic and fibrotic functions are regulated at transcriptional, post-transcriptional and epigenetic levels

In order to assess the molecular mechanisms that underlie the effects of CXCL4 on morphology, phenotype, and function of moDCs, in **Chapter 4** we performed whole genome transcriptome and methylation analysis of moDCs and CXCL4-moDCs, both during differentiation and after stimulation with polyI:C.

We described that CXCL4 drives dramatic changes in transcription and DNA methylation, disturbing cytokine and TLR signalling, metabolic pathways and ECM remodelling. Remarkably, we showed that CXCL4 potentiates pro-inflammatory and pro-fibrotic responses both directly in moDCs and indirectly in dermal fibroblasts. Furthermore, as we observed that the changes in DNA methylation (mostly hypermethylation) occur primarily during moDC differentiation, we hypothesize that CXCL4-driven inflammatory and fibrotic responses upon TLR triggering are epigenetically imprinted during moDC differentiation. By applying a new methodology (RegEnrich), we identified multiple co-expression and co-methylation modules of clustered genes involved in immune responses, ECM organization and metabolic reprograming. We found little overlap between CXCL4-moDC specific co-expression and co-methylation modules, suggesting that DNA methylation has little influence on the transcriptional reprogramming prompted by CXCL4. Using data driven gene regulatory network analyses, we showed that CXCL4 modulates pro-inflammatory and pro-fibrotic responses via key transcription regulators, such as CIITA (Class II Major Histocompatibility Complex Transactivator) and IRF8 (Interferon Regulatory Factor 8). Taken together, our study reveals that CXCL4 is a key driver of innate immune training and a modulator of inflammatory and fibrotic responses. Our results further elucidate the contribution of CXCL4 to the development of chronic autoimmune fibrotic conditions.

The effects of CXCL4 on the phenotype and immune responses described in **Chapters 2, 3 and 4**, suggest a critical immune-stimulatory role of CXCL4 in moDC function, rather than a tolerogenic role. In **Chapter 5,** we therefore focused on

comparing the expression of immunogenic and tolerogenic markers in moDCs and CXCL4-moDCs. We found that CXCL4 exposure induces the up-regulation of gene sets associated with immunogenic DCs and down-regulation of several genes associated with tolerogenic DCs. C1q, a gene up-regulated in tolerogenic DCs, was dramatically down-regulated in CXCL4-moDCs, both at the mRNA and protein level. C1q is part of a trimeric protein complex (also including C1r and C1s) of the complement system, as part of the innate branch of the immune system. DNA methylation analysis led us to propose that CXCL4 transcriptional repression of C1q could possibly be explained by the strong hypermethylation, specifically at the promoter regions of *C1QA*, *C1QB* and *C1QC* genes.

Finally, in **Chapter 6**, we investigated how CXCL4 potentiates pro-inflammatory cytokine production in moDCs. As cytokines are tightly regulated by transcriptional, but also post-transcriptional mechanisms, we examined whether a subset of cytokines found overexpressed in stimulated CXCL4-moDCs were regulated at the level of mRNA decay. We found that the aberrant production of IL-6 and TNF, but not IL-12 and IL-23, was a consequence of enhanced cytokine mRNA stability, dictated by the inactivation of the RNA-binding protein tristetraprolin (TTP). In fact, siRNA-mediated knockdown of TTP, used to mimic TTP inactivation, resulted in enhanced IL6 and TNF expression in stimulated moDCs. Ultimately, we described that MAPK-p38 signalling plays a predominant role on CXCL4-induced cytokine production upon polyI:C stimulation, and mediates TTP phosphorylation (inactivation).

Altogether, this thesis highlights the role of CXCL4 in reprogramming moDC phenotype and function, and in driving transcriptional, post-transcriptional and epigenetic changes, which result in aberrant inflammatory and fibrotic responses. Targeting key players of these pathways represents promising possibilities for therapeutic intervention in diseases where CXCL4 is implicated, most notably SSc, RA and PsA.

A

Nederlandse samenvatting

CXCL4 (ook bekend als bloedplaatjesfactor 4/ *platelet factor 4*, PF4) is een chemokine die betrokken is bij fysiologische processen zoals bloedstolling, remming van hematopoëse en bijsturen van de immuunreacties. Hoge concentraties van CXCL4, zowel in circulatie als in inflammatoire weefsels, waren eerder al geassocieerd met verschillende auto-immuunziekten zoals reumatoïde artritis (RA) en het syndroom van Sjögren (SS). Onze onderzoeksgroep heeft CXCL4 geïdentificeerd als een biomarker voor Systemische Sclerose (SSc), ook wel sclerodermie genaamd.

SSc is een heterogene aandoening. Er zijn verschillende kenmerken van SSc, waaronder vasculopathie, immuuncel disfunctie, productie van autoreactieve antilichamen en afwijkende afzetting van extracellulaire matrixcomponenten (ECM), zoals fibronectine. Van de verschillende subsets van immuuncellen die mogelijk kunnen bijdragen aan SSc-pathologie, werd eerder al aangetoond dat dendritische cellen (DC's) van SSc-patiënten versterkte TLR-gemedieerde responsen vertoonden. Ook werden DC-infiltraten waargenomen in fibrotische weefsels van SSc patiënten, samen met T-cellen die daarbij vooral een Th2- en Th17-fenotype vertonen.

In dit proefschrift heb ik de rol van CXCL4 in het sturen van immuun responsen onderzocht, en de door CXCL4 gemoduleerde moleculaire mechanismen bestudeerd die bijdragen tot chronische inflammatoire en fibrotisch afwijkende responsen in SSc. Voor de ontwikkeling van therapeutische strategieën gericht op ziekten waarbij CXCL4 betrokken is, is namelijk de identificatie van CXCL4-gemoduleerde doelen een noodzakelijke stap.

CXCL4 versterkt aangeboren en adaptieve immuunresponsen

CXCL4 moduleert het fenotype en de functie van DC's en T-cellen. In **Hoofdstuk 2** hebben we de rol van CXCL4 in het aansturen van aangeboren en adaptieve immuunresponsen opgehelderd in humane moDC's (*monocyte-derived DCs*). Deze cellen hebben we gebruikt als model voor inflammatoire DC's. We hebben aangetoond dat CXCL4 de opregulatie van co-stimulatie- en rijpingsmoleculen in moDC's aanstuurt. Bovendien hebben we voor de eerste keer waargenomen dat wanneer moDC's zijn blootgesteld aan CXCL4 tijdens hun cel differentiatie, ze al worden voorbestemd richting afwijkende productie van pro-inflammatoire cytokines, zoals we waarnemen na triggering van TLR3 (polyI: C) of TLR7 / 8 (R848 en CL075). Verder toonden we aan dat door aanwezigheid van CXCL4 tijdens moDC differentiatie, moDC's versterkt worden in hun capaciteit om autologe

$CD4^+$ en $CD8^+$ T-cel responsen te stimuleren, en ook antigeen-specifieke $CD8^+$ T-cel ontstekingsreacties te versterken.

Hoge CXCL4 concentraties worden gelinkt aan Th17-geassocieerde ontstekingsziekten, zoals RA, psoriasis en SSc. Daarom hebben we in **Hoofdstuk 3** de rol van CXCL4 bij T-cel activatie en het richten van differentiatie tot Th17 onderzocht. We hebben aangetoond dat CXCL4 de activering van $CD4^+$ T-cellen naar IL17-producerende cellen bevordert, hetzij na CD3 / CD28-stimulatie, hetzij in co-kweekexperimenten met monocyten, myeloïde DC's (mDC's) en CXCL4-moDC's. Om duidelijk te krijgen over hoe CXCL4-niveaus in verband staan tot IL-17-productie bij psoriatische artritis (PsA), een door Th17 gemedieerde aandoening, hebben we concentraties gemeten van CXCL4- en IL-17 in plasma en het synoviaal vocht van PsA-patiënten. We vonden dat CXCL4 verhoogd aanwezig is in de circulatie van PsA-patiënten, en dat er een positieve correlatie bestaat tussen de hoeveelheden CXCL4 en IL-17 in de synoviale vloeistof.

CXCL4-aangestuurde immunogene en fibrotische functies worden gereguleerd op transcriptioneel, post-transcriptioneel en epigenetisch niveau

Om de moleculaire mechanismen te beoordelen die de effecten van CXCL4 op de cel morfologie, het fenotype en de functie van moDC's bepalen, hebben we in **Hoofdstuk 4** het volledige genoom-brede transcriptoom en methylatie-analyse van moDC's en CXCL4-moDC's uitgevoerd, zowel tijdens differentiatie als na stimulatie met polyI: C.

We hebben beschreven dat CXCL4 dramatische veranderingen in transcriptie en DNA-methylatie veroorzaakt, en zo cytokine- en TLR-signalering, metabolische processen en ECM-hermodellering verstoort. Hier hebben we aangetoond dat CXCL4 pro-inflammatoire en pro-fibrotische reacties versterkt, zowel direct in moDC's als indirect in dermale fibroblasten. Verder hebben we vastgesteld dat de veranderingen in DNA-methylatie (meestal hypermethylatie) voornamelijk tijdens differentiatie van moDC voorkomen. Hieruit volgde onze hypothese dat CXCL4-aangestuurde ontstekings- en fibrotische responsen na TLR-triggering epigenetisch geprogrammeerd worden tijdens moDC-differentiatie. Aan de hand van een nieuwe methodologie (RegEnrich), hebben we meerdere modules van co-expressie en co-methylatie van geclusterde genen geïdentificeerd die betrokken zijn bij immuunresponsen, ECM-organisatie en metabole herprogrammering. We vonden weinig overlap tussen CXCL4-moDC specifieke co-expressie en co-methylatie modules. Dit resultaat geeft aan dat DNA methylatie weinig invloed uitoefent op het

door CXCL4 geinduceerde reprogammering van het transcriptioom. Gebruik makende van *data-driven gene regulatory network* analyse, brachten we aan het licht dat CXCL4 pro-inflammatoire en pro-fibrotische responses moduleert via key transcriptie regulatoren, zoals CIITA (Class II Major Histocompatibility Complex Transactivator) en IRF8 (Interferon Regulatory Factor 8). Alles bij elkaar toont onze studie aan dat CXCL4 een sleutelfunctie heeft in het aansturen van aangeboren immuun training en een modulator is van inflammatoire en fibrotische responsen. CXCL4 draagt daarmee ook bij aan de ontwikkeling van chronische fibrotische autoimmuun condities.

Op basis van de effecten van CXCL4 op het fenotype en de immuunresponsen (beschreven in hoofdstukken 2, 3 en 4), lijkt CXCL4 een cruciale immuunstimulerende rol te spelen in de moDC-functie, eerder dan een tolerogene. In **Hoofdstuk 5** focusten we ons daarom op het vergelijken van de expressie van immunogene en tolerogene markers in moDCs en CXCL4-moDCs. We stelden vast dat blootstelling aan CXCL4 leidde tot inductie van expressie van genen sets die geassocieerd worden met immunogene DCs en remming van expressie van verschillende genen sets geassocieerd met tolerogene DCs. C1q, een gen dat versterkt tot expressie komt in tolerogene DCs, werd geremd in CXCL4-moDCs, zowel op mRNA- als op eiwit-niveau. C1q maakt deel uit van een trimeric eiwitcomplex (samen met C1r en C1s) van het complementsysteem, onderdeel van het aangeboren immuunsysteem. DNA-methylatie-analyse liet zien dat C1QA, C1QB en C1QC genen sterk hypermethyleerd waren, specifiek op de promotor regio; een mogelijke verklaring hiervoor is dat C1q transcriptioneel onderdrukt wordt door CXCL4.

Ten slotte, in **Hoofdstuk 6**, hebben we onderzocht hoe CXCL4 de pro-inflammatoire cytokine productie in moDCs versterkt. Omdat cytokines strak gereguleerd worden door transcriptionele, maar ook post-transcriptionele mechanismen, hebben we getracht te achterhalen of een subset van cytokines die in gestimuleerde CXCL4-moDCs versterkt tot expressie komen, gereguleerd werden op het niveau van mRNA-afbraak. We stelden vast dat een afwijkende productie van IL-6 en TNF, maar niet van IL-12 en IL-23, een gevolg was van bestendiging van de stabiliteit van cytokine mRNA, ingegeven door de inactivatie van het RNA-bindend proteïne tristetraprolin (TTP). SiRNA-gemedieerde knockdown van TTP op moDC´s, die werd gebruikt om TTP-inactivatie na te bootsen, resulteerde in verhoogde IL6- en TNF-expressie in gestimuleerde moDC's. Uiteindelijk hebben we beschreven dat MAPK-p38-signalering een dominante rol speelt bij door CXCL4 geïnduceerde cytokine productie na polyI:C-stimulatie, en TTP-fosforylering (inactivatie) medieert.

In zijn geheel heeft deze thesis de rol van CXCL4 onder de aandacht gebracht bij de herprogrammering van het fenotype en de functie van moDC, en bij het aansturen van de transcriptionele en post-transcriptionele epigenische veranderingen, die leiden tot kwalijke inflammatoire en fibrotische responses. De sleutelspelers van de

processen die ik in dit proefschrift heb beschreven, dienen als kansrijke beloftes voor therapeutische interventies bij ziektes waar CXCL4 bij betrokken is, in het bijzonder SSc, RA en PsA.

Acknowledgments

A todos os que têm estado ao meu lado, diretamente ou indiretamente, perto ou á distância, com mais ou menos frequência, especialmente durante esta aventura, um Muito Obrigada!
To everyone that have been by my side, directly or indirectly, close by or far away, more or less frequently, especially during this big adventure, Thank you!

E tudo começou com uma conversa fantástica num banco de um jardim, no Rossio de Viseu à quase 10 anos atrás com alguém que pela primeira vez despertou em mim a curiosidade em investigação, na área da imunologia e reumatologia, **José António Pereira da Silva**. Depressa aprendi que para além de um cientista brilhante por quem eu me orgulho muito, tinha ao meu lado também um amigo para a vida toda, um bom ouvinte e conselheiro, um segundo Pai. Ao maior 'culpado' de toda esta aventura, Muito Obrigada, não há palavras que possam descrever a minha eterna gratidão!

Leaving my 'comfort zone' in Coimbra/Portugal it was the most challenging thing it ever happened to me, in that time, 2012. With the unconditional support and motivation transmitted by Pereira da Silva and Margarida Carneiro I had the opportunity to move to Utrecht for an Erasmus internship within the Department of Rheumatology and Clinical immunology under the supervision of **Hans** and **Ruth**.
Hans, thank you very much for giving me the opportunity and trust to work with you, and for all your help with the necessary procedures to make it possible! Dank U wel!
Ruth, dear Ruth, can't thank you enough for all you have done for me! Since the first day I have met you and worked with you, I never felt worried, foreign, bored, unmotivated, hopeless.. You have transmitted and inspired on me so much good energy, hope, creativity, you always tried to find a way out with me, in work related things and personal issues. I miss our work discussions in the AZU or in your house with thousands of folders, and several USBs, hard disks, and folders inside of folders that never ended, back-ups everywhere! I have learned so much with you about so many things! You are definitely one of the most brilliant and special persons and scientists that more inspired me! Thank you for bringing me to your house, for letting me play with Philippe and Charlotte, such a wonderful kids! Thanks Jan, for helping and trusting on me! I'm waiting for your visit!

This is a great opportunity to thank to everyone from the Department of Rheumatology, either for the help in the lab, the paper work, or the great conversations in the office, during lunch, and outside UMCU, **Marion, Kim**, **Dorien, Katja, Arno, Rieneke, Maud, Sandhya, Marlies, Jos** (and **Joële**), Bedankt!!

Dear **Tim,** seven years ago, when you moved to Utrecht with your group, we had our first meeting in your office in AZU with Renoud. You gave me your support to apply for a PhD fellowship from Portugal to work in your group. If writing the proposal with you, Mark and Renoud was straightforward and super enthusiastic, getting feedback from FCT and fair grant conditions was a big pain for more than one year right? Thank you for this opportunity; for your support; for listening to me (even if I couldn't say 'but, however, although' hahaha); brainstorming with me; to help me to keep focus on the project's goals or many times to challenge me with 'spannend' ideas. Thanks for trusting on me (even during the period I was absent because of the restaurant and family) and believing so much on the projects until the end!

I want to truly thank to the first members I met of Tim's group: Grazie Mille and Bedankt especially to **Marta, Lenny, Kim, Mark, Koen, Nick, Annelies,** and **Renoud**.
Lenny and **Marta,** amazing colleagues that besides trusting so much on me their knowledge and creativity on working with CXCL4, were always so patience and so kind. **Marta**, bella, you are really genuine, hard worker, a fighter! Grazie mille for all our scientific discussions and for your support, not just during the victories. The way you shared your knowledge and enthusiasm definitely had a huge impact on me back in 2012/2013, sei grande!
Kim and **Mark,** thank you so much for your patience, for teaching me so much and helping me finding my way in the lab, starting the cell cultures, planning experiments and much more, meanwhile you were so overloaded on moving to Utrecht, finishing your own experiments and writing. Super bedankt for everything!
Renoud, together with **Mark** you both made sure to write and apply with me to the PhD fellowship, step up with me all the project and teach me all the basic steps in the lab and organization skills that made all the difference on my PhD traject. Renoud, thank you so much for always caring with my well-being inside and outside the lab, even after you leaving; I have learned a lot with you and you definitely inspired me!

Super Bedankt to all Radstake group, not just for the scientific discussions but also for the gezellig time: **Marzia, Alsya, Elena, Wiola, Nadia, Maili, Luuk, Cornelis, Bea, Samu, Emmerik** (and sweet **Willemijn**), **Tessa, Andrea, Nila, Jorre, Ralph,**

Fréderique, Weiyang, Kamil, Sarita, Rina, Sanne, Michel, Anne-Mieke, Jonas, Fleurieke, Abi, Anneline, Maarten Hillen, Sofie, Eefje, Maarten vd Kroef, Kris, Joel and Aridaman.

To my CXCL4-buddy of all these years, **Alsya**, a big Obrigada! Thanks for sharing so much, for your kindness and caring! Keep being such a hard worker, resilient and a great human been!
Maili, thank you for your kindness and for our brainstorming in this last year! It seems like CXCL4 it's contagious (it also caught you hahaha)! Letting go the project of CXCL4 role on DC metabolism was definitely very 'painful' to me after so many weeks/weekends and evenings trying to optimize methodologies specially the seahorse (it should be called instead 'the nightmare', much more suitable). But it was a great pleasure to have you as my CXCL4-metabolism-buddy and thinking along with you! Welcome to the CXCL4 (not always cheerful) world!
Dear **Fréderique** thank you so much for your friendship since the AZU time in 2012, you have such an amazing heart! Thanks for our gezellig conversations about everything; you always inspired me hope and peace!
Weiyang thank you for all the time and patience you have dedicated to our collaboration, for making an effort to teach me soooo new and complex field, and for trying to learn with me. No one has told us it would be easy, right? And we did it!
Cornelis a special bedankt to you, for your time, help, patience! Collaborating with you this last year definitely pushed forward our research projects, really appreciated!
Bea and **Samu,** muchas gracias for all the fun we had and for thinking with me during troubleshooting. **Bea,** gracias for helping me several times with WB, elisa, etc and for finalizing the runs of my last project! When are the four of you coming to eat polvo in my restaurant?

During the last year of my PhD, we decided to nicely close our big CXCL4 project on moDCs performing transcriptomics and on study DNA methylation in a complex set of experiments. **Aridaman** without your help and guidance it would have been impossible to finish my PhD seeing the project finishing with so cool data. All our work now explain all the observations that we have seen happening to the cells in the dish and probably what may happen in patients. I'm honestly very proud of our work! Thank you for accepting to supervise me on this project (that I agree, it's quite of a challenge because I'm so stubborn), for beveling on it and trusting so much on me!

Marianne, my dear supervisor, first of all Obrigada for giving me the opportunity of being supervised by you when Tim proposed it! Bedankt for your guidance, patience and care throughout these years! I'm very grateful for our brainstorming, for being

part of the Boes lab, and for always helping making the bridge with some else that could help me/us.
A big bedankt to all Boes lab, **Lotte, Willemijn, Lieneke, Robert, Ewoud, Thijs, Marthe, Sarah, Francesca.**
Willemijn, sweet Willemijn, thanks for all the great time we shared, so much laughing, brainstorming, hard work, long days and coffe/beer time! Miss you!

To all other colleagues I have met in the **LTI** a big thanks for the nice working environment, especially to **Zuzana, Mojtaba, Sweet Maarten, Arjan, Shamir, Kuldeep, Alessandra, Mariona, Lucas, Julia, Matevz.**
Big thanks to **Maud** and **Enric** for all our brainstorming, Thanks for sharing so much with me!
A very big *Obrigada* to **Gerrit** and **Sigrid**; **Niels, Amelia** and **Jan Meeldik** (protein facility); to **Wilco, Rianne, Jenny, Mariska, Barbara** (Luminex facility); to **Jeroen** and **Pien** (FACS facility).
Bedankt to our secretaries **Yvonne, Saskia, Anja** and **Diana** for all the patience and help.

Kristin Denzer obrigada for your kindness and great conversations about saudade, Sintra, and many other things we shared missing from Portugal.

Mathew (Peprotech) thank you for your help many times and for all conversations about everything, I will be waiting for your visit!!
I would like to acknowledge the **Fundação para a Ciência e Tecnologia** (FCT, Portugal) for granting me with an international PhD fellowship that allowed me to accomplish my PhD in the Netherlands. Thanks to **Peprotech**, **ChipSoft**, the PhD program **Infection and Immunity** from the UMCU, the **Department of Rheumatology and Clinical Immunology** and the **Stichting NVLE founds** for sponsoring the printing costs of my thesis, Obrigada!

I would like to thank to the **members of the reading commitee** for assessing my thesis.

To all the OIO kamer roomies especially to **Zsolt, Nadia, Chiara, Elena, Lotte, Luuk, Sjanna, Eveline, Sarah, Caroline, Nanette** for all the gezellig moments we shared inside and outside the WKZ.
Luuk, bedankt for your help and patience many times with translating paper work or simply by guiding me through the steps. Thank you for caring, for our brainstorming and reasoned criticism, and making me laugh so much (Suavementeee…hahaha).

Lotte, it was great to seat next to you these years, our brainstorming about so many things, pipetting, sharing chocolates or beer, when we got good and bad results! Thank you for your support and friendship!
Nadia Schat, thank you for having such a great heart, taking care of me and trusting on me! You are a great friend and feeder! Thanks for your patience many times on translating boring stuff to help me!
Elenina, Elena Chouriço, sweetheart! Let's laugh even more now about everything we have shared, so many unforgettable memories in the lab, in the office, in your house, in my house, going for food or dancing! Music and laughing was always present, even in the terrible days ('girls just want to have fun')! Thank you so much for making me laugh so much (dressing unicorn is on the top 10), for sharing and taking care of me, for the late dinners and company in the lab in the weekends! Terrible to say, but I would not change a thing! These all made us this strong!

Pawluska, such a great scientist and friend! I'm glad I have met you better, and learned so much every time we were thinking together! Obrigada por tudo!

Marzia, my unofficial supervisor for long time, thank you! Grazie mille for teaching me so much, for your patience, for your support, for always opening the door from your office, even when you were so overloaded! Proud of you and for working with you! Brainstorming and pipetting with you, made for sure, a huge difference in my projects, I will always be very thankful for all you have done for me dear!

Besides growing so much as a person and as scientist, the best thing Holland gave me was the opportunity to meet wonderful persons, that made all the difference during these years: OBRIGADA ÀS CRIATURAS FANTÀSTICAS: **Rúben, Ana e Tiago, Inês, Barbara and Daniele, Popi, Chiara** e **Gianluca, Ana** e **Diederik** for supporting me in the bad moments and celebrating with me my victories!
Thank you for all your support during my project in the Netherlands and for being so supportive while I was setting up my new project that would completely change my life. You were the only persons that were truly next to me and supporting since the day I got the news about it until the day I have inaugurated the restaurant.

Rúben querido, o segundo português a conhecer nos corredores do WKZ enquanto falava com a única portuguesa que conhecia em terras holandesas. Mal eu sabia que estava a falar com os dois futuros meus melhores amigos, os meus pilares naquele país. Obrigada por nunca mais teres desarredado pé da minha beira, nem sabes a força que me deste todos estes anos diariamente, mesmo que não nos víssemos. Obrigada pela companhia no cappuccino da manhã, almoços, jantares em

tantos sítios diferentes e nas corridas; por tantas vezes me ajudares em casa (e nas mudanças que serão sempre motivo de gargalhadas); de pensares comigo nos meus projetos; por tornares os fins de semana no laboratório mais leves (desculpa se isto soa injusto hahaha); por me fazeres rir e cuidares de mim! Ir para o trabalho ou para casa de bike (ou até para o centro) nunca era a mesma coisa sem ti, ou porque não tinha ninguém a quem bater com a minha bicicleta, ou porque apanhava menos vezes molhas. Obrigada por tornares o meu tempo na Holanda inesquecível!

Amigos **Ana e Tiago,** estarei para sempre grata por todo o apoio, amizade, partilha, paciência, por tomarem conta de mim, por toda a ajuda no laboratório, mesmo nas horas e fins de semana 'de corpo presente' porque a alminha já tinha ido para casa; obrigada por todas as discussões científicas que tivemos a qualquer hora do dia e lugar, por pensarem comigo tantas vezes, por ouvirem os meus desabafos e rirem comigo (ou de mim) nos momentos que em que eu mais precisava! Obrigada por me ajudarem quando eu andava com a casa às costas, e quando o Mickey me veio visitar (hahaha, também não acabou lá muito bem). Que continuemos a partilhar muito mais!

Querida **Inesinha**, a nossa última criatura a entrar nos Banana! Obrigada por todo o carinho e apoio, por toda a paciência para discutirmos ensaios ou resultados mesmo durante as tuas correrias entre milhões de ensaios ou applications. Estamos à tua espera para vires fazer o controlo de qualidade do arroz de cabidela e fazermos no nosso restaurante o dia do maranho (vais aterrorizar metade da clientela com o cheiro dessa coisa manhosa, mas vai valer ainda mais apena ter-te cá).

Barbara, my Italian mom, can't thank you enough! You saved me since the first day I met you in the AZU, when Ruth introduced each other. You taught me so much in the lab in the AZU and WKZ these years; you helped me moving thousand times; hosting and taking care of me; You and **Daniele** made me fell at Home, grazie per tutto quello che hai fatto per me!

Popi, my dear, when I met you in the first days of February 2012, in the streets of the Uithof searching for the place for the introduction to the new students, I felt so lucky for finding someone so special, fighter, with big heart! Together, we went through so much, besides the -15ºC in Utrecht, we laugh, we cried, we supported each other in many moments, we danced together, we moved, cooked, we drank Vinho do Porto, biked, travelled, brainstormed about work and life. Obrigada for being such a wonderful friend!

Marta e **Shiva** obrigada por toda a inspiração e motivação que me transmitiram desde o dia em que vos conheci! Vocês não têm (provavelmente) a noção do grande impacto que pessoas fantásticas, humanas, sensíveis e motivadas como vocês

têm no percurso de pessoas como eu. Obrigada por todo o trabalho que fazem no Science Xplore, e da motivação que transmitem, que teve sem duvida um grande impacto em mim.

André Almeida, obrigada por todo o apoio, paciência, toda a motivação e inspiração que sempre me transmitiste, por todas as visitas a Viseu, Coimbra e Utrecht sempre preenchidas de gargalhadas. Não sabes tu próprio a diferença que fizeste desde o momento que decidi mudar-me para a Holanda; foste incansável em me ajudar na mudança, fizeste questão de na minha primeira viagem me deixares nas portas de embarque em Lisboa; estiveste incondicionalmente ao meu lado no meu retorno por causa da minha avó; procuras-te comigo soluções varias vezes, mesmo quando a minha teimosia não o permitia. Obrigada por seres simplesmente tu!

Aurea, conhecer-te durante a minha estadia em Coimbra foi das melhores coisas que me aconteceu nesse período! Querida, obrigada por apesar de estarmos meses e meses sem nos vermos, continuares a ser uma das minhas melhores amigas, sempre lá para mim!

Ni, querida obrigada por toda a amizade e apoio que apesar da distância conseguimos dar uma à outra! Obrigada por seres aquele porto de abrigo quando retomava a Casa!

Minha selermoon, **Vanessa**! Não existe forma de agradecer por todo o apoio, carinho, força que me transmites diariamente, por toda a confiança e amizade genuína, por toda a paciência! Já á mais de 25 anos, e muitos mais virão! Tenho muito orgulho em ti, sei tropo bravíssima!

Alla mia grande amica, sorella italiana e paranymph **Chiara**, Grazie mille per tutti! How amazing it is to meet such an amazing person and friend, already half a way of my stay in the Netherlands? And sharing the office, friends, pipetting, projects? Even CXCL4 (hahaha)? Really amazing!! Thank you for all your friendship, unconditional support, inspiration, trust, patience and honesty! Sono molto felice di averti nella mia vita! **Gianluca** grazie mille for the great time we shared (especially cooking, eating, drinking beer and enjoying life right? What Italian and Portuguese people do best together? hahaha). I hope we visit each other many many times, in Portugal, in Italy, in the Netherlands or any place in the world!

Minha paranymph **Ana**, a minha mana do coração, desde o dia que te conheci! Quando me mudei para o WKZ o Zsolt falou-me pela primeira vez em ti, que havia outra portuguesa no departamento; fiquei radiante! Obrigada por seres o melhor ser humano que eu alguma vez conheci, por cuidares sempre tão bem de mim, por rires e chorares comigo, por me ouvires e por todos os conselhos. **Diederik,** tens sido incansável, obrigada por toda a confiança, amizade, partilha, pelos teus cozinhados

e cerveja fantástica! Ana, Diederik, vou guardar para sempre no coração os nossos almoços ou cafés no WKZ, AZU, nos momentos inesquecíveis em vossa casa, no parque, no jardim, nas nossas idas ás compras, no nascimento dos vossos príncipes, nas nossas celebrações, do quanto me recarrega baterias e me deixa de coração cheio ver o **Tiago** e **Lucas** a crescer e tê-los ao colo! As vossas vitórias serão sempre as minha vitórias! Só desejo que continuemos a partilhar muito mais por aí ou por aqui, as minhas duas casas, porque vocês fizeram com que me sentisse em casa ao vosso lado.

Um grande obrigada à minha **Equipa**, pela confiança deste o primeiro dia que eu propus começar este novo projeto. Obrigada pelo apoio e resiliência, mesmo nos dias mais complicados!

À **Fernanda, Romão** e **Filipe**, um obrigada muito especial por estarem do meu lado, por todos os conselhos, por acreditarem em mim, e cuidarem de mim como filha / irmã! Por sempre, e desde sempre me receberem tão bem! Sou uma sortuda!

Aos meus **pais** por me apoiarem incondicionalmente e por acreditarem em mim.
Mãe, és a minha guerreira, tudo o que alcancei até hoje foi sempre a pensar em ti e por tudo o que fazes para permitires que eu realize os meus sonhos!
Mana, nunca te conseguirei agradecer por tudo o que fazes por mim! Eu deixar a nossa casa e saber que tu lá estavas por um lado sempre me trouxe a tranquilidade que eu precisava para me focar na minha formação e realização; por outro lado sempre me causou uma grande angustia por não estar ao teu lado a lutar contigo. Obrigada por seres a melhor irmã do Mundo! Terás sempre o meu apoio incondicional!
Tenho muito orgulho em vocês!

A

Curriculum Vitae

Sandra Cristina Silva Cardoso was born on September 6th, 1988 in Viseu, Portugal. In 2009 she achieved her bachelor's degree in Biotechnology Engineering and in 2011 her master´s degree in Biotechnology at the Instituto Politécnico de Bragança. For her Master thesis, Sandra joined a research project on the phenotypic and functional characterization of $CD8^+$ T-cells from patients with Rheumatoid Arthritis, under the supervision of Dr. Margarida Carneiro and Prof. Dr. J. A. Pereira da Silva, at the Centro de Neurociências e Biologia Celular in Coimbra (CNC). In the frame of an ERASMUS scholarship program, in 2012 Sandra moved to the Netherlands to participate on a research project under the supervision of Dr. Ruth Fritsch and Prof. Dr. Hans Bijlsma at the University Medical Center, Utrecht. She investigated differences on gene expression of $CD4^+$ T-cells and monocytes between glucocorticoid-responsive and glucocorticoid-non responsive patients with rheumatoid arthritis, In 2013 she received an international fellowship from the Fundação para a Ciência e Tecnologia to perform her PhD research at the Department of Rheumatology and Clinical Immunology and Laboratory of Translational Immunology under the supervision of Dr. Marianne Boes, Prof. Dr. Timothy Radstake and Dr. Aridaman Pandit. During her PhD, Sandra and collaborators focused on deciphering the role of the chemokine CXCL4 on immune and fibrotic responses orchestrated by human monocyte-derived dendritic cells, and underlying molecular mechanisms. In 2018 she moved back to Viseu, opened a new restaurant on traditional Portuguese food and is bringing forward her family business.

List of publications

This thesis

Silva-Cardoso SC, Tao W, Fernández BM, Boes M, Radstake TRDJ, Pandit A. CXCL4 suppresses tolerogenic immune signature of monocyte-derived dendritic cells. *Submitted for publication*

Silva-Cardoso SC[*], Tao W[*], Angiolilli C, Lopes AP, Bekker CPJ, Devaprasad A, Giovannone B, van Laar J, Cossu M, Marut W, Hack E, de Boer RJ, Boes M, Pandit A, Radstake TRDJ. CXCL4 links inflammation and fibrosis through transcriptional and epigenetic reprogramming of inflammatory monocyte-derived cells. *Submitted for publication*

Silva-Cardoso SC, Bekker CPJ, Boes M, Radstake TRDJ, Angiolilli C. CXCL4 is a driver of cytokine mRNA stability in monocyte-derived dendritic cells. *Mol Immunol.* 2019; 114:524-534.

Affandi AJ, **Silva-Cardoso SC**, Garcia S, Leijten EFA, van Kempen TS, Marut W, van Roon JAG, Radstake TRDJ. CXCL4 is a novel inducer of human Th17 cells and correlates with IL17 and IL22 in psoriatic arthritis. *Eur J Immunol.* 2018;48(3):522-531.

Silva-Cardoso SC, Affandi AJ, Spel L, Cossu M, van Roon JAG, Boes M, Radstake TRDJ. CXCL4 Exposure Potentiates TLR-Driven Polarization of Human Monocyte-Derived Dendritic Cells and Increases Stimulation of T Cells. *J Immunol.* 2017;199(1):253-262.

[*]Authors contributed equally to the work

Other publications

van der Kroef M, van den Hoogen LL, Mertens JS, Blokland SLM, Haskett S, Devaprasad A, Carvalheiro T, Chouri E, Vazirpanah N, Cossu M, MD, Wichers CGK, **Silva-Cardoso SC**, Affandi AJ, Bekker CPJ, Lopes AP, Hillen MR, Bonte-Mineur F, Kok MR, Beretta L, Rossato M, Mingeneau M, van Roon JAG, Radstake TRDJ. Cytometry by time of flight identifies distinct signatures in patients with systemic sclerosis, systemic lupus erythematosus and Sjögrens syndrome. *Eur J Immunol.* 2019; doi: 10.1002/eji.201948129.

van der Kroef M, Castellucci M, Mokry M, Cossu M, Garonzi M, Bossini-Castillo L, Chouri E, Wichers CGK, Beretta L, Trombetta E, **Silva-Cardoso S**, Vazirpanah N, Carvalheiro T, Angiolilli C, Bekker CPJ, Affandi AJ, Reedquist AK, Bonte-Mineur F, Zirkzee EJM, Bazzoni F, Radstake TRDJ, Rossato M. Histone modifications underlie monocyte dysregulation in patients with systemic sclerosis, underlining the treatment potential of epigenetic targeting. *Ann Rheuma Dis*. 2019; 78(4):529-538.

Chouri E, Servaas NH, Bekker CPJ, Affandi AJ, Cossu M, Hillen MR, Angiolilli C, Mertens JS, van den Hoogen LL, **Silva-Cardoso S**, van der Kroef M, Vazirpanah N, Wichers CGK, Carvalheiro T, Blokland SLM, Giovannone B, Porretti L, Marut W, Vigone B, van Roon JAG, Beretta L, Rossato M, Radstake TRDJ. Serum microRNA screening and functional studies reveal miR-483-5p as a potential driver of fibrosis in systemic sclerosis. *J Autoimmun.* 2018; 89:162-170.

Rossato M, Affandi AJ, Thordardottir S, Wichers CGK, Cossu M, Broen JCA, Moret FM, Bossini-Castillo L, Chouri E, van Bon L, Wolters F, Marut W, van der Kroef M, **Silva-Cardoso S**, Bekker CPJ, Dolstra H, van Laar JM, Martin J, van Roon JAG, Reedquist KA, Beretta L, Radstake TRDJ. Association of MicroRNA-618 Expression With Altered Frequency and Activation of Plasmacytoid Dendritic Cells in Patients With Systemic Sclerosis. Arthritis *Rheumatol*. 2017; 69(9):1891-1902.

Fritsch-Stork RD, **Silva-Cardoso SC**, Groot Koerkamp MJ; Broen JC, Lafeber FF, Bijlsma JW. Expression of ERAP2 and LST1 is increased before start of therapy in rheumatoid arthritis patients with good clinical response to glucocorticoids. *Clin Exp Rheumatol.* 2016; 34(4):685-9

Carvalheiro H, Duarte C*, **Silva-Cardoso S***, da Silva JA, Souto-Carneiro MM. CD8+ T cell profiles in patients with rheumatoid arthritis and their relationship to disease activity. *Arthritis Rheumatol*. 2015;67(2):363-71

*Authors contributed equally to the work